frontiers
RESEARCH TOPICS

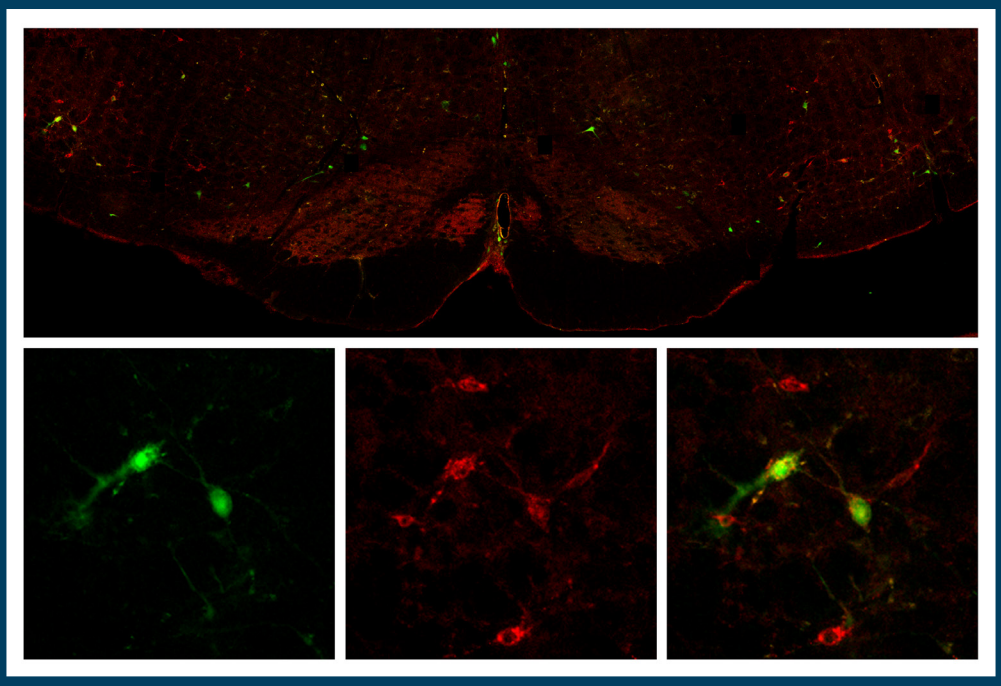

CENTRAL CONTROL OF AUTONOMIC FUNCTIONS IN HEALTH AND DISEASE

Topic Editors
Stuart J. McDougall, Heike Münzberg,
Andrei V. Derbenev and Andrea Zsombok

frontiers in
NEUROSCIENCE

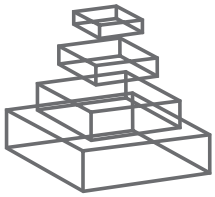

frontiers

ISSN 1664-8714
ISBN 978-2-88919-475-9
DOI 10.3389/978-2-88919-475-9

ABOUT FRONTIERS

Frontiers is more than just an open-access publisher of scholarly articles: it is a pioneering approach to the world of academia, radically improving the way scholarly research is managed. The grand vision of Frontiers is a world where all people have an equal opportunity to seek, share and generate knowledge. Frontiers provides immediate and permanent online open access to all its publications, but this alone is not enough to realize our grand goals.

FRONTIERS JOURNAL SERIES

The Frontiers Journal Series is a multi-tier and interdisciplinary set of open-access, online journals, promising a paradigm shift from the current review, selection and dissemination processes in academic publishing.
All Frontiers journals are driven by researchers for researchers; therefore, they constitute a service to the scholarly community. At the same time, the Frontiers Journal Series operates on a revolutionary invention, the tiered publishing system, initially addressing specific communities of scholars, and gradually climbing up to broader public understanding, thus serving the interests of the lay society, too.

DEDICATION TO QUALITY

Each Frontiers article is a landmark of the highest quality, thanks to genuinely collaborative interactions between authors and review editors, who include some of the world's best academicians. Research must be certified by peers before entering a stream of knowledge that may eventually reach the public - and shape society; therefore, Frontiers only applies the most rigorous and unbiased reviews.
Frontiers revolutionizes research publishing by freely delivering the most outstanding research, evaluated with no bias from both the academic and social point of view.
By applying the most advanced information technologies, Frontiers is catapulting scholarly publishing into a new generation.

WHAT ARE FRONTIERS RESEARCH TOPICS?

Frontiers Research Topics are very popular trademarks of the Frontiers Journals Series: they are collections of at least ten articles, all centered on a particular subject. With their unique mix of varied contributions from Original Research to Review Articles, Frontiers Research Topics unify the most influential researchers, the latest key findings and historical advances in a hot research area!
Find out more on how to host your own Frontiers Research Topic or contribute to one as an author by contacting the Frontiers Editorial Office: researchtopics@frontiersin.org

CENTRAL CONTROL OF AUTONOMIC FUNCTIONS IN HEALTH AND DISEASE

Topic Editors:
Stuart J. McDougall, University of Melbourne, Australia
Heike Münzberg, Louisiana State University, USA
Andrei V. Derbenev, Tulane University, USA
Andrea Zsombok, Tulane University, USA

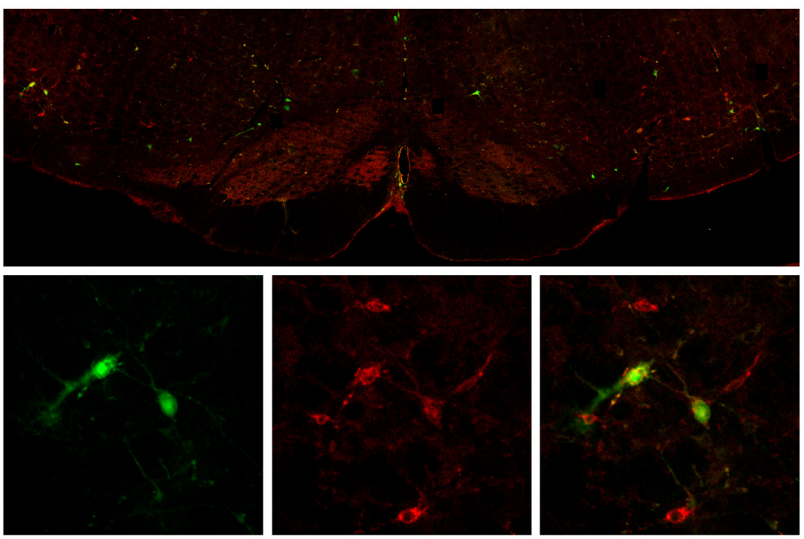

Brainstem localization of leptin receptors (red) and pseudo rabies virus infected cells (green) resulting from renal injection. Adapted from Barnes & McDougal, this issue.

The field of autonomic neuroscience research concentrates on those neural pathways and processes that ultimately modulate parasympathetic and sympathetic output to alter peripheral organ function. In the following ebook, laboratories from across the field have contributed reviews and original research to summarize current views on the role of the brain in tuning peripheral organ performance to regulate body temperature, glucose homeostasis and blood pressure.

Table of Contents

04 ***Central Control of Autonomic Functions in Health and Disease***
Stuart J. McDougall, Heike Münzberg, Andrei V. Derbenev and Andrea Zsombok

06 ***Autonomic Regulation of Brown Adipose Tissue Thermogenesis in Health and Disease: Potential Clinical Applications for Altering BAT Thermogenesis***
Domenico Tupone, Christopher J. Madden and Shaun F. Morrison

20 ***Neural Pathways that Control the Glucose Counterregulatory Response***
Anthony J. M. Verberne, Azadeh Sabetghadam and Willian S. Korim

32 ***Alterations in Blood Glucose and Plasma Glucagon Concentrations During Deep Brain Stimulation in the Shell Region of the Nucleus Accumbens in Rats***
Charlene Diepenbroek, Geoffrey van der Plasse, Leslie Eggels, Merel Rijnsburger, Matthijs G. P. Feenstra, Andries Kalsbeek, Damiaan Denys, Eric Fliers, Mireille J. Serlie and Susanne E. la Fleur

40 ***Modulation of Gastrointestinal Vagal Neurocircuits by Hyperglycemia***
Kirsteen N. Browning

49 ***Astrocytes in the Nucleus of the Solitary Tract are Activated by Low Glucose or Glucoprivation: Evidence for Glial Involvement in Glucose Homeostasis***
David H. McDougal, Gerlinda E. Hermann and Richard C. Rogers

59 ***Regulation of Neurons in the Dorsal Motor Nucleus of the Vagus by SIRT1***
Yanyan Jiang and Andrea Zsombok

67 ***Isolation of TRPV1 Independent Mechanisms of Spontaneous and Asynchronous Glutamate Release at Primary Afferent to NTS Synapses***
Axel J. Fenwick, Shaw-wen Wu and James H. Peters

77 ***TRPV1-Dependent Regulation of Synaptic Activity in the Mouse Dorsal Motor Nucleus of the Vagus Nerve***
Imran J. Anwar and Andrei V. Derbenev

85 ***Leptin Into the Rostral Ventral Lateral Medulla (RVLM) Augments Renal Sympathetic Nerve Activity and Blood Pressure***
Maria J. Barnes and David H. McDougal

frontiers in
NEUROSCIENCE

EDITORIAL
published: 09 January 2015
doi: 10.3389/fnins.2014.00440

Central control of autonomic functions in health and disease

Stuart J. McDougall[1]*, Heike Münzberg[2], Andrei V. Derbenev[3] and Andrea Zsombok[3]

[1] *Florey Institute of Neuroscience and Mental Health, University of Melbourne, Parkville, VIC, Australia*
[2] *Pennington Biomedical Research Center, Louisiana State University, Baton Rouge, LA, USA*
[3] *Department of Physiology, Tulane University, New Orleans, LA, USA*
**Correspondence: stuart.mcdougall@florey.edu.au*

Edited and reviewed by:
Joel C. Bornstein, The University of Melbourne, Australia

Keywords: thermogenesis, glucose, TRPV cation channels, hypoglycemia, vagal afferents

There is a lack of knowledge about the neurophysiology of disease states such as obesity and related disorders. Recognizing this, basic scientists are actively investigating and learning more about how the brain controls energy homeostasis from the perspective of autonomic function.

The central nervous system controls many fundamental systems including whole body metabolism, body temperature and blood pressure. Autonomic reflexes are mediated by neural pathways in the brainstem and spinal cord and generally regulate organ and system performance very rapidly (ms). Autonomic control is also mediated by specific brain regions, such as the hypothalamus, which is responsible for mid-term (min) and long-term (hours/days) regulation of internal organ systems. Importantly, autonomic reflexes are dynamic, where adaptations can alter rapid homeostatic control over longer time scales. In this respect, an understanding of the basic neurophysiology is required to subsequently discover how these processes contribute to, or are impacted by, disease states - ranging from diabetes mellitus to hypertension.

The field of autonomic neuroscience research concentrates on those neural pathways and processes that ultimately modulate parasympathetic and sympathetic output to alter peripheral organ function. In the following eBook, laboratories from across the field have contributed reviews and original research to summarize current views on the role of the brain in tuning peripheral organ performance to regulate body temperature, glucose homeostasis and blood pressure. These mechanisms include experimental approaches ranging from the whole system to synaptic levels.

One of the most basic requirements for mammalian life is the maintenance of core body temperature and as such, this factor is tightly regulated. Tupone et al. (2014) review the central nervous system nuclei and circuitry involved in brown adipose tissue thermogenesis, a sympathetically driven mechanism to increase body temperature that has been demonstrated in species from rodents to adult humans. The Morrison laboratory has been consistently at the forefront in unraveling the brain regions involved in this mechanism and in this review, the authors also discuss the potential advantages of activation or inhibition of brown adipose tissue thermogenesis for the treatment of obesity or cardiac ischemia.

A second basic requirement for life is energy availability, with glucose as the basic substrate in mammals. Verberne et al. (2014) review the current understanding of the neural pathways that control glucose homeostasis with specific emphasis on the counter-regulatory response to hypoglycemia. This mechanism highlights the coordination between endocrine and neural outflows in regulating the supply of glucose. Diepenbroek et al. (2013) present original research indicating that deep brain stimulation of the nucleus accumbens shell in rats alters blood glucose and glucagon, a mechanism that may be mediated via the lateral hypothalamus, a site that receives strong innervation from the nucleus accumbens. Such an interaction complements the central scheme presented in the review by Verberne et al. (2014). Meanwhile, Browning (2013) presents a perspective article on the role of glucose in modulating gastrointestinal vagal afferent reflex function. Figure 2 neatly and concisely summarizes the known mechanisms by which glucose impacts the viscerosensory arm of autonomic reflexes.

The site where viscerosensory information enters the brainstem is the nucleus of the solitary tract (NTS) and this region plays a crucial role in many autonomic functions. In this context, McDougal et al. (2013) highlights an important role of astrocytes in glucose homeostasis. Specifically, the authors demonstrate that cytoplasmic calcium increases in astrocytes under low glucose conditions, an effect that could not be prevented by the neurotoxin tetrodotoxin. These data suggest that astrocytes are able to directly sense changes in central glucose levels.

The dorsal motor nucleus of the vagus (DMV) is positioned downstream to vagal afferents and receives viscerosensory information via the NTS. In the original work of Jiang and Zsombok (2014), the role of a Sirtuin in the DMV in regulating energy homeostasis is investigated. The authors show that SIRT1 modulates excitatory inputs to DMV motor neurons, which relies on potassium channel modulation to increase glutamate release from presynaptic terminals.

Taken together, these studies illustrate the overlapping and integrated mechanisms that are involved in glucose homeostasis.

Two papers investigate the role of the transient receptor potential cation channel subfamily V member 1 (TRPV1) in the dorsomedial complex and both utilized temperature as a tool in their respective assay systems. First Fenwick et al. (2014) test

the hypothesis that other TRP channels apart from TRPV1 contribute to the excitatory primary afferent drive to NTS neurons. In knock out TRPV1 mice, approximately 50% of NTS neurons received primary afferent input where glutamate release could be modulated by temperature, suggesting involvement of other TRP channels in this neurotransmitter release process. The authors subsequently demonstrate nodose neurons express TRPV3 and propose this channel may be involved. While one to two steps later in the reflex circuitry Anwar and Derbenev (2013) explore the role of the TRPV1 in the DMV and observe both glutamatergic and GABAergic release is modulated by TRPV1 activation. Both papers further illustrate just how heterogeneous the dorsomedial complex is and continues to challenge efforts to investigate the neurophysiology in this region.

Finally on the sympathetic output side, at the level of the rostroventrolateral medulla (RVLM), Barnes and McDougal (2014) investigate the impact of leptin in modulating arterial pressure and renal nerve activity. The authors first utilized transneuronal tracing techniques to demonstrate leptin receptor expression in tyrosine hydroxylase positive RVLM neurons that ultimately innervate the kidney cortex. Then demonstrated that leptin microinjected into the RVLM evokes a sympathoexcitatory response to increases blood pressure and renal sympathetic nerve activity. These findings indicate a possible mechanism by which hypertension develops with obesity.

From whole system to synaptic levels, this collection of work represents the diverse range of central mechanisms that contribute to the regulation of autonomic function in relation to body temperature, energy and blood pressure homeostasis. This basic research sets the foundation for understanding how the brain coordinates and modulates peripheral organ systems. Defining these neurophysiological mechanisms will facilitate the development of advanced therapeutic approaches in the treatment of autonomic related disease states into the future.

REFERENCES

Anwar, I. J., and Derbenev, A. V. (2013). TRPV1-dependent regulation of synaptic activity in the mouse dorsal motor nucleus of the vagus nerve. *Front. Neurosci.* 7:238. doi: 10.3389/fnins.2013.00238

Barnes, M. J., and McDougal, D. H. (2014). Leptin into the rostral ventral lateral medulla (RVLM) augments renal sympathetic nerve activity and blood pressure. *Front. Neurosci.* 8:232. doi: 10.3389/fnins.2014.00232

Browning, K. N. (2013). Modulation of gastrointestinal vagal neurocircuits by hyperglycemia. *Front. Neurosci.* 7:217. doi: 10.3389/fnins.2013.00217

Diepenbroek, C., van der Plasse, G., Eggels, L., Rijnsburger, M., Feenstra, M. G., Kalsbeek, A., et al. (2013). Alterations in blood glucose and plasma glucagon concentrations during deep brain stimulation in the shell region of the nucleus accumbens in rats. *Front. Neurosci.* 7:226. doi: 10.3389/fnins.2013.00226

Fenwick, A. J., Wu, S. W., and Peters, J. H. (2014). Isolation of TRPV1 independent mechanisms of spontaneous and asynchronous glutamate release at primary afferent to NTS synapses. *Front. Neurosci.* 8:6. doi: 10.3389/fnins.2014.00006

Jiang, Y., and Zsombok, A. (2014). Regulation of neurons in the dorsal motor nucleus of the vagus by SIRT1. *Front. Neurosci.* 7:270. doi: 10.3389/fnins.2013.00270

McDougal, D. H., Hermann, G. E., and Rogers, R. C. (2013). Astrocytes in the nucleus of the solitary tract are activated by low glucose or glucoprivation: evidence for glial involvement in glucose homeostasis. *Front. Neurosci.* 7:249. doi: 10.3389/fnins.2013.00249

Tupone, D., Madden, C. J., and Morrison, S. F. (2014). Autonomic regulation of brown adipose tissue thermogenesis in health and disease: potential clinical applications for altering BAT thermogenesis. *Front. Neurosci.* 8:14. doi: 10.3389/fnins.2014.00014

Verberne, A. J., Sabetghadam, A., and Korim, W. S. (2014). Neural pathways that control the glucose counterregulatory response. *Front. Neurosci.* 8:38. doi: 10.3389/fnins.2014.00038

Conflict of Interest Statement: The authors declare that the research was conducted in the absence of any commercial or financial relationships that could be construed as a potential conflict of interest.

Received: 28 November 2014; accepted: 15 December 2014; published online: 09 January 2015.

Citation: McDougall SJ, Münzberg H, Derbenev AV and Zsombok A (2015) Central control of autonomic functions in health and disease. Front. Neurosci. ***8****:440. doi: 10.3389/fnins.2014.00440*

This article was submitted to Autonomic Neuroscience, a section of the journal Frontiers in Neuroscience.

frontiers in
NEUROSCIENCE

REVIEW ARTICLE
published: 07 February 2014
doi: 10.3389/fnins.2014.00014

Autonomic regulation of brown adipose tissue thermogenesis in health and disease: potential clinical applications for altering BAT thermogenesis

Domenico Tupone*, Christopher J. Madden and Shaun F. Morrison

Department of Neurological Surgery, Oregon Health and Science University, Portland, OR, USA

Edited by:
Andrea Zsombok, Tulane University, USA

Reviewed by:
Heike Muenzberg-Gruening, Pennington Biomedical Research Center, USA
Youichirou Ootsuka, Flinders University of South Australia, Australia

****Correspondence:***
Domenico Tupone, Neurological Surgery (Mail Code L-472), Oregon Health and Science University, 3181 SW Sam Jackson Park Rd., Portland, OR 97239, USA
e-mail: tupone@ohsu.edu

From mouse to man, brown adipose tissue (BAT) is a significant source of thermogenesis contributing to the maintenance of the body temperature homeostasis during the challenge of low environmental temperature. In rodents, BAT thermogenesis also contributes to the febrile increase in core temperature during the immune response. BAT sympathetic nerve activity controlling BAT thermogenesis is regulated by CNS neural networks which respond reflexively to thermal afferent signals from cutaneous and body core thermoreceptors, as well as to alterations in the discharge of central neurons with intrinsic thermosensitivity. Superimposed on the core thermoregulatory circuit for the activation of BAT thermogenesis, is the permissive, modulatory influence of central neural networks controlling metabolic aspects of energy homeostasis. The recent confirmation of the presence of BAT in human and its function as an energy consuming organ have stimulated interest in the potential for the pharmacological activation of BAT to reduce adiposity in the obese. In contrast, the inhibition of BAT thermogenesis could facilitate the induction of therapeutic hypothermia for fever reduction or to improve outcomes in stroke or cardiac ischemia by reducing infarct size through a lowering of metabolic oxygen demand. This review summarizes the central circuits for the autonomic control of BAT thermogenesis and highlights the potential clinical relevance of the pharmacological inhibition or activation of BAT thermogenesis.

Keywords: brown adipose tissue, hypothermia, adenosine, hibernation, torpor, therapeutic hypothermia, fever, obesity

INTRODUCTION

The presence of uncoupling protein-1 (UCP-1) in the mitochondria of brown and beige adipocytes confers on brown adipose tissue (BAT) the unique capacity to generate heat through dissociation of the energy derived from the electron transport chain from the production of ATP. BAT thermogenesis is under the direct control of central sympathetic circuits such that the release of norepinephrine onto β3 receptors in the membrane of brown adipocytes contributes to increased lipolysis and β-oxidation of fatty acids leading to the activation of the mitochondrial process for heat production (Cannon and Nedergaard, 2004). Cold exposure produces BAT activation, both in human (Christensen et al., 2006; Cypess et al., 2009; Nedergaard et al., 2010) and rodents (Nakamura and Morrison, 2011; Morrison et al., 2012), and exposure to a warm environment leads to a reduction in the sympathetic drive to BAT, maintaining an inhibition of thermogenesis (Nakamura and Morrison, 2010).

BAT thermogenesis requires the consumption of energy stores, initially those in the BAT lipid droplets and, with extended BAT activation, those derived from catabolism of white adipose tissue. During restricted energy availability, BAT thermogenesis and its energy expenditure are inhibited, as exemplified in the suspension of the thermogenic response to cold in hibernating animals (Cannon and Nedergaard, 2004) and during food restriction or hypoglycemia (Egawa et al., 1989; Madden, 2012). Thus, in addition to the core thermoregulatory network, BAT thermogenesis can be modulated by CNS circuits not directly involved in thermoregulation, but in regulating other aspects of overall energy homeostasis. We hypothesize that such a metabolic regulation of BAT thermogenesis plays a permissive role in determining BAT thermogenesis, potentiating, or reducing transmission through the core thermoregulatory circuit controlling BAT. In this review, we will describe the core thermoregulatory circuit controlling BAT thermogenesis in response to cold or warm exposure, as well as other CNS regions whose neurons may be modulatory or permissive for the BAT thermogenesis. Additionally, we will suggest examples in which the understanding of the circuits regulating BAT thermogenesis, and thus, the opportunities for pharmacological inhibition or activation of BAT, could be clinically relevant in pathologies such as intractable fever, obesity, or brain or myocardial ischemia.

CORE THERMOREGULATORY CIRCUIT REGULATING BAT THERMOGENESIS

The autonomic regulation of BAT thermogenesis is effected primarily through the core thermoregulatory network (**Figure 1**) in the CNS. This neural network can be viewed as a reflex circuit through which changes in skin (and visceral) thermoreceptor discharge leads to alterations in the activation of BAT sympathetic nerve activity (SNA), to counter or protect against changes in

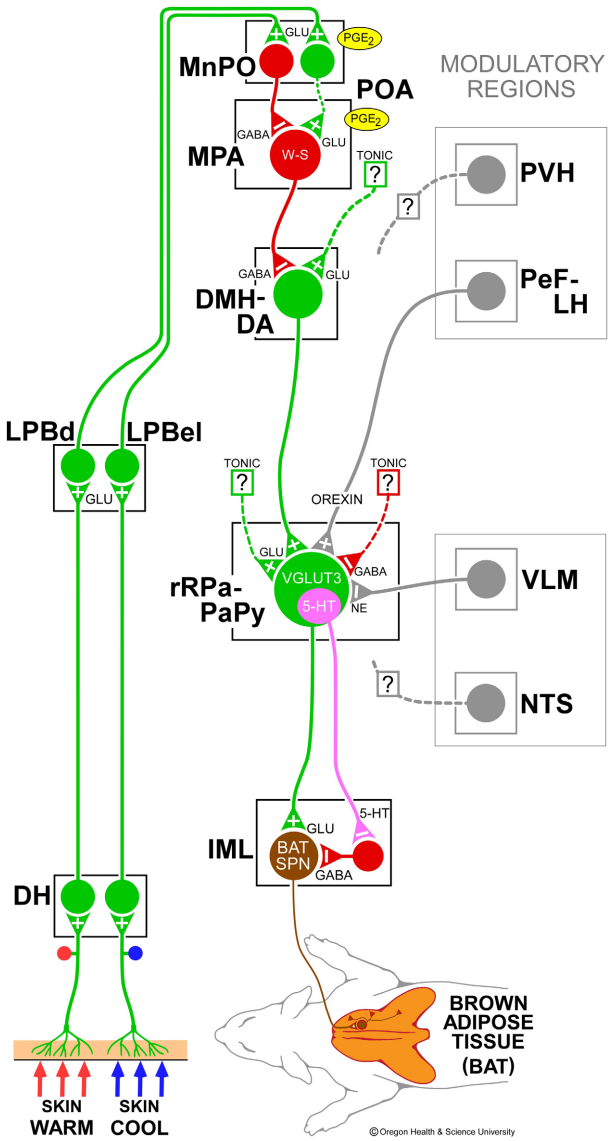

FIGURE 1 | Schematic model of the central autonomic thermoregulatory pathway and neurotransmitters regulating brown adipose tissue (BAT). Cool and warm cutaneous thermal sensory receptors excite primary sensory neurons in the dorsal root ganglia which relay thermal information to second-order thermal sensory neurons in the dorsal horn (DH). Cool and warm sensory neurons in DH release glutamate to activate third-order sensory neurons in the external lateral (LPBel) and dorsal (LPBd) subnuclei, respectively, of the lateral parabrachial nucleus. Thermal signals for involuntary thermoregulatory responses are transmitted from the LPB to the preoptic area (POA) which contains a population of BAT-regulating, GABAergic, warm-sensitive (W-S) neurons in the medial preoptic area (MPA) that project to inhibit glutamatergic, BAT sympathoexcitatory neurons in the dorsomedial hypothalamus and dorsal hypothalamic area (DMH-DA). In the median preoptic (MnPO) subnucleus, we postulate that GABAergic interneurons, activated by cool-activated neurons in LPBel, inhibit W-S neurons, while excitatory interneurons, excited by warm-activated neurons in LPBd, excite W-S neurons. Prostaglandin (PG) E_2 binds to EP3 receptors to inhibit the activity of W-S neurons in the POA. The activity of BAT sympathoexcitatory neurons in the DMH-DA, determined by the balance of a glutamatergic excitation of

(Continued)

FIGURE 1 | Continued
unknown origin and a GABAergic inhibition from W-S POA neurons, excites BAT sympathetic premotor neurons in the rostral ventromedial medulla, including the rostral raphe pallidus (rRPa) and parapyramidal area (PaPy), that project to BAT sympathetic preganglionic neurons (SPN) in the spinal intermediolateral nucleus (IML). Some BAT premotor neurons can release glutamate (GLU) to excite BAT SPNs and increase BAT sympathetic nerve activity, while others can release serotonin (5-HT) to interact with 5-HT_{1A} receptors, potentially on inhibitory interneurons in the IML, to increase the BAT sympathetic outflow, and thermogenesis. Regions with modulatory inputs to the thermoregulatory pathway include the paraventricular hypothalamic nucleus (PVH) which exerts an inhibitory influence on BAT thermogenesis. Orexinergic neurons in the perifornical lateral hypothalamus (PeF-LH) project to the rRPa to increase the excitability of BAT sympathetic premotor neurons. Activation of neurons in the ventrolateral medulla (VLM) or in the nucleus of the solitary tract (NTS) produces an inhibition of BAT thermogenesis. Norepinephrine (NE) release from the rRPa terminals of VLM catecholaminergic neurons contributes to the VLM-evoked BAT sympathoinhibition via alpha 2 adrenergic receptors on BAT sympathetic premotor neurons. VGLUT3, vesicular glutamate transporter 3.

the temperature of the brain and other critical organ tissues. The synaptic integration sites and neurotransmitter systems in the core thermoregulatory network constitute potential sites where non-thermal signals and pharmacological agents could modulate BAT thermogenesis.

CUTANEOUS THERMAL RECEPTOR AFFERENT PATHWAY

The skin contains both cool and warm thermoreceptors (Andrew and Craig, 2001; Craig et al., 2001). The predominant cold receptors are lightly myelinated Aδ fibers, active between 10°C and 40°C and less abundant warm receptors are unmyelinated C fibers, activated between 30°C and 50°C, such that both warm and cold thermoreceptors would be active at temperatures between 30°C and 35°C (Hensel and Kenshalo, 1969). The molecular mechanisms underlying activation of cutaneous thermoreceptors reside in the transient receptor potential (TRP) family of cation channels whose conductances are temperature dependent (Pogorzala et al., 2013). TRPM8, activated by menthol and cooling is the primary candidate for the cutaneous cold receptor TRP channel (McKemy et al., 2002). BAT activity and core temperature are reduced by blockade of peripheral TRPM8 (Almeida et al., 2012) or neonatal capsaicin treatment that reduces TRPM8 mRNA in dorsal root ganglia (Yamashita et al., 2008). By virtue of their location at the interface between the environment and subcutaneous tissue, the discharge of cool and warm skin thermoreceptors will be influenced by both the ambient temperature (modulated by the degree of hairiness of the skin site) and the level of cutaneous blood flow and degree of anastomosis of the cutaneous vasculature. Thus, upon exposure to a cold environment, an increase in the discharge of skin cool thermoreceptors will be sustained by the fall in ambient temperature as well as by the reflex-evoked cutaneous vasoconstriction which reduces the flow of warm blood to the skin in order to limit heat loss.

Primary thermal somatosensory fibers deliver thermal information to lamina I neurons in the spinal (or trigeminal) dorsal horn (Craig, 2002) (**Figure 1**). Cold-defensive, sympathetic BAT

thermogenesis is driven, not by the spinothalamocortical pathway mediating perception, localization and discrimination of cutaneous thermal stimuli, but rather by a spinoparabrachiopreoptic pathway, in which collateral axons of spinothalamic and trigeminothalamic lamina I dorsal horn neurons (Hylden et al., 1989; Li et al., 2006) activate lateral parabrachial nucleus (LPB) neurons projecting to thermoregulatory networks in the preoptic area (POA). Specifically, neurons in the external lateral subnucleus (LPBel) of the lateral parabrachial nucleus (LPB) and projecting to the median subnucleus (MnPO) of the POA are glutamatergically activated following cold exposure (Bratincsak and Palkovits, 2004; Nakamura and Morrison, 2008b), and third-order warm sensory neurons in the dorsal subnucleus (LPBd) are activated in response to skin warming (Bratincsak and Palkovits, 2004; Nakamura and Morrison, 2010). Although nociceptive inputs play only a minor role (Nakamura and Morrison, 2008b), there may be other non-thermal signals that are integrated with cutaneous thermal afferent inputs to LPB neurons in the afferent pathway contributing to regulate BAT thermogenesis.

HYPOTHALAMIC MECHANISMS IN THE THERMOREGULATORY CONTROL OF BAT THERMOGENESIS

Within the neural circuits regulating BAT thermogenesis, the hypothalamus, prominently including the POA and the dorsomedial hypothalamus/dorsal hypothalamic area (DMH/DA), occupies a pivotal position between the cutaneous signaling related to ambient temperature and the premotor and spinal motor pathways controlling BAT thermogenesis (**Figure 1**). Other hypothalamic nuclei, including the perifornical lateral hypothalamus (PeF/LH) and the paraventricular nucleus (PVH), can modulate BAT SNA (see below), but are not within the core thermoregulatory pathway.

Glutamatergic activation of MnPO neurons by their LPBel inputs is an essential step in the central mechanism for eliciting cold-defensive BAT thermogenesis. Specifically, stimulation of BAT thermogenesis by activation of LPBel neurons or by skin cooling is blocked by inhibiting neuronal activity or by antagonizing glutamate receptors in the MnPO (Nakamura and Morrison, 2008a,b). MnPO neurons receiving cutaneous cold signals from LPBel neurons also presumably receive other synaptic inputs that could influence the regulation of BAT thermogenesis by cutaneous thermal afferents. For example, tuberoinfundibular peptide of 39 residues (TIP39)-mediated activation of the parathyroid hormone 2 receptor (PTH2R) on glutamatergic terminals presynaptic to MnPO neurons projecting to DMH/DA increases core temperature, likely including a stimulation of BAT thermogenesis, and interruption of TIP39 signaling in MnPO reduces cold defense capability (Dimitrov et al., 2011). Additionally, neurons in MnPO contain receptors for leptin (Zhang et al., 2011) and for PGE_2(Lazarus et al., 2007) that also influence the activation of BAT thermogenesis. The strong activation of BAT thermogenesis by local nanoinjections of bicuculline into MnPO (Nakamura and Morrison, 2008a) is consistent with a tonic GABAergic inhibition of skin cooling-activated neurons in MnPO.

The conceptual foundation of our current understanding of the role of the hypothalamus in normal body temperature regulation and in the elevated body temperature during fever is the discovery (Nakayama et al., 1963; Boulant and Hardy, 1974) of a class of hypothalamic neurons, perhaps concentrated in the medial preoptic area (MPA), which have intrinsic temperature sensitivity: in the absence of synaptic inputs, their discharge frequency increases as the temperature of their local environment increases. The neurophysiological mechanism underlying the thermosensitivity of warm-sensitive neurons in the POA is thought to reside in a warming-dependent facilitation of the rate of rise of a depolarizing prepotential, due to an heat-induced increase in the inactivation rate of an A-type potassium current, which shortens the intervals between action potentials and thereby increases their firing rates (Boulant, 2006). Thus, cold-defensive and febrile activation of BAT thermogenesis is postulated to occur via a disinhibitory mechanism in which MnPO neurons receiving cutaneous cool signals from LPBel neurons provide a GABAergic inhibition to warm-sensitive, GABAergic (Lundius et al., 2010) inhibitory projection neurons in the MPA (**Figure 1**) to reduce their tonic activity, thereby resulting in disinhibition of BAT sympathoexcitatory neurons in caudal brain regions such as DMH/DA and rostral raphe pallidus (rRPa), whose excitation increases the sympathetic outflow to BAT. Consistent with this hypothesis, increases in BAT thermogenesis evoked by skin cooling or by stimulation of MnPO neurons are reversed completely by antagonizing $GABA_A$ receptors in the MPA (Nakamura and Morrison, 2008a).

The DMH/DA contains the BAT sympathoexcitatory neurons antecedent to medullary BAT sympathetic premotor neurons in rRPa (**Figure 1**) that are critical for the cold-defense and febrile activation of BAT thermogenesis (reviewed in Dimicco and Zaretsky, 2007). The direct activation of DMH/DA neurons by local injection of NMDA or leptin (Enriori et al., 2011) increases the sympathetic tone to BAT. Bicuculline-mediated disinhibition of DMH/DA neurons increases BAT SNA (Cao et al., 2004) and BAT thermogenesis (Zaretskaia et al., 2002), consistent with a tonically-active GABAergic input, likely from warm-sensitive POA neurons, to BAT sympathoexcitatory neurons in the DMH/DA (**Figure 1**) (Nakamura et al., 2005). In addition, inhibition of neurons in the DMH/DA or blockade of local glutamate receptors in the DMH/DA reverses febrile and cold-evoked excitations of BAT SNA and BAT thermogenesis (Zaretskaia et al., 2003; Madden and Morrison, 2004; Morrison et al., 2004; Nakamura et al., 2005; Nakamura and Morrison, 2007). Neurons in the DMH/DA do not project directly to BAT sympathetic preganglionic neurons, but their monosynaptic projection to the rostral ventromedial medulla (Hermann et al., 1997; Samuels et al., 2002; Nakamura et al., 2005; Yoshida et al., 2009), including the principal site of BAT sympathetic premotor neurons in the rRPa (see below), has been implicated in mediating the effects of DMH/DA neurons on BAT thermogenesis. Glutamate receptor activation in the rRPa is necessary for the increase in BAT SNA and BAT thermogenesis evoked by disinhibition of neurons in the DMH/DA (Cao and Morrison, 2006). Neurons in the DMH/DA that are retrogradely-labeled from tracer injections into the rRPa express Fos in response to BAT thermogenic stimuli such as endotoxin, cold exposure or stress (Sarkar et al., 2007; Yoshida et al., 2009; Madden, 2012) and some DMH/DA neurons that project to the rRPa receive close

GABAergic appositions from neurons in the MPA (Nakamura et al., 2005).

While there is evidence suggesting a role for neurons in the periaqueductal gray (PAG) in determining the level of BAT thermogenesis, potentially by influencing the output from the DMH/DA, no consistent picture has emerged of the functional organization of the PAG influence on the sympathetic outflow to BAT. Some DMH/DA neurons projecting to the caudal PAG (cPAG) express Fos in response to cold exposure (Yoshida et al., 2005) and some neurons in the cPAG are multisynaptically-connected to BAT (Cano et al., 2003), presumably including those that project directly to the raphe (Hermann et al., 1997). Neurons in the cPAG express Fos in response to cold (Cano et al., 2003), although these may not project to the rRPa (Yoshida et al., 2009). Excitation of neurons in cPAG increases BAT temperature, but without a concomitant increase in core temperature (Chen et al., 2002), while similar excitation of neurons in the lateral and dorsolateral PAG (dl/lPAG) of conscious rats does increase core temperature, in a manner dependent on activity within the DMH (De Menezes et al., 2009). In contrast, in anesthetized and paralyzed rats, skin cooling-evoked stimulation of BAT thermogenesis was unaffected by muscimol injections into the cPAG (Nakamura and Morrison, 2007). The area of the rostral ventromedial PAG (rvmPAG) contains neurons with an inhibitory effect on BAT thermogenesis that are capable of reversing the BAT thermogenesis evoked by PGE_2 injections into POA or by disinhibition of neurons in DMH/DA (Rathner and Morrison, 2006).

BAT SYMPATHETIC PREMOTOR NEURONS IN THE rRPa

Within the hierarchical organization of the central thermoregulatory network, neurons in the rostral ventromedial medulla, centered in the rRPa and extending into nearby raphe magnus nucleus and over the pyramids to the parapyramidal area (PaPy) (Bamshad et al., 1999; Oldfield et al., 2002; Cano et al., 2003; Yoshida et al., 2003), play a key role as BAT sympathetic premotor neurons—providing an essential excitatory drive to BAT sympathetic preganglionic neurons (SPNs) in the intermediolateral nucleus (IML) of the thoracolumbar spinal cord, which, in turn, excite sympathetic ganglion cells innervating the BAT pads (**Figure 1**). BAT sympathetic premotor neurons in the rRPa respond to local application of agonists for NMDA and non-NMDA subtypes of glutamate receptors and receive a potent glutamatergic excitation (Madden and Morrison, 2003; Cao and Morrison, 2006). They also receive GABAergic inhibitory inputs, which predominate under warm conditions to reduce BAT thermogenesis. Relief of this tonically-active, GABAergic inhibition as well as an increase in glutamate-mediated excitation, including that from the DMH (Cao and Morrison, 2006), contributes to the cold-evoked and febrile increases in BAT premotor neuronal discharge that drives BAT SNA and BAT heat production (Madden and Morrison, 2003). Reduced activity of rRPa neurons produces dramatic falls in body temperature in conscious rats (Zaretsky et al., 2003). The activity of rRPa neurons is required for the increases in BAT SNA and BAT thermogenesis elicited by a variety of thermogenic stimuli, including not only skin cooling and fever (Nakamura et al., 2002; Madden and Morrison, 2003; Nakamura and Morrison, 2007; Ootsuka et al., 2008), but also disinhibition of neurons in the DMH (Cao et al., 2004) or PeF/LH (Cerri and Morrison, 2005); activation of central mu-opioid receptors (Cao and Morrison, 2005), central melanocortin receptors (Fan et al., 2007) or preoptic CRF receptors (Cerri and Morrison, 2006) and systemic administration of the adipose tissue hormone, leptin (Morrison, 2004). BAT thermogenesis is driven by the activity of both VGLUT3-expressing and serotonin-containing neurons in the rostral ventromedial medulla, as indicated by the findings that a significant percentage of VGLUT3-containing neurons in the rRPa express c-fos in response to cold exposure or icv PGE_2 (Nakamura et al., 2004), that serotonergic neurons in the rRPa increase their firing rate in response to PGE_2 administration or cold exposure (Martin-Cora et al., 2000), that blockade of spinal glutamatergic receptors attenuates increases in BAT SNA evoked by disinhibition of neurons in the raphe pallidus (Nakamura et al., 2004), and that blockade of spinal serotonin receptors markedly attenuates cold-evoked increases in BAT SNA (Madden and Morrison, 2010). Thus, the rRPa and PaPy regions of the ventromedial medulla contain the principal populations of BAT sympathetic premotor neurons that provide the final common medullospinal pathway (**Figure 1**) for the BAT sympathoexcitatory drive to the spinal network controlling BAT SNA and that are both necessary and sufficient for the BAT thermogenic responses to thermoregulatory (**Figure 1**) and febrile stimuli and to a variety of neurochemical mediators that influence body temperature.

SPINAL SYMPATHETIC MECHANISMS INFLUENCING BAT THERMOGENESIS

The discharge of BAT SPNs that determines the level of BAT SNA and BAT thermogenesis, as well as the rhythmic bursting characteristic of BAT SNA, is governed by their supraspinal and segmental inputs as well as those to the network of spinal interneurons that influence BAT SPN excitability. A significant fraction of the BAT sympathetic premotor neurons in rRPa and in the PaPy are glutamatergic and/or serotonergic and/or GABAergic neurons (Cano et al., 2003; Nakamura et al., 2004; Stornetta et al., 2005). In addition, IML-projecting neurons located in the rRPa and the PaPy can contain thyrotropin-releasing hormone (TRH) and substance P (Sasek et al., 1990), but a role for these neurotransmitters in the spinal mechanisms regulating BAT thermogenesis has yet to be demonstrated. GABAergic and serotonergic inhibitory inputs to GABAergic spinal interneurons likely play a role in the regulation of BAT thermogenesis (Stornetta et al., 2005; Madden and Morrison, 2008). Glutamate and 5-HT play critical roles in the descending excitation of BAT sympathetic preganglionic neurons by their antecedent premotor neurons in the rRPa (Nakamura et al., 2004; Madden and Morrison, 2006, 2010). The significant role of serotonin-containing neurons in normal cold defense responses is also supported by the finding that mice that lack almost all central serotonergic neurons show blunted BAT thermogenesis during cold exposure (Hodges et al., 2008).

NON-THERMOREGULATORY MODULATION OF BAT THERMOGENESIS

The CNS circuit described above (**Figure 1**) represents the thermoregulatory backbone pathway controlling the BAT sympathetic outflow in response to changes in skin thermoreceptor

discharge. However, BAT thermogenesis can be markedly influenced by a variety of metabolic signals (e.g., oxygen or energy status) and BAT thermogenesis can contribute to the elevations in core temperature that characterize various behavioral states (e.g., wakefulness or stress). With the view that cold-defense is the primary function of BAT thermogenesis, we propose that such influences on BAT thermogenesis are effected by modulating, perhaps in a "permissive" manner, transmission through the synaptic integration sites in the backbone thermoregulatory pathway driving BAT SNA by a diverse array of non-thermoregulatory inputs. Since it is only for the regulation of BAT thermogenesis by skin thermoreceptors that the reflex pathway from stimulus to effector has been delineated, we can only speculate about the "functional" role underlying the myriad of neurochemical and site-specific effects on BAT thermogenesis that have been described. Although we categorize these influences as "modulatory," it should be clear that some (e.g., hypoxia or hypoglycemia) are capable of completely abrogating thermoregulatory activation of BAT thermogenesis. On the other hand, it is expected that modulatory influences that increase BAT thermogenesis (e.g., orexin) will require activation of the core thermoregulatory system.

OREXIN NEURONS IN THE PeF/LH INCREASE BAT THERMOGENESIS

Orexin neurons, a population of glutamatergic neurons co-expressing the peptides orexin A and B (De Lecea et al., 1998; Sakurai et al., 1998), are located exclusively in the PeF/LH and regulate a variety of physiological functions, including BAT thermogenesis, through their projections to several regions of the CNS (Peyron et al., 1998). A subpopulation of orexin neurons project to BAT sympathetic premotor neurons in the rRPa and PaPy (Oldfield et al., 2002; Berthoud et al., 2005; Tupone et al., 2011). Administration of orexin into the 4th ventricle increased c-fos expression in rRPa (Berthoud et al., 2005) and direct nanoinjection of orexin in RPa/PaPy, or activation of LH by activation of local NMDA receptors (Tupone et al., 2011) or by disinhibition with the $GABA_A$ antagonist, bicuculline (Cerri and Morrison, 2005), increases BAT SNA and BAT thermogenesis. Orexin in rRPa, as well as activation of neurons in PeF-LH by NMDA, potentiates an ongoing BAT SNA but fails to increase BAT SNA if the ongoing level of BAT SNA is low, as during normothermia. These data are interpreted to indicate that the orexin input to the rRPa can amplify BAT thermoregulatory responses elicited at the level of the BAT sympathetic premotor neuron (Tupone et al., 2011). Of interest is the finding that disinhibition of PeF-LH neurons with local nanoinjection of bicuculline evokes an increase in BAT SNA even in a thermoneutral condition with an initial low level of BAT SNA and this stimulation of BAT SNA requires the activity of BAT sympathoexcitatory neurons in the DMH/DA (Cerri and Morrison, 2005). Furthermore, PeF-LH orexinergic neurons, but not their release of orexin, are required for febrile and stress-induced thermogenesis (Takahashi et al., 2013). Thus, glutamate release from orexin (and non-orexinergic) neurons in PeF-LH at projection sites of these neurons such as the DMH (Peyron et al., 1998) and the rRPa (Tupone et al., 2011; Madden, 2012) could also be an important modulator of BAT thermogenesis. The modulatory role of orexin release in rRPa on cold-defensive BAT thermogenesis (Tupone et al., 2011); the increase in body weight together with the dysregulation of body temperature observed in orexin neuron-ablated mice (Hara et al., 2001, 2005; Perez-Leighton et al., 2013); and the association between a propensity for obesity and thermoregulatory dysfunction in narcoleptic disease (Plazzi et al., 2011), a pathology characterized by the lack of the orexinergic neurons, suggests that the influence of the orexin input to the core thermoregulatory network controlling BAT SNA plays a significant role in the maintenance of thermoregulatory and metabolic homeostasis.

HYPOXIC INHIBITION OF BAT THERMOGENESIS

To conserve metabolic fuel reserves and oxygen for the metabolic demands of essential tissues such as the brain and heart, BAT thermogenesis is markedly influenced by the energy status of the animal: adequate fuel substrate and oxygen availability are permissive for the activation of BAT thermogenesis, while a reduced supply of nutrient fuels (Rothwell and Stock, 1982; Buchanan et al., 1991; Madden, 2012) or of oxygen (Madden and Morrison, 2005) inhibits BAT thermogenesis. Although the neural mechanisms through which metabolic homeostasis regulates the permissive control of BAT energy expenditure are only beginning to be elucidated, recent evidence supports a role for the integration of metabolic signals with the regulation of BAT thermogenesis within the nucleus tractus solitarius (NTS) (Cao et al., 2010; Grill and Hayes, 2012), the paraventricular nucleus of the hypothalamus (PVH) and the ventrolateral medulla (VLM) (Ritter et al., 2001; Cao et al., 2010; Madden, 2012).

Systemic hypoxia produces a prompt and complete reversal of the elevated BAT SNA resulting from cold exposure or PGE_2 injection into the POA (Madden and Morrison, 2005). These effects arise from stimulation of the arterial chemoreceptors since they are eliminated by transection of the carotid sinus nerves or by inhibition of second-order arterial chemoreceptor sensory neurons in the commissural region of the nucleus of the tractus solitarius (commNTS) (Madden and Morrison, 2005). Interestingly, hypoxia also eliminates the BAT SNA activation resulting from bicuculline nanoinjection into the rRPa (Madden and Morrison, 2005), suggesting that the hypoxic inhibition of BAT thermogenesis is unlikely to arise from activation of a GABAergic input to BAT sympathetic premotor neurons in rRPa. Similarly to arterial hypoxia, disinhibition of neurons in the rostral ventrolateral medulla (rVLM) inhibits the increase in BAT SNA following nanoinjection of bicuculline into the rRPa (Cao et al., 2010). The neuroanatomical pathway for the arterial chemoreceptor-mediated inhibition of BAT SNA and BAT thermogenesis may parallel that described for the hypoxic activation of vasoconstrictor sympathetic outflow (Guyenet, 2000). Interestingly, both anatomical (Stornetta et al., 2004) and electrophysiological (Deuchars et al., 1997) studies support the existence of a bulbospinal inhibitory pathway from the rVLM to SPNs thus providing a putative descending inhibitory substrate for the hypoxic inhibition of SPNs governing BAT thermogenesis.

ROLE OF NTS IN METABOLIC REGULATION OF BAT

The intermediate NTS (iNTS) contains second-order sensory neurons receiving visceral vagal input that includes metabolic signals related, at least in part, to fuel substrate availability. The

iNTS also contains BAT sympathoinhibitory neurons: disinhibition of iNTS neurons elicits a prompt and complete inhibition of the increases in BAT SNA and BAT thermogenesis due to cold exposure, to injections of PGE_2 into the MPA, to disinhibition of neurons in DMH/DA or in rRPa, or to pontomedullary transection (Cao et al., 2010). Further, nanoinjection of an A1 adenosine receptor agonist in iNTS inhibits cold-evoked BAT SNA and this BAT sympathoinhibition is reversed by inhibition of iNTS neurons (**Figure 2A**) (Tupone et al., 2013a). The inhibition of BAT thermogenesis and BAT energy expenditure by upregulation of hepatic glucokinase may also be mediated by BAT sympathoinhibitory neurons in NTS since it is dependent on a vagal afferent input (Tsukita et al., 2012). The circuit through which iNTS neurons inhibit BAT SNA is debated and remains to be further elucidated. In the mouse, a direct GABAergic projection from NTS to BAT sympathetic premotor neurons in rRPa has been suggested to mediate the NTS-evoked inhibition of BAT activity (Kong et al., 2012). However, perhaps due to a species difference, retrograde tracing from the rat rRPa failed to identify a direct projection from iNTS to rRPa (Tupone et al., 2013a). Additionally, the long survival times necessary to transynaptically label iNTS neurons after inoculation of BAT with pseudorabies virus (Cano et al., 2003) is not consistent with a direct projection from iNTS to rRPa in rat. Moreover, activation of iNTS neurons in the rat inhibits BAT SNA and BAT thermogenesis after bicuculline injection into rRPa (Cao et al., 2010), a finding that is also inconsistent with a direct GABAergic input from the iNTS to BAT sympathetic premotor neurons in the rRPa. A species difference notwithstanding, these data could also be explained by the inability to narrowly target tracer injections into rRPa in mice and the existence of a GABAergic connection between parts of the NTS and RPa that are different from those examined in the rat. Nonetheless, the iNTS-evoked inhibition of BAT SNA in rat appears to be mediated by a multisynaptic pathway from iNTS neurons to BAT sympathetic premotor neurons in rRPa and eventually to BAT SPNs or the projection of iNTS neurons to more rostral or caudal area of the RPa. The iNTS also contains BAT sympathoexcitatory neurons, as suggested by the increase in BAT temperature following injection of leptin and/or TRH into the 4th ventricle (Hermann et al., 2006; Rogers et al., 2009), although injection of leptin alone into the NTS failed to alter BAT SNA (Mark et al., 2009). Additionally, the activation of BAT thermogenesis by duodenal lipid is dependent on cholecystokinin A receptor activation and on a vagal input to iNTS neurons (Blouet and Schwartz, 2012). Thus, multiple populations of neurons in the NTS can make significant contributions to the autonomic regulation BAT thermogenesis, particularly in response to peripheral metabolic signaling.

NEURONS IN THE VLM CONTRIBUTE TO THE HYPOGLYCEMIC INHIBITION OF BAT THERMOGENESIS

Activation of neurons throughout the rostral-caudal extent of the VLM from the facial nucleus to the lateral reticular nucleus produces an inhibition of BAT SNA (Cao et al., 2010). In particular, disinhibition of rostral VLM neurons elicits a prompt and complete inhibition of BAT SNA and BAT thermogenesis elicited by cold, by injection of PGE_2 into the MPA, by disinhibition of neurons in DMH/DA or the rRPa, or by pontomedullary transection (Cao et al., 2010). Feeding and adrenal medullary responses to the glucopenia produced by systemic administration of 2-Deoxy-D-glucose (2-DG) are mediated by neurons in the intermediate VLM, including those that project to the PVH (Ritter et al., 2001) or the spinal cord (Madden et al., 2006). Direct injection of the glucoprivic agent, 5-Thio-D-glucose (5-TG), into the intermediate VLM (**Figure 2B**) inhibits BAT SNA and BAT thermogenesis (Madden, 2012). Although the inhibition of BAT SNA and BAT thermogenesis from activation of iVLM neurons is mediated in part by a direct catecholaminergic projection to rRPa and dependent on α2 adrenergic receptors in rRPa (Madden et al., 2013), it's role in the glucoprivic inhibition of BAT SNA remains to be determined. In this regard, the rRPa does not receive a direct input from neurons in the rostral VLM (Madden et al., 2013), a VLM region from which potent inhibition of BAT SNA can be elicited (Cao et al., 2010), suggesting that there are multiple

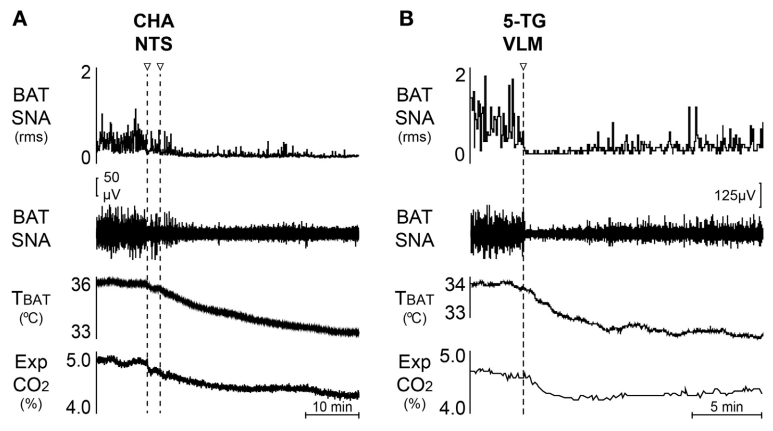

FIGURE 2 | Inhibition of BAT thermogenesis through central modulatory areas. (A) Bilateral injection of the A1 adenosine receptor agonist, CHA, induces a rapid inhibition of the cold-evoked BAT SNA and reduces BAT temperature and expired CO_2. Modified from Tupone et al. (2013a). **(B)** Unilateral nanoinjection of the glucoprivic agent, 5-TG, into the VLM induces a rapid inhibition of cold-evoked BAT SNA and a fall in BAT temperature and expired CO_2. Modified from Madden (2012), Tupone et al. (2013a).

BAT sympathoinhibitory systems over the rostral-caudal extent of the VLM.

NEURONS IN THE PVH MODULATE BAT SNA

The PVH plays a major role in the regulation of energy homeostasis through its influence on food intake (Atasoy et al., 2012) and energy expenditure (Madden and Morrison, 2009). Although the pauci-synaptic connections of neurons in the PVH to BAT (Bamshad et al., 1999; Oldfield et al., 2002; Cano et al., 2003; Yoshida et al., 2003) strongly supports a role for these neurons in the sympathetic regulation of BAT thermogenesis, their influence on the regulation of BAT thermogenesis has been controversial. Initially, neurons in the PVH were thought to play a role in the excitation of BAT SNA, since neurons in the dorsal PVH with direct projections to the spinal SPNs are activated during fever (Zhang et al., 2000) and lesions of PVH attenuated fever (Horn et al., 1994; Caldeira et al., 1998; Lu et al., 2001), although, curiously, cold-evoked BAT thermogenesis was unaffected by lesions of the PVH (Lu et al., 2001). In contrast, disinhibition of neurons in PVH or their glutamatergic activation with NMDA injections completely inhibits BAT SNA and BAT thermogenesis induced by cold exposure, injections of PGE_2 into the MPA, or disinhibition of neurons in DMH/DA (Madden and Morrison, 2009). Although activation of PVH neurons could attenuate the increases in BAT SNA and BAT thermogenesis evoked by injections of NMDA into the rRPa, those resulting from bicuculline injections into rRPa were unaffected by disinhibition of PVH neurons, consistent with the PVH-evoked inhibition of BAT SNA being mediated by $GABA_A$ receptors in the rRPa. That neurons in the PVH provide an inhibitory influence on BAT SNA is also supported by the observations that NPY presynaptically inhibits GABA release onto PVH neurons (Cowley et al., 1999) and microinjection of NPY into the PVH decreases BAT SNA (Egawa et al., 1991). These apparent controversies in the relation of PVH neurons to BAT thermogenesis, particularly during fever, might be explained by the presence of subpopulations of PVH neurons mediating contrasting effects on BAT thermogenesis or by a role of PVH neurons during fever that involves the stimulation of other fever-supporting effector systems such as the cutaneous vasculature or hormone release.

Controversy also exists concerning the role of melanocortin receptor activation in the PVH on energy expenditure and on the activation of BAT thermogenesis. Selective rescue of melanocortin-4 receptor (MC4R) expression in neurons of the PVH (and the medial amygdala) in mice lacking expression of MC4R, failed to normalize (elevate) their oxygen consumption to wild-type levels (Balthasar et al., 2005). Based on these data it was suggested that PVH MC4Rs do not mediate the energy expenditure effects of melanocortins. In contrast, other groups have demonstrated that microinjection of melanocortin receptor agonists into the PVH increases core and BAT temperatures (Song et al., 2008; Skibicka and Grill, 2009). These effects of melanocortin receptor activation could be mediated by activation of presynaptic MC4Rs, which potentiate GABAergic inputs to PVH neurons (Cowley et al., 1999). Indeed, this explanation would reconcile such a controversy, since the rescue of MC4R in the study of Balthasar et al. would only rescue the postsynaptic MC4R in PVH neurons and not those that are located presynaptically and are potentially responsible for the effects of exogenously administered melanocortin receptor agonists. This explanation is also consistent with the existence of BAT sympathoinhibitory neurons in the PVH (Madden and Morrison, 2009). The physiological conditions which stimulate the BAT sympathoinhibitory output from the PVH are unknown, but may include hypoglycemia (Madden, 2012) and hypoxia (Madden and Morrison, 2005), as well as chronic intermittent hypoxia (Sharpe et al., 2013). Another interesting possibility is that neurons in the PVH provide a tonic inhibition of BAT thermogenesis and release from this inhibition under specific conditions, such as changes in dietary composition or leptin binding to arcuate neurons (Kong et al., 2012), may activate BAT SNA and BAT energy expenditure.

PATHOLOGY

BAT THERMOGENESIS CONTRIBUTES TO FEVER

Fever is a hyperthermia (i.e., increase in core temperature) mediated by increased thermogenesis and cutaneous vasoconstriction in response to inflammatory mediators that influence central thermoregulatory circuits. Inflammatory mediators such as interleukin (IL)-1 (Rothwell, 1989), macrophage inflammatory protein-1 (MIP-1) (Zampronio et al., 1994) and tumor necrosis factor alpha (TNF-α) (Rothwell, 1988) are secreted in response to invading pathogens. With the exception of MIP-1 and IL-8, the febrile response to these inflammatory mediators requires the production of prostaglandin E_2 (PGE_2). BAT thermogenesis contributes significantly to the heat production necessary to raise core body temperature during the febrile response driven by the increased synthesis of prostaglandin E_2 (PGE_2) in response to pathogen invasion. PGE_2, which is synthesized in peripheral tissues and in the brain vasculature in response to immune signals (Elmquist et al., 1997; Matsumura et al., 1998; Yamagata et al., 2001), acts through its EP3 receptor (EP3-R) on neurons in POA, particularly the MPO and MnPO (Scammell et al., 1996; Nakamura et al., 2000, 2002; Lazarus et al., 2007) to activate BAT thermogenesis and increase body temperature during fever. The central role played by the POA neurons in fever is highlighted by the demonstration that elimination of EP3-R selectively in the POA is sufficient to prevent lipopolysaccharide (LPS) fever (Lazarus et al., 2007). However, EP3 receptors expressed in other brain areas such as the PVH and parabrachial nucleus may play a minor role in the generation of fever, since a thermogenic response follows nanoinjection of PGE_2 into these regions (Skibicka et al., 2011). Anatomical evidence supporting the role of POA neurons in fever includes the demonstration of a population of EP3-R- positive, PRV-infected neurons in POA following virus inoculation of interscapular BAT (Yoshida et al., 2003). Also, EP3-R-positive neurons in POA heavily and directly project to DMH and to rRPa (Nakamura et al., 2002, 2005, 2009) (**Figures 3A,B,D**). Moreover, the majority of EP3-R-expressing POA neurons (Nakamura et al., 2002) and of warm-sensitive neurons in POA (Lundius et al., 2010) are GABAergic. Physiologically, the muscimol-evoked inhibition of POA neurons elicits hyperthermic, cardiovascular, and neuroendocrine responses similar to those evoked by a PGE_2 nanoinjection into the same site (Zaretsky et al., 2006). Consistent with these results,

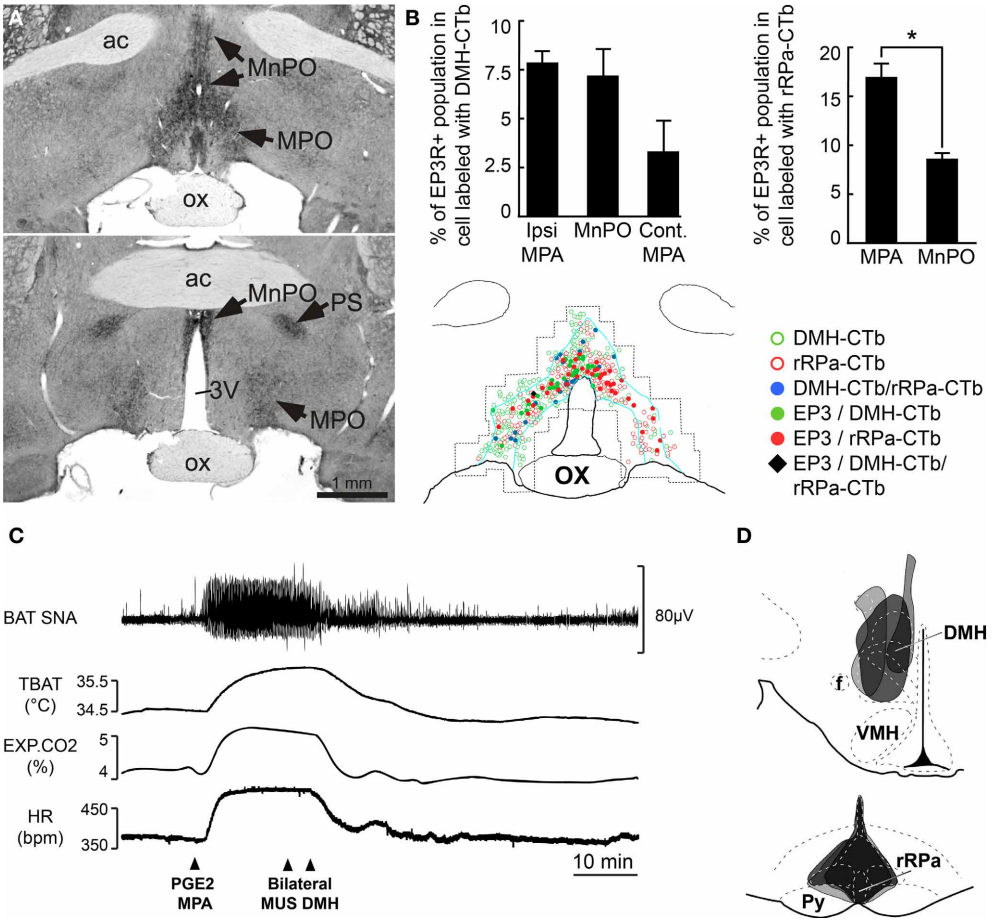

FIGURE 3 | Role of POA neurons in the generation of the fever response mediated by PGE_2. (A) Intense immunoreactivity for the EP3-R in the rat POA is particularly distributed in the MnPO, MPA, and parastrial nucleus (PS). Modified from Nakamura et al. (1999). **(B)** Counting of double-labeled neurons in MnPO and MPA that were EP3-R immunoreactive and retrogradely labeled following injection (**D**) of Alexa488-conjugated CTb and Alexa594-conjugated CTb in DMH and in rRPa, respectively, thereby suggesting their role in mediating the febrile response. $*P < 0.05$, paired *t*-test. Modified from Nakamura et al. (2009). **(C)** PGE_2-evoked increases in BAT SNA, BAT temperature (TBAT), Exp CO_2, and HR were immediately reversed by bilateral muscimol injections into the DMH. Modified from Madden and Morrison (2004).

a fever like response is elicited by the bicuculline-evoked disinhibition of DMH neurons (Morrison, 1999; Zaretskaia et al., 2002; Cao et al., 2004). Currently, the febrile response is postulated to arise from PGE_2 binding to EP3-R and inhibiting, via inhibitory GTP-binding proteins (Narumiya et al., 1999), the activity of warm-sensitive neurons in POA. This results in the disinhibition of DMH BAT sympathoexcitatory neurons projecting to BAT sympathetic premotor neurons rRPa, and the activation of BAT thermogenesis (**Figure 3C**).

THE ROLE OF BAT IN OBESITY

Sympathetic activation of BAT increases lipolysis and β-oxidation of fatty acids in BAT, allowing heat production, via mitochondrial UCP1, at the expense of stored lipids (Cannon and Nedergaard, 2004). Reduced thermogenesis, and thus reduced lipid consumption, in BAT may contribute to the etiology of some forms of obesity. Indeed, humans with low body temperature, suggesting a reduced thermogenesis, are more prone to obesity (Rising et al., 1995; Van Marken Lichtenbelt and Daanen, 2003) and obesity in humans is correlated with decreased BAT activity (Oberkofler et al., 1997; Rousseau et al., 2006; Van Marken Lichtenbelt et al., 2009). Furthermore, treatments that impair BAT thermogenesis (**Figure 4A**), such as ablation of the tissue itself or deletion of UCP-1 or β-adrenergic receptors, render rodents prone to excess weight gain (**Figure 4B**) (Lowell et al., 1993; Hamann et al., 1996; Bachman et al., 2002; Kontani et al., 2005; Feldmann et al., 2009). Conversely, increased BAT activity is protective against obesity (Kopecky et al., 1995, 1996; Guerra et al., 1998; Stanford et al., 2013). Regardless of the specific role that decreased expression or activation of BAT has in the development or maintenance of obesity in humans, it is clear that adult humans possess BAT (Cypess et al., 2009; Saito et al., 2009; Van Marken Lichtenbelt et al., 2009; Virtanen et al., 2009; Zingaretti et al., 2009) and that sympathetic activation of this tissue regulates the metabolism of fat in this tissue. Therefore, a greater understanding of the sympathetic regulation of BAT could suggest targets for therapeutic approaches

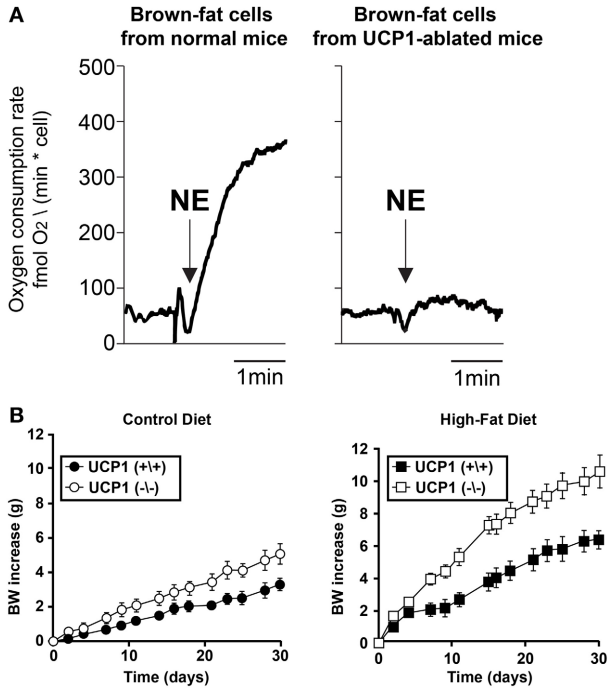

FIGURE 4 | Impairment of BAT thermogenic function leads to body weight increase. (A) Brown fat cells isolated from normal mice or from UCP1-ablated mice were stimulated with 1 μM norepinephrine (NE). Thermogenic responses (oxygen consumption) were impaired in the UCP1-abated mice compared to wild type. Adapted from Matthias et al. (2000). **(B)** Body weight (BW) increase of wild-type and UCP1(−/−) mice. Average slope was significantly different ($p < 0.05$) between both wild-type and UCP1-ablated mice for control diet and high-fat diet. From Feldmann et al. (2009).

to increase energy expenditure in this tissue and thereby combat obesity.

CLINICAL RELEVANCE OF BAT INHIBITION

Although BAT is activated during human cold defense (Christensen et al., 2006), its role in human febrile thermogenesis has not been directly demonstrated. Nonetheless, since the central thermoregulatory pathways for cold-defensive and febrile thermogenesis are overlapping in rats (Nakamura and Morrison, 2011), it is highly likely that BAT thermogenesis is recruited in human fever as well. Thus, a potentially significant role for a pharmacological inhibition of BAT thermogenesis could be the inhibition of potentially lethal febrile responses, especially those resistant to treatment with COX inhibitors, such as in malaria, head trauma (neurogenic fever), meningitis, or AIDS. Although not a lethal febrile response, LPS-induced fever was reversed and prevented by central inhibition of BAT (and shivering) thermogenesis following systemic delivery of an agonist for the alpha2 adrenergic receptor (**Figures 5C,D**) (Madden et al., 2013), which is present in the rRPa and leads to inhibition of the activity of BAT sympathetic premotor neurons and a fall in BAT thermogenesis (Madden et al., 2013). Additionally, febrile responses were reversed by treatment with an A1 adenosine receptor agonist (Muzzi et al., 2012), which inhibits BAT thermogenesis (Tupone et al., 2013b).

Another important role for pharmacological inhibition BAT thermogenesis is the facilitation of a reduction in body temperature for therapeutic use in patients with brain or cardiac ischemia. Although hypothermia can be protective in the settings of myocardial infarction and brain ischemia (Hemmen and Lyden, 2009), the hypothermia is often induced by the use of cooling approaches (Schwartz et al., 2012) which also elicit a thermoregulatory response including BAT and shivering thermogenesis (Nakamura and Morrison, 2008b, 2011), thereby preventing a rapid and deep cooling of the body. Since BAT plays a role in the human thermogenic response during cold exposure, the pharmacological inhibition of BAT thermogenesis could contribute to a more rapid and controlled body core cooling for therapeutic hypothermia (Tupone et al., 2013b). Thus, understanding the central circuits controlling BAT thermogenesis is of fundamental importance for the development of drugs to induce hypothermia. For instance, the neural circuit described above shows several CNS sites and some of the pharmacological agents acting on specific thermoregulatory areas through which inhibition of BAT thermogenesis could be obtained. However, to be therapeutically useful, a pharmacologically-induced inhibition of thermoregulation and the associated hypothermia should not interfere with other important physiological functions and should be easily reversible. In this regard, the injection of muscimol in rRPa (Cerri et al., 2013) or the central administration of an A1 adenosine receptor agonist (Tupone et al., 2013a) inhibited BAT SNA and BAT thermogenesis in rat, which, in a cool ambient temperature, led to a deep hypothermia and hypometabolic state (**Figures 5A,B**) which also characterizes torpor, from which rats recovered spontaneously with no apparent physiological dysfunction. This demonstrates the possibility to produce a safe, hypothermic, and torpid state in a nonhibernating animal. We suggest that a pharmacological inhibition of BAT thermogenesis could be clinically useful in human for the rapid induction of therapeutic hypothermia or as an alternative antipyretic.

SUMMARY

BAT thermogenesis is finely controlled by the CNS. Cold and warm input from the skin are received in the parabrachial nuclei of the brain stem and transmitted to the POA, a center for the integration of the thermal information. Neurons in the POA provide an inhibitory regulation of BAT activation through a serial neuronal network including the DMH and the rRPa excitatory projection to the spinal sympathetic preganglionic neurons, to maintain the temperature homeostasis of the body in response to changes in the ambient temperature. However, the regulation of BAT thermogenesis is also directly related to overall energetic status. As described here, robust metabolic signals such as hypoxia and hypoglycemia inhibit BAT thermogenesis via neurons in the NTS, PVH or VLM. It is likely that these brain regions, which are also involved in the control of energy homeostasis, can exert more subtle inhibitory effects on BAT activation that are reflective of a permissive metabolic control of BAT thermogenesis. In this regard, malfunction of those metabolic controllers

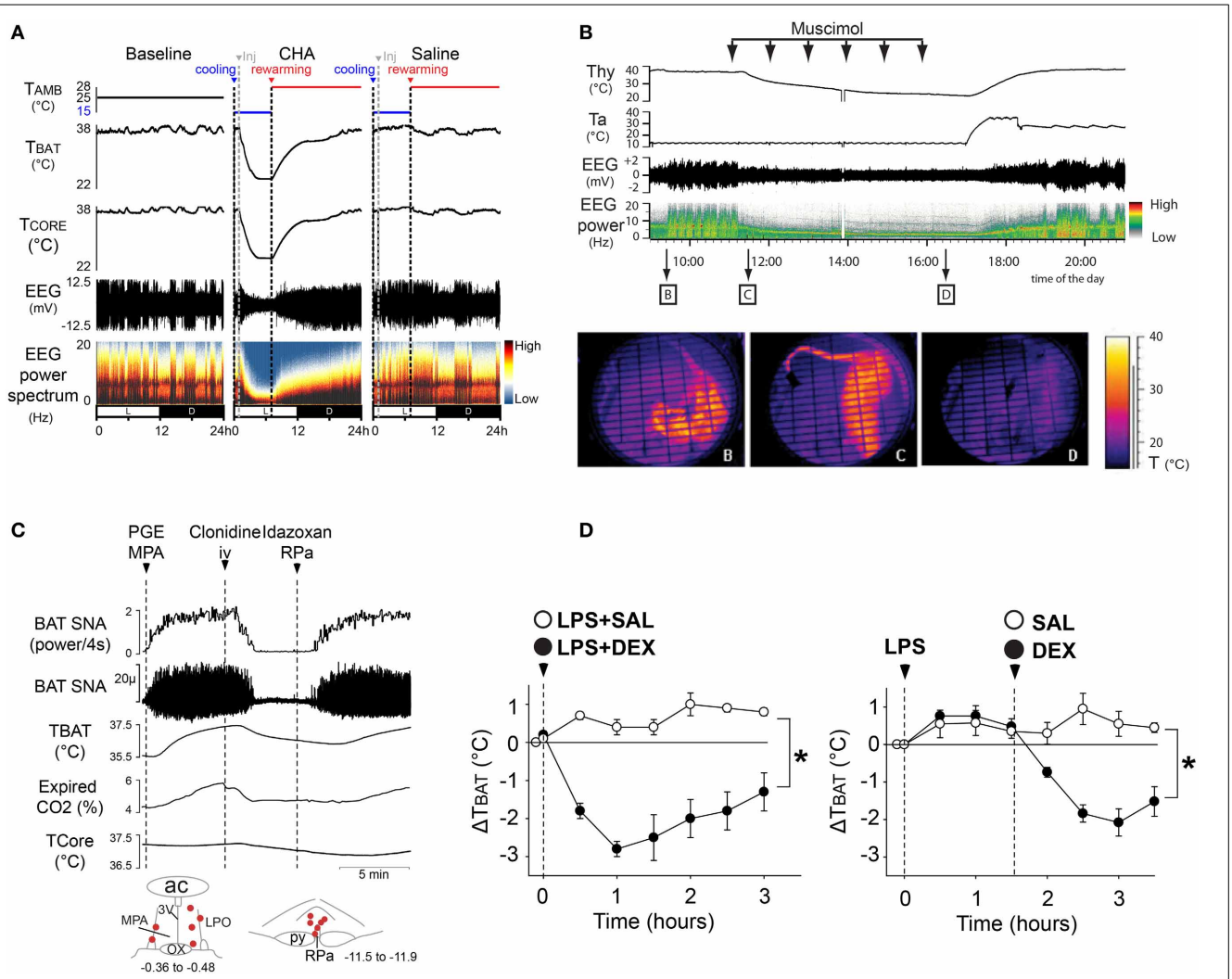

FIGURE 5 | Inhibition of BAT thermogenesis could be used to induce therapeutic hypothermia or to treat fever. (A) Central activation of the A1 adenosine receptor (A1AR), induces a deep hypothermia and reduction of EEG amplitude and power, characteristic of a torpor-like state in rat, a non-hibernating species. External re-warming reversed the hypothermic torpor-like state, allowing recovery from this state with no apparent dysfunction in physiological and sleep characteristics. Adapted from Tupone et al. (2013a). **(B)** The inhibition of thermogenesis following administration of $GABA_A$ agonist, muscimol, into the rRPa produced a deep hypothermia and reduction in EEG amplitude and a shift of the theta power resembling the torpor-like state of hibernating mammals. Adapted from Cerri et al. (2013). **(C)** Alpha2 adrenergic receptor agonist, clonidine, inhibits PGE_2-evoked BAT SNA that is reversed by direct injection of α2 receptor antagonist in rRPa. **(D)** Alpha2 receptor agonist treatment blocks the febrile response elicited by LPS injection in a free-behaving rat. The asterisk indicates two-way repeated measures ANOVA: drug effect, p 0.001; time effect, p 0.001; and interaction effect, p 0.001. Adapted from Madden et al. (2013).

could result in chronic downregulation of BAT activity and BAT thermogenesis which could contribute to metabolic pathologies such as obesity and diabetes. On the other hand, it may be possible, with pharmacological stimulation of BAT thermogenesis in obese patients, to increase the energy expenditure to reduce body weight. Additionally, a better comprehension of the inhibitory regulation of BAT thermogenesis, could contribute to the discovery of novel pharmacological approaches to block cold-defensive BAT thermogenesis, which would be useful to induce therapeutic hypothermia or to treat intractable fevers. Centrally-acting drugs interacting with the A1 adenosine receptor or with the alpha2 adrenergic receptor may be applicable for such therapeutic approaches. In conclusion, control of the autonomic regulation of BAT thermogenesis, primarily a thermoregulatory function, could play a significant role in ameliorating pathologies like obesity or high fevers, or for the induction of a therapeutic hypothermic state following myocardial infarction or stroke.

ACKNOWLEDGMENTS

Support of the research contributing to this review: National Institutes of Health NS40987 (Shaun F. Morrison), Collins Medical Trust (Domenico Tupone), American Heart Association (Christopher J. Madden).

REFERENCES

Almeida, M. C., Hew-Butler, T., Soriano, R. N., Rao, S., Wang, W., Wang, J., et al. (2012). Pharmacological blockade of the cold receptor TRPM8 attenuates autonomic and behavioral cold defenses and decreases deep body temperature. *J. Neurosci.* 32, 2086–2099. doi: 10.1523/JNEUROSCI.5606-11.2012

Andrew, D., and Craig, A. D. (2001). Spinothalamic lamina I neurons selectively sensitive to histamine: a central neural pathway for itch. *Nat. Neurosci.* 4, 72–77. doi: 10.1038/82924

Atasoy, D., Betley, J. N., Su, H. H., and Sternson, S. M. (2012). Deconstruction of a neural circuit for hunger. *Nature* 488, 172–177. doi: 10.1038/nature 11270

Bachman, E. S., Dhillon, H., Zhang, C. Y., Cinti, S., Bianco, A. C., Kobilka, B. K., et al. (2002). betaAR signaling required for diet-induced thermogenesis and obesity resistance. *Science* 297, 843–845. doi: 10.1126/science.1073160

Balthasar, N., Dalgaard, L. T., Lee, C. E., Yu, J., Funahashi, H., Williams, T., et al. (2005). Divergence of melanocortin pathways in the control of food intake and energy expenditure. *Cell* 123, 493–505. doi: 10.1016/j.cell.2005.08.035

Bamshad, M., Song, C. K., and Bartness, T. J. (1999). CNS origins of the sympathetic nervous system outflow to brown adipose tissue. *Am. J. Physiol.* 276, R1569–R1578.

Berthoud, H. R., Patterson, L. M., Sutton, G. M., Morrison, C., and Zheng, H. (2005). Orexin inputs to caudal raphe neurons involved in thermal, cardiovascular, and gastrointestinal regulation. *Histochem. Cell Biol.* 123, 147–156. doi: 10.1007/s00418-005-0761-x

Blouet, C., and Schwartz, G. J. (2012). Duodenal lipid sensing activates vagal afferents to regulate non-shivering brown fat thermogenesis in rats. *PLoS ONE* 7:e51898. doi: 10.1371/journal.pone.0051898

Boulant, J. A. (2006). Counterpoint: heat-induced membrane depolarization of hypothalamic neurons: an unlikely mechanism of central thermosensitivity. *Am. J. Physiol. Regul. Integr. Comp. Physiol.* 290, R1481–R1484; discussion: R1484. doi: 10.1152/ajpregu.00655.2005

Boulant, J. A., and Hardy, J. D. (1974). The effect of spinal and skin temperatures on the firing rate and thermosensitivity of preoptic neurones. *J. Physiol.* 240, 639–660.

Bratincsak, A., and Palkovits, M. (2004). Activation of brain areas in rat following warm and cold ambient exposure. *Neuroscience* 127, 385–397. doi: 10.1016/j.neuroscience.2004.05.016

Buchanan, T. A., Cane, P., Eng, C. C., Sipos, G. F., and Lee, C. (1991). Hypothermia is critical for survival during prolonged insulin-induced hypoglycemia in rats. *Metabolism* 40, 330–334. doi: 10.1016/0026-0495(91)90118-G

Caldeira, J. C., Franci, C. R., and Pela, I. R. (1998). Bilateral lesion of hypothalamic paraventricular nucleus abolishes fever induced by endotoxin and bradykinin in rats. *Ann. N. Y. Acad. Sci.* 856, 294–297. doi: 10.1111/j.1749-6632.1998.tb08342.x

Cannon, B., and Nedergaard, J. (2004). Brown adipose tissue: function and physiological significance. *Physiol. Rev.* 84, 277–359. doi: 10.1152/physrev.00015.2003

Cano, G., Passerin, A. M., Schiltz, J. C., Card, J. P., Morrison, S. F., and Sved, A. F. (2003). Anatomical substrates for the central control of sympathetic outflow to interscapular adipose tissue during cold exposure. *J. Comp. Neurol.* 460, 303–326. doi: 10.1002/cne.10643

Cao, W. H., Fan, W., and Morrison, S. F. (2004). Medullary pathways mediating specific sympathetic responses to activation of dorsomedial hypothalamus. *Neuroscience* 126, 229–240. doi: 10.1016/j.neuroscience.2004.03.013

Cao, W. H., Madden, C. J., and Morrison, S. F. (2010). Inhibition of brown adipose tissue thermogenesis by neurons in the ventrolateral medulla and in the nucleus tractus solitarius. *Am. J. Physiol. Regul. Integr. Comp. Physiol.* 299, R277–R290. doi: 10.1152/ajpregu.00039.2010

Cao, W. H., and Morrison, S. F. (2005). Brown adipose tissue thermogenesis contributes to fentanyl-evoked hyperthermia. *Am. J. Physiol. Regul. Integr. Comp. Physiol.* 288, R723–R732. doi: 10.1152/ajpregu.00669.2004

Cao, W. H., and Morrison, S. F. (2006). Glutamate receptors in the raphe pallidus mediate brown adipose tissue thermogenesis evoked by activation of dorsomedial hypothalamic neurons. *Neuropharmacology* 51, 426–437. doi: 10.1016/j.neuropharm.2006.03.031

Cerri, M., Mastrotto, M., Tupone, D., Martelli, D., Luppi, M., Perez, E., et al. (2013). The inhibition of neurons in the central nervous pathways for thermoregulatory cold defense induces a suspended animation state in the rat. *J. Neurosci.* 33, 2984–2993. doi: 10.1523/JNEUROSCI.3596-12.2013

Cerri, M., and Morrison, S. F. (2005). Activation of lateral hypothalamic neurons stimulates brown adipose tissue thermogenesis. *Neuroscience* 135, 627–638. doi: 10.1016/j.neuroscience.2005.06.039

Cerri, M., and Morrison, S. F. (2006). Corticotropin releasing factor increases in brown adipose tissue thermogenesis and heart rate through dorsomedial hypothalamus and medullary raphe pallidus. *Neuroscience* 140, 711–721. doi: 10.1016/j.neuroscience.2006.02.027

Chen, X. M., Nishi, M., Taniguchi, A., Nagashima, K., Shibata, M., and Kanosue, K. (2002). The caudal periaqueductal gray participates in the activation of brown adipose tissue in rats. *Neurosci. Lett.* 331, 17–20. doi: 10.1016/S0304-3940(02)00757-7

Christensen, C. R., Clark, P. B., and Morton, K. A. (2006). Reversal of hypermetabolic brown adipose tissue in F-18 FDG PET imaging. *Clin. Nucl. Med.* 31, 193–196. doi: 10.1097/01.rlu.0000204199.33136.05

Cowley, M. A., Pronchuk, N., Fan, W., Dinulescu, D. M., Colmers, W. F., and Cone, R. D. (1999). Integration of NPY, AGRP, and melanocortin signals in the hypothalamic paraventricular nucleus: evidence of a cellular basis for the adipostat. *Neuron* 24, 155–163. doi: 10.1016/S0896-6273(00)80829-6

Craig, A. D. (2002). How do you feel? Interoception: the sense of the physiological condition of the body. *Nat. Rev. Neurosci.* 3, 655–666. doi: 10.1038/nrn894

Craig, A. D., Krout, K., and Andrew, D. (2001). Quantitative response characteristics of thermoreceptive and nociceptive lamina I spinothalamic neurons in the cat. *J. Neurophysiol.* 86, 1459–1480.

Cypess, A. M., Lehman, S., Williams, G., Tal, I., Rodman, D., Goldfine, A. B., et al. (2009). Identification and importance of brown adipose tissue in adult humans. *N. Engl. J. Med.* 360, 1509–1517. doi: 10.1056/NEJMoa0810780

De Lecea, L., Kilduff, T. S., Peyron, C., Gao, X., Foye, P. E., Danielson, P. E., et al. (1998). The hypocretins: hypothalamus-specific peptides with neuroexcitatory activity. *Proc. Natl. Acad. Sci. U.S.A.* 95, 322–327. doi: 10.1073/pnas.95.1.322

De Menezes, R. C., Zaretsky, D. V., Fontes, M. A., and Dimicco, J. A. (2009). Cardiovascular and thermal responses evoked from the periaqueductal grey require neuronal activity in the hypothalamus. *J. Physiol.* 587, 1201–1215. doi: 10.1113/jphysiol.2008.161463

Deuchars, S. A., Spyer, K. M., and Gilbey, M. P. (1997). Stimulation within the rostral ventrolateral medulla can evoke monosynaptic GABAergic IPSPs in sympathetic preganglionic neurons *in vitro*. *J. Neurophysiol.* 77, 229–235.

Dimicco, J. A., and Zaretsky, D. V. (2007). The dorsomedial hypothalamus: a new player in thermoregulation. *Am. J. Physiol. Regul. Integr. Comp. Physiol.* 292, R47–R63. doi: 10.1152/ajpregu.00498.2006

Dimitrov, E. L., Kim, Y. Y., and Usdin, T. B. (2011). Regulation of hypothalamic signaling by tuberoinfundibular peptide of 39 residues is critical for the response to cold: a novel peptidergic mechanism of thermoregulation. *J. Neurosci.* 31, 18166–18179. doi: 10.1523/jneurosci.2619-11.2011

Egawa, M., Yoshimatsu, H., and Bray, G. A. (1989). Effects of 2-deoxy-D-glucose on sympathetic nerve activity to interscapular brown adipose tissue. *Am. J. Physiol.* 257, R1377–R1385.

Egawa, M., Yoshimatsu, H., and Bray, G. A. (1991). Neuropeptide Y suppresses sympathetic activity to interscapular brown adipose tissue in rats. *Am. J. Physiol.* 260, R328–R334.

Elmquist, J. K., Scammell, T. E., and Saper, C. B. (1997). Mechanisms of CNS response to systemic immune challenge: the febrile response. *Trends Neurosci.* 20, 565–570. doi: 10.1016/S0166-2236(97)01138-7

Enriori, P. J., Sinnayah, P., Simonds, S. E., Garcia Rudaz, C., and Cowley, M. A. (2011). Leptin action in the dorsomedial hypothalamus increases sympathetic tone to brown adipose tissue in spite of systemic leptin resistance. *J. Neurosci.* 31, 12189–12197. doi: 10.1523/JNEUROSCI.2336-11.2011

Fan, W., Morrison, S. F., Cao, W. H., and Yu, P. (2007). Thermogenesis activated by central melanocortin signaling is dependent on neurons in the rostral raphe pallidus (rRPa) area. *Brain Res.* 1179, 61–69. doi: 10.1016/j.brainres.2007.04.006

Feldmann, H. M., Golozoubova, V., Cannon, B., and Nedergaard, J. (2009). UCP1 ablation induces obesity and abolishes diet-induced thermogenesis in mice exempt from thermal stress by living at thermoneutrality. *Cell Metab.* 9, 203–209. doi: 10.1016/j.cmet.2008.12.014

Grill, H. J., and Hayes, M. R. (2012). Hindbrain neurons as an essential hub in the neuroanatomically distributed control of energy balance. *Cell Metab.* 16, 296–309. doi: 10.1016/j.cmet.2012.06.015

Guerra, C., Koza, R. A., Yamashita, H., Walsh, K., and Kozak, L. P. (1998). Emergence of brown adipocytes in white fat in mice is under genetic control.

Effects on body weight and adiposity. *J. Clin. Invest.* 102, 412–420. doi: 10.1172/JCI3155

Guyenet, P. G. (2000). Neural structures that mediate sympathoexcitation during hypoxia. *Respir. Physiol.* 121, 147–162. doi: 10.1016/S0034-5687(00)00125-0

Hamann, A., Flier, J. S., and Lowell, B. B. (1996). Decreased brown fat markedly enhances susceptibility to diet-induced obesity, diabetes, and hyperlipidemia. *Endocrinology* 137, 21–29. doi: 10.1210/endo.137.1.8536614

Hara, J., Beuckmann, C. T., Nambu, T., Willie, J. T., Chemelli, R. M., Sinton, C. M., et al. (2001). Genetic ablation of orexin neurons in mice results in narcolepsy, hypophagia, and obesity. *Neuron* 30, 345–354. doi: 10.1016/S0896-6273(01)00293-8

Hara, J., Yanagisawa, M., and Sakurai, T. (2005). Difference in obesity phenotype between orexin-knockout mice and orexin neuron-deficient mice with same genetic background and environmental conditions. *Neurosci. Lett.* 380, 239–242. doi: 10.1016/j.neulet.2005.01.046

Hemmen, T. M., and Lyden, P. D. (2009). Hypothermia after acute ischemic stroke. *J. Neurotrauma* 26, 387–391. doi: 10.1089/neu.2008.0574

Hensel, H., and Kenshalo, D. R. (1969). Warm receptors in the nasal region of cats. *J. Physiol.* 204, 99–112.

Hermann, D. M., Luppi, P. H., Peyron, C., Hinckel, P., and Jouvet, M. (1997). Afferent projections to the rat nuclei raphe magnus, raphe pallidus and reticularis gigantocellularis pars alpha demonstrated by iontophoretic application of choleratoxin (subunit b). *J. Chem. Neuroanat.* 13, 1–21. doi: 10.1016/S0891-0618(97)00019-7

Hermann, G. E., Barnes, M. J., and Rogers, R. C. (2006). Leptin and thyrotropin-releasing hormone: cooperative action in the hindbrain to activate brown adipose thermogenesis. *Brain Res.* 1117, 118–124. doi: 10.1016/j.brainres.2006.08.018

Hodges, M. R., Tattersall, G. J., Harris, M. B., McEvoy, S. D., Richerson, D. N., Deneris, E. S., et al. (2008). Defects in breathing and thermoregulation in mice with near-complete absence of central serotonin neurons. *J. Neurosci.* 28, 2495–2505. doi: 10.1523/JNEUROSCI.4729-07.2008

Horn, T., Wilkinson, M. F., Landgraf, R., and Pittman, Q. J. (1994). Reduced febrile responses to pyrogens after lesions of the hypothalamic paraventricular nucleus. *Am. J. Physiol.* 267, R323–R328.

Hylden, J. L., Anton, F., and Nahin, R. L. (1989). Spinal lamina I projection neurons in the rat: collateral innervation of parabrachial area and thalamus. *Neuroscience* 28, 27–37. doi: 10.1016/0306-4522(89)90229-7

Kong, D., Tong, Q., Ye, C., Koda, S., Fuller, P. M., Krashes, M. J., et al. (2012). GABAergic RIP-Cre neurons in the arcuate nucleus selectively regulate energy expenditure. *Cell* 151, 645–657. doi: 10.1016/j.cell.2012.09.020

Kontani, Y., Wang, Y., Kimura, K., Inokuma, K. I., Saito, M., Suzuki-Miura, T., et al. (2005). UCP1 deficiency increases susceptibility to diet-induced obesity with age. *Aging Cell* 4, 147–155. doi: 10.1111/j.1474-9726.2005.00157.x

Kopecky, J., Clarke, G., Enerback, S., Spiegelman, B., and Kozak, L. P. (1995). Expression of the mitochondrial uncoupling protein gene from the aP2 gene promoter prevents genetic obesity. *J. Clin. Invest.* 96, 2914–2923. doi: 10.1172/JCI118363

Kopecky, J., Rossmeisl, M., Hodny, Z., Syrovy, I., Horakova, M., and Kolarova, P. (1996). Reduction of dietary obesity in aP2-Ucp transgenic mice: mechanism and adipose tissue morphology. *Am. J. Physiol.* 270, E776–E786.

Lazarus, M., Yoshida, K., Coppari, R., Bass, C. E., Mochizuki, T., Lowell, B. B., et al. (2007). EP3 prostaglandin receptors in the median preoptic nucleus are critical for fever responses. *Nat. Neurosci.* 10, 1131–1133. doi: 10.1038/nn1949

Li, J., Xiong, K., Pang, Y., Dong, Y., Kaneko, T., and Mizuno, N. (2006). Medullary dorsal horn neurons providing axons to both the parabrachial nucleus and thalamus. *J. Comp. Neurol.* 498, 539–551. doi: 10.1002/cne.21068

Lowell, B. B., S-Susulic, V., Hamann, A., Lawitts, J. A., Himms-Hagen, J., Boyer, B. B., et al. (1993). Development of obesity in transgenic mice after genetic ablation of brown adipose tissue. *Nature* 366, 740–742. doi: 10.1038/366740a0

Lu, J., Zhang, Y. H., Chou, T. C., Gaus, S. E., Elmquist, J. K., Shiromani, P., et al. (2001). Contrasting effects of ibotenate lesions of the paraventricular nucleus and subparaventricular zone on sleep-wake cycle and temperature regulation. *J. Neurosci.* 21, 4864–4874.

Lundius, E. G., Sanchez-Alavez, M., Ghochani, Y., Klaus, J., and Tabarean, I. V. (2010). Histamine influences body temperature by acting at H1 and H3 receptors on distinct populations of preoptic neurons. *J. Neurosci.* 30, 4369–4381. doi: 10.1523/JNEUROSCI.0378-10.2010

Madden, C. J. (2012). Glucoprivation in the ventrolateral medulla decreases brown adipose tissue sympathetic nerve activity by decreasing the activity of neurons in raphe pallidus. *Am. J. Physiol. Regul. Integr. Comp. Physiol.* 302, R224–R232. doi: 10.1152/ajpregu.00449.2011

Madden, C. J., and Morrison, S. F. (2003). Excitatory amino acid receptor activation in the raphe pallidus area mediates prostaglandin-evoked thermogenesis. *Neuroscience* 122, 5–15. doi: 10.1016/S0306-4522(03)00527-X

Madden, C. J., and Morrison, S. F. (2004). Excitatory amino acid receptors in the dorsomedial hypothalamus mediate prostaglandin-evoked thermogenesis in brown adipose tissue. *Am. J. Physiol. Regul. Integr. Comp. Physiol.* 286, R320–R325. doi: 10.1152/ajpregu.00515.2003

Madden, C. J., and Morrison, S. F. (2005). Hypoxic activation of arterial chemoreceptors inhibits sympathetic outflow to brown adipose tissue in rats. *J. Physiol.* 566, 559–573. doi: 10.1113/jphysiol.2005.086322

Madden, C. J., and Morrison, S. F. (2006). Serotonin potentiates sympathetic responses evoked by spinal NMDA. *J. Physiol.* 577, 525–537. doi: 10.1113/jphysiol.2006.116574

Madden, C. J., and Morrison, S. F. (2008). Brown adipose tissue sympathetic nerve activity is potentiated by activation of 5-hydroxytryptamine (5-HT)(1A)/5-HT(7) receptors in the rat spinal cord. *Neuropharmacology* 54, 487–496. doi: 10.1016/j.neuropharm.2007.10.019

Madden, C. J., and Morrison, S. F. (2009). Neurons in the paraventricular nucleus of the hypothalamus inhibit sympathetic outflow to brown adipose tissue. *Am. J. Physiol. Regul. Integr. Comp. Physiol.* 296, R831–R843. doi: 10.1152/ajpregu.91007.2008

Madden, C. J., and Morrison, S. F. (2010). Endogenous activation of spinal 5-hydroxytryptamine (5-HT) receptors contributes to the thermoregulatory activation of brown adipose tissue. *Am. J. Physiol. Regul. Integr. Comp. Physiol.* 298, R776–R783. doi: 10.1152/ajpregu.00614.2009

Madden, C. J., Stocker, S. D., and Sved, A. F. (2006). Attenuation of homeostatic responses to hypotension and glucoprivation after destruction of catecholaminergic rostral ventrolateral medulla neurons. *Am. J. Physiol. Regul. Integr. Comp. Physiol.* 291, R751–R759. doi: 10.1152/ajpregu.00800.2005

Madden, C. J., Tupone, D., Cano, G., and Morrison, S. F. (2013). alpha2 Adrenergic receptor-mediated inhibition of thermogenesis. *J. Neurosci.* 33, 2017–2028. doi: 10.1523/JNEUROSCI.4701-12.2013

Mark, A. L., Agassandian, K., Morgan, D. A., Liu, X., Cassell, M. D., and Rahmouni, K. (2009). Leptin signaling in the nucleus tractus solitarii increases sympathetic nerve activity to the kidney. *Hypertension* 53, 375–380. doi: 10.1161/HYPERTENSIONAHA.108.124255

Martin-Cora, F. J., Fornal, C. A., Metzler, C. W., and Jacobs, B. L. (2000). Single-unit responses of serotonergic medullary and pontine raphe neurons to environmental cooling in freely moving cats. *Neuroscience* 98, 301–309. doi: 10.1016/S0306-4522(00)00133-0

Matsumura, K., Cao, C., Ozaki, M., Morii, H., Nakadate, K., and Watanabe, Y. (1998). Brain endothelial cells express cyclooxygenase-2 during lipopolysaccharide-induced fever: light and electron microscopic immunocytochemical studies. *J. Neurosci.* 18, 6279–6289.

Matthias, A., Ohlson, K. B., Fredriksson, J. M., Jacobsson, A., Nedergaard, J., and Cannon, B. (2000). Thermogenic responses in brown fat cells are fully UCP1-dependent. UCP2 or UCP3 do not substitute for UCP1 in adrenergically or fatty scid-induced thermogenesis. *J. Biol. Chem.* 275, 25073–25081. doi: 10.1074/jbc.M000547200

McKemy, D. D., Neuhausser, W. M., and Julius, D. (2002). Identification of a cold receptor reveals a general role for TRP channels in thermosensation. *Nature* 416, 52–58. doi: 10.1038/nature719

Morrison, S. F. (1999). RVLM and raphe differentially regulate sympathetic outflows to splanchnic and brown adipose tissue. *Am. J. Physiol.* 276, R962–R973.

Morrison, S. F. (2004). Activation of 5-HT1A receptors in raphe pallidus inhibits leptin-evoked increases in brown adipose tissue thermogenesis. *Am. J. Physiol. Regul. Integr. Comp. Physiol.* 286, R832–R837. doi: 10.1152/ajpregu.00678.2003

Morrison, S. F., Cao, W.-H., and Madden, C. J. (2004). Dorsomedial hypothalamic and brainstem pathways controlling thermogenesis in brown adipose tissue. *J. Ther. Biol.* 29, 333–337. doi: 10.1016/j.jtherbio.2004.08.006

Morrison, S. F., Madden, C. J., and Tupone, D. (2012). Central control of brown adipose tissue thermogenesis. *Front. Endocrinol. (Lausanne)* 3:5. doi: 10.3389/fendo.2012.00005

Muzzi, M., Blasi, F., Masi, A., Coppi, E., Traini, C., Felici, R., et al. (2012). Neurological basis of AMP-dependent thermoregulation and its relevance to central and peripheral hyperthermia. *J. Cereb. Blood Flow Metab.* 33, 183–190. doi: 10.1038/jcbfm.2012.157

Nakamura, K., Kaneko, T., Yamashita, Y., Hasegawa, H., Katoh, H., Ichikawa, A., et al. (1999). Immunocytochemical localization of prostaglandin EP3 receptor in the rat hypothalamus. *Neurosci. Lett.* 260, 117–120. doi: 10.1016/S0304-3940(98)00962-8

Nakamura, K., Kaneko, T., Yamashita, Y., Hasegawa, H., Katoh, H., and Negishi, M. (2000). Immunohistochemical localization of prostaglandin EP3 receptor in the rat nervous system. *J. Comp. Neurol.* 421, 543–569. doi: 10.1002/(SICI)1096-9861(20000612)421:4%3C543::AID-CNE6%3E3.0.CO;2-3

Nakamura, K., Matsumura, K., Hubschle, T., Nakamura, Y., Hioki, H., Fujiyama, F., et al. (2004). Identification of sympathetic premotor neurons in medullary raphe regions mediating fever and other thermoregulatory functions. *J. Neurosci.* 24, 5370–5380. doi: 10.1523/JNEUROSCI.1219-04.2004

Nakamura, K., Matsumura, K., Kaneko, T., Kobayashi, S., Katoh, H., and Negishi, M. (2002). The rostral raphe pallidus nucleus mediates pyrogenic transmission from the preoptic area. *J. Neurosci.* 22, 4600–4610.

Nakamura, K., and Morrison, S. F. (2007). Central efferent pathways mediating skin cooling-evoked sympathetic thermogenesis in brown adipose tissue. *Am. J. Physiol. Regul. Integr. Comp. Physiol.* 292, R127–R136. doi: 10.1152/ajpregu.00427.2006

Nakamura, K., and Morrison, S. F. (2008a). Preoptic mechanism for cold-defensive responses to skin cooling. *J. Physiol.* 586, 2611–2620. doi: 10.1113/jphysiol.2008.152686

Nakamura, K., and Morrison, S. F. (2008b). A thermosensory pathway that controls body temperature. *Nat. Neurosci.* 11, 62–71. doi: 10.1038/nn2027

Nakamura, K., and Morrison, S. F. (2010). A thermosensory pathway mediating heat-defense responses. *Proc. Natl. Acad. Sci. U.S.A.* 107, 8848–8853. doi: 10.1073/pnas.0913358107

Nakamura, K., and Morrison, S. F. (2011). Central efferent pathways for cold-defensive and febrile shivering. *J. Physiol.* 589, 3641–3658. doi: 10.1113/jphysiol.2011.210047

Nakamura, Y., Nakamura, K., Matsumura, K., Kobayashi, S., Kaneko, T., and Morrison, S. F. (2005). Direct pyrogenic input from prostaglandin EP3 receptor-expressing preoptic neurons to the dorsomedial hypothalamus. *Eur. J. Neurosci.* 22, 3137–3146. doi: 10.1111/j.1460-9568.2005.04515.x

Nakamura, Y., Nakamura, K., and Morrison, S. F. (2009). Different populations of prostaglandin EP3 receptor-expressing preoptic neurons project to two fever-mediating sympathoexcitatory brain regions. *Neuroscience* 161, 614–620. doi: 10.1016/j.neuroscience.2009.03.041

Nakayama, T., Hammel, H., Hardy, J., and Eisenman, J. (1963). Thermal stimulation of electrical activity of single units of the preoptic region. *Am. J. Physiol.* 204, 1122–1126.

Narumiya, S., Sugimoto, Y., and Ushikubi, F. (1999). Prostanoid receptors: structures, properties, and functions. *Physiol. Rev.* 79, 1193–1226.

Nedergaard, J., Bengtsson, T., and Cannon, B. (2010). Three years with adult human brown adipose tissue. *Ann. N. Y. Acad. Sci.* 1212, E20–E36. doi: 10.1111/j.1749-6632.2010.05905.x

Oberkofler, H., Dallinger, G., Liu, Y. M., Hell, E., Krempler, F., and Patsch, W. (1997). Uncoupling protein gene: quantification of expression levels in adipose tissues of obese and non-obese humans. *J. Lipid Res.* 38, 2125–2133.

Oldfield, B. J., Giles, M. E., Watson, A., Anderson, C., Colvill, L. M., and McKinley, M. J. (2002). The neurochemical characterisation of hypothalamic pathways projecting polysynaptically to brown adipose tissue in the rat. *Neuroscience* 110, 515–526. doi: 10.1016/S0306-4522(01)00555-3

Ootsuka, Y., Blessing, W. W., Steiner, A. A., and Romanovsky, A. A. (2008). Fever response to intravenous prostaglandin E2 is mediated by the brain but does not require afferent vagal signaling. *Am. J. Physiol. Regul. Integr. Comp. Physiol.* 294, R1294–R1303. doi: 10.1152/ajpregu.00709.2007

Perez-Leighton, C. E., Billington, C. J., and Kotz, C. M. (2013). Orexin modulation of adipose tissue. *Biochim. Biophys. Acta*. doi: 10.1016/j.bbadis.2013.06.007

Peyron, C., Tighe, D. K., Van Den Pol, A. N., De Lecea, L., Heller, H. C., Sutcliffe, J. G., et al. (1998). Neurons containing hypocretin (orexin) project to multiple neuronal systems. *J. Neurosci.* 18, 9996–10015.

Plazzi, G., Moghadam, K. K., Maggi, L. S., Donadio, V., Vetrugno, R., Liguori, R., et al. (2011). Autonomic disturbances in narcolepsy. *Sleep Med. Rev.* 15, 187–196. doi: 10.1016/j.smrv.2010.05.002

Pogorzala, L. A., Mishra, S. K., and Hoon, M. A. (2013). The cellular code for mammalian thermosensation. *J. Neurosci.* 33, 5533–5541. doi: 10.1523/jneurosci.5788-12.2013

Rathner, J. A., and Morrison, S. F. (2006). Rostral ventromedial periaqueductal gray: a source of inhibition of the sympathetic outflow to brown adipose tissue. *Brain Res.* 1077, 99–107. doi: 10.1016/j.brainres.2006.01.035

Rising, R., Fontvieille, A. M., Larson, D. E., Spraul, M., Bogardus, C., and Ravussin, E. (1995). Racial difference in body core temperature between Pima Indian and Caucasian men. *Int. J. Obes. Relat. Metab. Disord.* 19, 1–5.

Ritter, S., Bugarith, K., and Dinh, T. T. (2001). Immunotoxic destruction of distinct catecholamine subgroups produces selective impairment of glucoregulatory responses and neuronal activation. *J. Comp. Neurol.* 432, 197–216. doi: 10.1002/cne.1097

Rogers, R. C., Barnes, M. J., and Hermann, G. E. (2009). Leptin "gates" thermogenic action of thyrotropin-releasing hormone in the hindbrain. *Brain Res.* 1295, 135–141. doi: 10.1016/j.brainres.2009.07.063

Rothwell, N. J. (1988). Central effects of TNF alpha on thermogenesis and fever in the rat. *Biosci. Rep.* 8, 345–352. doi: 10.1007/BF01115225

Rothwell, N. J. (1989). CRF is involved in the pyrogenic and thermogenic effects of interleukin 1 beta in the rat. *Am. J. Physiol.* 256, E111–E115.

Rothwell, N. J., and Stock, M. J. (1982). Effect of chronic food restriction on energy balance, thermogenic capacity, and brown-adipose-tissue activity in the rat. *Biosci. Rep.* 2, 543–549. doi: 10.1007/BF01314214

Rousseau, C., Bourbouloux, E., Campion, L., Fleury, N., Bridji, B., Chatal, J. F., et al. (2006). Brown fat in breast cancer patients: analysis of serial (18)F-FDG PET/CT scans. *Eur. J. Nucl. Med. Mol. Imaging* 33, 785–791. doi: 10.1007/s00259-006-0066-x

Saito, M., Okamatsu-Ogura, Y., Matsushita, M., Watanabe, K., Yoneshiro, T., Nio-Kobayashi, J., et al. (2009). High incidence of metabolically active brown adipose tissue in healthy adult humans: effects of cold exposure and adiposity. *Diabetes* 58, 1526–1531. doi: 10.2337/db09-0530

Sakurai, T., Amemiya, A., Ishii, M., Matsuzaki, I., Chemelli, R. M., Tanaka, H., et al. (1998). Orexins and orexin receptors: a family of hypothalamic neuropeptides and G protein-coupled receptors that regulate feeding behavior. *Cell* 92, 573–585. doi: 10.1016/S0092-8674(00)80949-6

Samuels, B. C., Zaretsky, D. V., and Dimicco, J. A. (2002). Tachycardia evoked by disinhibition of the dorsomedial hypothalamus in rats is mediated through medullary raphe. *J. Physiol.* 538, 941–946. doi: 10.1113/jphysiol.2001.013302

Sarkar, S., Zaretskaia, M. V., Zaretsky, D. V., Moreno, M., and Dimicco, J. A. (2007). Stress- and lipopolysaccharide-induced c-fos expression and nNOS in hypothalamic neurons projecting to medullary raphe in rats: a triple immunofluorescent labeling study. *Eur. J. Neurosci.* 26, 2228–2238. doi: 10.1111/j.1460-9568.2007.05843.x

Sasek, C. A., Wessendorf, M. W., and Helke, C. J. (1990). Evidence for co-existence of thyrotropin-releasing hormone, substance P and serotonin in ventral medullary neurons that project to the intermediolateral cell column in the rat. *Neuroscience* 35, 105–119. doi: 10.1016/0306-4522(90)90125-N

Scammell, T. E., Elmquist, J. K., Griffin, J. D., and Saper, C. B. (1996). Ventromedial preoptic prostaglandin E2 activates fever-producing autonomic pathways. *J. Neurosci.* 16, 6246–6254.

Schwartz, B. G., Kloner, R. A., Thomas, J. L., Bui, Q., Mayeda, G. S., Burstein, S., et al. (2012). Therapeutic hypothermia for acute myocardial infarction and cardiac arrest. *Am. J. Cardiol.* 110, 461–466. doi: 10.1016/j.amjcard.2012.03.048

Sharpe, A. L., Calderon, A. S., Andrade, M. A., Cunningham, J. T., Mifflin, S. W., and Toney, G. M. (2013). Chronic intermittent hypoxia increases sympathetic control of blood pressure: role of neuronal activity in the hypothalamic paraventricular nucleus. *Am. J. Physiol. Heart Circ. Physiol.* 305, H1772–H1780. doi: 10.1152/ajpheart.00592.2013

Skibicka, K. P., Alhadeff, A. L., Leichner, T. M., and Grill, H. J. (2011). Neural controls of prostaglandin 2 pyrogenic, tachycardic, and anorexic actions are anatomically distributed. *Endocrinology* 152, 2400–2408. doi: 10.1210/en.2010-1309

Skibicka, K. P., and Grill, H. J. (2009). Hypothalamic and hindbrain melanocortin receptors contribute to the feeding, thermogenic, and cardiovascular

action of melanocortins. *Endocrinology* 150, 5351–5361. doi: 10.1210/en.2009-0804

Song, C. K., Vaughan, C. H., Keen-Rhinehart, E., Harris, R. B., Richard, D., and Bartness, T. J. (2008). Melanocortin-4 receptor mRNA expressed in sympathetic outflow neurons to brown adipose tissue: neuroanatomical and functional evidence. *Am. J. Physiol. Regul. Integr. Comp. Physiol.* 295, R417–R428. doi: 10.1152/ajpregu.00174.2008

Stanford, K. I., Middelbeek, R. J., Townsend, K. L., An, D., Nygaard, E. B., Hitchcox, K. M., et al. (2013). Brown adipose tissue regulates glucose homeostasis and insulin sensitivity. *J. Clin. Invest.* 123, 215–223. doi: 10.1172/JCI62308

Stornetta, R. L., McQuiston, T. J., and Guyenet, P. G. (2004). GABAergic and glycinergic presympathetic neurons of rat medulla oblongata identified by retrograde transport of pseudorabies virus and in situ hybridization. *J. Comp. Neurol.* 479, 257–270. doi: 10.1002/cne.20332

Stornetta, R. L., Rosin, D. L., Simmons, J. R., McQuiston, T. J., Vujovic, N., Weston, M. C., et al. (2005). Coexpression of vesicular glutamate transporter-3 and gamma-aminobutyric acidergic markers in rat rostral medullary raphe and intermediolateral cell column. *J. Comp. Neurol.* 492, 477–494. doi: 10.1002/cne.20742

Takahashi, Y., Zhang, W., Sameshima, K., Kuroki, C., Matsumoto, A., Sunanaga, J., et al. (2013). Orexin neurons are indispensable for prostaglandin E2-induced fever and defence against environmental cooling in mice. *J. Physiol*. 591, 5623–5643. doi: 10.1113/jphysiol.2013.261271

Tsukita, S., Yamada, T., Uno, K., Takahashi, K., Kaneko, K., Ishigaki, Y., et al. (2012). Hepatic glucokinase modulates obesity predisposition by regulating BAT thermogenesis via neural signals. *Cell Metab.* 16, 825–832. doi: 10.1016/j.cmet.2012.11.006

Tupone, D., Madden, C. J., Cano, G., and Morrison, S. F. (2011). An orexinergic projection from perifornical hypothalamus to raphe pallidus increases rat brown adipose tissue thermogenesis. *J. Neurosci.* 31, 15944–15955. doi: 10.1523/JNEUROSCI.3909-11.2011

Tupone, D., Madden, C. J., and Morrison, S. F. (2013a). Central activation of the A1 adenosine receptor (A1AR) induces a hypothermic, torpor-like state in the rat. *J. Neurosci.* 33, 14512–14525. doi: 10.1523/JNEUROSCI.1980-13.2013

Tupone, D., Madden, C. J., and Morrison, S. F. (2013b). Highlights in basic autonomic neurosciences: central adenosine A1 receptor - the key to a hypometabolic state and therapeutic hypothermia? *Auton. Neurosci.* 176, 1–2. doi: 10.1016/j.autneu.2013.02.004

Van Marken Lichtenbelt, W. D., and Daanen, H. A. (2003). Cold-induced metabolism. *Curr. Opin. Clin. Nutr. Metab. Care* 6, 469–475. doi: 10.1097/01.mco.0000078992.96795.5f

Van Marken Lichtenbelt, W. D., Vanhommerig, J. W., Smulders, N. M., Drossaerts, J. M., Kemerink, G. J., Bouvy, N. D., et al. (2009). Cold-activated brown adipose tissue in healthy men. *N. Engl. J. Med.* 360, 1500–1508. doi: 10.1056/NEJMoa0808718

Virtanen, K. A., Lidell, M. E., Orava, J., Heglind, M., Westergren, R., Niemi, T., et al. (2009). Functional brown adipose tissue in healthy adults. *N. Engl. J. Med.* 360, 1518–1525. doi: 10.1056/NEJMoa0808949

Yamagata, K., Matsumura, K., Inoue, W., Shiraki, T., Suzuki, K., Yasuda, S., et al. (2001). Coexpression of microsomal-type prostaglandin E synthase with cyclooxygenase-2 in brain endothelial cells of rats during endotoxin-induced fever. *J. Neurosci.* 21, 2669–2677.

Yamashita, H., Wang, Z., Wang, Y., Furuyama, T., Kontani, Y., Sato, Y., et al. (2008). Impaired basal thermal homeostasis in rats lacking capsaicin-sensitive peripheral small sensory neurons. *J. Biochem.* 143, 385–393. doi: 10.1093/jb/mvm233

Yoshida, K., Konishi, M., Nagashima, K., Saper, C. B., and Kanosue, K. (2005). Fos activation in hypothalamic neurons during cold or warm exposure: projections to periaqueductal gray matter. *Neuroscience* 133, 1039–1046. doi: 10.1016/j.neuroscience.2005.03.044

Yoshida, K., Li, X., Cano, G., Lazarus, M., and Saper, C. B. (2009). Parallel preoptic pathways for thermoregulation. *J. Neurosci.* 29, 11954–11964. doi: 10.1523/JNEUROSCI.2643-09.2009

Yoshida, K., Nakamura, K., Matsumura, K., Kanosue, K., Konig, M., Thiel, H. J., et al. (2003). Neurons of the rat preoptic area and the raphe pallidus nucleus innervating the brown adipose tissue express the prostaglandin E receptor subtype EP3. *Eur. J. Neurosci.* 18, 1848–1860. doi: 10.1046/j.1460-9568.2003.02919.x

Zampronio, A. R., Souza, G. E., Silva, C. A., Cunha, F. Q., and Ferreira, S. H. (1994). Interleukin-8 induces fever by a prostaglandin-independent mechanism. *Am. J. Physiol.* 266, R1670–R1674.

Zaretskaia, M. V., Zaretsky, D. V., and Dimicco, J. A. (2003). Role of the dorsomedial hypothalamus in thermogenesis and tachycardia caused by microinjection of prostaglandin E2 into the preoptic area in anesthetized rats. *Neurosci. Lett.* 340, 1–4. doi: 10.1016/S0304-3940(03)00047-8

Zaretskaia, M. V., Zaretsky, D. V., Shekhar, A., and Dimicco, J. A. (2002). Chemical stimulation of the dorsomedial hypothalamus evokes non-shivering thermogenesis in anesthetized rats. *Brain Res.* 928, 113–125. doi: 10.1016/S0006-8993(01)03369-8

Zaretsky, D. V., Hunt, J. L., Zaretskaia, M. V., and Dimicco, J. A. (2006). Microinjection of prostaglandin E2 and muscimol into the preoptic area in conscious rats: comparison of effects on plasma adrenocorticotrophic hormone (ACTH), body temperature, locomotor activity, and cardiovascular function. *Neurosci. Lett.* 397, 291–296. doi: 10.1016/j.neulet.2005.12.032

Zaretsky, D. V., Zaretskaia, M. V., and Dimicco, J. A. (2003). Stimulation and blockade of GABAA receptors in the raphe pallidus: effects on body temperature, heart rate, and blood pressure in conscious rats. *Am. J. Physiol. Regul. Integr. Comp. Physiol.* 285, R110–R116. doi: 10.1152/ajpregu.00016.2003

Zhang, Y., Kerman, I. A., Laque, A., Nguyen, P., Faouzi, M., Louis, G. W., et al. (2011). Leptin-receptor-expressing neurons in the dorsomedial hypothalamus and median preoptic area regulate sympathetic brown adipose tissue circuits. *J. Neurosci.* 31, 1873–1884. doi: 10.1523/JNEUROSCI.3223-10.2011

Zhang, Y. H., Lu, J., Elmquist, J. K., and Saper, C. B. (2000). Lipopolysaccharide activates specific populations of hypothalamic and brainstem neurons that project to the spinal cord. *J. Neurosci.* 20, 6578–6586.

Zingaretti, M. C., Crosta, F., Vitali, A., Guerrieri, M., Frontini, A., Cannon, B., et al. (2009). The presence of UCP1 demonstrates that metabolically active adipose tissue in the neck of adult humans truly represents brown adipose tissue. *FASEB J.* 23, 3113–3120. doi: 10.1096/fj.09-133546

Conflict of Interest Statement: The authors declare that the research was conducted in the absence of any commercial or financial relationships that could be construed as a potential conflict of interest.

Received: 05 December 2013; accepted: 20 January 2014; published online: 07 February 2014.

Citation: Tupone D, Madden CJ and Morrison SF (2014) Autonomic regulation of brown adipose tissue thermogenesis in health and disease: potential clinical applications for altering BAT thermogenesis. Front. Neurosci. ***8****:14. doi: 10.3389/fnins.2014.00014*

This article was submitted to Autonomic Neuroscience, a section of the journal Frontiers in Neuroscience.

frontiers in
NEUROSCIENCE

REVIEW ARTICLE
published: 26 February 2014
doi: 10.3389/fnins.2014.00038

Neural pathways that control the glucose counterregulatory response

Anthony J. M. Verberne*, Azadeh Sabetghadam and Willian S. Korim

Clinical Pharmacology and Therapeutics Unit, Department of Medicine, Austin Health Heidelberg, The University of Melbourne, Melbourne, VIC, Australia

Edited by:
Andrea Zsombok, Tulane University, USA

Reviewed by:
Pieter V. Berghe, Center for Gastroenterological Research, Belgium
Kirsteen Browning, Penn State College of Medicine, USA
Vanessa Routh, Rutgers New Jersey Medical School, USA

****Correspondence:***
Anthony J. M. Verberne, Clinical Pharmacology and Therapeutics Unit, Department of Medicine, Austin Health Heidelberg, The University of Melbourne, Melbourne, VIC 3084, Australia
e-mail: antonius@unimelb.edu.au

Glucose is an essential metabolic substrate for all bodily tissues. The brain depends particularly on a constant supply of glucose to satisfy its energy demands. Fortunately, a complex physiological system has evolved to keep blood glucose at a constant level. The consequences of poor glucose homeostasis are well-known: hyperglycemia associated with uncontrolled diabetes can lead to cardiovascular disease, neuropathy and nephropathy, while hypoglycemia can lead to convulsions, loss of consciousness, coma, and even death. The glucose counterregulatory response involves detection of declining plasma glucose levels and secretion of several hormones including glucagon, adrenaline, cortisol, and growth hormone (GH) to orchestrate the recovery from hypoglycemia. Low blood glucose leads to a low brain glucose level that is detected by glucose-sensing neurons located in several brain regions such as the ventromedial hypothalamus, the perifornical region of the lateral hypothalamus, the arcuate nucleus (ARC), and in several hindbrain regions. This review will describe the importance of the glucose counterregulatory system and what is known of the neurocircuitry that underpins it.

Keywords: glucose sensing, glucagon, adrenaline, rostral ventrolateral medulla, perifornical hypothalamus, ventromedial hypothalamus, counterregulation, hypoglycemia

INTRODUCTION

Glucose is a major source of energy for all cells in mammals. In particular, the nervous system requires a continuous supply of glucose to support its energy requirements and maintain metabolic homeostasis. A large proportion of energy provided by glucose is used only to support the neuronal resting membrane potential. In addition, marked regional differences in glucose utilization may be associated with changes in cognitive function even at steady state. As such, multifaceted physiological mechanisms were selected for during the evolution of mammalian species to adjust and maintain blood glucose within a narrow range. By contrast, in Type 1 diabetes, pathological increases in blood glucose, known as hyperglycemia, may lead to adverse, chronic consequences including cardiovascular disease, neuropathy, retinopathy and nephropathy. In Type 1 diabetes, hyperglycemia is treated with insulin to restore normoglycemia. However, diabetic patients may also experience hypoglycemia, as a result of inappropriate doses of insulin. Similarly, ∼30% of patients with advanced Type 2 diabetes treated with hypoglycemic agents can experience hypoglycemia. If severe, hypoglycemia can result in convulsions, loss of consciousness, coma and even death. In order to restore normoglycemia, the body activates a series of defense mechanisms that act in conjunction and are referred to as the "glucose counterregulatory response." The autonomic and neuroendocrine responses associated with the glucose counterregulatory response are usually accompanied by other behaviors such as arousal and feeding.

Although the mechanisms that underpin glucose homeostasis reside partly in the periphery, it is apparent that the central nervous system plays an important role in glucose counterregulation. For instance, adrenaline release in response to hypoglycemia or glucoprivation (local glucose deprivation) is essentially mediated by the sympathetic nervous system. Glucose sensors are distributed throughout several bodily regions and are capable of detecting decreases in glucose levels in the plasma and in the brain extracellular milieu. Activation of some of these sensors results in glucose counterregulation by adjusting the secretion of several hormones. In response to declining plasma glucose there is a decrease in insulin secretion and increases in glucagon, adrenaline, cortisol, and GH secretion. Decreases in glucose levels are detected by glucose-sensing neurons that are found in several brain regions including the ventromedial hypothalamus, the perifornical region of the lateral hypothalamus (PeH), the arcuate nucleus (ARC), as well as in several hindbrain regions and in the periphery e.g., pancreas, carotid body, liver, and gastrointestinal tract. This review addresses the central and peripheral neural pathways involved in blood glucose homeostasis.

GLUCOSE SENSING

GLUCOSE SENSING IN THE PERIPHERY

Apart from glucose-sensing by pancreatic β-cells, which will not be dealt with in this review, peripheral glucose sensing has been demonstrated at several sites including the liver, via the hepatic portal vein, vagal (Adachi, 1981) and sympathetic afferents, intestinal vagal glucose sensors, and possibly the carotid body (**Figure 1**). Hepatic glucose sensors appear to be necessary for expression of the sympathoadrenal response to hypoglycemia (Donovan et al., 1991) and are located close to or in the portal vein. Portal vein denervation blunts the adrenal catecholamine response to slowly-developing hypoglycemia (Hevener et al., 2000). These portal vein sensory afferents contain calcitonic gene-related peptide since they are capsaicin sensitive,

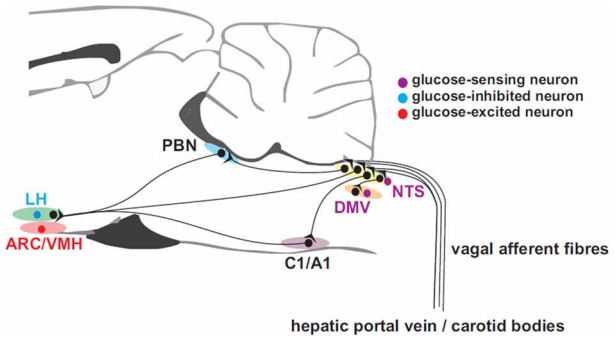

FIGURE 1 | Afferent inputs from the periphery to brain neurons involved in glucose homeostasis. Glucose-sensing vagal and sympathetic afferents arise from the liver and gastrointestinal tract and convey information to the nucleus of the solitary tract (NTS). Unlike their sympathetic sensory counter-parts arising near the portal vein, vagal glucose sensors probably do not contribute the counter-regulatory response. Carotid body glucose sensors may also contribute to the counter-regulatory response. Information is relayed from NTS to the dorsal motor nucleus of the vagus (DMV) which provides parasympathetic drive to the pancreatic islets and via the parabrachial nucleus (PBN) top supramedullary structures. C1 adrenergic neurons with projections ascending to hypothalamic sub-regions such as the arcuate (ARC), lateral (LH), and ventromedial hypothalamic (VMH) nuclei, are involved in the feeding response to insulin-induced hypoglycemia.

but probably do not travel in the vagus (Fujita et al., 2007). The carotid body may also sense glucose (Pardal and Lopez-Barneo, 2002; Conde et al., 2007; Garcia-Fernandez et al., 2007) and contribute to the counterregulatory modulation of glucagon secretion (Koyama et al., 2000). However, its chemosensitivity to CO_2 and O_2 hampers the interpretation of glucose-sensing afferent signals. In man, hyperoxia attenuates the counterregulatory hormonal responses to insulin-induced hypoglycemia (Wehrwein et al., 2010). Nevertheless, the glucose-sensing locus seems to shift from the portal-mesenteric vein to a different site (e.g., central nervous system) during fast developing hypoglycemia (Saberi et al., 2008).

GLUCOSE SENSING IN THE BRAIN

In the central nervous system glucose levels are necessarily maintained at ∼0.4–2.5 mM, in which glucose-sensing involves the interplay of neurons and astrocytes (Marty et al., 2005). Their machinery involves the activity of glucokinase, adenosine triphosphate-sensitive K^+ (K_{ATP}) channels, AMP-activated protein kinase (AMPK), odium-glucose co-transporters, and glucose transporter type 2 (Glut2). The membrane potential of glucosensing neurons changes according to their intracellular metabolism (Oomura et al., 1974; Rowe et al., 1996) and to potentials produced by the interaction of glucose with glucose transporters (O'Malley et al., 2006; Williams et al., 2008). Signaling in glucose-sensing neurons and astrocytes involves glucose uptake by Glut2. Following glycolysis in astrocytes, lactate is produced and released into the extracellular space. Extracellular glucose and lactate from astrocytes are internalized by neurons. Lactate is internalized via monocarboxylate transporter 2 whereas glucose is phosphorylated by glucokinase (Levin et al., 2004) and converted to pyruvate (Lam et al., 2005; Marty et al., 2007).

In glucose excited (GE) neurons (Oomura et al., 1964, 1974), oxidative phosphorylation of glucose and the internalization of lactate by monocarboxylate transporters increases the intracellular ATP/ADP ratio resulting in closure of KATP channels (Lee et al., 1999; Miki et al., 2001). Subsequent membrane depolarization leads to action potential generation resulting in activation of voltage-gated calcium channels and neurotransmitter release (Amoroso et al., 1990; Moriyama et al., 2004). Glucose inhibited (GI) cells (Oomura et al., 1964, 1974) have a glucose-sensing mechanism that involves glucokinase in part. It has been speculated, however, that a rise in the intracellular ATP/ADP ratio results in augmented activity of the Na^+/K^+ ATPase pump (Oomura et al., 1974; Song and Routh, 2005). Alternatively, a reduction in extracellular glucose increases intracellular AMP raising the activity of AMPK (Murphy et al., 2009). This mechanism is potentiated by augmented concentrations of guanylate cyclase driven by nitric oxide, which production is stimulated by AMPK. The increase in concentration of AMPK activates the cystic fibrosis transmembrane conductance regulator, increasing chloride conductance and hyperpolarizing the cell (Murphy et al., 2009).

Nonetheless, the presence of the aforementioned transporters, channels, and kinases does not define a glucose sensing neuron. For instance, in the ventromedial hypothalamic nucleus (VMH) ∼65% of GE and 45% of GI neurons have their responses gated by glucokinase (Kang et al., 2004). In addition, KATP channels are ubiquitous and contribute to diverse physiological functions. Finally, these mechanisms also fail to explain why neurons in the VMH do not express Fos in response to systemic glucoprivation or hypoglycemia (Briski and Sylvester, 2001; Cai et al., 2001). Hence, electrophysiological characterization is the most effective method for identification of glucosensing neurons.

The role of the hindbrain in glucose sensing and control of the counterregulatory response has been reviewed recently by Ritter et al. (2011). It was proposed that the hindbrain contains all of the elements necessary for orchestration of the counterregulatory response. Glucose counterregulatory responses to neuroglucoprivation remained following decerebration, or obstruction of the cerebral aqueduct in rat (DiRocco and Grill, 1979; Ritter et al., 1981). The evidence for this notion is convincing and it is possible that hypothalamic and hindbrain systems operate cooperatively as redundant or "fail-safe" mechanisms. Glucose-sensing neurons have been identified in the dorsal motor nucleus of the vagus (DMV) and the solitary tract nucleus (NTS) (Adachi et al., 1995). However, these sites do not clearly overlap with sites identified using localized glucoprivation (Andrew et al., 2007). Perhaps this is because the relatively large injection volumes that were used in these studies do not allow fine discrimination of the regions that are sensitive to localized neuroglucoprivation. Early studies that support an important role for the hindbrain (DiRocco and Grill, 1979; Ritter et al., 1981) did not unequivocally identify the participation of the sympathoadrenal system. Nevertheless, immunotoxic destruction of the rostral C1 medullospinal neurons in the RVLM eliminates the hyperglycemia, adrenaline secretion and

adrenal medullary Fos expression in response to the glucoprivic agent 2-deoxy-D-glucose (2DG) (Ritter et al., 2001; Madden et al., 2006). This is in agreement with our report that the rostral ventrolateral medulla (RVLM) contains medullospinal neurons that are activated by 2DG and that stimulation of these neurons results in hyperglycemia that is markedly reduced by prior adrenalectomy (Verberne and Sartor, 2010). In the studies that used the immunotoxin it is somewhat surprising that a rise in glucagon secretion did not compensate for the loss of adrenaline secretion in response to 2-DG (Karlsson and Ahren, 1991).

In the forebrain, glucose-sensing occurs primarily in the hypothalamus. A strong case has been made for the importance of the VMH in orchestration of the counterregulatory response to hypoglycemia (Borg et al., 1994, 1995, 1997, 1999; Tong et al., 2007). Glucose-sensing neurons have been identified in the VMH, PeH, and the ARC (Oomura et al., 1974; Burdakov et al., 2005a,b; Routh, 2010). It is likely that these different groups of glucose-sensing neurons subserve different physiological roles that may include the counterregulatory response, energy balance and sensations of hunger.

NEURAL CIRCUITRY INVOLVED IN THE GLUCOSE COUNTERREGULATORY RESPONSE

GLUCOSE CONTROL BY HYPOTHALAMIC NEURONS

The involvement of hypothalamic neurons in blood glucose control has been determined by neuroanatomy, neurochemistry, electrophysiology, and neuropharmacology. Hypoglycemia (Moriguchi et al., 1999; Cai et al., 2001) or systemic glucoprivation (Briski and Sylvester, 2001) excites neurons in the ARC, the paraventricular nucleus (PVN), dorsomedial hypothalamic nucleus (DMH), VMH, and lateral hypothalamus (LH; including the perifornical area), as determined by Fos expression in these neurons. Additionally, some of those neurons were characterized according to their electrophysiological properties in response to changes in glucose levels and glucoprivation (Oomura et al., 1964, 1969, 1974; Burdakov et al., 2005a, 2006; Gonzalez et al., 2008). The majority of the GE neurons are positioned laterally in the hypothalamus, whereas GI neurons are located ventromedially.

Studies using neurotropic viruses have shown that in the perifornical hypothalamus only orexin- and MCH-containing neurons project to adrenal sympathetic premotor neurons in the RVLM (Kerman et al., 2007). In addition, insulin-induced hypoglycemia or neuroglucoprivation induces Fos expression in orexin neurons of the PeH suggesting a possible role in glucose sensing (Moriguchi et al., 1999; Briski and Sylvester, 2001; Cai et al., 2001; Paranjape et al., 2006; Tkacs et al., 2007). On the other hand, an *in vitro* study has shown that GI orexin neurons respond in an identical fashion to both glucose and 2DG through a K^+ channel-mediated mechanism. In addition, these studies showed that this glucose-sensing mechanism is direct and operates independently of glucose metabolism (Gonzalez et al., 2008). This suggests that the orexin neurons are not the principal glucose-sensors involved in the counterregulatory response. This discrepancy may be explained if the site of action of 2DG may not be directly at the PeH orexin neurons but at some other synaptically connected location. In addition, the complexity of hypothalamic interconnections limit the precision with which we can identify glucose-sensing neurons that modulate the counterregulatory response.

HYPOTHALAMIC DESCENDING PATHWAYS

Hypothalamic responses to hypoglycemia occur via connections with sympathetic and parasympathetic efferent neurons in the brainstem and spinal cord (**Figure 2**). Anterograde and retrograde transport studies show that neurons in the PVN and

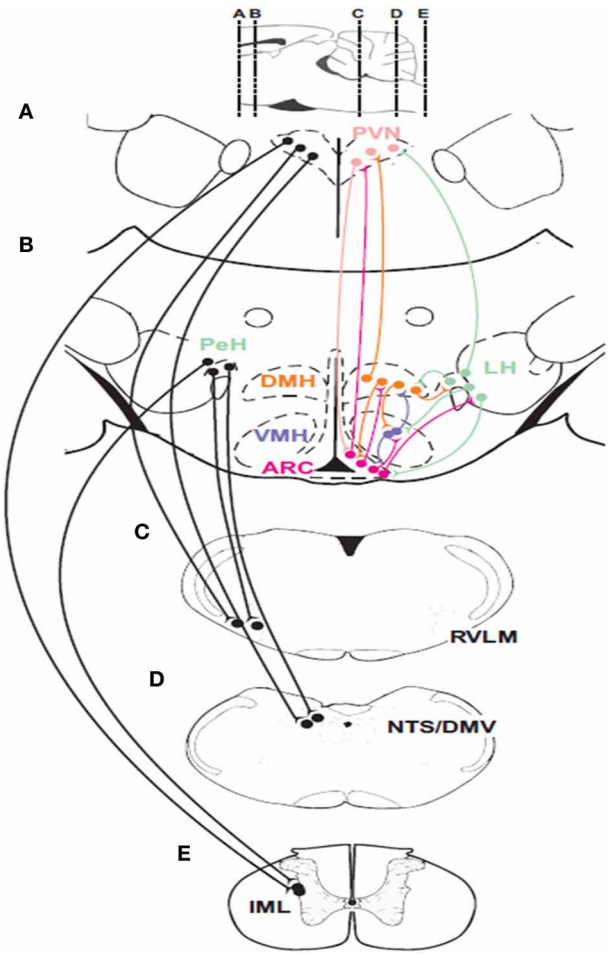

FIGURE 2 | Descending connections and intrahypothalamic pathways involved in glucose homeostasis. Neurons in the paraventricular nucleus of the hypothalamus (PVN) and the perifornical region of the hypothalamus (PeH) have connections with important premotor sympathetic and parasympathetic neuronal groups located in the rostral ventrolateral medulla (RVLM) and the dorsal motor nucleus of the vagus (DMV) as well as to the major sensory relay structure the nucleus of the solitary tract (NTS) and sympathetic preganglionic neurons (SPNs) located in the intermediolateral cell column (IML) of the spinal cord. Glucose-sensing neurons are found in the ARC, the ventromedial hypothalamic nucleus (VMH) and the perifornical region (PeH) of the lateral hypothalamic (LH) area. Parasympathetic efferents to the pancreatic islets can activate insulin and glucagon secretion while C1 neurons in the RVLM provide drive to adrenal SPNs. Parasagittal section at the top of the figure indicates rostrocaudal locations of coronal sections **(A–E)**.

LH project directly to sympathetic preganglionic motor neurons (SPN) in the spinal cord (Saper et al., 1976; Luiten et al., 1985), and catecholaminergic sympathetic premotor neurons (C1) (Ter Horst et al., 1984; Luiten et al., 1985; Allen and Cechetto, 1992; Shafton et al., 1998) in the RVLM. Furthermore, orexinergic and MCH neurons in the LH project to both sympathetic groups (Bittencourt et al., 1992; Peyron et al., 1998; Kerman et al., 2007). However, the evidence for differential sympathetic control of adrenaline and glucagon release is scarce. Although neurotropic viral transport studies (Strack et al., 1989a,b; Kerman et al., 2007) confirm that these pathways are involved in the control of the chromaffin cells, they coincide with the sympathetic pathways that control the pancreas (Jansen et al., 1997). Additionally, the synergism between the PVN and LH extends outside their communication through neural pathways. For example, an increase in circulating adrenaline stimulates corticotropin-releasing factor (CRF) secretion by pituitary corticotrophic cells (Mezey et al., 1984).

Apart from the LH and PVN, medullary sympathetic premotor neurons contribute to glucose homeostasis by driving SPNs that control adrenaline release (Verberne and Sartor, 2010). Studies by Ritter and colleagues have identified the importance of catecholaminergic medullary neurons in mediation of the counterregulatory responses to glucoprivation (Ritter et al., 1998, 2001, 2006; Li et al., 2006, 2009). Systemic glucoprivation increases the firing rate of slow-conducting (<1 m/s) RVLM adrenal premotor medullospinal neurons (Verberne and Sartor, 2010), implying that they are C1 catecholaminergic cells (Schreihofer and Guyenet, 1997). Glucoprivation also elicits phosphorylation (Damanhuri et al., 2012), and expression of Fos (Ritter et al., 1998) and dopamine β-hydroxylase mRNA (Ritter et al., 2006) in RVLM C1 neurons. By contrast, neurotoxic ablation of C1 neurons eliminates the glucose response to the glucoprivic agent 2DG (Ritter et al., 2001; Madden et al., 2006). Interestingly, medullary orexinergic terminals (De Lecea et al., 1998; Peyron et al., 1998) make close appositions with RVLM C1 neurons (Puskas et al., 2010). Presumably, these close appositions arise from the orexin neurons labeled after injection of a neurotropic virus into the adrenal gland (Kerman et al., 2007). A subpopulation of these catecholaminergic neurons also expresses NPY (Li and Ritter, 2004). These neurons are located at the C1/A1 level and project rostrally to the hypothalamus (Verberne et al., 1999; Li and Ritter, 2004; Li et al., 2009) and are probably involved in the feeding response to neuroglucoprivation (Ritter et al., 2001; Li and Ritter, 2004). Finally, RVLM sympathetic premotor neurons make monosynaptic (McAllen et al., 1994; Zagon and Bacon, 1991; Oshima et al., 2008), glutamatergic (Morrison et al., 1989a; Morrison and Cao, 2000) connections with adrenal SPN (Morrison and Cao, 2000) to form a sympathoexcitatory pathway.

Studies using neuronal tracers have also identified direct projections from the PVN (Luiten et al., 1985) and the LH (Ter Horst et al., 1984; Allen and Cechetto, 1992) to parasympathetic motor neurons (Fox and Powley, 1986), particularly in the NTS/DMV area (Loewy et al., 1994). Furthermore, orexinergic terminals are found in the DMV (Date et al., 1999) and direct injection of orexin increases gastric motility (Krowicki et al., 2002) presumably mediated by an increase in parasympathetic nerve activity. An orexinergic input to the DMV has also been implicated in the increase in pancreatic parasympathetic nerve discharge produced by insulin-induced hypoglycemia (Wu et al., 2004). These findings suggest that the PVN and LH act as the major hypothalamic gateways for descending pathways that modulate glucose homeostasis (Luiten et al., 1985; Ter Horst and Luiten, 1987; Sim and Joseph, 1991).

The ARC/VMH and DMH neurons project to the DMV in the dorsal medulla, but they do not communicate with sympathetic premotor neurons in the ventral medulla. In fact, direct projections from the ARC/VMH and DMH to DMV motor neurons have been confirmed by anterograde (Ter Horst and Luiten, 1986; Sim and Joseph, 1991; Canteras et al., 1994) and retrograde (Ter Horst et al., 1984) tracer studies. However, there is no evidence for projections from ARC/VMH and DMH neurons to RVLM sympathetic premotor neurons. Although the studies by Borg and colleagues suggest that glucoprivation of VMH neurons induces glucagon, adrenaline and noradrenaline release, the microdialysis technique used in their studies is likely to have allowed diffusion of the glucoprivic agent throughout several hypothalamic regions, confounding the interpretation of these findings (Borg et al., 1995, 1997). Therefore, it is conceivable that additional inputs from ARC-VMH-DMH neurons to DMV neurons drive glucagon release, whereas adrenaline release is modulated in parallel by neurons in the LH (Yardley and Hilton, 1987) and PVN (Blair et al., 1996). Nevertheless, Chan and colleagues have clearly demonstrated that suppression of GABAergic drive in the VMH enhances the secretion of glucagon and adrenaline but not corticosterone in response to insulin-induced hypoglycemia (Chan et al., 2006). In STZ diabetic rats, blockade of VMH GABA receptors restores the glucagon response to hypoglycemia more effectively than the adrenaline response (Chan et al., 2011). Furthermore, these investigators have shown an inverse relationship between counterregulatory hormone release and VMH extracellular GABA (Zhu et al., 2010). On the other hand, Elmquist and colleagues have shown that reduction of VMH glutamatergic drive during hypoglycemia reduces the glucagon response to a greater extent than the adrenaline response (Tong et al., 2007).

INTRAMEDULLARY PROJECTIONS—EVIDENCE FOR INDEPENDENT GLUCOSE CONTROL IN THE BRAINSTEM

Several pieces of evidence suggest that the glucose counterregulatory network is confined to the brainstem, rather than involving the hypothalamus. Following decerebration (DiRocco and Grill, 1979) or obstruction of the cerebral aqueduct (Ritter et al., 1981), systemic glucoprivation with 2DG or injection of 5-thio-D-glucose (5TG) into the fourth ventricle elicits hyperglycemia, supposedly resulting from adrenaline release. However, these early studies assumed the involvement of adrenaline secretion based on glucose measurements alone, a role that could be fairly attributed to glucagon, as previously discussed in this review. Vagal afferent fibers conveying signals from the portal vein terminate onto the NTS and DMV neurons (Adachi et al., 1984; Berthoud et al., 1992).

Neurons in the DMV/NTS-A2 express Fos in response to hypoglycemia or glucoprivation (Ritter et al., 1998; Cai et al.,

2001; Damanhuri et al., 2012) and a small proportion (21%) are glucose-sensing as based on electrophysiological characterization. This finding is supported by the presence of K_{ATP} channels and glucokinase in DMV (Balfour et al., 2006) and NTS (Briski et al., 2009) neurons. Nevertheless, activation of adrenal premotor neurons by an intrinsic drive from brainstem neurons cannot be disregarded. For instance, C1 sympathetic premotor neurons receive excitatory inputs from other brainstem nuclei including the NTS (Aicher et al., 1996), a structure which provides a high proportion of asymmetric synapses onto C1 neurons. By contrast, although sympathetic premotor neurons in the ventral medulla are activated by glucoprivation, evidence supporting the notion that they are intrinsically glucose-sensitive is poor.

Based on the evidence discussed here, it can be inferred that a rudimentary brainstem circuit is sufficient to counteract hypoglycemia and maintain life (DiRocco and Grill, 1979). It seems that NTS and DMV neurons constitute the first line of defense against hypoglycemia by mediating the release of glucagon. A proportion of these cells is intrinsically glucose sensitive, and receives input signals from vagal afferent neurons. However, whether the excitatory drive to adrenal premotor neurons following hypoglycemia or glucoprivation directly originates from brainstem neurons, or derives from descending hypothalamic projections is unknown. Moreover, if the former assumption is proven true, the question arises as to what is the role of the aforementioned hypothalamic circuitry. On the other hand, it can be speculated that the brainstem neurons that mediate the autonomic apparatus for glucose homeostasis, whereas hypothalamic neurons integrate complex behaviors such as feeding and arousal. This hierarchical structure of the neuroaxis adds a new dimension to the counterregulatory response to hypoglycemia. During the execution of these behaviors, it seems that the hypothalamic neurons can override the activity of brainstem neurons in order to adjust the autonomic outputs to a new metabolic demand. For instance, selective pharmacogenetic activation of ARC- AGRP neurons and optogenetic activation of orexinergic neurons elicit feeding (Krashes et al., 2011) and arousal (Adamantidis et al., 2007), respectively; behaviors that work in conjunction to increase glycemia.

EFFERENT PATHWAYS FOR COUPLING TO AUTONOMIC EFFECTORS

The nervous system activates counterregulatory mechanisms to hypoglycemia in order to restore the blood glucose to normal levels. These mechanisms respond at different glycaemic levels (Cryer, 1997). In clinical studies the thresholds are: ∼4.5 mM at which the pancreatic β-cell responds with a decrease in insulin secretion. At ∼3.6–3.8 mM release of counterregulatory hormones (glucagon, adrenaline, GH, and cortisol) occurs. Furthermore, distinct subsets of neurons within the nervous system seem to selectively regulate these responses. In this section, we review the descending neural pathways and mechanisms controlling glucose counterregulatory hormones via sympathetic and parasympathetic motor neurons which originate in the hypothalamus and brainstem where the premotor neurons are found (**Figure 3**). Therefore, we first provide an insight of the neural mechanisms, at the motor level, that control insulin and glucagon secretion. Secondly, we discuss the neural control of adrenaline release, and finally, the modulation of GH and cortisol release.

NEURAL CONTROL OF PANCREATIC α- AND β-CELLS

Insulin secreting β-cells and glucagon secreting α-cells are innervated by sympathetic and parasympathetic neurons

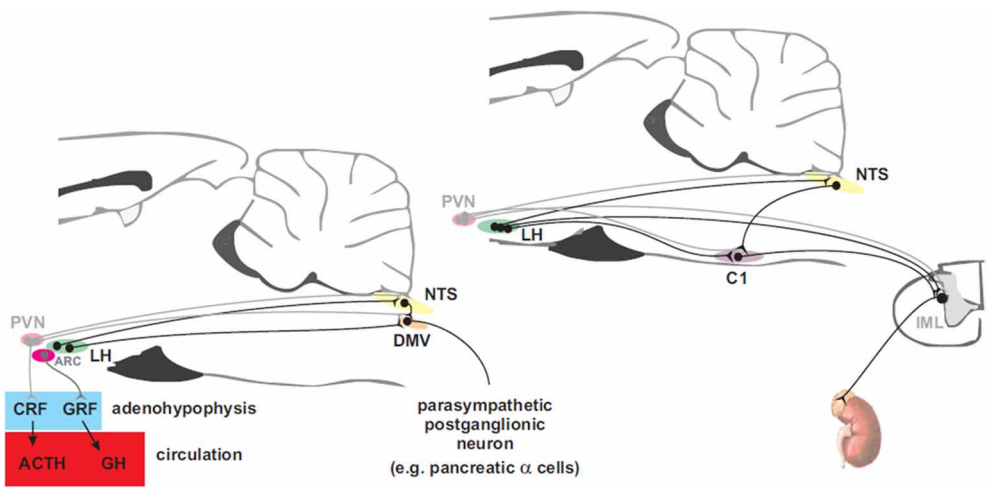

FIGURE 3 | Hypothalamic projections to the adenohypophysis and to parasympathetic motorneurons that innervate the pancreas (left panel) and to sympathetic premotor neurons that supply the adrenal gland (right panel). Neurons in the paraventricular nucleus of the hypothalamus (PVN) control the release of adrenocorticotropin (ACTH) into the circulation via corticotropin releasing factor (CRF) to promote secretion of cortisol from the adrenal cortex while arcuate (ARC) neurons control release of growth hormone (GH) via the release of growth hormone releasing factor (GRF). Preganglionic parasympathetic neurons of the dorsal motor nucleus of the vagus (DMV) receive inputs from neurons in the ARC and the lateral hypothalamus (LH). PVN and LH neurons send direct projections to the nucleus of the solitary tract (NTS) and to sympathetic preganglionic neurons in the intermediolateral cell column (IML). Adrenal catecholamine release is controlled by inputs from LH to C1 neurons in the rostral ventrolateral medulla (RVLM) that drive the adrenal sympathetic outflow.

(Gerich et al., 1976). The branches of the subdiaphragmatic vagus and of the splanchnic nerves form a mixed nerve connecting to the pancreas (Woods and Porte, 1974; Gerich et al., 1976). Electron microscopy has shown that both adrenergic and cholinergic terminals make contact with pancreatic islets (Madden and Sarras, 1989). These nerve terminals consist of both myelinated (Lever, 1964; Esterhuizen et al., 1968) and unmyelinated (Watari, 1968) fibers, which can be found in the periphery and within the center of the islets (Morgan and Lobl, 1968), in addition to ganglion cells (Honjin, 1956; Kobayashi and Fujita, 1969). In the nerve terminals found in the islets, electron microscopy reveals two major types of vesicles: cholinergic agranular vesicles and adrenergic granular cores (Richardson, 1964).

The pancreas receives parasympathetic cholinergic fibers in the vagus nerve, which originate in the DMV. *In vitro* and *in vivo* administration of acetylcholine induces insulin and glucagon secretion (Malaisse et al., 1967; Iversen, 1973a). These responses are mediated by activation of muscarinic receptors. Atropine reduces basal levels of insulin (Bloom et al., 1974a) and glucagon (Bloom et al., 1974b) induced by hypoglycemia and intravenous injection of arginine, respectively. *In vitro*, atropine also blocks the release of insulin and glucagon in response to acetylcholine (Malaisse et al., 1967; Iversen, 1973a). Stimulation of the vagus nerve elicits insulin and glucagon secretion in different species (Daniel and Henderson, 1967; Frohman et al., 1967; Kaneto et al., 1967, 1974), although bilateral section of the vagus fails to produce a sustained change in resting levels of insulin and glucagon (Hakanson et al., 1971; Bloom et al., 1974b). On the other hand, in humans, vagal section increases the periodicity of insulin secretion (Matthews et al., 1983). The cell bodies of vagal preganglionic neurons that regulate insulin and glucagon secretion are found in the DMV (Kalia, 1981). DMV neurons are located bilaterally ventral and medial to the nucleus of the solitary tract (NTS) in the dorsal surface of the caudal medulla, and are identified by choline acetyltransferase (ChAT) immunoreactivity (Takanaga et al., 2003; Llewellyn-Smith et al., 2013; Zheng et al., 2013). Injections of neurotropic pseudorabies virus into the pancreas retrogradely labels cell bodies of cholinergic neurons in the DMV (Jansen et al., 1997). Excitation of DMV neurons augments plasma insulin levels, whereas inhibition of these neurons reduces plasma insulin levels (Ionescu et al., 1983; Siaud et al., 1991).

Activation of sympathetic drive to the pancreas reduces insulin secretion and increases the secretion of glucagon. In experimental conditions, noradrenaline or adrenaline mimic the pancreatic response to sympathoexcitation, reducing insulin release and eliciting glucagon release (Coore and Randle, 1964; Karam et al., 1966; Porte and Williams, 1966; Iversen, 1973b). Similar results are observed following electrical stimulation of the splanchnic or the pancreatic mixed nerve, in the presence of atropine (Marliss et al., 1973; Bloom and Edwards, 1978). Anatomical findings further support this mechanism. The sympathetic projections to the pancreas originate in the celiac and superior mesenteric plexi, and converge at the greater and middle splanchnic nerves (Baron et al., 1985, 1988). Immunohistochemical studies show that the terminals of these nerves contain catecholamines (Miller, 1981). Thus, it is likely that these terminals belong to sympathetic postganglionic neurons, whose cell bodies are located in the sympathetic chain ganglia. The afferent inputs to these neurons are cholinergic (Feldberg, 1943; Feldberg et al., 1951; Oesch and Thoenen, 1973) and originate from SPN located in both the intermediolateral column (lamina VII) and the central autonomic area (lamina X) of the thoracolumbar spinal cord (Torigoe et al., 1985; Bacon and Smith, 1988; Pyner and Coote, 1994).

Apart from the noradrenergic and cholinergic inputs, neuropeptides also contribute to the innervation of the pancreatic islets. Neuropeptides released by the pancreatic nerve terminals probably also control islet function by modulating the release of insulin and glucagon (Ahren et al., 1986). Immunohistochemical studies have identified a variety of peptides in nerve terminals projecting to the pancreas. These include vasoactive intestinal polypeptide (VIP) (Bishop et al., 1980), cholecystokinin (CCK) (Rehfeld et al., 1980), gastrin releasing polypeptide (GRP) (Moghimzadeh et al., 1983), galanin (Dunning et al., 1986), NPY (Pettersson et al., 1987), calcitonin gene-related peptide (CGRP) (Pettersson et al., 1986), substance P and enkephalin (Larsson, 1979). In functional studies, VIP, CCK, and GRP appear to be excitatory while the inhibitory peptides are galanin, NPY, and CGRP and substance P and enkephalin produce diverse responses (Larsson, 1979).

ADRENAL SYMPATHETIC OUTFLOW

Adrenaline counters hypoglycemia by acting in the liver and pancreas. In the pancreas, adrenaline inhibits insulin release (Coore and Randle, 1964; Karam et al., 1966; Malaisse et al., 1967) and stimulates glucagon release (Iversen, 1973b; Gerich et al., 1974) whereas, in the liver, adrenaline activates gluconeogenesis and glycogenolysis (Exton, 1985; Pilkis et al., 1988; Kraus-Friedmann and Feng, 1996; Fabbri et al., 1998). In addition, adrenaline acts on skeletal muscle to reduce glucose uptake and also promotes lipolysis via an action at β_2-adrenoceptors. Adrenaline is released by chromaffin cells in the adrenal medulla, under the control of SPN. Sympathetic projections to the adrenal gland are comprised of sympathetic pre- and post-ganglionic fibers (Carlsson et al., 1992). The preganglionic fibers to the adrenal gland are axons from a subset of SPNs, located in the T4–T13 segments of the spinal cord; the postganglionic fibers projecting to the adrenal gland originate from neurons in the sympathetic chain ganglion, and receive inputs from SPNs (Baron et al., 1988; Strack et al., 1988, 1989b). Neuroglucoprivation induces Fos expression in the adrenal medulla and in the intermediolateral cell column, primarily at spinal cord segments T7–T10, where adrenomedullary preganglionic neurons are found (Ritter et al., 1995). Neuroglucoprivation also activates the adrenal sympathetic outflow but not the renal sympathetic outflow (Niijima, 1975).

Systemic glucoprivation produces increases in levels of adrenaline and blood glucose, suggesting increase in the sympathoexcitatory drive to the adrenal gland (Ritter et al., 1995; Elman et al., 2004).

Adrenal-projecting SPNs can be functionally segregated according to electrophysiological properties and neurochemical phenotype. At least two subpopulations of SPN have been electrophysiologically differentiated: one group is involved in control

of adrenaline secretion, while the other is related to the control of noradrenaline release (Morrison and Cao, 2000). The former subset of neurons is responsive to systemic glucoprivation, whereas the latter is exclusively inhibited by increases in blood pressure. The SPN clusters can be alternatively differentiated according to their neurochemical content. For instance, SPN that participate in cardiovascular regulation are immunoreactive for cocaine and amphetamine-regulated transcript peptide (CART); and in the adrenal, CART positive terminals selectively target noradrenergic chromaffin cells (Gonsalvez et al., 2010). On the other hand, enkephalin is likely to be a selective marker for adrenal-projecting SPN that control adrenaline release (Kumar et al., 2010). In fact, neuroglucoprivation produces c-Fos expression in prepro-enkephalin mRNA positive neurons, but fails to activate prepro-CART mRNA positive neurons (Parker et al., 2013). Although enkephalin is an inhibitory peptide used as a neurochemical marker, it does not imply that it inhibits chromaffin cells. Enkephalin produces variable responses in pancreatic islets (Green et al., 1983). Patients with type 1 or severe type 2 diabetes are at high risk of life-threatening hypoglycemia, due to a combination of intensive insulin treatment and impaired glucagon secretion (Halimi, 2010). Hypoglycemia usually occurs as a result of a mismatch between insulin dose, the amount of food consumed, and energy expended. Due to the destruction of pancreatic α-cells, in these patients adrenaline is the major glucose counterregulatory hormone secreted in response to hypoglycemia. Although slow-acting counterregulatory hormones contribute to rescue glucose levels (see below), the importance of adrenaline lies on the fact that it is the only remaining fast-acting counterregulatory hormone.

SLOW-ACTING GLUCOSE COUNTERREGULATORY HORMONES

The slow-acting hormones, GH, and cortisol, contribute to glucose counterregulation by shifting metabolism of non-neural tissues away from glucose utilization (Schwartz et al., 1987). Cortisol activates fatty acid oxidation, gluconeogenesis and ketogenesis (Gerich et al., 1980). On the other hand, GH increases lipolysis, fatty acid oxidation and induces the insulin resistance noted in pregnancy (Barbour et al., 2002). Cortisol secretion is activated by adrenocorticotropic hormone (ACTH) release, which is modulated by CRF. Insulin-induced hypoglycemia is a stressor that produces large increases in plasma CRF (Engler et al., 1989) and ACTH (Pacak et al., 1995). CRF is synthetized by parvocellular neuroendocrine cells in the PVN of the hypothalamus and is released into the hypothalamo-hypophyseal portal system and transported to the anterior pituitary (adenohypophysis) where it stimulates corticotropes to secrete ACTH into the circulation. At the adrenal cortex, ACTH stimulates the synthesis of cortisol, glucocorticoids, mineralocorticoids, and dehydroepiandrosterone. Alternatively, hypoglycemia can also trigger the release of GH (Roth et al., 1963). This hormone is directly released by the adenohypophysis, and is primarily stimulated by the growth hormone-releasing factor (GRF) (Barinaga et al., 1985) produced in the ARC (Sawchenko et al., 1985). Nonetheless, growth hormone-secretagogues (Howard et al., 1996) and somatostatin (Plotsky and Vale, 1985), respectively, can stimulate and inhibit GH release.

CONCLUSION

The preceding discussion provides a brief overview of the neural circuitry involved in the control of glucose homeostasis. However, in order to define how the neural pathways interplay to control glucose homeostasis, more detailed knowledge of the important neurons and their connections is still required. In contrast to brainstem neurons, we believe that further neuropharmacological and neurochemical characterization of hypothalamic neurons is necessary to understand their role in glucose control. Most of the current evidence relies on direct injections of drugs and neuronal tracers which, due to short projections within the hypothalamus, hamper the interpretation of the findings. Fortunately, new techniques are arising to overcome this issue. For instance, new pharmaco- and opto-genetic tools will help to determine the links between the neurochemical, pharmacological, and electrophysiological properties of hypothalamic neurons.

Two important questions about the role of hypothalamic neurons in the control of glucose homeostasis remain to be answered. The first is to define the hypothalamic gateway for downstream information, with an emphasis on the communication between the motor and premotor outputs and the glucose-sensing brainstem circuitry. Identification of neurons that control the release of adrenaline, glucagon, ACTH and GH will allow us to understand how these are controlled differentially and to determine the respective roles of the hypothalamic and brainstem nuclei. Secondly, a better knowledge of the hypothalamic circuitry involved in the control of blood glucose has yet to be elucidated. It will allow us to determine the structures and mechanisms underlying complex behaviors in response to hypoglycemia, which are related but distinct from autonomic and endocrine glucose homeostasis. For example, it can be speculated that brainstem neurons provide the essential output for autonomic responses while the hypothalamus integrates feeding, arousal and "fight or flight" behaviors associated with these responses. By answering these questions we may delineate the multi-layered neural apparatus that underpins glucose control and determine how it tunes different body systems to the brain's energy demand in mammals, a condition simply necessary for life.

REFERENCES

Adachi, A. (1981). Electrophysiological study of hepatic vagal projection to the medulla. *Neurosci. Lett.* 24, 19–23. doi: 10.1016/0304-3940(81)90352-9

Adachi, A., Kobashi, M., and Funahashi, M. (1995). Glucose-responsive neurons in the brainstem. *Obes. Res.* 3, 735S–740S. doi: 10.1002/j.1550-8528.1995.tb00493.x

Adachi, A., Shimizu, N., Oomura, Y., and Kobashi, M. (1984). Convergence of hepatoportal glucose-sensitive afferent signals to glucose-sensitive units within the nucleus of the solitary tract. *Neurosci. Lett.* 46, 215–218. doi: 10.1016/0304-3940(84)90444-0

Adamantidis, A. R., Zhang, F., Aravanis, A. M., Deisseroth, K., and de Lecea, L. (2007). Neural substrates of awakening probed with optogenetic control of hypocretin neurons. *Nature* 450, 420–424. doi: 10.1038/nature06310

Ahren, B., Taborsky, G. J. Jr., and Porte, D. Jr. (1986). Neuropeptidergic versus cholinergic and adrenergic regulation of islet hormone secretion. *Diabetologia* 29, 827–836. doi: 10.1007/BF00870137

Aicher, S. A., Saravay, R. H., Cravo, S., Jeske, I., Morrison, S. F., Reis, D. J., et al. (1996). Monosynaptic projections from the nucleus tractus solitarii to C1 adrenergic neurons in the rostral ventrolateral medulla: comparison with input from the caudal ventrolateral medulla. *J. Comp. Neurol.* 373, 62–75. doi: 10.1002/(SICI)1096-9861(19960909)373:1%3C62::AID-CNE6%3E3.0.CO;2-B

Allen, G. V., and Cechetto, D. F. (1992). Functional and anatomical organization of cardiovascular pressor and depressor sites in the lateral hypothalamic area: I. Descending projections. *J. Comp. Neurol.* 315, 313–332. doi: 10.1002/cne.903150307

Amoroso, S., Schmid-Antomarchi, H., Fosset, M., and Lazdunski, M. (1990). Glucose, sulfonylureas, and neurotransmitter release: role of ATP-sensitive K+ channels. *Science* 247, 852–854. doi: 10.1126/science.2305257

Andrew, S. F., Dinh, T. T., and Ritter, S. (2007). Localized glucoprivation of hindbrain sites elicits corticosterone and glucagon secretion. *Am. J. Physiol.* 292, R1792–R1798. doi: 10.1152/ajpregu.00777.2006

Bacon, S. J., and Smith, A. D. (1988). Preganglionic sympathetic neurones innervating the rat adrenal medulla: immunocytochemical evidence of synaptic input from nerve terminals containing substance P, GABA or 5-hydroxytryptamine. *J. Auton. Nerv. Syst.* 24, 97–122. doi: 10.1016/0165-1838(88)90140-3

Balfour, R. H., Hansen, A. M., and Trapp, S. (2006). Neuronal responses to transient hypoglycaemia in the dorsal vagal complex of the rat brainstem. *J. Physiol.* 570, 469–484. doi: 10.1113/jphysiol.2005.098822

Barbour, L. A., Shao, J., Qiao, L., Pulawa, L. K., Jensen, D. R., Bartke, A., et al. (2002). Human placental growth hormone causes severe insulin resistance in transgenic mice. *Am. J. Obstet. Gynecol.* 186, 512–517. doi: 10.1067/mob.2002.121256

Barinaga, M., Bilezikjian, L. M., Vale, W. W., Rosenfeld, M. G., and Evans, R. M. (1985). Independent effects of growth hormone releasing factor on growth hormone release and gene transcription. *Nature* 314, 279–281. doi: 10.1038/314279a0

Baron, R., Janig, W., and Kollmann, W. (1988). Sympathetic and afferent somata projecting in hindlimb nerves and the anatomical organization of the lumbar sympathetic nervous system of the rat. *J. Comp. Neurol.* 275, 460–468. doi: 10.1002/cne.902750310

Baron, R., Janig, W., and McLachlan, E. M. (1985). The afferent and sympathetic components of the lumbar spinal outflow to the colon and pelvic organs in the cat. II. The lumbar splanchnic nerves. *J. Comp. Neurol.* 238, 147–157. doi: 10.1002/cne.902380203

Berthoud, H. R., Kressel, M., and Neuhuber, W. L. (1992). An anterograde tracing study of the vagal innervation of rat liver, portal vein and biliary system. *Anat. Embryol. (Berl.)* 186, 431–442. doi: 10.1007/BF00185458

Bishop, A. E., Polak, J. M., Green, I. C., Bryant, M. G., and Bloom, S. R. (1980). The location of VIP in the pancreas of man and rat. *Diabetologia* 18, 73–78. doi: 10.1007/BF01228307

Bittencourt, J. C., Presse, F., Arias, C., Peto, C., Vaughan, J., Nahon, J. L., et al. (1992). The melanin-concentrating hormone system of the rat brain: an immuno- and hybridization histochemical characterization. *J. Comp. Neurol.* 319, 218–245. doi: 10.1002/cne.903190204

Blair, M. L., Piekut, D., Want, A., and Olschowka, J. A. (1996). Role of the hypothalamic paraventricular nucleus in cardiovascular regulation. *Clin. Exp. Pharmacol. Physiol.* 23, 161–165. doi: 10.1111/j.1440-1681.1996.tb02590.x

Bloom, S. R., and Edwards, A. V. (1978). Certain pharmacological characteristics of the release of pancreatic glucagon in response to stimulation of the splanchnic nerves. *J. Physiol.* 280, 25–35.

Bloom, S. R., Edwards, A. V., and Vaughan, N. J. (1974a). The role of the autonomic innervation in the control of glucagon release during hypoglycaemia in the calf. *J. Physiol.* 236, 611–623.

Bloom, S. R., Vaughan, N. J., and Russell, R. C. (1974b). Vagal control of glucagon release in man. *Lancet* 2, 546–549. doi: 10.1016/S0140-6736(74)91875-3

Borg, M. A., Borg, W. P., Tamborlane, W. V., Brines, M. L., Shulman, G. I., and Sherwin, R. S. (1999). Chronic hypoglycemia and diabetes impair counterregulation induced by localized 2-deoxy-glucose perfusion of the ventromedial hypothalamus in rats. *Diabetes* 48, 584–587. doi: 10.2337/diabetes.48.3.584

Borg, M. A., Sherwin, R. S., Borg, W. P., Tamborlane, W. V., and Shulman, G. I. (1997). Local ventromedial hypothalamus glucose perfusion blocks counterregulation during systemic hypoglycemia in awake rats. *J. Clin. Invest.* 99, 361–365. doi: 10.1172/JCI119165

Borg, W. P., During, M. J., Sherwin, R. S., Borg, M. A., Brines, M. L., and Shulman, G. I. (1994). Ventromedial hypothalamic lesions in rats suppress counterregulatory responses to hypoglycemia. *J. Clin. Invest.* 93, 1677–1682. doi: 10.1172/JCI117150

Borg, W. P., Sherwin, R. S., During, M. J., Borg, M. A., and Shulman, G. I. (1995). Local ventromedial hypothalamus glucopenia triggers counterregulatory hormone release. *Diabetes* 44, 180–184. doi: 10.2337/diab.44.2.180

Briski, K. P., Cherian, A. K., Genabai, N. K., and Vavaiya, K. V. (2009). *In situ* coexpression of glucose and monocarboxylate transporter mRNAs in metabolic-sensitive caudal dorsal vagal complex catecholaminergic neurons: transcriptional reactivity to insulin-induced hypoglycemia and caudal hindbrain glucose or lactate repletion during insulin-induced hypoglycemia. *Neuroscience* 164, 1152–1160. doi: 10.1016/j.neuroscience.2009.08.074

Briski, K. P., and Sylvester, P. W. (2001). Hypothalamic orexin-A-immunopositive neurons express Fos in response to central glucopenia. *Neuroreport* 12, 531–534. doi: 10.1097/00001756-200103050-00020

Burdakov, D., Gerasimenko, O., and Verkhratsky, A. (2005a). Physiological changes in glucose differentially modulate the excitability of hypothalamic melanin-concentrating hormone and orexin neurons *in situ*. *J. Neurosci.* 25, 2429–2433. doi: 10.1523/JNEUROSCI.4925-04.2005

Burdakov, D., Jensen, L. T., Alexopoulos, H., Williams, R. H., Fearon, I. M., O'Kelly, I., et al. (2006). Tandem-pore K+ channels mediate inhibition of orexin neurons by glucose. *Neuron* 50, 711–722. doi: 10.1016/j.neuron.2006.04.032

Burdakov, D., Luckman, S. M., and Verkhratsky, A. (2005b). Glucose-sensing neurons of the hypothalamus. *Philos. Trans. R. Soc. Lond. B Biol. Sci.* 360, 2227–2235. doi: 10.1098/rstb.2005.1763

Cai, X. J., Evans, M. L., Lister, C. A., Leslie, R. A., Arch, J. R., Wilson, S., et al. (2001). Hypoglycemia activates orexin neurons and selectively increases hypothalamic orexin-B levels: responses inhibited by feeding and possibly mediated by the nucleus of the solitary tract. *Diabetes* 50, 105–112. doi: 10.2337/diabetes.50.1.105

Canteras, N. S., Simerly, R. B., and Swanson, L. W. (1994). Organization of projections from the ventromedial nucleus of the hypothalamus: a *Phaseolus vulgaris*-leucoagglutinin study in the rat. *J. Comp. Neurol.* 348, 41–79. doi: 10.1002/cne.903480103

Carlsson, S., Skarphedinsson, J. O., Delle, M., Hoffman, P., and Thoren, P. (1992). Differential responses in post- and pre-ganglionic adrenal sympathetic nerve activity and renal sympathetic nerve activity after injection of 2-deoxy-D-glucose and insulin in rats. *Acta Physiol. Scand.* 145, 169–175. doi: 10.1111/j.1748-1716.1992.tb09352.x

Chan, O., Paranjape, S., Czyzyk, D., Horblitt, A., Zhu, W., Ding, Y., et al. (2011). Increased GABAergic output in the ventromedial hypothalamus contributes to impaired hypoglycemic counterregulation in diabetic rats. *Diabetes* 60, 1582–1589. doi: 10.2337/db10-1579

Chan, O., Zhu, W., Ding, Y., McCrimmon, R. J., and Sherwin, R. S. (2006). Blockade of GABA(A) receptors in the ventromedial hypothalamus further stimulates glucagon and sympathoadrenal but not the hypothalamo-pituitary-adrenal response to hypoglycemia. *Diabetes* 55, 1080–1087. doi: 10.2337/diabetes.55.04.06.db05-0958

Conde, S. V., Obeso, A., and Gonzalez, C. (2007). Low glucose effects on rat carotid body chemoreceptor cells' secretory responses and action potential frequency in the carotid sinus nerve. *J. Physiol. (Lond.)* 585, 721–730. doi: 10.1113/jphysiol.2007.144261

Coore, H. G., and Randle, P. J. (1964). Regulation of insulin secretion studied with pieces of rabbit pancreas incubated *in vitro*. *Biochem. J.* 93, 66–78.

Cryer, P. E. (1997). Hierarchy of physiological responses to hypoglycemia: relevance to clinical hypoglycemia in type I (insulin dependent) diabetes mellitus. *Horm. Metab. Res.* 29, 92–96. doi: 10.1055/s-2007-978997

Damanhuri, H. A., Burke, P. G., Ong, L. K., Bobrovskaya, L., Dickson, P. W., Dunkley, P. R., et al. (2012). Tyrosine hydroxylase phosphorylation in catecholaminergic brain regions: a marker of activation following acute hypotension and glucoprivation. *PLoS ONE* 7:e50535. doi: 10.1371/journal.pone.0050535

Daniel, P. M., and Henderson, J. R. (1967). The effect of vagal stimulation on plasma insulin and glucose levels in the baboon. *J. Physiol.* 192, 317–327.

Date, Y., Ueta, Y., Yamashita, H., Yamaguchi, H., Matsukura, S., Kangawa, K., et al. (1999). Orexins, orexigenic hypothalamic peptides, interact with autonomic, neuroendocrine and neuroregulatory systems. *Proc. Natl. Acad. Sci. U.S.A.* 96, 748–753. doi: 10.1073/pnas.96.2.748

De Lecea, L., Kilduff, T. S., Peyron, C., Gao, X., Foye, P. E., Danielson, P. E., et al. (1998). The hypocretins: hypothalamus-specific peptides with neuroexcitatory activity. *Proc. Natl. Acad. Sci. U.S.A.* 95, 322–327. doi: 10.1073/pnas.95.1.322

DiRocco, R. J., and Grill, H. J. (1979). The forebrain is not essential for sympathoadrenal hyperglycemic response to glucoprivation. *Science* 204, 1112–1114. doi: 10.1126/science.451558

Donovan, C. M., Halter, J. B., and Bergman, R. N. (1991). Importance of hepatic glucoreceptors in sympathoadrenal response to hypoglycemia. *Diabetes* 40, 155–158. doi: 10.2337/diab.40.1.155

Dunning, B. E., Ahren, B., Veith, R. C., Bottcher, G., Sundler, F., and Taborsky, G. J. Jr. (1986). Galanin: a novel pancreatic neuropeptide. *Am. J. Physiol.* 251, E127–E133.

Elman, I., Rott, D., Green, A. I., Langleben, D. D., Lukas, S. E., Goldstein, D. S., et al. (2004). Effects of pharmacological doses of 2-deoxyglucose on plasma catecholamines and glucose levels in patients with schizophrenia. *Psychopharmacology (Berl.)* 176, 369–375. doi: 10.1007/s00213-004-1890-y

Engler, D., Pham, T., Fullerton, M. J., Ooi, G., Funder, J. W., and Clarke, I. J. (1989). Studies of the secretion of corticotropin-releasing factor and arginine vasopressin into the hypophysial-portal circulation of the conscious sheep. I. Effect of an audiovisual stimulus and insulin-induced hypoglycemia. *Neuroendocrinology* 49, 367–381. doi: 10.1159/000125141

Esterhuizen, A. C., Spriggs, T. L., and Lever, J. D. (1968). Nature of islet-cell innervation in the cat pancreas. *Diabetes* 17, 33–36.

Exton, J. H. (1985). Mechanisms involved in alpha-adrenergic phenomena. *Am. J. Physiol.* 248, E633–E647.

Fabbri, E., Capuzzo, A., and Moon, T. W. (1998). The role of circulating catecholamines in the regulation of fish metabolism: an overview. *Comp. Biochem. Physiol. C Pharmacol. Toxicol. Endocrinol.* 120, 177–192. doi: 10.1016/S0742-8413(98)10017-8

Feldberg, W. (1943). Synthesis of acetylcholine in sympathetic ganglia and cholinergic nerves. *J. Physiol.* 101, 432–445.

Feldberg, W., Harris, F. W., and Lin, R. C. (1951). Observations on the presence of cholinergic and non-cholinergic neurones in the central nervous system. *J. Physiol.* 112, 400–404.

Fox, E. A., and Powley, T. L. (1986). Tracer diffusion has exaggerated CNS maps of direct preganglionic innervation of pancreas. *J. Auton. Nerv. Syst.* 15, 55–69. doi: 10.1016/0165-1838(86)90079-2

Frohman, L. A., Ezdinli, E. Z., and Javid, R. (1967). Effect of vagotomy and vagal stimulation on insulin secretion. *Diabetes* 16, 443–448.

Fujita, S., Bohland, M. A., Sanchez-Watts, G., Watts, A. G., and Donovan, C. M. (2007). Hypoglycemic detection at the portal vein is mediated by capsaicin-sensitive primary sensory neurons. *Am. J. Physiol.* 293, E96–E101. doi: 10.1152/ajpendo.00415.2006

Garcia-Fernandez, M., Ortega-Saenz, P., Castellano, A., and Lopez-Barneo, J. (2007). Mechanisms of low-glucose sensitivity in carotid body glomus cells. *Diabetes* 56, 2893–2900. doi: 10.2337/db07-0122

Gerich, J., Cryer, P., and Rizza, R. (1980). Hormonal mechanisms in acute glucose counterregulation: the relative roles of glucagon, epinephrine, norepinephrine, growth hormone, and cortisol. *Metabolism* 29, 1164–1175. doi: 10.1016/0026-0495(80)90026-8

Gerich, J. E., Charles, M. A., and Grodsky, G. M. (1976). Regulation of pancreatic insulin and glucagon secretion. *Annu. Rev. Physiol.* 38, 353–388. doi: 10.1146/annurev.ph.38.030176.002033

Gerich, J. E., Langlois, M., Noacco, C., Schneider, V., and Forsham, P. H. (1974). Adrenergic modulation of pancreatic glucagon secretion in man. *J. Clin. Invest.* 53, 1441–1446. doi: 10.1172/JCI107692

Gonsalvez, D. G., Kerman, I. A., McAllen, R. M., and Anderson, C. R. (2010). Chemical coding for cardiovascular sympathetic preganglionic neurons in rats. *J. Neurosci.* 30, 11781–11791. doi: 10.1523/JNEUROSCI.0796-10.2010

Gonzalez, J. A., Jensen, L. T., Fugger, L., and Burdakov, D. (2008). Metabolism-independent sugar sensing in central orexin neurons. *Diabetes* 57, 2569–2576. doi: 10.2337/db08-0548

Green, I. C., Ray, K., and Perrin, D. (1983). Opioid peptide effects on insulin release and c-AMP in islets of Langerhans. *Horm. Metab. Res.* 15, 124–128. doi: 10.1055/s-2007-1018648

Hakanson, R., Liedberg, G., and Lundquist, I. (1971). Effect of vagal denervation on insulin release after oral and intravenous glucose. *Experientia* 27, 460–461. doi: 10.1007/BF02137312

Halimi, S. (2010). Acute consequences of hypoglycaemia in diabetic patients. *Diabetes Metab* 36 (Suppl. 3), S75–S83. doi: 10.1016/S1262-3636(10)70471-7

Hevener, A. L., Bergman, R. N., and Donovan, C. M. (2000). Portal vein afferents are critical for the sympathoadrenal response to hypoglycemia. *Diabetes* 49, 8–12. doi: 10.2337/diabetes.49.1.8

Honjin, R. (1956). The innervation of the pancreas of the mouse, with special reference to the structure of the peripheral extension of the vegetative nervous system. *J. Comp. Neurol.* 104, 331–371. doi: 10.1002/cne.901040302

Howard, A. D., Feighner, S. D., Cully, D. F., Arena, J. P., Liberator, P. A., Rosenblum, C. I., et al. (1996). A receptor in pituitary and hypothalamus that functions in growth hormone release. *Science* 273, 974–977. doi: 10.1126/science.273.5277.974

Ionescu, E., Rohner-Jeanrenaud, F., Berthoud, H. R., and Jeanrenaud, B. (1983). Increases in plasma insulin levels in response to electrical stimulation of the dorsal motor nucleus of the vagus nerve. *Endocrinology* 112, 904–910. doi: 10.1210/endo-112-3-904

Iversen, J. (1973a). Effect of acetyl choline on the secretion of glucagon and insulin from the isolated, perfused canine pancreas. *Diabetes* 22, 381–387. doi: 10.1172/JCI107395

Iversen, J. (1973b). Adrenergic receptors and the secretion of glucagon and insulin from the isolated, perfused canine pancreas. *J. Clin. Invest.* 52, 2102–2116. doi: 10.1172/JCI107395

Jansen, A. S., Hoffman, J. L., and Loewy, A. D. (1997). CNS sites involved in sympathetic and parasympathetic control of the pancreas: a viral tracing study. *Brain Res.* 766, 29–38. doi: 10.1016/S0006-8993(97)00532-5

Kalia, M. (1981). Brain stem localization of vagal preganglionic neurons. *J. Auton. Nerv. Syst.* 3, 451–481. doi: 10.1016/0165-1838(81)90081-3

Kaneto, A., Kosaka, K., and Nakao, K. (1967). Effects of stimulation of the vagus nerve on insulin secretion. *Endocrinology* 80, 530–536. doi: 10.1210/endo-80-3-530

Kaneto, A., Miki, E., and Kosaka, K. (1974). Effects of vagal stimulation on glucagon and insulin secretion. *Endocrinology* 95, 1005–1010. doi: 10.1210/endo-95-4-1005

Kang, L., Routh, V. H., Kuzhikandathil, E. V., Gaspers, L. D., and Levin, B. E. (2004). Physiological and molecular characteristics of rat hypothalamic ventromedial nucleus glucosensing neurons. *Diabetes* 53, 549–559. doi: 10.2337/diabetes.53.3.549

Karam, J. H., Grasso, S. G., Wegienka, L. C., Grodsky, G. M., and Forsham, P. H. (1966). Effect of selected hexoses, of epinephrine and of glucagon on insulin secretion in man. *Diabetes* 15, 571–578.

Karlsson, S., and Ahren, B. (1991). Contribution of adrenergic nerves and the adrenals to 2-deoxy-D-glucose-induced insulin and glucagon secretion in the mouse. *Int. J. Pancreatol.* 10, 207–215.

Kerman, I. A., Bernard, R., Rosenthal, D., Beals, J., Akil, H., and Watson, S. J. (2007). Distinct populations of presympathetic-premotor neurons express orexin or melanin-concentrating hormone in the rat lateral hypothalamus. *J. Comp. Neurol.* 505, 586–601. doi: 10.1002/cne.21511

Kobayashi, S., and Fujita, T. (1969). Fine structure of mammalian and avian pancreatic islets with special reference to D cells and nervous elements. *Z. Zellforsch. Mikrosk. Anat.* 100, 340–363. doi: 10.1007/BF00571491

Koyama, Y., Coker, R. H., Stone, E. E., Lacy, D. B., Jabbour, K., Williams, P. E., et al. (2000). Evidence that carotid bodies play an important role in glucoregulation *in vivo*. *Diabetes* 49, 1434–1442. doi: 10.2337/diabetes.49.9.1434

Krashes, M. J., Koda, S., Ye, C., Rogan, S. C., Adams, A. C., Cusher, D. S., et al. (2011). Rapid, reversible activation of AgRP neurons drives feeding behavior in mice. *J. Clin. Invest.* 121, 1424–1428. doi: 10.1172/JCI46229

Kraus-Friedmann, N., and Feng, L. (1996). The role of intracellular Ca^{2+} in the regulation of gluconeogenesis. *Metabolism* 45, 389–403. doi: 10.1016/S0026-0495(96)90296-6

Krowicki, Z. K., Burmeister, M. A., Berthoud, H. R., Scullion, R. T., Fuchs, K., and Hornby, P. J. (2002). Orexins in rat dorsal motor nucleus of the vagus potently stimulate gastric motor function. *Am. J. Physiol.* 283, G465–G472. doi: 10.1152/ajpgi.00264.2001

Kumar, N. N., Allen, K., Parker, L., Damanhuri, H., and Goodchild, A. K. (2010). Neuropeptide coding of sympathetic preganglionic neurons; focus on adrenally projecting populations. *Neuroscience* 170, 789–799. doi: 10.1016/j.neuroscience.2010.07.047

Lam, T. K., Gutierrez-Juarez, R., Pocai, A., and Rossetti, L. (2005). Regulation of blood glucose by hypothalamic pyruvate metabolism. *Science* 309, 943–947. doi: 10.1126/science.1112085

Larsson, L. I. (1979). Innervation of the pancreas by substance P, enkephalin, vasoactive intestinal polypeptide and gastrin/CCK immunoractive nerves. *J. Histochem. Cytochem.* 27, 1283–1284. doi: 10.1177/27.9.479572

Lee, K., Dixon, A. K., Richardson, P. J., and Pinnock, R. D. (1999). Glucose-receptive neurones in the rat ventromedial hypothalamus express KATP channels composed of Kir6.1 and SUR1 subunits. *J. Physiol.* 515(Pt 2), 439–452. doi: 10.1111/j.1469-7793.1999.439ac.x

Lever, J. D. (1964). Structural aspects of endocrine secretion. *Arch. Biol. (Liege)* 75, 437–452.

Levin, B. E., Routh, V. H., Kang, L., Sanders, N. M., and Dunn-Meynell, A. A. (2004). Neuronal glucosensing: what do we know after 50 years? *Diabetes* 53, 2521–2528. doi: 10.2337/diabetes.53.10.2521

Li, A. J., and Ritter, S. (2004). Glucoprivation increases expression of neuropeptide Y mRNA in hindbrain neurons that innervate the hypothalamus. *Eur. J. Neurosci.* 19, 2147–2154. doi: 10.1111/j.1460-9568.2004.03287.x

Li, A. J., Wang, Q., Dinh, T. T., and Ritter, S. (2009). Simultaneous silencing of NPY and DBH expression in hindbrain A1/C1 catecholamine cells suppresses glucoprivic feeding. *J. Neurosci.* 29, 280–287. doi: 10.1523/JNEUROSCI.4267-08.2009

Li, A. J., Wang, Q., and Ritter, S. (2006). Differential responsiveness of dopamine-beta-hydroxylase gene expression to glucoprivation in different catecholamine cell groups. *Endocrinology* 147, 3428–3434. doi: 10.1210/en.2006-0235

Llewellyn-Smith, I. J., Gnanamanickam, G. J., Reimann, F., Gribble, F. M., and Trapp, S. (2013). Preproglucagon (PPG) neurons innervate neurochemically identified autonomic neurons in the mouse brainstem. *Neuroscience* 229, 130–143. doi: 10.1016/j.neuroscience.2012.09.071

Loewy, A. D., Franklin, M. F., and Haxhiu, M. A. (1994). CNS monoamine cell groups projecting to pancreatic vagal motor neurons: a transneuronal labeling study using pseudorabies virus. *Brain Res.* 638, 248–260. doi: 10.1016/0006-8993(94)90657-2

Luiten, P. G., ter Horst, G. J., Karst, H., and Steffens, A. B. (1985). The course of paraventricular hypothalamic efferents to autonomic structures in medulla and spinal cord. *Brain Res.* 329, 374–378. doi: 10.1016/0006-8993(85)90554-2

Madden, C. J., Stocker, S. D., and Sved, A. F. (2006). Attenuation of homeostatic responses to hypotension and glucoprivation after destruction of catecholaminergic rostral ventrolateral medulla neurons. *Am. J. Physiol.* 291, R751–R759. doi: 10.1152/ajpregu.00800.2005

Madden, M. E., and Sarras, M. P. Jr. (1989). The pancreatic ductal system of the rat: cell diversity, ultrastructure, and innervation. *Pancreas* 4, 472–485. doi: 10.1097/00006676-198908000-00013

Malaisse, W., Malaisse-Lagae, F., Wright, P. H., and Ashmore, J. (1967). Effects of adrenergic and cholinergic agents upon insulin secretion *in vitro*. *Endocrinology* 80, 975–978. doi: 10.1210/endo-80-5-975

Marliss, E. B., Girardier, L., Seydoux, J., Wollheim, C. B., Kanazawa, Y., Orci, L., et al. (1973). Glucagon release induced by pancreatic nerve stimulation in the dog. *J. Clin. Invest.* 52, 1246–1259. doi: 10.1172/JCI107292

Marty, N., Dallaporta, M., Foretz, M., Emery, M., Tarussio, D., Bady, I., et al. (2005). Regulation of glucagon secretion by glucose transporter type 2 (glut2) and astrocyte-dependent glucose sensors. *J. Clin. Invest.* 115, 3545–3553. doi: 10.1172/JCI26309

Marty, N., Dallaporta, M., and Thorens, B. (2007). Brain glucose sensing, counter-regulation, and energy homeostasis. *Physiology* 22, 241–251. doi: 10.1152/physiol.00010.2007

Matthews, D. R., Lang, D. A., Burnett, M. A., and Turner, R. C. (1983). Control of pulsatile insulin secretion in man. *Diabetologia* 24, 231–237. doi: 10.1007/BF00282705

McAllen, R. M., Habler, H.-J., Michaelis, M., Peters, O., and Janig, W. (1994). Monosynaptic excitation of preganglionic vasomotor neurons by subretrofacial neurons of the rostral ventrolateral medulla. *Brain Res.* 634, 227–234. doi: 10.1016/0006-8993(94)91925-9

Mezey, E., Kiss, J. Z., Skirboll, L. R., Goldstein, M., and Axelrod, J. (1984). Increase of corticotropin-releasing factor staining in rat paraventricular nucleus neurones by depletion of hypothalamic adrenaline. *Nature* 310, 140–141. doi: 10.1038/310140a0

Miki, T., Liss, B., Minami, K., Shiuchi, T., Saraya, A., Kashima, Y., et al. (2001). ATP-sensitive K+ channels in the hypothalamus are essential for the maintenance of glucose homeostasis. *Nat. Neurosci.* 4, 507–512. doi: 10.1038/87455

Miller, R. E. (1981). Pancreatic neuroendocrinology: peripheral neural mechanisms in the regulation of the islets of Langerhans. *Endocr. Rev.* 2, 471–494. doi: 10.1210/edrv-2-4-471

Moghimzadeh, E., Ekman, R., Hakanson, R., Yanaihara, N., and Sundler, F. (1983). Neuronal gastrin-releasing peptide in the mammalian gut and pancreas. *Neuroscience* 10, 553–563. doi: 10.1016/0306-4522(83)90152-5

Morgan, C. R., and Lobl, R. T. (1968). A histochemical study of neuro-insular complexes in the pancreas of the rat. *Anat. Rec.* 160, 231–237. doi: 10.1002/ar.1091600209

Moriguchi, T., Sakurai, T., Nambu, T., Yanagisawa, M., and Goto, K. (1999). Neurons containing orexin in the lateral hypothalamic area of the adult rat brain are activated by insulin-induced acute hypoglycemia. *Neurosci. Lett.* 264, 101–104. doi: 10.1016/S0304-3940(99)00177-9

Moriyama, R., Tsukamura, H., Kinoshita, M., Okazaki, H., Kato, Y., and Maeda, K. (2004). *In vitro* increase in intracellular calcium concentrations induced by low or high extracellular glucose levels in ependymocytes and serotonergic neurons of the rat lower brainstem. *Endocrinology* 145, 2507–2515. doi: 10.1210/en.2003-1191

Morrison, S. F., Callaway, J., Milner, T. A., and Reis, D. J. (1989a). Glutamate in the spinal sympathetic intermediolateral nucleus: localization by light and electron microscopy. *Brain Res.* 503, 5–15. doi: 10.1016/0006-8993(89)91696-X

Morrison, S. F., and Cao, W. H. (2000). Different adrenal sympathetic preganglionic neurons regulate epinephrine and norepinephrine secretion. *Am. J. Physiol.* 279, R1763–R1775.

Morrison, S. F., Ernsberger, P., Milner, T. A., Callaway, J., Gong, A., and Reis, D. J. (1989b). A glutamate mechanism in the intermediolateral nucleus mediates sympathoexcitatory responses to stimulation of the rostral ventrolateral medulla. *Prog. Brain Res.* 81, 159–169. doi: 10.1016/S0079-6123(08)62006-3

Murphy, B. A., Fakira, K. A., Song, Z., Beuve, A., and Routh, V. H. (2009). AMP-activated protein kinase and nitric oxide regulate the glucose sensitivity of ventromedial hypothalamic glucose-inhibited neurons. *Am. J. Physiol.* 297, C750–C758. doi: 10.1152/ajpcell.00127.2009

Niijima, A. (1975). The effect of 2-deoxy-D-glucose and D-glucose on the efferent discharge rate of sympathetic nerves. *J. Physiol.* 251, 231–243.

Oesch, F., and Thoenen, H. (1973). Increased activity of the peripheral sympathetic nervous system: induction of choline acetyltransferase in the preganglionic cholinergic neurone. *Nature* 242, 536–537. doi: 10.1038/242536a0

O'Malley, D., Reimann, F., Simpson, A. K., and Gribble, F. M. (2006). Sodium-coupled glucose cotransporters contribute to hypothalamic glucose sensing. *Diabetes* 55, 3381–3386. doi: 10.2337/db06-0531

Oomura, Y., Kimura, K., Ooyama, H., Maeno, T., Iki, M., and Kuniyoshi, M. (1964). Reciprocal activities of the ventromedial and lateral hypothalamic areas of cats. *Science* 143, 484–485. doi: 10.1126/science.143.3605.484

Oomura, Y., Ono, T., Ooyama, H., and Wayner, M. J. (1969). Glucose and osmosensitive neurones of the rat hypothalamus. *Nature* 222, 282–284. doi: 10.1038/222282a0

Oomura, Y., Ooyama, H., Sugimori, M., Nakamura, T., and Yamada, Y. (1974). Glucose inhibition of the glucose-sensitive neurone in the rat lateral hypothalamus. *Nature* 247, 284–286. doi: 10.1038/247284a0

Oshima, N., Kumagai, H., Onimaru, H., Kawai, A., Pilowsky, P. M., Iigaya, K., et al. (2008). Monosynaptic excitatory connection from the rostral ventrolateral medulla to sympathetic preganglionic neurons revealed by simultaneous recordings. *Hypertens. Res.* 31, 1445–1454. doi: 10.1291/hypres.31.1445

Pacak, K., Palkovits, M., Kvetnansky, R., Yadid, G., Kopin, I. J., and Goldstein, D. S. (1995). Effects of various stressors on *in vivo* norepinephrine release in the hypothalamic paraventricular nucleus and on the pituitary-adrenocortical axis. *Ann. N.Y. Acad. Sci.* 771, 115–130. doi: 10.1111/j.1749-6632.1995.tb44675.x

Paranjape, S. A., Vavaiya, K. K., Kale, A. Y., and Briski, K. P. (2006). Habituation of insulin-induced hypoglycemic transcription activation of lateral hypothalamic orexin-A-containing neurons to recurring exposure. *Regul. Pept.* 135, 1–6. doi: 10.1016/j.regpep.2006.02.002

Pardal, R., and Lopez-Barneo, J. (2002). Low glucose-sensing cells in the carotid body. *Nat. Neurosci.* 5, 197–198. doi: 10.1038/nn812

Parker, L. M., Kumar, N. N., Lonergan, T., Goodchild, A. K. (2013). Neurochemical codes of sympathetic preganglionic neurons activated by glucoprivation. *J. Comp. Neurol.* 521, 2703–2718. doi: 10.1002/cne.23310

Pettersson, M., Ahren, B., Bottcher, G., and Sundler, F. (1986). Calcitonin gene-related peptide: occurrence in pancreatic islets in the mouse and the rat and inhibition of insulin secretion in the mouse. *Endocrinology* 119, 865–869. doi: 10.1210/endo-119-2-865

Pettersson, M., Ahren, B., Lundquist, I., Bottcher, G., and Sundler, F. (1987). Neuropeptide Y: intrapancreatic neuronal localization and effects on insulin secretion in the mouse. *Cell Tissue Res.* 248, 43–48. doi: 10.1007/BF01239960

Peyron, C., Tighe, D. K., van den Pol, A. N., de Lecea, L., Heller, H. C., Sutcliffe, J. G., et al. (1998). Neurons containing hypocretin (orexin) project to multiple neuronal systems. *J. Neurosci.* 18, 9996–10015.

Pilkis, S. J., el-Maghrabi, M. R., and Claus, T. H. (1988). Hormonal regulation of hepatic gluconeogenesis and glycolysis. *Annu. Rev. Biochem.* 57, 755–783. doi: 10.1146/annurev.bi.57.070188.003543

Plotsky, P. M., and Vale, W. (1985). Patterns of growth hormone-releasing factor and somatostatin secretion into the hypophysial-portal circulation of the rat. *Science* 230, 461–463. doi: 10.1126/science.2864742

Porte, D. Jr., and Williams, R. H. (1966). Inhibition of insulin release by norepinephrine in man. *Science* 152, 1248–1250. doi: 10.1126/science.152.3726.1248

Puskas, N., Papp, R. S., Gallatz, K., and Palkovits, M. (2010). Interactions between orexin-immunoreactive fibers and adrenaline or noradrenaline-expressing neurons of the lower brainstem in rats and mice. *Peptides* 31, 1589–1597. doi: 10.1016/j.peptides.2010.04.020

Pyner, S., and Coote, J. H. (1994). Evidence that sympathetic preganglionic neurones are arranged in target-specific columns in the thoracic spinal cord of the rat. *J. Comp. Neurol.* 342, 15–22. doi: 10.1002/cne.903420103

Rehfeld, J. F., Larsson, L. I., Goltermann, N. R., Schwartz, T. W., Holst, J. J., Jensen, S. L., et al. (1980). Neural regulation of pancreatic hormone secretion by the C-terminal tetrapeptide of CCK. *Nature* 284, 33–38. doi: 10.1038/284033a0

Richardson, K. C. (1964). The fine structure of the albino rabbit iris with special reference to the identification of adrenergic and cholinergic nerves and nerve endings in its intrinsic muscles. *Am. J. Anat.* 114, 173–205. doi: 10.1002/aja.1001140202

Ritter, R. C., Slusser, P. G., and Stone, S. (1981). Glucoreceptors controlling feeding and blood glucose: location in the hindbrain. *Science* 213, 451–452. doi: 10.1126/science.6264602

Ritter, S., Bugarith, K., and Dinh, T. T. (2001). Immunotoxic destruction of distinct catecholamine subgroups produces selective impairment of glucoregulatory responses and neuronal activation. *J. Comp. Neurol.* 432, 197–216. doi: 10.1002/cne.1097

Ritter, S., Dinh, T. T., and Li, A. J. (2006). Hindbrain catecholamine neurons control multiple glucoregulatory responses. *Physiol. Behav.* 89, 490–500. doi: 10.1016/j.physbeh.2006.05.036

Ritter, S., Li, A. J., Wang, Q., and Dinh, T. T. (2011). Minireview: the value of looking backward: the essential role of the hindbrain in counterregulatory responses to glucose deficit. *Endocrinology* 152, 4019–4032. doi: 10.1210/en.2010-1458

Ritter, S., Llewellyn-Smith, I. J., and Dinh, T. T. (1998). Subgroups of hindbrain catecholamine neurons are selectively activated by 2-deoxy-D-glucose induced metabolic challenge. *Brain Res.* 805, 41–54. doi: 10.1016/S0006-8993(98)00655-6

Ritter, S., Scheurink, A., and Singer, L. K. (1995). 2-Deoxy-D-glucose but not 2-mercaptoacetate increases Fos-like immunoreactivity in adrenal medulla and sympathetic preganglionic neurons. *Obes. Res.* 3 (Suppl. 5), 729S–734S.

Roth, J., Glick, S. M., Yalow, R. S., and Berson, S. A. (1963). Hypoglycemia: a potent stimulus to secretion of growth hormone. *Science* 140, 987–988. doi: 10.1126/science.140.3570.987

Routh, V. H. (2010). Glucose sensing neurons in the ventromedial hypothalamus. *Sensors (Basel)* 10, 9002–9025. doi: 10.3390/s101009002

Rowe, I. C., Treherne, J. M., and Ashford, M. L. (1996). Activation by intracellular ATP of a potassium channel in neurones from rat basomedial hypothalamus. *J. Physiol.* 490, 97–113.

Saberi, M., Bohland, M., and Donovan, C. M. (2008). The locus for hypoglycemic detection shifts with the rate of fall in glycemia: the role of portal-superior mesenteric vein glucose sensing. *Diabetes* 57, 1380–1386. doi: 10.2337/db07-1528

Saper, C. B., Loewy, A. D., Swanson, L. W., and Cowan, W. M. (1976). Direct hypothalamo-autonomic connections. *Brain Res.* 117, 305–312. doi: 10.1016/0006-8993(76)90738-1

Sawchenko, P. E., Swanson, L. W., Rivier, J., and Vale, W. W. (1985). The distribution of growth-hormone-releasing factor (GRF) immunoreactivity in the central nervous system of the rat: an immunohistochemical study using antisera directed against rat hypothalamic GRF. *J. Comp. Neurol.* 237, 100–115. doi: 10.1002/cne.902370108

Schreihofer, A. M., and Guyenet, P. G. (1997). Identification of C1 presympathetic neurons in rat rostral ventrolateral medulla by juxtacellular labeling *in vivo*. *J. Comp. Neurol.* 387, 524–536. doi: 10.1002/(SICI)1096-9861(19971103)387:4%3C524::AID-CNE4%3E3.0.CO;2-4

Schwartz, N. S., Clutter, W. E., Shah, S. D., and Cryer, P. E. (1987). Glycemic thresholds for activation of glucose counterregulatory systems are higher than the threshold for symptoms. *J. Clin. Invest.* 79, 777–781. doi: 10.1172/JCI112884

Shafton, A. D., Ryan, A., and Badoer, E. (1998). Neurons in the hypothalamic paraventricular nucleus send collaterals to the spinal cord and to the rostral ventrolateral medulla in the rat. *Brain Res.* 801, 239–243. doi: 10.1016/S0006-8993(98)00587-3

Siaud, P., Puech, R., Assenmacher, I., and Alonso, G. (1991). Microinjection of oxytocin into the dorsal vagal complex decreases pancreatic insulin secretion. *Brain Res.* 546, 190–194. doi: 10.1016/0006-8993(91)91480-O

Sim, L. J., and Joseph, S. A. (1991). Arcuate nucleus projections to brainstem regions which modulate nociception. *J. Chem. Neuroanat.* 4, 97–109. doi: 10.1016/0891-0618(91)90034-A

Song, Z., and Routh, V. H. (2005). Differential effects of glucose and lactate on glucosensing neurons in the ventromedial hypothalamic nucleus. *Diabetes* 54, 15–22. doi: 10.2337/diabetes.54.1.15

Strack, A. M., Sawyer, W. B., Hughes, J. H., Platt, K. B., and Loewy, A. D. (1989a). A general pattern of CNS innervation of the sympathetic outflow demonstrated by transneuronal pseudorabies viral infections. *Brain Res.* 491, 156–162. doi: 10.1016/0006-8993(89)90098-X

Strack, A. M., Sawyer, W. B., Marubio, L. M., and Loewy, A. D. (1988). Spinal origin of sympathetic preganglionic neurons in the rat. *Brain Res.* 455, 187–191. doi: 10.1016/0006-8993(88)90132-1

Strack, A. M., Sawyer, W. B., Platt, K. B., and Loewy, A. D. (1989b). CNS cell groups regulating the sympathetic outflow to adrenal gland as revealed by transneuronal cell body labeling with pseudorabies virus. *Brain Res.* 491, 274–296. doi: 10.1016/0006-8993(89)90063-2

Takanaga, A., Hayakawa, T., Tanaka, K., Kawabata, K., Maeda, S., and Seki, M. (2003). Immunohistochemical characterization of cardiac vagal preganglionic neurons in the rat. *Auton. Neurosci.* 106, 132–137. doi: 10.1016/S1566-0702(03)00127-9

Ter Horst, G. J., and Luiten, P. G. (1986). The projections of the dorsomedial hypothalamic nucleus in the rat. *Brain Res. Bull.* 16, 231–248. doi: 10.1016/0361-9230(86)90038-9

Ter Horst, G. J., and Luiten, P. G. (1987). *Phaseolus vulgaris* leuco-agglutinin tracing of intrahypothalamic connections of the lateral, ventromedial, dorsomedial and paraventricular hypothalamic nuclei in the rat. *Brain Res. Bull.* 18, 191–203. doi: 10.1016/0361-9230(87)90190-0

Ter Horst, G. J., Luiten, P. G. M., and Kuipers, F. (1984). Descending pathways from hypothalamus to dorsal motor vagus and ambiguus nuclei in the rat. *J. Auton. Nerv. Syst.* 11, 59–75. doi: 10.1016/0165-1838(84)90008-0

Tkacs, N. C., Pan, Y., Sawhney, G., Mann, G. L., and Morrison, A. R. (2007). Hypoglycemia activates arousal-related neurons and increases wake time in adult rats. *Physiol. Behav.* 91, 240–249. doi: 10.1016/j.physbeh.2007.03.003

Tong, Q., Ye, C., McCrimmon, R. J., Dhillon, H., Choi, B., Kramer, M. D., et al. (2007). Synaptic glutamate release by ventromedial hypothalamic neurons is part of the neurocircuitry that prevents hypoglycemia. *Cell Metab.* 5, 383–393. doi: 10.1016/j.cmet.2007.04.001

Torigoe, Y., Cernucan, R. D., Nishimoto, J. A., and Blanks, R. H. (1985). Sympathetic preganglionic efferent and afferent neurons mediated by the greater splanchnic nerve in rabbit. *Exp. Neurol.* 87, 334–348. doi: 10.1016/0014-4886(85)90224-9

Verberne, A. J., and Sartor, D. M. (2010). Rostroventrolateral medulla neurons modulate glucose homeostasis in the rat. *Am. J. Physiol.* 299, E802–E807. doi: 10.1152/ajpendo.00466.2010

Verberne, A. J. M., Stornetta, R. L., and Guyenet, P. G. (1999). Properties of C1 and other ventrolateral medullary neurones with hypothalamic projections in the rat. *J. Physiol.* 517, 477–494. doi: 10.1111/j.1469-7793.1999.0477t.x

Watari, N. (1968). Fine structure of nervous elements in the pancreas of some vertebrates. *Z. Zellforsch. Mikrosk. Anat.* 85, 291–314. doi: 10.1007/BF00328843

Wehrwein, E. A., Basu, R., Basu, A., Curry, T. B., Rizza, R. A., and Joyner, M. J. (2010). Hyperoxia blunts counterregulation during hypoglycaemia in humans: possible role for the carotid bodies? *J. Physiol.* 588, 4593–4601. doi: 10.1113/jphysiol.2010.197491

Williams, R. H., Alexopoulos, H., Jensen, L. T., Fugger, L., and Burdakov, D. (2008). Adaptive sugar sensors in hypothalamic feeding circuits. *Proc. Natl. Acad. Sci. U.S.A.* 105, 11975–11980. doi: 10.1073/pnas.0802687105

Woods, S. C., and Porte, D. Jr. (1974). Neural control of the endocrine pancreas. *Physiol. Rev.* 54, 596–619.

Wu, X., Gao, J., Yan, J., Owyang, C., and Li, Y. (2004). Hypothalamus-brain stem circuitry responsible for vagal efferent signaling to the pancreas evoked by hypoglycemia in rat. *J. Neurophysiol.* 91, 1734–1747. doi: 10.1152/jn.00791.2003

Yardley, C. P., and Hilton, S. M. (1987). Vasodilatation in hind-limb skeletal muscle evoked as part of the defence reaction in the rat. *J. Auton. Nerv. Syst.* 19, 127–136. doi: 10.1016/0165-1838(87)90006-3

Zagon, A., and Bacon, S. J. (1991). Evidence of a monosynaptic pathway between cells of the ventromedial medulla and the motoneuron pool of the thoracic spinal cord in rat: electron microscopic analysis of synaptic contacts. *Eur. J. Neurosci.* 3, 55–65. doi: 10.1111/j.1460-9568.1991.tb00811.x

Zheng, L. F., Zhang, Y., Chen, C. L., Song, J., Fan, R. F., Cai, Q. Q., et al. (2013). Alterations in TH- and ChAT-immunoreactive neurons in the DMV and gastric dysmotility in an LPS-induced PD rat model. *Auton. Neurosci.* 177, 194–198. doi: 10.1016/j.autneu.2013.04.012

Zhu, W., Czyzyk, D., Paranjape, S. A., Zhou, L., Horblitt, A., Szabo, G., et al. (2010). Glucose prevents the fall in ventromedial hypothalamic GABA that is required for full activation of glucose counterregulatory responses during hypoglycemia. *Am. J. Physiol.* 298, E971–E977. doi: 10.1152/ajpendo.00749.2009

Conflict of Interest Statement: The authors declare that the research was conducted in the absence of any commercial or financial relationships that could be construed as a potential conflict of interest.

Received: 09 October 2013; accepted: 10 February 2014; published online: 26 February 2014.

*Citation: Verberne AJM, Sabetghadam A and Korim WS (2014) Neural pathways that control the glucose counterregulatory response. Front. Neurosci. **8**:38. doi: 10.3389/fnins.2014.00038*

This article was submitted to Autonomic Neuroscience, a section of the journal Frontiers in Neuroscience.

frontiers in
NEUROSCIENCE

ORIGINAL RESEARCH ARTICLE
published: 10 December 2013
doi: 10.3389/fnins.2013.00226

Alterations in blood glucose and plasma glucagon concentrations during deep brain stimulation in the shell region of the nucleus accumbens in rats

Charlene Diepenbroek[1]*†, Geoffrey van der Plasse[2,3]†, Leslie Eggels[1], Merel Rijnsburger[1], Matthijs G. P. Feenstra[4,5], Andries Kalsbeek[1,6], Damiaan Denys[4,5], Eric Fliers[1], Mireille J. Serlie[1] and Susanne E. la Fleur[1]

[1] Department of Endocrinology and Metabolism, Academic Medical Center, University of Amsterdam, Amsterdam, Netherlands
[2] Department of Psychiatry, Brain Center Rudolf Magnus, University Medical Center, Utrecht, Netherlands
[3] Department of Translational Neuroscience, Brain Center Rudolf Magnus, University Medical Center Utrecht, Utrecht, Netherlands
[4] Department of Psychiatry, Academic Medical Center, University of Amsterdam, Amsterdam, Netherlands
[5] Department of Neuromodulation and Behaviour, Netherlands Institute for Neuroscience, an institute of the Royal Netherlands Academy of Arts and Sciences, Amsterdam, Netherlands
[6] Department of Hypothalamic Integration Mechanisms, Netherlands Institute for Neuroscience, an institute of the Royal Netherlands Academy of Arts and Sciences, Amsterdam, Netherlands

Edited by:
Heike Muenzberg-Gruening, Pennington Biomedical Research Center, USA

Reviewed by:
Ronald M. Harper, University of California Los Angeles School of Medicine, USA
Kirsteen Browning, Penn State College of Medicine, USA

***Correspondence:**
Charlene Diepenbroek, Department of Endocrinology and Metabolism Academic Medical Center, University of Amsterdam, Meibergdreef 9, F2-131-1, 1105 AZ Amsterdam, Netherlands
e-mail: c.diepenbroek@amc.uva.nl
† *These authors have contributed equally to this work.*

Deep brain stimulation (DBS) of the nucleus accumbens (NAc) is an effective therapy for obsessive compulsive disorder (OCD) and is currently under investigation as a treatment for eating disorders. DBS of this area is associated with altered food intake and pharmacological treatment of OCD is associated with the risk of developing type 2 diabetes. Therefore we examined if DBS of the NAc-shell (sNAc) influences glucose metabolism. Male Wistar rats were subjected to DBS, or sham stimulation, for a period of 1 h. To assess the effects of stimulation on blood glucose and glucoregulatory hormones, blood samples were drawn before, during and after stimulation. Subsequently, all animals were used for quantitative assessment of Fos immunoreactivity in the lateral hypothalamic area (LHA) using computerized image analysis. DBS of the sNAc rapidly increased plasma concentrations of glucagon and glucose while sham stimulation and DBS outside the sNAc were ineffective. In addition, the increase in glucose was dependent on DBS intensity. In contrast, the DBS-induced increase in plasma corticosterone concentrations was independent of intensity and region, indicating that the observed DBS-induced metabolic changes were not due to corticosterone release. Stimulation of the sNAc with 200 μA increased Fos immunoreactivity in the LHA compared to sham or 100 μA stimulated animals. These data show that DBS of the sNAc alters glucose metabolism in a region- and intensity- dependent manner in association with neuronal activation in the LHA. Moreover, these data illustrate the need to monitor changes in glucose metabolism during DBS-treatment of OCD patients.

Keywords: deep brain stimulation (DBS), nucleus accumbens shell, lateral hypothalamic area, glucose, glucoregulatory hormones, neural activity

INTRODUCTION

Deep brain stimulation (DBS) of the nucleus accumbens (NAc) is used to treat obsessive compulsive disorder (OCD), depression and addiction (Denys et al., 2010; Bewernick et al., 2012; Muller et al., 2013) and is currently under investigation for the treatment of eating-disorders (eg., Halpern et al., 2008). Although the precise mechanisms through which DBS exerts its effects remain to be elucidated, recent data from human and animal studies suggest that DBS directly affects neuronal network activity (McCracken and Grace, 2007; Vandehey et al., 2010; Tan et al., 2011; Figee et al., 2013) and alters neurotransmitter release (van Dijk et al., 2012; Halpern et al., 2013).

Effective pharmacological treatment of OCD, such as anti-depressants and serotonin reuptake inhibitors target the dopaminergic- and serotoninergic system. This suggests that modulation of these neurotransmitter systems could well be involved in the effects of DBS. Unfortunately, drugs targeting these neurotransmitter systems increase the risk to develop type 2 diabetes, through direct modulation of glucose metabolism, independent of alterations in body weight. In addition, DBS of the NAc has been associated with changes in food intake (van der Plasse et al., 2012; Halpern et al., 2013). In light of these findings, and the current interest in DBS as a treatment for eating-disorders (Benabid and Torres, 2012), it is imperative to determine whether DBS might influence glucose metabolism and thus induce side effects.

Central control of glucose metabolism is mediated by multiple brain areas and neurotransmitter systems that include serotonergic neurons in the raphe nucleus, noradrenergic neurons in the locus coeruleus, and hypothalamic nuclei that project,

directly and indirectly to brainstem nuclei that regulate autonomic outflow (Lechin and van der Dijs, 2006; Marino et al., 2011). Of these, hypothalamic nuclei are ideally situated to sense and integrate peripheral metabolic signals and regulate autonomic tone to maintain a positive energy balance. With respect to possible NAc DBS-induced alterations in glucose metabolism and food intake, early viral tracing experiments in rats revealed a neural connection between the NAc (part of the ventral striatum) and pancreas (Buijs et al., 2001). Specifically, the shell region of the NAc (sNAc) projects to the lateral hypothalamic area (LHA), directly as well as via the ventral pallidum (Zahm and Brog, 1992). The LHA, in turn, projects to the dorsal motor nucleus of the vagus, the ventral lateral medulla and preganglionic spinal cord neurons, all of which project to the pancreas to regulate endocrine pancreatic functions, but also project to the liver and thus may alter glucose metabolism (Buijs et al., 2001; Berthoud, 2004; Wu et al., 2004; Yi et al., 2010).

It is well documented that the projection between the sNAc and the LHA plays a role in food directed behavior (Kelley and Swanson, 1997; Stratford and Kelley, 1999). Recently, van der Plasse et al. (2012) showed that DBS of the sNAc in free-fed rats with access to normal chow elicits feeding behavior. However, to date, a role for this neuroanatomical connection in the regulation of glucose metabolism has not been investigated. We hypothesized that the neural connection between the sNAc and pancreas (and liver) is functional in glucose metabolism. To investigate this hypothesis, we implanted stimulation electrodes in the sNAc of rats and studied the effects of local stimulation on blood glucose and glucoregulatory hormones. In addition, to test if the LHA is involved in the effects of sNAc stimulation we measured the Fos response in the LHA following DBS of the sNAc, as a marker for neuronal activity. We subjected rats to 1h stimulation at two different intensities. Prior to-, during-, and after cessation of stimulation, blood samples were drawn and concentrations of blood glucose and plasma glucoregulatory hormones were measured. Subsequently, brain sections were stained and Fos activation in the LHA was quantified. This study shows for the first time the effects of electrical stimulation in the sNAc on neural activity in the LHA and on glucose metabolism.

METHODS

ANIMALS

Twenty five male Wistar rats (250–280 g; Harlan, Horst, the Netherlands) were individually housed in Plexiglas cages in a temperature (20 ± 2°C), humidity (60 ± 2%) and light controlled room with a 12/12 h light-dark schedule (lights on at 7:00 h AM). All animals had *ad libitum* access to laboratory chow (Teklad Global 18% Protein Rodent Diet, Harlan, Horst, Netherlands) and tap water prior to testing.

Rats were adapted to handling in the period prior to surgery. The experiment was performed in the rat's home cage. The experiment was approved by the Committee for Animal Experimentation of the Academic Medical Center of the University of Amsterdam, Netherlands.

SURGERY

Rats were anaesthetized with an i.p. injection of 80 mg/kg Ketamine (Eurovet Animal Health, Bladel, Netherlands), 8 mg/kg Rompun® (xylazine, Bayer Health Care, Mijdrecht, Netherlands) and 0.1 mg/kg Atropine (Pharmachemie B. V., Haarlem, Netherlands), after which an intra-atrial silicone catheter was implanted in the jugular vein, according to the method of Steffens (1969). After catheter implantation, rats were bilaterally implanted with bipolar electrodes (dual stainless steel electrodes, 300 μm length, 125 μm diameter, distance between poles was 100 μm, 325 μm of the end of the electrodes was stripped; PlasticOne) aimed at the sNAc (A + 1.44 mm, L + 3 mm, V −7.3 mm, angle 17°), using a stereotaxic apparatus (Kopf). Catheters and electrodes were fixed on the skull with dental cement. Rats received a recovery period of 7 days.

STIMULATION

Four hours prior to stimulation food was removed (i.e., at 8:00h AM). Animals were connected to the blood-sampling catheter and electrode implants were attached to stimulation cables which were, via an electrically-shielded dual channel swivel (Med Associates, St Albans, VT, USA), connected to stimulation equipment. The sampling catheter and cables were kept out of reach by means of a counterbalanced beam. This allowed the animals to move freely during the experiment and allowed all manipulations to be performed outside the cages without handling the animals.

On experimental days a total of 25 rats were subjected to 60 min of either 100 μA ($n = 12$) or 200 μA ($n = 13$) or sham (all animals) stimulation. Each animal served as its own control and was, controlled for body weight, randomly assigned to an experimental group. Each experimental day all three stimulation conditions were applied. Rats received 7 days of recovery before being switched in experimental condition.

Stimulations were performed with a digital stimulator (DS8000, World Precision Instruments, Sarasota, USA) and stimulus isolator (DLS100, World Precision Instruments, Sarasota, USA). Stimulation parameters were as follows; biphasic square pulses, 60 μs duration, 200 μs 'zero' time, frequency 130 Hz. Blood samples were drawn prior ($t = -1$ min, baseline) during ($t = 5$, $t = 10$, $t = 15$, $t = 30$, $t = 60$ min) and following cessation of stimulation ($t = 90$ and $t = 120$ min).

ANALYTICAL METHODS

Blood glucose concentrations were measured directly during the experiment, using a custom glucose meter (Freestyle Freedom Lite, Abbot, Hoofddorp, Netherlands). Blood samples were immediately chilled on ice in Eppendorf tubes with 5 μL heparin: saline (10x) solution and centrifuged at 4°C (15 min, 3000 rpm). Plasma samples were stored at −20°C until further analysis. Plasma insulin, glucagon and corticosterone concentrations were measured using radioimmunoassay kits (Millipore, St Charles, MO, USA and Biochemicals, Costa Mesa, CA, respectively). The amount of sample-, standards-, label-, antibody and precipitating reagent, described in the manufacture's protocol, were divided by four. The variation-coefficient of the immunoassays was < 10%.

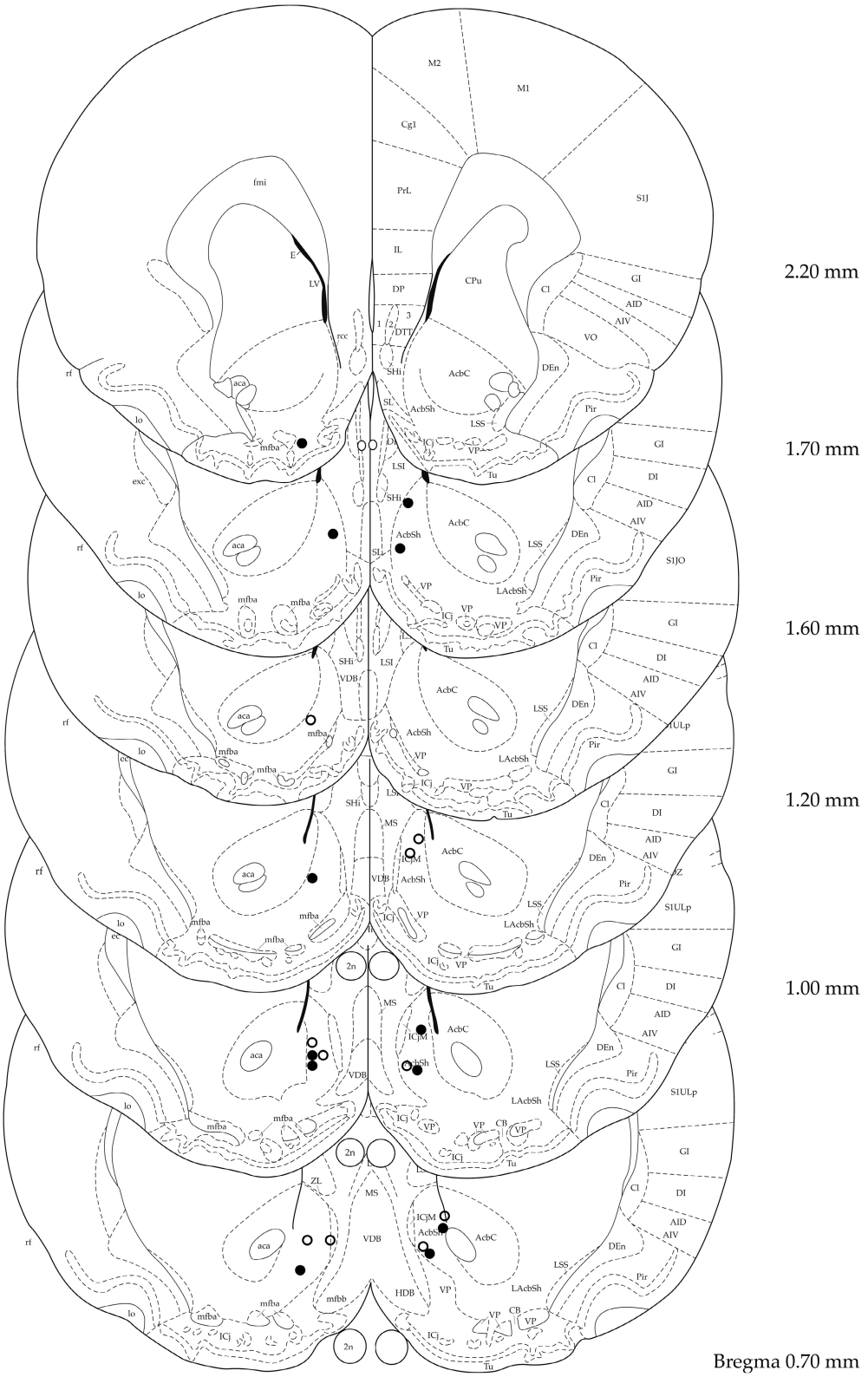

FIGURE 1 | Localization of electrode tips in 100 μA (black circles) and 200 μA (white circles) stimulated animals. Adapted from (Paxinos and Watson, 1998).

HISTOLOGY AND IMMUNOCYTOCHEMISTRY

At the end of the experiment ($t = 120$), animals were anaesthetized with a CO_2/O_2 mixture (6:4) followed by 100% CO_2 and killed by decapitation. Brains were then rapidly removed, frozen on dry ice and stored at −80°. Brain tissue was cut on a cryostat in 35 μm sections. Sections were collected on gelatin coated slides and fixed for 10 min in 4% paraformaldehyde at room temperature. For verification of electrode placement, slides were Nissl-stained after fixation and examined with a microscope to determine precise location of the electrodes. Given the functional specificity of the sNAc in the (para)sympathetic projection to the pancreas and liver, electrode placement was considered misplaced when electrode tips were observed outside the sNAc according to the delineation of Paxinos and Watson (1998).

For immunohistochemical staining, sections were incubated with 10% methanol, 3% H_2O_2 in Tris-buffered saline (TBS, 0.06 M Tris, 0.2 M NaCl, pH 7.6) for 10 min. Slides were then rinsed in TBS (3 times, 10 min) and incubated overnight at 4°C with goat anti-Fos IgG (1:1500; Santa Cruz Biotechnology, Inc., California) diluted in supermix (SUMI, 0.25% gelatin, 0.5% Triton X-100 in TBS (pH 7.6)). Following incubation, slides were rinsed in TBS (3 times, 10 min), incubated for 1 h in biotinylated horse anti-goat IgG (1:400 in SUMI; Vector Laboratories Inc., Burlingame, CA), rinsed in TBS (3 times, 10 min), and incubated for 1 h in avidin-biotin complex (ABC in SUMI, Vector Laboratories Inc., Burlingame, CA). Following incubation, slides were rinsed in TBS (3 times, 10 min). The reaction product was visualized by incubation in 1% diaminobenzidine (DAB) (0.05% nickel ammonium sulphate was added to the DAB solution to darken the reaction product) with 0.01% H_2O_2 for 7 min. After incubation, slides were rinsed with water. Finally, slides were run through ethanol and xylene and covered for observation by light microscopy.

ANALYSIS OF Fos IMMUNOREACTIVITY

Fos immunoreactivity in the LHA was identified and displayed with a computerized image analysis system consisting of a Zeiss Axioskop and a Media Cybermetrics evolution 9801 video camera (Media Cybernetics, Silver Spring, MD, USA). The LHA was manually outlined in every captured image. The Fos-postive nuclear profiles were manually counted using locally programmed software developed at the Netherlands Institute for Neuroscience. Quantification of Fos was performed by an experimenter who was blind to the experimental conditions. For each rat, one section was measured every 1.80 mm (from bregma −1.20 to −4.56 mm). Subsequently, the mean number of Fos-positive cells in these sections was calculated.

STATISTICS

All data are presented as means ± SEM. Statistical analysis was performed using a repeated-measure analysis of variance (rmANOVA) (SPSS Inc, Chicago, USA) to test for effects of *time, stimulation* and *time* ∗ *stimulation* interaction. When a treatment or interaction effect was detected, a paired-samples *t*-test test was used to test for group differences. Data were tested on outliers with the Grubbs'outlier test (GraphPad Sofware, Inc, La Jolla, USA). Fos immunoreactivity was statistically analyzed using the non-parametric Kruskall Wallis test. A difference was considered significant when $p < 0.05$ and as a trend when $p < 0.10$.

RESULTS

HISTOLOGY

Figure 1 shows electrode placement of all animals that were bilaterally stimulated in the target area and were included in the analysis. Verification of electrode placement revealed correct placement of the electrodes in the sNAc in 6 out of 12 and 5 out of 13 animals in the 100 and 200 μA groups, respectively. Data of animals with misplaced electrodes were analyzed per condition (100 μA: $n = 3$, 200 μA: $n = 5$) and used to assess the topographical specificity of sNAc stimulation. In four animals ($n = 2$ for both stimulation conditions), electrode placement could not be verified due to absence of traces in brain tissue. Two animals could not be used for analysis due to incomplete data sets.

CONCENTRATIONS OF BLOOD GLUCOSE AND PLASMA GLUCOREGULATORY HORMONES

Baseline concentrations of blood glucose and plasma concentrations of glucagon, insulin and corticosterone were not significantly different between the 100 μA, 200 μA or sham condition (**Table 1**).

Although blood glucose concentrations changed over time, there were no differences between rats stimulated with 100 μA compared to controls (**Figure 2A**). In contrast, blood glucose concentrations showed a significant increase during bilateral sNAc stimulation with 200 μA, which was significant at $t = 5$ and $t = 30$ compared to the sham condition while a trend was detected for $t = 10$ (**Figure 2B**, see figure legends for statistics).

Bilateral sNAc stimulation with 200 μA increased plasma glucagon concentrations compared to the sham condition with

Table 1 | Basal concentrations of blood glucose, plasma glucagon, corticosterone and insulin in the 100 ($n = 6$) and 200 μA ($n = 5$) stimulated animals and their sham condition.

	sham 100 μA	DBS 100 μA	sham 200 μA	DBS 200 μA
Glucose (mmol/l)	6.4 ± 0.1	6.6 ± 0.1	6.6 ± 0.1	6.4 ± 0.1
Glucagon (ng/l)	87.5 ± 5.5	89.9 ± 6.7	77.2 ± 11.7	81.0 ± 8.1
Corticosterone (nmol/l)	33.1 ± 9.5	73.9 ± 35.4	35.0 ± 14.8	44.7 ± 12.2
Insulin (pmol/l) kloppen de	635.9 ± 104.2	692.2 ± 174.0	516.3 ± 135.0	535.9 ± 269.3

Data are means ± SEM.

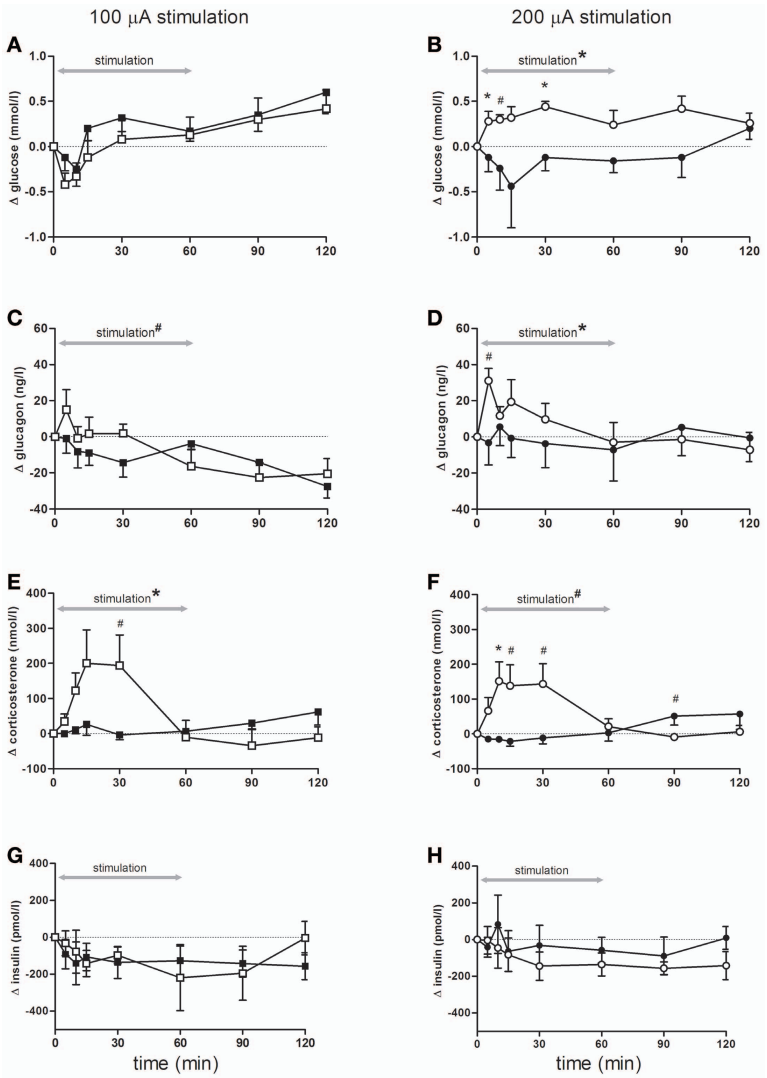

FIGURE 2 | Blood glucose concentrations (A,B), and plasma- glucagon (C,D), corticosterone (E,F) and insulin (G,H) concentrations during and following stimulation. Effects of 100 μA stimulation ($n = 6$) are shown in the left column, black squares = sham stimulation, white squares = 100 μA stimulation (**A,C,E,G**), the right column (**B,D,F,H**) shows stimulation at 200 μA ($n = 5$), black circles = sham stimulation, white circles = 200 μA stimulation. All data are presented as mean ± SEM. $^{*}p < 0.05$, $^{\#}p < 0.10$. (**A–B**) Blood glucose concentrations were significantly elevated following stimulation at 200 μA compared with sham stimulation. (A) An overall time effect ($p < 0.001$), but no stimulation or interaction effect. **(B)** rmANOVA indicated an effect of stimulation ($p = 0.03$), post-hoc testing showed that glucose concentrations were significant higher at $t = 5$, and $t = 30$ (both $p = 0.04$), a trend was detected for $t = 10$ ($p = 0.06$). **(C,D)** Plasma glucagon concentrations significantly increased following stimulation at 200 μA compared with sham. **(C)** An effect of time ($p < 0.001$) and a trend for time ∗ stimulation ($p = 0.09$). **(D)** rmANOVA revealed a significant effect of time ($p = 0.05$) and time ∗ stimulation ($p = 0.03$). A trend for higher glucagon elevations was detected at $t = 5$ ($p = 0.07$). **(E,F)** Stimulation at both intensities increased plasma corticosterone concentrations. **(E)** rmANOVA revealed a time ($p < 0.001$) and an interaction effect between time and stimulation ($p < 0.001$). *Post-hoc* analysis revealed a trend for $t = 30$ ($p = 0.09$). **(F)** rmANOVA revealed a trend for time ($p = 0.10$), a significant effect of time ∗ stimulation ($p < 0.001$) and a trend for stimulation ($p = 0.07$). Corticosterone elevation was significant at $t = 10$ ($p = 0.05$) and a trend was detected for $t = 15$, $t = 30$, $t = 90$ ($p = 0.07$, $p = 0.06$ and $p = 0.08$ respectively). **(G,H)** Plasma insulin concentrations were not significant different between the stimulation and sham condition of either 100 or 200 μA stimulated animals.

the highest glucagon concentrations measured at 5 min after DBS onset (**Figure 2D**). After cessation of stimulation, plasma glucagon concentrations returned to pre-stimulation concentrations and were comparable to plasma concentrations of the sham condition. Statistical analysis showed a significant effect of time, and a trend toward a significant effect of bilateral sNAc stimulation with 100 μA (**Figure 2C**).

Plasma corticosterone concentrations significantly increased during 100 μA and showed a trend for an increase during 200 μA stimulation when compared to their own sham condition (**Figures 2E,F**). *Post-hoc* analysis revealed that plasma corticosterone concentrations with 100 μA stimulation showed an increase compared to the sham condition at $t = 30$, although this did not reach significance (**Figure 2E**).

There were no significant differences in plasma insulin concentrations in animals stimulated with 100 μA or 200 μA compared to their non-stimulation condition (**Figures 2G,H**).

Statistical analysis of blood glucose and plasma glucoregulatory hormones in the animals with misplaced electrodes revealed a significant increase in plasma corticosterone concentrations during both 100 μA and 200 μA stimulation while concentrations of blood glucose and plasma concentrations of glucagon and insulin were not significantly changed.

NEURAL ACTIVATION IN THE LATERAL HYPOTHALAMIC AREA

The results of Fos immunoreactivity quantification, and a representative histological section showing Fos-positive cells for each stimulation condition are presented in **Figure 3**. Quantification of neuronal activity revealed that stimulation of the sNAc with 200 μA increased Fos expression in the LHA compared to no stimulation (sham) or stimulation with 100 μA. One animal in the 100 μA stimulation group had to be excluded after being identified as an outlier ($p < 0.05$).

DISCUSSION

We here show that DBS of the sNAc affects systemic concentrations of glucose and glucagon in a region- and intensity-dependent manner. These data thus suggest a role for the sNAc in glucose metabolism through controlling pancreatic and/or hepatic output. Importantly, these data indicate that DBS stimulation used for treating OCD and, which may in future be used for treating eating disorders, may induce metabolic changes.

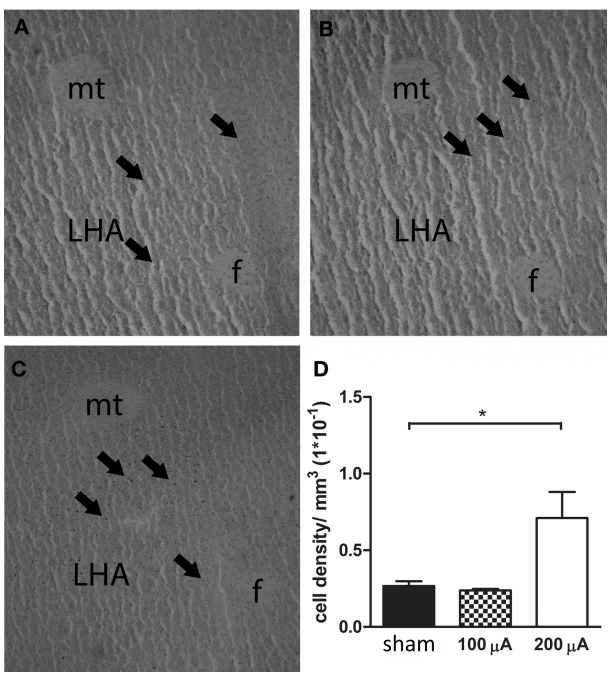

FIGURE 3 | Representative histological section of a sham (A), 100 μA (B) and 200 μA (C) stimulated rat showing Fos-positive cells in the lateral hypothalamic area (LHA). Arrows indicate Fos-positive nuclei. *f*, fornix, *mt*, mammillothalamic tract. **(D)** Number of Fos positive cells in the LHA of sham, 100 μA and 200 μA stimulated animals ($n = 3$–5). Fos staining was significantly increased in 200 μA stimulated animals compared to sham stimulated animals (*$p = 0.035$).

Following onset of stimulation, concentrations of both blood glucose and plasma glucagon acutely increased and, in the case of glucose, lasted for the duration of the stimulation. These increases were stimulation intensity dependent as DBS at 100 μA did not yield these effects. DBS did not affect plasma insulin concentrations at either intensity tested, but it did increase plasma corticosterone concentrations at both stimulation intensities (100 and 200 μA). Especially the latter result is of interest as it indicates that DBS of the sNAc can induce a physiological stress-like response, although behavioral experiments in rodents show no increased anxiety or altered locomotor activity after acute sNAc stimulation (van Dijk et al., 2013).

The increase in plasma corticosterone concentrations at both stimulation intensities (100 and 200 μA), observed in our study, indicates that the higher glucose concentrations are not driven by a DBS-induced increase in general arousal/stress, as only 200 μA increased plasma glucose concentrations. This is further supported by the finding that also in animals with misplaced electrodes plasma corticosterone concentrations increased but blood glucose or plasma glucagon concentrations did not. Importantly, the latter observation suggests that the increased concentrations of glucagon and glucose are specific to DBS of the sNAc as stimulation just outside this area did not evoke a response.

With respect to the neural network that might mediate these effects, it is interesting that the sNAc is anatomically connected to the pancreas, via projections to the LHA and brainstem (Buijs et al., 2001). Indeed, we observed specific activation of the LHA following stimulation, whereas no activation was observed in other areas within the hypothalamus (data not shown). Future experiments are needed to elucidate whether brainstem nuclei are also activated. Interestingly, the Fos expression in the LHA appeared intensity dependent, showing increased expression only at the higher stimulation intensity. This suggests that the higher intensity affects projection areas of the sNAc, whereas the stimulation at 100μA does not, which is also in line with the finding that glucose and glucagon levels were only affected with high intensity stimulation. It is however, unclear at this point which subsets of neurons are activated in the LHA. Several neuropeptides are expressed in the LHA that are known to be involved in energy metabolism. Of special interest are the orexin neurons, which have been shown to receive input from the NAc (Zheng et al., 2003) and are involved in the regulation of glucose metabolism (Yi et al., 2009).

We hypothesize that the increase in blood glucose concentrations is driven by the DBS-stimulated release of glucagon from pancreatic alpha cells. Although the rise in glucagon is small, it has been shown that, in isolated perfused rat livers, small glucagon peaks of 0.4 ug/l induce glycogenolysis and increase glucose concentrations (Sokal et al., 1964). The rise in blood glucose might, however, also result from a direct effect of DBS on the muscle or liver via neural innervation. Sudo et al. (1991), for example, showed that peripheral glucose uptake is under hypothalamic control. Furthermore, we previously showed that the LHA is neurally connected to the liver, and that a GABA antagonist administered to the LHA increased plasma glucose

concentrations, which could be prevented by a sympathetic liver denervation (Yi et al., 2009). Administering a GABA antagonist in the LHA did not, however, affect plasma glucagon concentrations making it unlikely that this projection to the liver, if involved, is also underlying the effects of DBS on plasma glucagon concentrations.

The increase in glucagon secretion from pancreatic alpha cells might be achieved via direct stimulation of sympathetic efferents or via sympathetic stimulation of adrenal-norepinephrine (NA) release [eg., Zsombok and Smith (2009); Taborsky and Mundinger (2012)]. As such, it is possible that DBS-induced activation of the HPA-axis contributed to the increase in glucagon via increased NA release. For a more detailed description of these alternative pathways we recommend a recent review by Taborsky and Mundinger (2012). As glucagon secretion is under para- as well as sympathetic control, we cannot distinguish from our data which nervous system is involved. Future experiments could shed light on the relative role of each of these pathways in the regulation of glucose metabolism during DBS and the relative contribution of sympathetic versus parasympathetic activity by combining DBS with the inclusion of independent measures of sympathetic/parasympathetic activity, such as heart rate variation.

In contrast to the effects of DBS on glucagon and glucose, we observed no changes in plasma insulin concentrations, suggesting that DBS of the sNAc does not directly act on pancreatic beta cells. This concept is supported by observations reported by others that electrical stimulation of the ventrolateral hypothalamic area (Helman et al., 1980) and LHA (Helman et al., 1983), induces a rise in glucagon without a rise in insulin. It could be surprising that the glucose increase we observed after DBS did not affect insulin concentrations as *ex vivo* experiments with perfused pancreatic islets from Wistar rats, showed that glucose oscillations with amplitudes between ∼0.5 and ∼1.5 mmol/L induces insulin secretory oscillations (Chou and Ipp, 1990). However, *in vivo* measurements support our findings by showing that higher glucose oscillations (≧1 mmol/L) were not accompanied by plasma insulin elevations (Yi et al., 2009). This may suggest that the increase in glucose, observed in animals stimulated with 200 μA, was not sufficient to induce an elevation in plasma insulin concentrations.

To date, the role of the sNAc in the regulation of glucose metabolism has received little attention whereas its role in food-motivated behavior is well established (Diepenbroek et al., 2013). The effects of DBS, we present here, point toward a role for this nucleus in the response to hypoglycaemia. Glucose-sensitive and, to a lesser extent, glucose-receptor cells are present in the sNAc (Papp et al., 2007). In addition, the sNAc is responsive to 2-deoxy-D-glucose (2DG), a glucose analog that inhibits glycolysis (Dodd et al., 2010). Hypoglycaemia could be sensed in the sNAc, and glucose homeostasis would be restored by the secretion of glucagon and stimulation of food consumption. The latter is supported by the study of (Dodd et al., 2010) that showed that the sNAc, as well as the orbitofrontal cortex and ventral pallidum are responsive to 2DG. Together, these regions form a corticostriatal connection with the hypothalamus via which processes of reward can influence the hypothalamic control of feeding behavior (Swanson, 2000; Fulton, 2010) and probably also glucose metabolism.

Apart from showing a functional role of the sNAc in glucose metabolism, these data are of great importance for the clinical use of DBS. These data show that stimulation of the sNAc with DBS for the treatment of psychiatric- and eating disorders may directly affect normal energy homeostasis and induce unwanted side-effects. Although interesting and potentially useful in employing DBS for eating-disorders, these data point out that the effects of DBS are not limited to the brain but also affect peripheral functions which should be taken into consideration when applying DBS.

In summary, we demonstrated that DBS of the sNAc in rats increased blood glucose concentrations and plasma glucagon concentrations in a region and intensity- dependent manner. These data are the first to show a direct relation between the use of DBS in the sNAc and changes in systemic concentrations of glucose and glucagon.

ACKNOWLEDGMENTS

The authors acknowledge Rianne van der Spek and José van den Heuvel of the Department of Endocrinolgy and Metabolism, Academic Medical Center, Amsterdam and Els Johannesma-Brian and Ruud Roozeboom of the Department of Clinical Chemistry, Laboratory of Endocrinology, Academic Medical Center, Amsterdam and Joop van Heerikhuize of the Netherlands Institute of Neuroscience, Amsterdam for excellent technical support.

FUNDING

This research was supported by Netherlands Organization for Scientific Research (ZonMw VIDI 917.96.331 & TOP 912.07.036).

REFERENCES

Benabid, A. L., and Torres, N. (2012). New targets for DBS. *Parkinsonism Relat. Disord.* 18(Suppl. 1), S21–S23. doi: 10.1016/S1353-8020(11)70009-8

Berthoud, H. R. (2004). Anatomy and function of sensory hepatic nerves. *Anat. Rec. A Discov. Mol. Cell. Evol. Biol.* 280, 827–835. doi: 10.1002/ar.a.20088

Bewernick, B. H., Kayser, S., Sturm, V., and Schlaepfer, T. E. (2012). Long-term effects of nucleus accumbens deep brain stimulation in treatment-resistant depression: evidence for sustained efficacy. *Neuropsychopharmacology* 37, 1975–1985. doi: 10.1038/npp.2012.44

Buijs, R. M., Chun, S. J., Niijima, A., Romijn, H. J., and Nagai, K. (2001). Parasympathetic and sympathetic control of the pancreas: a role for the suprachiasmatic nucleus and other hypothalamic centers that are involved in the regulation of food intake. *J. Comp. Neurol.* 431, 405–423. doi: 10.1002/1096-9861(20010319)431:4<405::AID-CNE1079>3.0.CO;2-D

Chou, H. F., and Ipp, E. (1990). Pulsatile insulin secretion in isolated rat islets. *Diabetes* 39, 112–117. doi: 10.2337/diacare.39.1.112

Denys, D., Mantione, M., Figee, M., van den Munckhof, P., Koerselman, F., Westenberg, H., et al. (2010). Deep brain stimulation of the nucleus accumbens for treatment-refractory obsessive-compulsive disorder. *Arch. Gen. Psychiatry* 67, 1061–1068. doi: 10.1001/archgenpsychiatry.2010.122

Diepenbroek, C., Serlie, M. J., Fliers, E., Kalsbeek, A., and la Fleur, S. E. (2013). Brain areas and pathways in the regulation of glucose metabolism. *Biofactors* 39, 505–513. doi: 10.1002/biof.1123

Dodd, G. T., Williams, S. R., and Luckman, S. M. (2010). Functional magnetic resonance imaging and c-Fos mapping in rats following a glucoprivic dose of 2-deoxy-D-glucose. *J. Neurochem.* 113, 1123–1132. doi: 10.1111/j.1471-4159.2010.06671.x

Figee, M., Luigjes, J., Smolders, R., Valencia-Alfonso, C. E., van, W. G., de, K. B., et al. (2013). Deep brain stimulation restores frontostriatal network activity in obsessive-compulsive disorder. *Nat. Neurosci.* 16, 386–387. doi: 10.1038/nn.3344

Fulton, S. (2010). Appetite and reward. *Front. Neuroendocrinol.* 31, 85–103. doi: 10.1016/j.yfrne.2009.10.003

Halpern, C. H., Tekriwal, A., Santollo, J., Keating, J. G., Wolf, J. A., Daniels, D., et al. (2013). Amelioration of binge eating by nucleus accumbens shell deep brain stimulation in mice involves D2 receptor modulation. *J. Neurosci.* 33, 7122–7129. doi: 10.1523/JNEUROSCI.3237-12.2013

Halpern, C. H., Wolf, J. A., Bale, T. L., Stunkard, A. J., Danish, S. F., Grossman, M., et al. (2008). Deep brain stimulation in the treatment of obesity. *J. Neurosurg.* 109, 625–634. doi: 10.3171/JNS/2008/109/10/0625

Helman, A. M., Amira, R., Nicolaidis, S., and Assan, R. (1980). Glucagon release induced by ventrolateral hypothalamic stimulation in the rat. *Endocrinology* 106, 1612–1619. doi: 10.1210/endo-106-5-1612

Helman, A. M., Giraud, P., Nicolaidis, S., Oliver, C., and Assan, R. (1983). Glucagon release after stimulation of the lateral hypothalamic area in rats: predominant beta-adrenergic transmission and involvement of endorphin pathways. *Endocrinology* 113, 1–6. doi: 10.1210/endo-113-1-1

Kelley, A. E., and Swanson, C. J. (1997). Feeding induced by blockade of AMPA and kainate receptors within the ventral striatum: a microinfusion mapping study. *Behav. Brain Res.* 89, 107–113. doi: 10.1016/S0166-4328(97)00054-5

Lechin, F., and van der Dijs, B. (2006). Central nervous system circuitry involved in the hyperinsulinism syndrome. *Neuroendocrinology* 84, 222–234. doi: 10.1159/000098005

Marino, J. S., Xy, Y., and Hill, J. W. (2011). Central insulin and leptin-mediated autonomic control of glucose homeostasis. *Trends Endocrinol. Metab.* 22, 254–284. doi: 10.1016/j.tem.2011.03.001

McCracken, C. B., and Grace, A. A. (2007). High-frequency deep brain stimulation of the nucleus accumbens region suppresses neuronal activity and selectively modulates afferent drive in rat orbitofrontal cortex *in vivo*. *J. Neurosci.* 27, 12601–12610. doi: 10.1523/JNEUROSCI.3750-07.2007

Muller, U. J., Voges, J., Steiner, J., Galazky, I., Heinze, H. J., Moller, M., et al. (2013). Deep brain stimulation of the nucleus accumbens for the treatment of addiction. *Ann. N. Y. Acad. Sci.* 1282, 119–128. doi: 10.1111/j.1749-6632.2012.06834.x

Papp, S., Lukats, B., Takacs, G., Szalay, C., and Karadi, Z. (2007). Glucose-monitoring neurons in the nucleus accumbens. *Neuroreport* 18, 1561–1565. doi: 10.1097/WNR.0b013e3281667eca

Paxinos, and Watson, (1998). The rat brain atlas in stereotaxic coordinates. San Diego, DA: Academic Press.

Sokal, E. J., Sarcione, E. J., and Henderson, A. M. (1964). Relative potency of glucagon and epinephrine as hepatic glycogenolytic agents: studies with the isolated perfused rat liver. *Endocrinology* 74, 930–938. doi: 10.1210/endo-74-6-930

Steffens, A. B. (1969). A method for frequent sampling blood and continuous infusion of fluids in the rat whithout disturbing the animal. *Physiol. Behav.* 4, 833–836. doi: 10.1016/0031-9384(69)90126-7

Stratford, T. R., and Kelley, A. E. (1999). Evidence of a functional relationship between the nucleus accumbens shell and lateral hypothalamus subserving the control of feeding behavior. *J. Neurosci.* 19, 11040–11048.

Sudo, M., Minokoshi, Y., and Shimazu, T. (1991). Ventromedial hypothalamic stimulation enhances peripheral glucose uptake in anesthetized rats. *Am. J. Physiol*. 261, E298–E303.

Swanson, L. W. (2000). Cerebral hemisphere regulation of motivated behavior. *Brain Res.* 886, 113–164. doi: 10.1016/S0006-8993(00)02905-X

Taborsky, G. J. Jr., and Mundinger, T. O. (2012). Minireview: the role of the autonomic nervous system in mediating the glucagon response to hypoglycemia. *Endocrinology* 153, 1055–1062. doi: 10.1210/en.2011-2040

Tan, S. K., Hartung, H., Sharp, T., and Temel, Y. (2011). Serotonin-dependent depression in Parkinson's disease: a role for the subthalamic nucleus. *Neuropharmacology* 61, 387–399. doi: 10.1016/j.neuropharm.2011.01.006

van der Plasse, G., Schrama, R., van Seters, S. P., Vanderschuren, L. J., and Westenberg, H. G. (2012). Deep brain stimulation reveals a dissociation of consummatory and motivated behaviour in the medial and lateral nucleus accumbens shell of the rat. *PLoS ONE* 7:e33455. doi: 10.1371/journal.pone.0033455

van Dijk, A., Klanker, M., van Oorschot, N., Post, R., Hamelink, R., Feenstra, M. G. P., et al. (2013). Deep brain stimulation affects conditioned and unconditioned anxiety in different brain areas. *Transl. Psychiatry* 3:e289, doi: 10.1038/tp.2013.56

van Dijk, A., Klompmakers, A. A., Feenstra, M. G., and Denys, D. (2012). Deep brain stimulation of the accumbens increases dopamine, serotonin, and noradrenaline in the prefrontal cortex. *J. Neurochem.* 123, 897–903. doi: 10.1111/jnc.12054

Vandehey, N. T., Moirano, J. M., Converse, A. K., Holden, J. E., Mukherjee, J., Murali, D., et al. (2010). High-affinity dopamine D2/D3 PET radioligands 18F-fallypride and 11C-FLB457: a comparison of kinetics in extrastriatal regions using a multiple-injection protocol. *J. Cereb. Blood Flow Metab.* 30, 994–1007. doi: 10.1038/jcbfm.2009.270

Wu, X., Gao, J., Yan, J., Owyang, C., and Li, Y. (2004). Hypothalamus-brain stem circuitry responsible for vagal efferent signaling to the pancreas evoked by hypoglycemia in rat. *J. Neurophysiol.* 91, 1734–1747. doi: 10.1152/jn.00791.2003

Yi, C. X., la Fleur, S. E., Fliers, E., and Kalsbeek, A. (2010). The role of the autonomic nervous liver innervation in the control of energy metabolism. *Biochim. Biophys. Acta.* 1802, 416–431. doi: 10.1016/j.bbadis.2010.01.006

Yi, C. X., Serlie, M. J., Ackermans, M. T., Foppen, E., Buijs, R. M., Sauerwein, H. P., et al. (2009). A major role for perifornical orexin neurons in the control of glucose metabolism in rats. *Diabetes* 58, 1998–2005. doi: 10.2337/db09-0385

Zahm, D. S., and Brog, J. S. (1992). On the significance of subterritories in the "accumbens" part of the rat ventral striatum. *Neuroscience* 50, 751–767. doi: 10.1016/0306-4522(92)90202-D

Zheng, H., Corkern, M., Stoyanova, I., Patterson, L. M., Tian, R., and Berthoud, H. R. (2003). Peptides that regulate food intake: appetite-inducing accumbens manipulation activates hypothalamic orexin neurons and inhibits POMC neurons. *Am. J. Physiol. Regul. Integr. Comp. Physiol*. 284, R1436-R1444. doi: 10.1152/ajpregu.00781.2002

Zsombok, A., and Smith, B. N. (2009). Plasticity of central autonomic neural circuits in diabetes. *Biochim. Biophys. Acta* 1792, 423–431. doi: 10.1016/j.bbadis.2008.12.001

Conflict of Interest Statement: The authors declare that the research was conducted in the absence of any commercial or financial relationships that could be construed as a potential conflict of interest.

Received: 25 July 2013; accepted: 06 November 2013; published online: 10 December 2013.

Citation: Diepenbroek C, van der Plasse G, Eggels L, Rijnsburger M, Feenstra MGP, Kalsbeek A, Denys D, Fliers E, Serlie MJ and la Fleur SE (2013) Alterations in blood glucose and plasma glucagon concentrations during deep brain stimulation in the shell region of the nucleus accumbens in rats. Front. Neurosci. 7:226. doi: 10.3389/fnins.2013.00226

This article was submitted to Autonomic Neuroscience, a section of the journal Frontiers in Neuroscience.

frontiers in
NEUROSCIENCE

PERSPECTIVE ARTICLE
published: 26 November 2013
doi: 10.3389/fnins.2013.00217

Modulation of gastrointestinal vagal neurocircuits by hyperglycemia

Kirsteen N. Browning*

Department of Neural and Behavioral Sciences, Penn State College of Medicine, Hershey, PA, USA

Edited by:
Andrea Zsombok, Tulane University, USA

Reviewed by:
Michael C. Andresen, Oregon Health and Science University, USA
Bret N. Smith, University of Kentucky College of Medicine, USA

****Correspondence:***
Kirsteen N. Browning, Department of Neural and Behavioral Sciences, Penn State College of Medicine, Room 3739B, 500 University Drive, MC H109, Hershey, PA 17033, USA
e-mail: knb13@psu.edu

Glucose sensing within autonomic neurocircuits is critical for the effective integration and regulation of a variety of physiological homeostatic functions including the co-ordination of vagally-mediated reflexes regulating gastrointestinal (GI) functions. Glucose regulates GI functions via actions at multiple sites of action, from modulating the activity of enteric neurons, endocrine cells, and glucose transporters within the intestine, to regulating the activity and responsiveness of the peripheral terminals, cell bodies and central terminals of vagal sensory neurons, to modifying both the activity and synaptic responsiveness of central brainstem neurons. Unsurprisingly, significant impairment in GI functions occurs in pathophysiological states where glucose levels are dysregulated, such as diabetes. A substantial obstacle to the development of new therapies to modify the disease, rather than treat the symptoms, are the gaps in our understanding of the mechanisms by which glucose modulates GI functions, particularly vagally-mediated responses and a more complete understanding of disease-related plasticity within these neurocircuits may open new avenues and targets for research.

Keywords: vagus, vagal reflex, afferent, 5-HT, gastric motility

VAGAL REFLEX CONTROL OF GASTROINTESTINAL FUNCTIONS

Autonomic neurocircuits are vitally important in the integration of homeostatic functions including the co-ordination of vago-vagal reflexes regulating gastric motility and emptying, nutrient absorption and satiety signaling. Data from several laboratories, including our own, have demonstrated that a wide variety of gastrointestinal (GI) neurohormones, and neurotransmitters act both centrally and peripherally to modulate vagal neurocircuits regulating GI functions (Dockray, 2004, 2009; Travagli et al., 2006).

Sensory information (mechanical, chemical, osmotic) from the GI tract is transduced and transmitted centrally via the afferent vagus nerve, the cell bodies of which lie in the paired nodose ganglia. While there does not appear to be strict somatotopic organization of neurons within the nodose ganglia there is a trend toward a rostro-caudal viscerotopy where neurons innervating the esophagus are located rostrally while neurons innervating the stomach are located more caudally (Zhuo et al., 1997). The central terminals of these sensory neurons enter the brainstem via the tractus solitarius (TS) and terminate on neurons of the nucleus of the tractus solitarius (NTS) using predominantly glutamate as a neurotransmitter (Andresen and Yang, 1990; Andresen and Kunze, 1994; Baptista et al., 2005). Unlike the nodose ganglion, neurons within the NTS are organized in a viscerotopic manner; activation of gastric vagal afferents, for example, activates neurons within the subnucleus gelatinosus of the NTS, while the subnucleus centralis receives information relating to the sensory control of swallowing (Altschuler et al., 1989, 1991; Barraco et al., 1992; Broussard and Altschuler, 2000). NTS neurons are heterogeneous with respect to their biophysical, neurochemical, and pharmacological properties (Bailey et al., 2002, 2006; Baptista et al., 2005; Browning et al., 2011) which contribute to their integration of this vast volume of sensory afferent information with metabolic and hormonal signals as well as neural inputs from brainstem and other CNS nuclei involved the regulation of autonomic functions. Once assimilated and integrated, NTS neurons relay this information to the adjacent dorsal motor nucleus of the vagus (DMV) which contains the preganglionic parasympathetic motoneurons which provide the output response back to the upper GI tract via the efferent vagus nerve.

In contrast to neurons within the NTS, DMV neurons are not organized viscerotopically but rather in columns or spindles that span the entire rostro-caudal extent of the nucleus related to each of the five subdiaphragmatic vagal branches that innervate the viscera (Shapiro and Miselis, 1985; Jarvinen and Powley, 1999; Travagli et al., 2006). While DMV neurons are also heterogeneous with respect to their biophysical, neurochemical and pharmacological properties (Fox and Powley, 1992; Browning et al., 1999, 2005; Jarvinen and Powley, 1999; Martinez de la Pena y Valenzuela et al., 2004; Babic et al., 2011), as preganglionic parasympathetic neurons they are all *a priori* cholinergic and activate postganglionic neurons within the target organ of interest via release of acetylcholine to activate nicotinic receptors. Postganglionic neurons within the upper GI tract form two distinct pathways to control gastric functions; an excitatory pathway that increases gastric tone, motility, and secretion via activation of muscarinic cholinergic receptors, and an inhibitory pathway that decreases gastric functions via release of non-adrenergic non-cholinergic (NANC) neurotransmitters, principally nitric

oxide and vasoactive intestinal polypeptide. Gastric relaxation, therefore, can be achieved by either inhibiting the tonically active cholinergic pathway or by activating the inhibitory NANC pathway (Travagli et al., 2006).

EFFECTS OF GLUCOSE ON GASTROINTESTINAL FUNCTIONS

Effective glucose sensing is critical for the efficient integration and regulation of a wide variety of physiological functions including the optimal regulation of glycemic levels. One of the most dramatic variations in physiological conditions occurs in response to meal ingestion when blood glucose levels increase dramatically. Glucose exerts profound vagally-mediated effects upon gastric motility and emptying, in part to stabilize excessive fluctuations in blood glucose levels following meal ingestion (MacGregor et al., 1976; Horowitz and Fraser, 1994; Ferreira et al., 2001; Rayner et al., 2001; Ishiguchi et al., 2002; Shi et al., 2003; Zhou et al., 2008). An increase in gastric motility in response to hypoglycemia accelerates nutrient delivery to the intestine allowing increased absorption and re-establishes plasma glucose levels whereas a hyperglycemia-induced decrease in gastric motility delays gastric emptying and reduces further glucose absorption preventing potentially prolonged, and damaging, elevations in glycemic levels.

Glucose is known to directly alter the activity of enteric nervous system neurons; intraintestinal infusions of glucose not only activates predominantly sensory neurons in the myenteric and submucosal plexuses of the upper small intestine (Liu et al., 1999; Sayegh et al., 2004; Vincent et al., 2011), it also appears to modulate the response of enteric neurons to other GI neurohormones such as cholecystokinin and serotonin (Roosen et al., 2012). Glucose appears to decrease gastric motility and delays gastric emptying primarily via indirect (paracrine) mechanisms of action, however. Glucose within the lumen of the intestine induces the release of neurohormones from enteroendocrine cells including releasing 5-HT from enterochromaffin cells within the proximal intestine as well as GLP-1 from L-cells in the distal intestine. These released neurohormones activate receptors (5-HT3 and GLP-1 receptors, respectively) on peripheral GI vagal afferent fiber terminals and the resulting excitatory signals are relayed centrally (Raybould, 1998, 1999, 2002; Glatzle et al., 2002; Raybould et al., 2003; Vincent et al., 2011). These sensory signals activate second order neurons within the NTS and, following integration, the subsequent vagal motor response induces gastric relaxation and delayed emptying (Zittel et al., 1994; Ferreira et al., 2001; Raybould et al., 2003; Zhou et al., 2008; Hayes et al., 2010; Vincent et al., 2011).

The vagal efferent pathway responsible for this glucose-induced gastric inhibition is somewhat controversial, however. Studies in rats have demonstrated that, within the brainstem, increasing extracellular glucose levels decreases gastric motility via inhibition of the excitatory cholinergic pathway rather than activation of the inhibitory NANC pathway (Ferreira et al., 2001; Shi et al., 2005) whereas other studies have suggested that the gastric relaxation induced following peripheral hyperglycemia was abolished by nitric oxide and VIP antagonists, suggesting that activation of the inhibitory NANC pathway was involved (Zhou et al., 2008). While differences in experimental protocols may account for some of these differences, it is unlikely to explain fully such divergent results. It is possible that different vagal efferent pathways are engaged by peripheral vs. central glucose, although this remains to be elucidated.

EFFECTS OF GLUCOSE ON VAGAL AFFERENT NEURONS

Once absorbed, however, glucose enters the bloodstream from where it continues to exert profound effects upon vagal neurocircuits controlling GI functions. While glucose increases the firing rate of vagal afferent fibers innervating the GI tract (Mei, 1978, 1985), it has also been known for some time that the responses of vagal afferents to intra-intestinal glucose is modulated by intravenous glucose (Mei, 1978) suggesting that circulating glucose may also modulate the activity and responsiveness of vagal sensory neurons.

Despite being contained within the relatively tough capsule of the nodose ganglion, vagal sensory neurons appear to be accessible to circulating factors (Lacolley et al., 2006a,b). While glucose is a universal fuel for neurons, some neurons possess the additional ability of using variations in extracellular glucose levels as a means of altering their excitability (Adachi et al., 1995; Levin et al., 2001; Kang et al., 2006). A subpopulation of vagal sensory neurons appears to display this sensitivity and are either excited or inhibited by elevations in glucose levels (Grabauskas et al., 2010). Further, the response to glucose appears to be related to the visceral organ that the vagal sensory neurons innervate; afferent neurons projecting to the stomach are more likely to exhibit excitatory responses to elevations in glucose levels while those that innervate the portal vein were more likely to be inhibitory in response to an increase in glucose, suggesting that the effects of glucose on vagal sensory transmission are specialized relative to the visceral information they transmit (Grabauskas et al., 2010). As with other neurons excited by elevations in glucose levels, this activation appears to involve the closure of an ATP-sensitive potassium channel (Dunn-Meynell et al., 1998; Ferreira et al., 2001; Raupach and Ballanyi, 2004; Balfour and Trapp, 2007; Grabauskas et al., 2010) while inhibition of vagal sensory neurons by glucose appears to involve an ATP-insensitive potassium channel although the ionic current involved remains to be elucidated (Grabauskas et al., 2010).

In addition to direct actions upon vagal afferent neurons, glucose also exerts indirect actions via modulation of neurotransmitter receptor density on the neuronal surface. In particular, we have demonstrated recently that glucose induces trafficking of 5-HT_3 receptors in GI vagal afferent neurons; following an increase in glucose levels, 5-HT_3 receptors are trafficked to the neuronal membrane (Babic et al., 2012). In contrast, a decrease in glucose levels results in receptor internalization (Babic et al., 2012). The functional consequence of this glucose-induced receptor trafficking is an increase or decrease in the inward current induced by 5-HT in response to an elevation or reduction of extracellular glucose level (Babic et al., 2012). Importantly, this glucose-induced modulation of 5-HT_3 receptor function occurs rapidly (within minutes) suggesting that, in addition to inducing the release of 5-HT from enterochromaffin cells, glucose may also increase the ability of GI vagal afferent neurons to respond

to released 5-HT. In this regard, it is also notable that, following the glucose-induced release of GI neurohormones and their activation of vagal afferent terminals within the intestine, these neurohormones also enter the circulation and gain access to vagal afferent neurons; circulating levels of platelet free 5-HT increase approximately 3-fold after meal ingestion (Houghton et al., 2003). Thus, the glucose-induced modulation of 5-HT_3 receptor density and function on vagal afferent neurons appears to be a means by which sensory signaling from the GI tract can be amplified or prolonged.

EFFECTS OF GLUCOSE ON CENTRAL VAGAL NEUROCIRCUITS

In addition to modulating the activity and functions of vagal sensory neurons and peripheral terminals, glucose also modulates the release of neurotransmitter from the central terminals of vagal sensory neurons; increasing the extracellular glucose concentration increased action potential-dependent and -independent glutamate release onto second order NTS neurons, while decreasing extracellular glucose levels inhibited glutamate release (Wan and Browning, 2008a). Further studies demonstrated that, as with vagal sensory somata, glucose induces the trafficking of 5-HT3 receptors to the membrane of vagal sensory nerve terminals, the activation of which increases glutamate release (Wan and Browning, 2008b). 5-HT_3 receptors on vagal afferent terminals appear to be activated tonically; in fact, the 5-HT_3 receptor antagonist, ondansetron, decreases action potential dependent and independent synaptic transmission to second order NTS neurons implying an ongoing activation of these receptors (Wan and Browning, 2008b). The NTS receives a dense serotonergic input from other brainstem nuclei, most prominently the medullary raphe nuclei (Steinbusch, 1981; Steinbusch and Nieuwenhuys, 1981; Thor and Helke, 1989) although vagal afferent neurons themselves contain 5-HT (Nosjean et al., 1990; Sykes et al., 1994).

Early studies using extracellular recording techniques showed that glucose is able to modulate the activity of subpopulations of neurons within the brainstem. Hepatic vagal afferent fibers that showed a decrease in activity in response to increased glucose exposure, for example, innervate NTS neurons that are also inhibited by local application of glucose (Adachi et al., 1984). Other NTS neurons, in contrast, increased their activity in response to elevated glucose levels (Adachi et al., 1995; Yettefti et al., 1995, 1997; Dallaporta et al., 2000); as described earlier for vagal sensory neurons, as well as for other glucose-sensitive central neurons (Dunn-Meynell et al., 1998; Levin et al., 2001), this increase in neuronal activity in response to increased extracellular glucose levels appear to involve ATP-sensitive potassium channels (Dallaporta et al., 2000; Balfour et al., 2006; Balfour and Trapp, 2007). The mechanism responsible for glucose-induced neuronal inhibition awaits further study, although modulation of chloride conductances may be involved (Balfour and Trapp, 2007).

The ability of glucose to modulate the activity of DMV neurons is more controversial, however. An earlier study using extracellular recording techniques suggested that a small subpopulation of DMV neurons that project via the ventral, or anterior, gastric branch increased or decreased their activity in response to topical glucose administration (Kobashi and Adachi, 1994; Adachi et al., 1995). Other studies using whole cell patch clamp recording techniques confirmed the presence of ATP-sensitive potassium channels on DMV neurons (Trapp et al., 1994; Karschin et al., 1998; Ferreira et al., 2001; Kulik et al., 2002; Raupach and Ballanyi, 2004; Balfour et al., 2006; Balfour and Trapp, 2007; Blake and Smith, 2012) suggesting their activity may be modulated by extracellular glucose levels. In contrast, later studies failed to observe any direct effects of glucose on DMV neuronal activity but, rather, demonstrated indirect effects via modulation of synaptic inputs presumably from NTS neurons (Ferreira et al., 2001). In part, these studies highlight the potential difficulties in separating direct from indirect effects when recording from neurons in brain slice preparations and the additional care required when examining ATP-sensitive potassium channels in neurons (to prevent unintentional channel closure via ATP supplied in the intracellular patch pipette solution).

One important caveat to the studies investigating the role of glucose within the brainstem is the concentration or dose of extracellular glucose used in most studies, which almost certainly exceeds physiological levels. Extracellular glucose levels in most CNS regions are assumed to be 15–20% of peripheral levels; hypothalamic glucose levels certainly vary in concert with blood glucose levels, but they do so within a very narrow range (∼0.25–1.0 mM; Dunn-Meynell et al., 2009) although other studies have measured cortical glucose levels between 0.2 and 4.5 mM (Silver and Erecinska, 1994). It should be borne in mind, however, that brainstem vagal neurons may be exposed to higher glucose levels than many other central nuclei since they are essentially circumventricular organs with a leaky blood-brain barrier and fenestrated capillaries (Cottrell and Ferguson, 2004). Regardless, our laboratory has demonstrated recently that, even at similarly low (0.5–5 mM, presumably more physiological) levels, glucose modulates glutamate release from the central terminals of vagal afferent neurons onto second order NTS neurons (**Figure 1**; Browning, unpublished data). This would suggest that the central terminals of some GI vagal sensory neurons may function as glucose sensors, in the sense that extracellular glucose levels regulate neurotransmitter release *in a linear* fashion across both physiological and pathophysiological ranges (Wan and Browning, 2008a).

ALTERATIONS IN ACTIONS OF GLUCOSE ON VAGALLY-MEDIATED GASTROINTESTINAL REFLEXES DURING PATHOPHYSIOLOGICAL STATES

As described earlier, GI functions including gastric motility and emptying are modulated by physiological alterations in blood glucose levels (Rayner et al., 2001). It is hardly surprising, therefore, that pathophysiological alterations in glucose levels result in profound disruption of GI functions. Although gastric hyperactivity has been observed in some rodent models of hyperglycemia and is experienced by some patients with diabetes, a significant proportion of animal models as well as patients exhibit diabetic gastroparesis, defined as delayed gastric emptying accompanied by other upper GI symptoms such as early satiety, fullness, abdominal pain, bloating, and nausea (Horowitz et al., 2002; Chaikomin et al., 2006). The severity of diabetic gastroparesis can vary widely from symptoms of mild discomfort up to

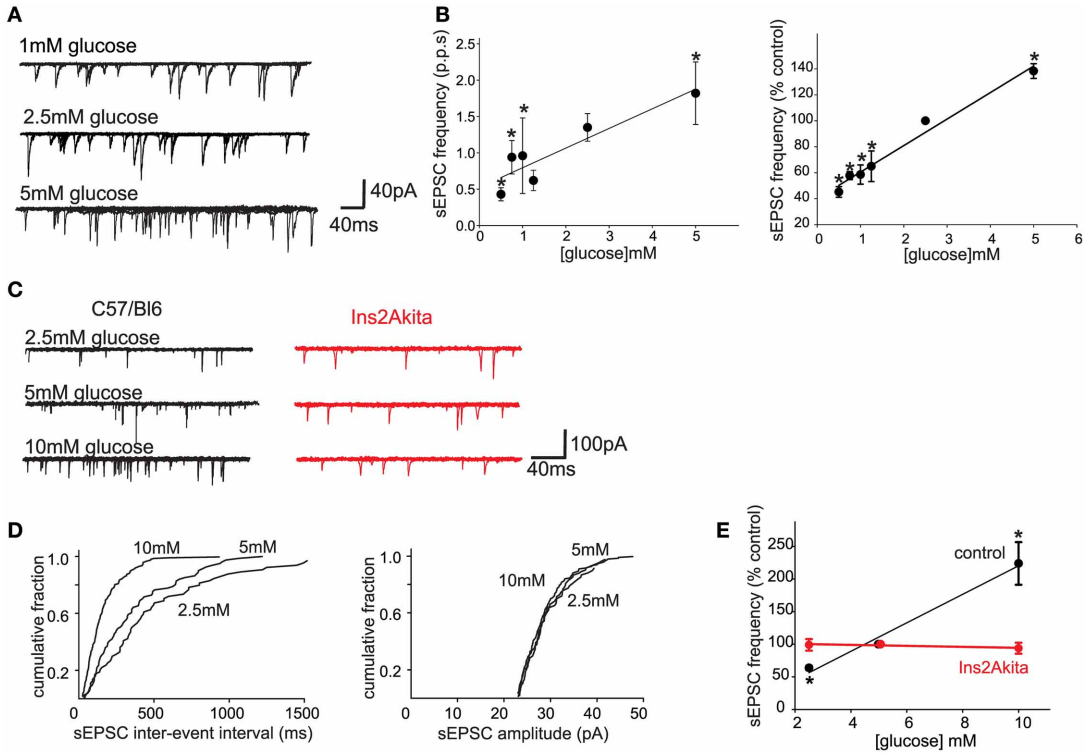

FIGURE 1 | Physiological extracellular glucose levels modulate glutamate release from the central terminals of vagal afferent neurons, an effect that is lost in diabetes. (A) Previously, we demonstrated that glucose acted presynaptically to increase the release of glutamate from the central terminals of vagal afferents (Wan and Browning, 2008b). To determine whether the release of glutamate is modulated by more physiological levels of glucose, whole cell patch clamp recordings were made from 27 neurons of the NTS subnucleus centralis (cNTS); neurons were voltage clamped at −60 mV and the effects of exposure to different physiological concentrations of extracellular glucose on spontaneous excitatory postsynaptic currents (sEPSCs) were recorded. A neuron was considered responsive if glucose altered either frequency or amplitude of sEPSCs by at least 20%. The proportion of neurons responding to a decrease in extracellular glucose concentration with a decrease in sEPSC frequency were as follows: from 2.5 to 0.5 mM, 4/6 neurons responded; from 0.5 to 0.75 mM, 6/7 neurons responded; from 2.5 to 1 mM, 5/6 neurons responded; from 2.5 to 1.25 mM, 4/6 neurons responded. In contrast, increasing extracellular glucose concentration from 2.5 to 5 mM increased sEPSC frequency in 6/7 neurons tested. Even within this narrow, presumably more physiological, range of glucose concentrations (0.5–5 mM), the frequency, but not amplitude, of sEPSCs was modulated by extracellular glucose concentration. **(B)** Summary graphics illustrating the relationship between extracellular glucose level and frequency of sEPSCs in cNTS neurons in rats. When expressed both as absolute frequency (pulse per second; p.p.ps; left) and as a percentage of sEPSC frequency at control glucose level (2.5 mM; right), the frequency of sEPSCs was dependent upon extracellular glucose concentration in a linear manner. $*P < 0.05$ vs. 2.5 mM glucose. These results suggest that the ability of glucose to modulate glutamate release from the central terminals of vagal afferents occurs across a wide range of conditions both physiological, as well as pathophysiological. The rapid alteration in glutamate transmission in response to extracellular glucose levels further suggests that glucose may set a background "tone" or ongoing level of transmission from the central terminals of gastrointestinal vagal afferents that can be up- or down-regulated in an ongoing, and rapidly reversible, manner. **(C)** To determine whether the sensitivity of vagal afferent terminals to glucose (Wan and Browning, 2008b) is (a) also present in the mouse and (b) altered during pathophysiological conditions such as diabetes, whole cell patch clamp recordings were made from NTS subnucleus centralis (cNTS) neurons ($n = 9$) in control (C57/Bl6) mice as well as from neurons ($n = 8$) in a mouse model of spontaneously developing Type 1 diabetes (Ins2Akita mice). As in the rat, the frequency of sEPSCs in cNTS neurons was dependent upon the extracellular glucose level in C57/Bl6 mice (left). In detail, in 5/6 neurons tested, decreasing the extracellular glucose concentration from 5 to 2.5 mM decreased sEPSC frequency; in contrast, in 6/7 neurons tested, increasing the extracellular glucose concentration from 5 to 10 mM increased sEPSC frequency. In no instance was any effect on sEPCS amplitude observed (113 ± 10% of control amplitude in 2.5 mM glucose and 100 ± 6% of control amplitude in 10 mM glucose; $P > 0.05$ in each case). In contrast, the ability of glucose to modulate the frequency of sEPSCs was lost in neurons from Ins2Akita mice (right). In detail, 4/5 neurons tested, decreasing the extracellular glucose concentration from 5 to 2.5 mM had no effect on sEPSC frequency while increasing extracellular glucose concentration from 5 to 10 mM had no effect on sEPSC frequency in any of the 5 neurons tested. **(D)** Computer generated graphics from the same control C57/Bl6 neuron as above showing that glucose increases the frequency (left) but not amplitude (right) of sEPSCs suggesting that, as in the rat, glucose acts at presynaptic sites to modulate glutamate release. **(E)** Summary graphic illustrating the relationship between extracellular glucose level and frequency of sEPSCs in cNTS neurons from control C57/Bl6 and diabetic Ins2Akita mice. When expressed a percentage of frequency at control glucose level (5 mM glucose), the ability of glucose to modulate the frequency of sEPSCs was lost in diabetes. $*P < 0.05$ vs. control frequency. These results suggest that the ability of glucose to modulate glutamatergic transmission from the central terminals of vagal afferents may be a more generalized phenomenon that occurs across species. The results further suggest that the glucose-dependent modulation of central vagal neurocircuits is compromised by chronic hyperglycemia. The timing of this loss in responsiveness, as well as its cause-or-effect response to the development of diabetes, may provide valuable insights into the effects of acute vs. chronic hyperglycemia on autonomic neurocircuitry and the consequence effects on gastrointestinal homeostatic regulation including the gastric dysmotility and delayed gastric emptying observed during hyperglycemia/diabetes.

impaired glycemic control, electrolyte imbalance, and malnutrition (Horowitz et al., 2002; Chaikomin et al., 2006). Despite the considerable healthcare and social costs associated with this disease, the pathophysiology of diabetic gastroparesis remains to be elucidated fully. That both Type 1 and Type 2 diabetic patients experience gastroparesis symptoms suggests that hyperglycemia, or dysregulated glycemic control *per se*, may play an important role in symptom development, although insulin itself certainly modulates the activity of central vagal motoneurons (Blake and Smith, 2012) and induces vagally-mediated increases in gastric motility (Krowicki et al., 1998).

The GI dysfunctions induced by either Type 1 or Type 2 diabetes may occur through actions at multiple sites (**Figure 2**). A loss of enteric neurons neurons, particularly inhibitory neurons (nitric oxide synthase-, vasoactive intestinal peptide-, neuropeptide Y- and galanin-immunoreactive) has been reported in rodent models of both Type 1 and Type 2 diabetes during the early stages of the disease [reviewed in Chandrasekharan and Srinivasan (2007)] which may contribute to the observed disordered motility patterns and decreased NANC-dependent muscle relaxations (Jenkinson and Reid, 2000; Yoneda et al., 2001; Demedts et al., 2013). Loss of Inhibitory Cells of Cajal (ICC) has also been reported in both Type 1 and Type 2 diabetes (Ordog et al., 2000; He et al., 2001; Iwasaki et al., 2006; Forrest et al., 2008; Wang et al., 2009; Grover et al., 2011) suggesting this may be another important means by which persistant hyperglycemia dysregulates GI motility although reduced levels of insulin and insulin signaling, rather than hyperglycemia *per se*, has also been shown to be involved in ICC depletion (Horvath et al., 2005).

Glucose sensing within enteroendocrine cells is also disrupted in diabetes (Lee et al., 2012) as are both the basal expression and function of intestinal sodium-glucose transporters (Bihler and Freund, 1975; Morton and Hanson, 1984; Dyer et al., 2002; Bhutta et al., 2013) suggesting that the increased absorption of glucose further amplifies the disrupted and dysregulated responses of GI neurocircuits to glucose. It is hardly surprising, therefore,

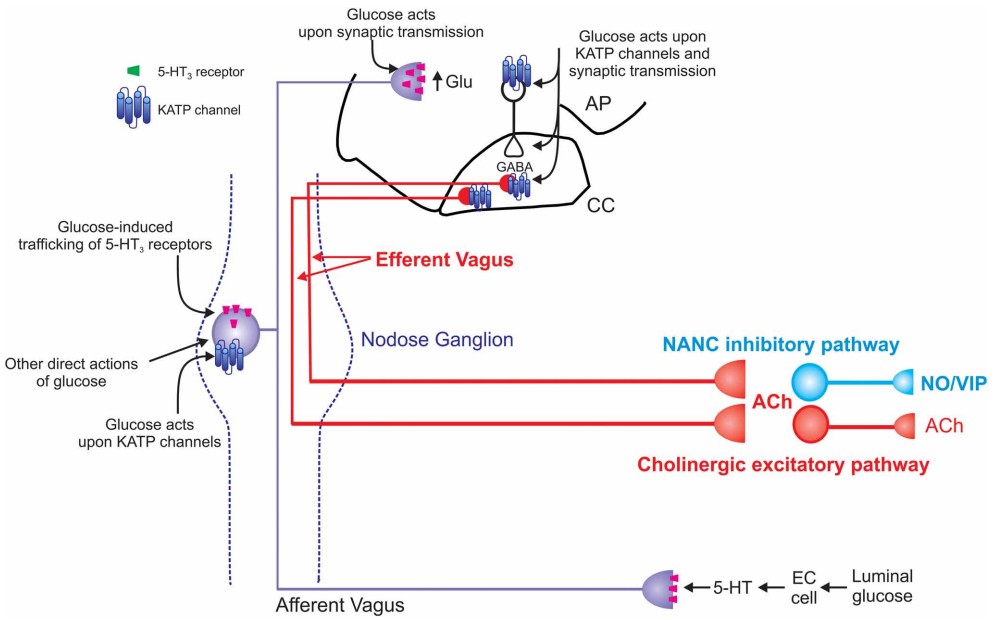

FIGURE 2 | Schematic representation of the effects of glucose on vago-vagal reflex control of the stomach. Glucose within the intestine induces the release of serotonin from enteroendocrine (EC) cells (Zhu et al., 2001; Freeman et al., 2006). The released 5-HT acts upon 5-HT3 receptors present on the peripheral terminals of vagal afferent neurons to cause their excitation (Hillsley et al., 1998; Raybould et al., 2003; Grundy, 2006); this peripheral signal is relayed centrally via the afferent vagus nerve. Once absorbed into the circulation, glucose is also able to act directly upon vagal afferent neurons within the nodose ganglion. Glucose induces neuronal excitation via actions upon ATP-sensitive potassium channels (KATP channels; Grabauskas et al., 2010) as well as causing neuronal inhibition via an as yet unidentified mechanism (Grabauskas et al., 2010). Glucose also rapidly and reversibly traffics 5-HT3 receptors to and from the membrane of gastrointestinal vagal afferent neurons (Babic et al., 2012). Since circulating platelet-free 5-HT levels increase following ingestion of a meal (Houghton et al., 2003), this provides a means by which glucose is able to modulate its own "perception" and amplify or prolong vagal afferent signaling. The central terminals of vagal afferent neurons enter the brainstem via the tractus solitarius and terminate on NTS neurons using predominantly glutamate as a neurotransmitter (Andresen and Yang, 1990; Andresen and Kunze, 1994). Glucose is also able to modulate the release of glutamate from the central terminals of vagal afferents by actions that involve 5-HT3 receptors (Wan and Browning, 2008a,b). Glucose can also activate NTS neurons via actions on KATP channels and increase synaptic transmission to gastric-projecting DMV neurons (Adachi et al., 1984, 1995; Ferreira et al., 2001). Glucose can also modulate the activity of DMV neurons directly (Trapp et al., 1994; Karschin et al., 1998; Balfour et al., 2006; Balfour and Trapp, 2007). The result of these central and peripheral actions of glucose is gastric relaxation and delayed gastric emptying (Schvarcz et al., 1997; Raymer et al., 2000; Rayner et al., 2001). The vagal efferent pathway involved in this gastric relaxation and delayed gastric emptying is still controversial. Peripheral actions of glucose appear to involve activation of a non-adrenergic, non-cholinergic pathway (Zhou et al., 2008) whereas central glucose appears to involve inhibition of the tonically active cholinergic pathway (Ferreira et al., 2001; Shi et al., 2003, 2005).

that altered vagal sensory and motor fiber functions have been reported in both humans (Tougas et al., 1992) and rodent models of diabetes (Yagihashi and Sima, 1986; Lee et al., 2001, 2012; Regalia et al., 2002). While frank autonomic neuropathy almost certainly contributes to the altered vagal sensory and motor functions observed in chronic diabetes, the actions of acute hyperglycemia to modulate vagal afferent and efferent functions (MacGregor et al., 1976; Shi et al., 2003; Takahashi et al., 2003; Zhou et al., 2008) suggests that poor glycemic control *per se* also negatively impacts vagal reflex functions.

While diabetes is most often considered a peripheral metabolic disease, an increasing body of evidence indicates a significant involvement of the central nervous system, including vagal neurocircuits within the hindbrain, in its development and functional outcomes. In a mouse model of spontaneously developing Type 1 diabetes, the Ins2(Akita) mouse, the ability of glucose to modulate synaptic transmission to second order NTS neurons is lost (see **Figures 1C,D**; Browning, unpublished data) suggesting an impairment of glucose sensitivity within vagal sensory neurocircuits. Recent studies have demonstrated that even short time periods of glycemic dysregulation result in significant modulation of synaptic transmission within vagal neurocircuits (Zsombok et al., 2011). This would suggest that the vagal control of GI functions may by disrupted even in the early stages of glycemic dysregulation, rather than as a consequence of autonomic neuropathy. In this regard, preliminary evidence that even short periods of exposure to a high fat diet disrupts the glucose-induced trafficking of 5-HT_3 receptors on GI vagal sensory neurons, well in advance of the development of obesity or hyperglycemia (Troy and Browning, 2013), raises the possibility that altered glucose signaling within vagal neurocircuits may precede, and even contribute to, disease development.

FUTURE DIRECTIONS

Glucose sensing within autonomic neurocircuits is critical for the effective integration and regulation of a variety of physiological homeostatic functions involved in the optimal regulation of blood glucose levels, including the co-ordination of vagally-mediated reflexes regulating GI functions (e.g., gastric motility and emptying, nutrient absorption and satiety signaling). Glucose regulates GI functions via actions at multiple sites of action, from modulating the activity of enteric neurons, endocrine cells and glucose transporters within the intestine, to regulating the activity and responsiveness of the peripheral terminals, cell bodies and central terminals of vagal sensory neurons, to modifying both the activity and synaptic responsiveness of NTS and DMV neurons. Unsurprisingly, significant impairment in GI functions results occurs in pathophysiological states where glucose levels are dysregulated, such as diabetes. A substantial obstacle to the development of new therapies to modify the disease, rather than treat the symptoms, are the gaps in our understanding of the mechanisms by which glucose modulates GI functions, particularly vagally-mediated responses. Vagal afferent and efferent fibers represent a much more readily available target for new therapies and a more complete understanding of disease-related plasticity within these neurocircuits may open new avenues and targets for research.

It will be of particular interest to elucidate the reversibility of hyperglycemia- and diabetes-induced vagal dysregulation—is there a period of exposure to hyperglycemia beyond which vagal neural damage is irreversible or is the neurocircuitry sufficiently plastic to recover with subsequent tight glycemic control? In this regard, the recent demonstration that the diet-induced obesity associated decrease in excitability and responsiveness of vagal motoneurons is reversed completely by Roux-en-Y gastric bypass surgery (Browning et al., 2013) suggests that vagal neurocircuits remain open to adaptation and that long-term dysregulation of their activity does not necessarily result in permanent and irrecoverable damage. The rapid remission of Type 2 diabetes following bariatric surgery, far in advance of weight loss, raises questions as to its mechanism of action and the degree to which recovery of glycemic regulation is related to the recovery of vagal afferent and efferent homeostatic control.

ACKNOWLEDGMENTS

Funding was provided by NIH DK078364 to Kirsteen N. Browning. The author thanks Dr R. Alberto Travagli for critical reviews of earlier versions of this manuscript and W.Nairn Browning for support and encouragement.

REFERENCES

Adachi, A., Kobashi, M., and Funahashi, M. (1995). Glucose-responsive neurons in the brainstem. *Obes. Res. 3 Suppl* 5, 735S–740S. doi: 10.1002/j.1550-8528.1995.tb00493.x

Adachi, A., Shimizu, N., Oomura, Y., and Kobashi, M. (1984). Convergence of hepatoportal glucose-sensitive afferent signals to glucose-sensitive units within the nucleus of the solitary tract. *Neurosci. Lett.* 46, 215–218. doi: 10.1016/0304-3940(84)90444-0

Altschuler, S. M., Bao, X., Bieger, D., Hopkins, D. A., and Miselis, R. R. (1989). Viscerotopic representation of the upper alimentary tract in the rat: sensory ganglia and nuclei of the solitary and spinal trigeminal tracts. *J. Comp. Neurol.* 283, 248–268. doi: 10.1002/cne.902830207

Altschuler, S. M., Ferenci, D. A., Lynn, R. B., and Miselis, R. R. (1991). Representation of the cecum in the lateral dorsal motor nucleus of the vagus nerve and commissural subnucleus of the nucleus tractus solitarii in rat. *J. Comp. Neurol.* 304, 261–274. doi: 10.1002/cne.903040209

Andresen, M. C., and Kunze, D. L. (1994). Nucleus tractus solitarius–gateway to neural circulatory control. *Annu. Rev. Physiol.* 56, 93–116. doi: 10.1146/annurev.physiol.56.1.93

Andresen, M. C., and Yang, M. (1990). Non-NMDA receptors mediate sensory afferent synaptic transmission in medial nucleus tractus solitarius. *Am. J. Physiol.* 259, H1307–H1311.

Babic, T., Browning, K. N., and Travagli, R. A. (2011). Differential organization of excitatory and inhibitory synapses within the rat dorsal vagal complex. *Am. J. Physiol. Gastrointest. Liver Physiol.* 300, G21–G32. doi: 10.1152/ajpgi.00363.2010

Babic, T., Troy, A. E., Fortna, S. R., and Browning, K. N. (2012). Glucose-dependent trafficking of 5-HT(3) receptors in rat gastrointestinal vagal afferent neurons. *Neurogastroenterol. Motil.* 24, e476–e488. doi: 10.1111/j.1365-2982.2012.01987.x

Bailey, T. W., Hermes, S. M., Andresen, M. C., and Aicher, S. A. (2006). Cranial visceral afferent pathways through the nucleus of the solitary tract to caudal ventrolateral medulla or paraventricular hypothalamus: target-specific synaptic reliability and convergence patterns. *J. Neurosci.* 26, 11893–11902. doi: 10.1523/JNEUROSCI.2044-06.2006

Bailey, T. W., Jin, Y. H., Doyle, M. W., and Andresen, M. C. (2002). Vanilloid-sensitive afferents activate neurons with prominent A-type potassium currents in nucleus tractus solitarius. *J. Neurosci.* 22, 8230–8237.

Balfour, R. H., Hansen, A. M., and Trapp, S. (2006). Neuronal responses to transient hypoglycaemia in the dorsal vagal complex of the rat brainstem. *J. Physiol.* 570, 469–484. doi: 10.1113/jphysiol.2005.098822

Balfour, R. H., and Trapp, S. (2007). Ionic currents underlying the response of rat dorsal vagal neurones to hypoglycaemia and chemical anoxia. *J. Physiol.* 579, 691–702. doi: 10.1113/jphysiol.2006.126094

Baptista, V., Zheng, Z. L., Coleman, F. H., Rogers, R. C., and Travagli, R. A. (2005). Characterization of neurons of the nucleus tractus solitarius pars centralis. *Brain Res.* 1052, 139–146. doi: 10.1016/j.brainres.2005.05.073

Barraco, R., el-Ridi, M., Ergene, E., Parizon, M., and Bradley, D. (1992). An atlas of the rat subpostremal nucleus tractus solitarius. *Brain Res. Bull.* 29, 703–765. doi: 10.1016/0361-9230(92)90143-L

Bhutta, H. Y., Deelman, T. E., Ashley, S. W., Rhoads, D. B., and Tavakkoli, A. (2013). Disrupted circadian rhythmicity of the intestinal glucose transporter SGLT1 in Zucker diabetic fatty rats. *Dig. Dis. Sci.* 58, 1537–1545. doi: 10.1007/s10620-013-2669-y

Bihler, I., and Freund, N. (1975). Sugar transport in the small intestine of obese hyperglycemic, fed and fasted mice. *Diabetologia* 11, 387–393. doi: 10.1007/BF00429905

Blake, C. B., and Smith, B. N. (2012). Insulin reduces excitation in gastric-related neurons of the dorsal motor nucleus of the vagus. *Am. J. Physiol. Regul. Integr. Comp. Physiol.* 303, R807–R814. doi: 10.1152/ajpregu.00276.2012

Broussard, D. L., and Altschuler, S. M. (2000). Central integration of swallow and airway-protective reflexes. *Am. J. Med.* 108(Suppl. 4a), 62S–67S. doi: 10.1016/S0002-9343(99)00340-X

Browning, K. N., Coleman, F. H., and Travagli, R. A. (2005). Characterization of pancreas-projecting rat dorsal motor nucleus of vagus neurons. *Am. J. Physiol. Gastrointest. Liver Physiol.* 288, G950–G955. doi: 10.1152/ajpgi.00549.2004

Browning, K. N., Fortna, S. R., and Hajnal, A. (2013). Roux-en-Y gastric bypass reverses the effects of diet-induced obesity to inhibit the responsiveness of central vagal motoneurones. *J. Physiol.* 591, 2357–2372. doi: 10.1113/jphysiol.2012.249268

Browning, K. N., Renehan, W. E., and Travagli, R. A. (1999). Electrophysiological and morphological heterogeneity of rat dorsal vagal neurones which project to specific areas of the gastrointestinal tract. *J. Physiol.* 517, 521–532. doi: 10.1111/j.1469-7793.1999.0521t.x

Browning, K. N., Wan, S., Baptista, V., and Travagli, R. A. (2011). Vanilloid, purinergic, and CCK receptors activate glutamate release on single neurons of the nucleus tractus solitarius centralis. *Am. J. Physiol. Regul. Integr. Comp. Physiol.* 301, R394–R401. doi: 10.1152/ajpregu.00054.2011

Chaikomin, R., Rayner, C. K., Jones, K. L., and Horowitz, M. (2006). Upper gastrointestinal function and glycemic control in diabetes mellitus. *World J. Gastroenterol.* 12, 5611–5621.

Chandrasekharan, B., and Srinivasan, S. (2007). Diabetes and the enteric nervous system. *Neurogastroenterol. Motil.* 19, 951–960. doi: 10.1111/j.1365-2982.2007.01023.x

Cottrell, G. T., and Ferguson, A. V. (2004). Sensory circumventricular organs: central roles in integrated autonomic regulation. *Regul. Pept.* 117, 11–23. doi: 10.1016/j.regpep.2003.09.004

Dallaporta, M., Perrin, J., and Orsini, J.-C. (2000). Involvement of adenosine triphosphate-sensitive K^+ channels in glucose-sensing in the rat solitary tract nucleus. *Neurosci. Lett.* 278, 77–80. doi: 10.1016/S0304-3940(99)00898-8

Demedts, I., Masaoka, T., Kindt, S., De, H. G., Geboes, K., Farre, R., et al. (2013). Gastrointestinal motility changes and myenteric plexus alterations in spontaneously diabetic biobreeding rats. *J. Neurogastroenterol. Motil.* 19, 161–170. doi: 10.5056/jnm.2013.19.2.161

Dockray, G. (2004). Gut endocrine secretions and their relevance to satiety. *Curr. Opin. Pharmacol.* 4, 557–560. doi: 10.1016/j.coph.2004.05.005

Dockray, G. J. (2009). The versatility of the vagus. *Physiol. Behav.* 97, 531–536. doi: 10.1016/j.physbeh.2009.01.009

Dunn-Meynell, A. A., Rawson, N. E., and Levin, B. E. (1998). Distribution and phenotype of neurons containing the ATP-sensitive K^+ channel in rat brain. *Brain Res.* 814, 41–54. doi: 10.1016/S0006-8993(98)00956-1

Dunn-Meynell, A. A., Sanders, N. M., Compton, D., Becker, T. C., Eiki, J., Zhang, B. B., et al. (2009). Relationship among brain and blood glucose levels and spontaneous and glucoprivic feeding. *J. Neurosci.* 29, 7015–7022. doi: 10.1523/JNEUROSCI.0334-09.2009

Dyer, J., Wood, I. S., Palejwala, A., Ellis, A., and Shirazi-Beechey, S. P. (2002). Expression of monosaccharide transporters in intestine of diabetic humans. *Am. J. Physiol. Gastrointest. Liver Physiol.* 282, G241–G248. doi: 10.1152/ajpgi.00310.2001

Ferreira, M. Jr., Browning, K. N., Sahibzada, N., Verbalis, J. G., Gillis, R. A., and Travagli, R. A. (2001). Glucose effects on gastric motility and tone evoked from the rat dorsal vagal complex. *J. Physiol.* 536, 141–152. doi: 10.1111/j.1469-7793.2001.t01-1-00141.x

Forrest, A., Huizinga, J. D., Wang, X. Y., Liu, L. W., and Parsons, M. (2008). Increase in stretch-induced rhythmic motor activity in the diabetic rat colon is associated with loss of ICC of the submuscular plexus. *Am. J. Physiol. Gastrointest. Liver Physiol.* 294, G315–G326. doi: 10.1152/ajpgi.00196.2007

Fox, E. A., and Powley, T. L. (1992). Morphology of identified preganglionic neurons in the dorsal motor nucleus of the vagus. *J. Comp. Neurol.* 322, 79–98. doi: 10.1002/cne.903220107

Freeman, S. L., Bohan, D., Darcel, N., and Raybould, H. E. (2006). Luminal glucose sensing in the rat intestine has characteristics of a sodium-glucose cotransporter. *Am. J. Physiol. Gastrointest. Liver Physiol.* 291, G439–G445. doi: 10.1152/ajpgi.00079.2006

Glatzle, J., Sternini, C., Robin, C., Zittel, T. T., Wong, H., Reeve, J. R. Jr., et al. (2002). Expression of 5-HT3 receptors in the rat gastrointestinal tract. *Gastroenterology* 123, 217–226. doi: 10.1053/gast.2002.34245

Grabauskas, G., Song, I., Zhou, S. Y., and Owyang, C. (2010). Electrophysiological identifications of glucose-sensing neurons in the rat nodose ganglia. *J. Physiol.* 588, 617–632. doi: 10.1113/jphysiol.2009.182147

Grover, M., Farrugia, G., Lurken, M. S., Bernard, C. E., Faussone-Pellegrini, M. S., Smyrk, T. C., et al. (2011). Cellular changes in diabetic and idiopathic gastroparesis. *Gastroenterology* 140, 1575–1585. doi: 10.1053/j.gastro.2011.01.046

Grundy, D. (2006). Serotonin and sensory signalling from the gastrointestinal lumen. *J. Physiol.* 575, 1–2. doi: 10.1113/jphysiol.2006.113472

Hayes, M. R., De Jonghe, B. C., and Kanoski, S. E. (2010). Role of the glucagon-like-peptide-1 receptor in the control of energy balance. *Physiol. Behav.* 100, 503–510. doi: 10.1016/j.physbeh.2010.02.029

He, C. L., Soffer, E. E., Ferris, C. D., Walsh, R. M., Szurszewski, J. H., and Farrugia, G. (2001). Loss of interstitial cells of cajal and inhibitory innervation in insulin-dependent diabetes. *Gastroenterology* 121, 427–434. doi: 10.1053/gast.2001.26264

Hillsley, K., Kirkup, A. J., and Grundy, D. (1998). Direct and indirect actions of 5-hydroxytryptamine on the discharge of mesenteric afferent fibres innervating the rat jejunum. *J. Physiol.* 506(Pt 2), 551–561. doi: 10.1111/j.1469-7793.1998.551bw.x

Horowitz, M., and Fraser, R. (1994). Disordered gastric motor function in diabetes mellitus. *Diabetologia* 37, 543–551. doi: 10.1007/BF00403371

Horowitz, M., O'Donovan, D., Jones, K. L., Feinle, C., Rayner, C. K., and Samsom, M. (2002). Gastric emptying in diabetes: clinical significance and treatment. *Diabet. Med.* 19, 177–194. doi: 10.1046/j.1464-5491.2002.00658x

Horvath, V. J., Vittal, H., and Ordog, T. (2005). Reduced insulin and IGF-I signaling, not hyperglycemia, underlies the diabetes-associated depletion of interstitial cells of Cajal in the murine stomach. *Diabetes* 54, 1528–1533. doi: 10.2337/diabetes.54.5.1528

Houghton, L. A., Atkinson, W., Whitaker, R. P., Whorwell, P. J., and Rimmer, M. J. (2003). Increased platelet depleted plasma 5-hydroxytryptamine concentration following meal ingestion in symptomatic female subjects with diarrhoea predominant irritable bowel syndrome. *Gut* 52, 663–670. doi: 10.1136/gut.52.5.663

Ishiguchi, T., Tada, H., Nakagawa, K., Yamamura, T., and Takahashi, T. (2002). Hyperglycemia impairs antro-pyloric coordination and delays gastric emptying in conscious rats. *Auton. Neurosci.* 95, 112–120. doi: 10.1016/S1566-0702(01)00383-6

Iwasaki, H., Kajimura, M., Osawa, S., Kanaoka, S., Furuta, T., Ikuma, M., and Hishida, A. (2006). A deficiency of gastric interstitial cells of Cajal accompanied by decreased expression of neuronal nitric oxide synthase and substance P in patients with type 2 diabetes mellitus. *J. Gastroenterol.* 41, 1076–1087. doi: 10.1007/s00535-006-1909-8

Jarvinen, M. K., and Powley, T. L. (1999). Dorsal motor nucleus of the vagus neurons: a multivariate taxonomy. *J. Comp. Neurol.* 403, 359–377.

Jenkinson, K. M., and Reid, J. J. (2000). Altered non-adrenergic non-cholinergic neurotransmission in gastric fundus from streptozotocin-diabetic rats. *Eur. J. Pharmacol.* 401, 251–258. doi: 10.1016/S0014-2999(00)00280-6

Kang, L., Dunn-Meynell, A. A., Routh, V. H., Gaspers, L. D., Nagata, Y., Nishimura, T., et al. (2006). Glucokinase is a critical regulator of ventromedial hypothalamic neuronal glucosensing. *Diabetes* 55, 412–420. doi: 10.2337/diabetes.55.02.06.db05-1229

Karschin, A., Brockhaus, J., and Ballanyi, K. (1998). K_{ATP} channel formation by the sulphonylurea receptors SUR1 with Kir6.2 subunits in rat dorsal vagal neurons *in situ*. *J. Physiol.* 509, 339–346. doi: 10.1111/j.1469-7793.1998.339bn.x

Kobashi, M., and Adachi, A. (1994). Effect of topical administration of glucose on neurons innervating abdominal viscera in dorsal motor nucleus of vagus in rats. *Jpn. J. Physiol.* 44, 729–734. doi: 10.2170/jjphysiol.44.729

Krowicki, Z. K., Nathan, N. A., and Hornby, P. J. (1998). Gastric motor and cardiovascular effects of insulin in dorsal vagal complex of the rat. *Am. J. Physiol.* 275, G964–G972.

Kulik, A., Brockhaus, J., Pedarzani, P., and Ballanyi, K. (2002). Chemical anoxia activates ATP-sensitive and blocks Ca(2+)-dependent K(+) channels in rat dorsal vagal neurons *in situ*. *Neuroscience* 110, 541–554. doi: 10.1016/S0306-4522(01)00468-7

Lacolley, P., Owen, J. R., Sandock, K., Lewis, T. H., Bates, J. N., Robertson, T. P., et al. (2006a). 5-HT activates vagal afferent cell bodies *in vivo*: role of 5-HT2 and 5-HT3 receptors. *Neuroscience* 143, 273–287. doi: 10.1016/j.neuroscience.2006.07.032

Lacolley, P., Owen, J. R., Sandock, K., Lewis, T. H., Bates, J. N., Robertson, T. P., et al. (2006b). Occipital artery injections of 5-HT may directly activate the cell bodies of vagal and glossopharyngeal afferent cell bodies in the rat. *Neuroscience* 143, 289–308. doi: 10.1016/j.neuroscience.2006.08.047

Lee, J., Cummings, B. P., Martin, E., Sharp, J. W., Graham, J. L., Stanhope, K. L., et al. (2012). Glucose sensing by gut endocrine cells and activation of the vagal afferent pathway is impaired in a rodent model of type 2 diabetes mellitus. *Am. J. Physiol. Regul. Integr. Comp. Physiol.* 302, R657–R666. doi: 10.1152/ajpregu.00345.2011

Lee, P. G., Cai, F., and Helke, C. J. (2002). Streptozotocin-induced diabetes reduces retrograde axonal transport in the afferent and efferent vagus nerve. *Brain Res.* 941, 127–136. doi: 10.1016/S0006-8993(02)02645-8

Lee, P. G., Hohman, T. C., Cai, F., Regalia, J., and Helke, C. J. (2001). Streptozotocin-induced diabetes causes metabolic changes and alterations in neurotrophin content and retrograde transport in the cervical vagus nerve. *Exp. Neurol.* 170, 149–161. doi: 10.1006/exnr.2001.7673

Levin, B. E., Dunn-Meynell, A. A., and Routh, V. H. (2001). Brain glucosensing and the K(ATP) channel. *Nat. Neurosci.* 4, 459–460. doi: 10.1038/87405

Liu, M. T., Seino, S., and Kirchgessner, A. L. (1999). Identification and characterization of glucoresponsive neurons in the enteric nervous system. *J. Neurosci.* 19, 10305–10317.

MacGregor, I. L., Gueller, R., Watts, H. D., and Meyer, J. H. (1976). The effect of acute hyperglycemia on gastric emptying in man. *Gastroenterology* 70, 190–196.

Martinez de la Pena y Valenzuela, I., Browning, K. N., and Travagli, R. A. (2004). Morphological differences between planes of section do not influence the electrophysiological properties of identified rat dorsal motor nucleus of the vagus neurons. *Brain Res.* 1003, 54–60. doi: 10.1016/j.brainres.2003.10.076

Mei, N. (1978). Vagal glucoreceptors in the small intestine of the cat. *J. Physiol.* 282, 485–506.

Mei, N. (1985). Intestinal chemosensitivity. *Physiol. Rev.* 65, 211–237.

Morton, A. P., and Hanson, P. J. (1984). Monosaccharide transport by the small intestine of lean and genetically obese (ob/ob) mice. *Q. J. Exp. Physiol.* 69, 117–126.

Nosjean, A., Compoint, C., Buisseret-Delmas, C., Orer, H. S., Merahi, N., Puizillout, J. J., et al. (1990). Serotonergic projections from the nodose ganglia to the nucleus tractus solitarius: an immunohistochemical and double labeling study in the rat. *Neurosci. Lett.* 114, 22–26. doi: 10.1016/0304-3940(90)90422-6

Ordog, T., Takayama, I., Cheung, W. K., Ward, S. M., and Sanders, K. M. (2000). Remodeling of networks of interstitial cells of Cajal in a murine model of diabetic gastroparesis. *Diabetes* 49, 1731–1739. doi: 10.2337/diabetes.49.10.1731

Raupach, T., and Ballanyi, K. (2004). Intracellular pH and KATP channel activity in dorsal vagal neurons of juvenile rats in situ during metabolic disturbances. *Brain Res.* 1017, 137–145. doi: 10.1016/j.brainres.2004.05.030

Raybould, H. E. (1998). Does your gut taste. Sensory transduction in the gastrointestinal tract. *News Physiol. Sci.* 13, 275–280.

Raybould, H. E. (1999). Nutrient tasting and signaling mechanisms in the gut. I. Sensing of lipid by the intestinal mucosa. *Am. J. Physiol.* 277, G751–G755.

Raybould, H. E. (2002). Visceral perception: sensory transduction in visceral afferents and nutrients. *Gut* 51(Suppl. 1), I11–I14. doi: 10.1136/gut.51.suppl_1.i11

Raybould, H. E., Glatzle, J., Robin, C., Meyer, J. H., Phan, T., Wong, H., and Sternini, C. (2003). Expression of 5-HT3 receptors by extrinsic duodenal afferents contribute to intestinal inhibition of gastric emptying. *Am. J. Physiol. Gastrointest. Liver Physiol.* 284, G367–G372. doi: 10.1152/ajpgi.00292.2001

Raymer, C. K., Park, H. S., Wishart, J. M., Kong, M.-F., Doran, S. M., and Horowitz, M. (2000). Effects of intraduodenal glucose and fructose on antropyloric motility and appetite in healthy humans. *Am. J. Physiol.* 278, R360–R366.

Rayner, C. K., Samsom, M., Jones, K. L., and Horowitz, M. (2001). Relationships of upper gastrointestinal motor and sensory function with glycemic control. *Diabetes Care* 24, 371–381. doi: 10.2337/diacare.24.2.371

Regalia, J., Cai, F., and Helke, C. (2002). Streptozotocin-induced diabetes and the neurochemistry of vagal afferent neurons. *Brain Res.* 938, 7–14. doi: 10.1016/S0006-8993(02)02456-3

Roosen, L., Boesmans, W., Dondeyne, M., Depoortere, I., Tack, J., and Vanden Berghe, P. (2012). Specific hunger- and satiety-induced tuning of guinea pig enteric nerve activity. *J. Physiol.* 590, 4321–4333. doi: 10.1113/jphysiol.2012.231134

Sayegh, A. I., Covasa, M., and Ritter, R. C. (2004). Intestinal infusions of oleate and glucose activate distinct enteric neurons in the rat. *Auton. Neurosci.* 115, 54–63. doi: 10.1016/j.autneu.2004.08.006

Schvarcz, E., Palmer, M., Aman, J., Horowitz, M., Stridsberg, M., and Berne, C. (1997). Physiological hyperglycemia slows gastric emptying in normal subjects and patients with insulin-dependent diabetes mellitus. *Gastroenterology* 113, 60–66. doi: 10.1016/S0016-5085(97)70080-5

Shapiro, R. E., and Miselis, R. R. (1985). The Central Organization of the Vagus Nerve Innervating the Stomach of the Rat. *J. Comp. Neurol.* 238, 473–488. doi: 10.1002/cne.902380411

Shi, M., Jones, A. R., Ferreira, M. Jr., Sahibzada, N., Gillis, R. A., and Verbalis, J. G. (2005). Glucose does not activate nonadrenergic, noncholinergic inhibitory neurons in the rat stomach. *Am. J. Physiol. Regul. Integr. Comp. Physiol.* 288, R742–R750. doi: 10.1152/ajpregu.00561.2004

Shi, M., Jones, A. R., Niedringhaus, M. S., Pearson, R. J., Biehl, A. M., Ferreira, M. Jr., et al. (2003). Glucose acts in the CNS to regulate gastric motility during hypoglycemia. *Am. J. Physiol. Regul. Integr. Comp. Physiol.* 285, R1192–R1202. doi: 10.1152/ajpregu.00179.2003

Silver, I. A., and Erecinska, M. (1994). Extracellular glucose concentration in mammalian brain: continuous monitoring of changes during increased neuronal activity and upon limitation in oxygen supply in normo-, hypo-, and hyperglycemic animals. *J. Neurosci.* 14, 5068–5076.

Steinbusch, H. W. (1981). Distribution of serotonin-immunoreactivity in the central nervous system of the rat-cell bodies and terminals. *Neuroscience* 6, 557–618. doi: 10.1016/0306-4522(81)90146-9

Steinbusch, H. W., and Nieuwenhuys, R. (1981). Localization of serotonin-like immunoreactivity in the central nervous system and pituitary of the rat, with special references to the innervation of the hypothalamus. *Adv. Exp. Med. Biol.* 133, 7–35. doi: 10.1007/978-1-4684-3860-4_1

Sykes, R. M., Spyer, K. M., and Izzo, P. N. (1994). Central distribution of substance P, calcitonin gene-related peptide and 5-hydroxytryptamine in vagal sensory afferents in the rat dorsal medulla. *Neuroscience* 59, 195–210. doi: 10.1016/0306-4522(94)90110-4

Takahashi, T., Matsuda, K., Kono, T., and Pappas, T. N. (2003). Inhibitory effects of hyperglycemia on neural activity of the vagus in rats. *Intens. Care Med.* 29, 309–311. doi: 10.1007/s00134-002-1580-3

Thor, K. B., and Helke, C. J. (1989). Serotonin and substance P colocalization in medullary projections to the nucleus tractus solitarius: dual-colour immunohistochemistry combined with retrograde tracing. *J. Chem. Neuroanat.* 2, 139–148.

Tougas, G., Hunt, R. H., Fitzpatrick, D., and Upton, A. R. (1992). Evidence of impaired afferent vagal function in patients with diabetes gastroparesis. *Pacing Clin. Electrophysiol.* 15, 1597–1602. doi: 10.1111/j.1540-8159.1992.tb02939.x

Trapp, S., Ballanyi, K., and Richter, D. W. (1994). Spontaneous activation of K_{ATP} current in rat dorsal vagal neurones. *Neuroreport* 5, 1285–1288. doi: 10.1097/00001756-199406020-00033

Travagli, R. A., Hermann, G. E., Browning, K. N., and Rogers, R. C. (2006). Brainstem circuits regulating gastric function. *Annu. Rev. Physiol.* 68, 279–305. doi: 10.1146/annurev.physiol.68.040504.094635

Troy, A. E., and Browning, K. N. (2013). High fat diet decreases glucose-dependent modulation of 5-HT responses in gastrointestinal vagal afferent neurons. *FASEB J.* 27, 1158.3.

Vincent, K. M., Sharp, J. W., and Raybould, H. E. (2011). Intestinal glucose-induced calcium-calmodulin kinase signaling in the gut-brain axis in awake rats. *Neurogastroenterol. Motil.* 23, e282–e293. doi: 10.1111/j.1365-2982.2011.01673.x

Wan, S., and Browning, K. N. (2008a). D-Glucose modulates synaptic transmission from the central terminals of vagal afferent fibers. *Am. J. Physiol. Gastrointest. Liver Physiol.* 294, G757–G763. doi: 10.1152/ajpgi.00576.2007

Wan, S., and Browning, K. N. (2008b). Glucose increases synaptic transmission from vagal afferent central nerve terminals via modulation of 5HT3 receptors. *Am. J. Physiol. Gastrointest. Liver Physiol.* 295, G1050–G1057. doi: 10.1152/ajpgi.90288.2008

Wang, X. Y., Huizinga, J. D., Diamond, J., and Liu, L. W. (2009). Loss of intramuscular and submuscular interstitial cells of Cajal and associated enteric nerves is related to decreased gastric emptying in streptozotocin-induced diabetes. *Neurogastroenterol. Motil.* 21, 1095–1099. doi: 10.1111/j.1365-2982.2009.01336.x

Yagihashi, S., and Sima, A. A. (1986). Diabetic autonomic neuropathy in BB rat. Ultrastructural and morphometric changes in parasympathetic nerves. *Diabetes* 35, 733–743. doi: 10.2337/diab.35.7.733

Yettefti, K., Orsini, J. C., El Ouazzain, T., Himmi, T., Boyer, A., and Perrin, J. (1995). Sensitivity of the nucleus tractus solitarius neurons to induced moderate hyperglycemia, with special reference to catecholaminergic regions. *J. Auton. Nerv. Syst.* 51, 191–197.

Yettefti, K., Orsini, J.-C., and Perrin, J. (1997). Characteristics of glycemia-sensitive neurons in the nucleus tractus solitarii: possible involvement in nutritional regulation. *Physiol. Behav.* 61, 93–100. doi: 10.1016/S0031-9384(96)00358-7

Yoneda, S., Kadowaki, M., Kuramoto, H., Fukui, H., and Takaki, M. (2001). Enhanced colonic peristalsis by impairment of nitrergic enteric neurons in spontaneously diabetic rats. *Auton. Neurosci.* 92, 65–71. doi: 10.1016/S1566-0702(01)00317-4

Zhou, S. Y., Lu, Y. X., and Owyang, C. (2008). Gastric relaxation induced by hyperglycemia is mediated by vagal afferent pathways in the rat. *Am. J. Physiol. Gastrointest. Liver Physiol.* 294, G1158–G1164. doi: 10.1152/ajpgi.00067.2008

Zhu, J. X., Wu, X. Y., Owyang, C., and Li, Y. (2001). Intestinal serotonin acts as a paracrine substance to mediate vagal signal transmission evoked by luminal factors in the rat. *J. Physiol.* 530, 431–442. doi: 10.1111/j.1469-7793.2001.0431k.x

Zhuo, H., Ichikawa, H., and Helke, C. J. (1997). Neurochemistry of the nodose ganglion. *Prog. Neurobiol.* 52, 79–107. doi: 10.1016/S0301-0082(97)00003-8

Zittel, T. T., De, G. R., Sternini, C., and Raybould, H. E. (1994). Fos protein expression in the nucleus of the solitary tract in response to intestinal nutrients in awake rats. *Brain Res.* 663, 266–270. doi: 10.1016/0006-8993(94)91272-6

Zsombok, A., Bhaskaran, M. D., Gao, H., Derbenev, A. V., and Smith, B. N. (2011). Functional plasticity of central TRPV1 receptors in brainstem dorsal vagal complex circuits of streptozotocin-treated hyperglycemic mice. *J. Neurosci.* 31, 14024–14031. doi: 10.1523/JNEUROSCI.2081-11.2011

Conflict of Interest Statement: The author declares that the research was conducted in the absence of any commercial or financial relationships that could be construed as a potential conflict of interest.

Received: 01 October 2013; accepted: 30 October 2013; published online: 26 November 2013.

*Citation: Browning KN (2013) Modulation of gastrointestinal vagal neurocircuits by hyperglycemia. Front. Neurosci. **7**:217. doi: 10.3389/fnins.2013.00217*

This article was submitted to Autonomic Neuroscience, a section of the journal Frontiers in Neuroscience.

frontiers in
NEUROSCIENCE

ORIGINAL RESEARCH ARTICLE
published: 20 December 2013
doi: 10.3389/fnins.2013.00249

Astrocytes in the nucleus of the solitary tract are activated by low glucose or glucoprivation: evidence for glial involvement in glucose homeostasis

David H. McDougal, Gerlinda E. Hermann* and Richard C. Rogers*

Laboratory for Autonomic Neuroscience, Pennington Biomedical Research Center, Baton Rouge, LA, USA

Edited by:
Andrea Zsombok, Tulane University, USA

Reviewed by:
Pieter V. Berghe, Center for Gastroenterological Research, Belgium
Ann Goodchild, Macquarie University, Australia

****Correspondence:***
Gerlinda E. Hermann and Richard C. Rogers, Laboratory for Autonomic Neuroscience, Pennington Biomedical Research Center, 6400 Perkins Rd, Baton Rouge, LA 70808, USA
e-mail: hermange@pbrc.edu; rogersrc@pbrc.edu

Glucose homeostasis is maintained through interplay between central and peripheral control mechanisms which are aimed at storing excess glucose following meals and mobilizing these same stores during periods of fasting. The nucleus of the solitary tract (NST) in the dorsal medulla has long been associated with the central detection of glucose availability and the control of glucose homeostasis. Recent evidence has emerged which supports the involvement of astrocytes in glucose homeostasis. The aim of the present study was to investigate whether NST-astrocytes respond to physiologically relevant decreases in glucose availability, *in vitro*, as well as to the presence of the glucoprivic compound 2-deoxy-D-Glucose. This report demonstrates that some NST-astrocytes are capable of responding to low glucose or glucoprivation by increasing cytoplasmic calcium; a change that reverses with restoration of normal glucose availability. While some NST-neurons also demonstrate an increase in calcium signaling during low glucose availability, this effect is smaller and somewhat delayed compared to those observed in adjacent astrocytes. TTX did not abolish these hypoglycemia mediated responses of astrocytes, suggesting that NST-astrocytes may be directly sensing low glucose levels as opposed to responding to neuronal detection of hypoglycemia. Thus, chemodetection of low glucose by NST-astrocytes may play an important role in the autonomic regulation of glucose homeostasis.

Keywords: astrocytes, calcium imaging, 2-deoxy-D-glucose, solitary nucleus, vago-vagal reflex, glucose homeostasis, hypoglycemia

INTRODUCTION

Glucose is the primary energy source for cellular metabolism. Therefore, the maintenance of appropriate serum glucose levels is critical for organismal survival. Glucose homeostasis is maintained through interplay between central and peripheral control mechanisms which are aimed at storing excess glucose following meals and mobilizing these same stores during periods of fasting. Central control of glucose homeostasis is accomplished by a distributed system of glucosensing elements, integrative neural networks which process signals from these elements, and pre-autonomic nuclei which control motor outflow and are modulated through inputs from these neural integrators (Watts and Donovan, 2010).

A principal site for neural integration of glucose availability is the nucleus of the solitary tract (NST), located in the dorsal medulla. Cells within NST have unique access to serum glucose levels due to the large numbers of fenestrated capillaries present in the nucleus (Gross et al., 1990) as well as its close apposition to the area postrema, a circumventricular organ (Cottrell and Ferguson, 2004). A subset of NST neurons have been shown to respond to physiologically relevant changes in extracellular glucose availability both *in vivo* (Yettefti et al., 1995, 1997) and *in vitro* (Mizuno and Oomura, 1984; Himmi et al., 1996; Dallaporta et al., 1999). In addition to containing these glucoresponsive cells, NST also receives input regarding peripheral glucose levels by way of glucosensors located in hepatic portal/mesenteric vein, which innervate NST via the hepatic branch of the vagus nerve (Niijima, 1984; Adachi et al., 1995; Grabauskas et al., 2010). Furthermore, NST also receives descending inputs from hypothalamic nuclei such as the lateral and paraventricular nuclei that are associated with glucose homeostasis (Marty et al., 2007; Geerling et al., 2010; Biag et al., 2012). Due to this confluence of signals regarding glucose availability as well as its inputs to pre-autonomic nuclei, the NST plays a predominate role in central control of glucose homeostasis (Adachi et al., 1995; Grill and Hayes, 2012).

The NST is also commonly associated with the physiological response to hypoglycemia. These autonomic counter-measures, often referred to collectively as the counter-regulatory response (CRR) include increases in serum levels of glucagon and stress hormones, increased food intake, and an overall increase in sympathetic tone. Systemic administration of the glucoprivic compound 2-deoxy-glucose (2-DG; a glucose analog commonly used to invoke the CRR) results in increased c-Fos expression in the NST (Ritter et al., 1998; Briski and Marshall, 2000; Sanders and Ritter, 2000; Dodd et al., 2010). Focal administration of a similar glucoprivic agent, 5-thio-D-glucose, directly into the NST of rats also drives CRRs such as increased food intake (Ritter et al., 2000) and increases in serum glucagon and stress hormone levels (Andrew et al., 2007).

In addition to its role in glucose homeostasis and hypoglycemic counter-regulation, the NST plays a critical role in a number of other autonomic functions such as regulation of cardiovascular, respiratory, and gastrointestinal reflexes (Blessing, 1997). There is increasing evidence that chemodetection by brainstem astrocytes can drive changes in these autonomic reflexes (Hermann and Rogers, 2009; Hermann et al., 2009; Gourine et al., 2010; Kasymov et al., 2013). Interestingly there is also strong evidence for astrocytic involvement in the autonomic response to hypoglycemia. Systemic administration of the selective glial toxin, methionine sulfoximine, blocks 2-DG induced c-Fos expression in NST (Young et al., 2000). In addition, transgenic mice which only express the type II glucose transporter (GLUT2) in pancreatic beta cells (i.e., expression of GLUT2 was knocked out centrally), demonstrate defects in the CRR (Burcelin and Thorens, 2001). However, these defects are rescued by the selective CNS re-expression of GLUT2 in astrocytes, but not neurons (Marty et al., 2005). Therefore, the aim of the present study was to investigate whether NST-astrocytes respond to physiologically relevant decreases in glucose availability, *in vitro*, as well as to the presence of the glucoprivic compound 2-DG.

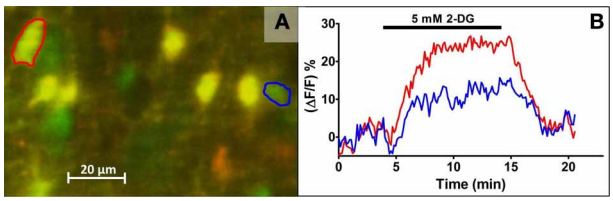

FIGURE 1 | Live cell calcium imaging of NST astrocytes in response to glucoprivic challenge. *In vivo* co-injection of the calcium indicator dye, Calcium Green 1-AM (CAG; green) and the glial vital stain sulforhodamine 101 (SR101; red) allows for simple discrimination of astrocytes and neurons in the *in situ* brain stem slice preparation. Following a dual exposure utilizing the 488 nm and 561 nm laser lines, a composite image is obtained in which astrocytes are clearly labeled yellow, i.e., positive for both CAG and SR101, while neurons remain green **(A)**. Time-lapse imaging with only the 488 nm laser line can then be used to follow changes in intracellular calcium concentrations, indicated by a proportional change in the intensity of the CAG signal, before, during, and after the application of glucoprivic or low glucose challenges. Regions of interest (ROI) were drawn around an individual neuron (blue circle) and astrocyte (red circle) in **(A)** for analysis of their time-lapse responses to 2-DG challenge **(B)**. Exposure time to 2-DG is represented by bar over graph.

METHODS

ANIMALS

All experimental procedures were conducted under the approval of the Pennington Biomedical Research Center's Institutional Animal Care and Use Committee. Long Evans rats of either sex (body weight between 150 and 250 g) were used in these studies. All animals were housed in a temperature controlled room under 12 h light/dark cycle and provided water and food *ad libitum*. All experimental protocols were performed according to the guidelines set forth by the National Institutes of Health.

In vivo PRE-LABELING OF NST AND HARVEST OF HINDBRAIN SLICES

Animals ($N = 22$) were deeply anesthetized with urethane (1.5 g/kg, ip; ethyl carbamate, Sigma) and placed in a stereotaxic frame. Using aseptic technique, the occipital plate of the skull was removed to expose the medullary brainstem. A micropipette 30 micron tip diameter; filled with 0.2% Calcium Green 1 AM (CAG; Life Technologies), 0.3% sulforhodamine 101 (SR101; Sigma Chemical) and 20% pluronic-DMSO (F-127, in pH 7.2 tris-PBS buffer) was directed toward the medial solitary nucleus using a stereotaxic carrier. Four injections (40 nL each) of the CAG-SR101 solution were made unilaterally into the NST at the level of calamus and 0.2, 0.4, and 0.6 mm anterior to calamus; all at a depth of 300 microns below the surface. This injection pattern labeled the entire ipsilateral medial NST (Hermann et al., 2009). CAG, a calcium reporter dye, is taken up by both neurons and glia while SR101 labels only astrocytes (Nimmerjahn et al., 2004; McDougal et al., 2011). SR101 does not interfere with CAG fluorescence (Hermann and Rogers, 2009). Thus, despite the similarity in size of NST neuronal and astrocytic cell bodies, this method made it possible to easily discriminate between these two cell types in the slice preparation (**Figure 1**). After a 30 min interval to allow for dye uptake, the anesthetized rat was decapitated and the brainstem was quickly harvested. The caudal brainstem was glued to an aluminum block and placed in cold (~4°C) carboxygenated (95% O_2; 5% CO_2) cutting solution (recipe below). Coronal sections (300 micron thick) were cut through the medulla using a Leica VT1200 tissue slicer equipped with a sapphire knife (Delaware Diamond Knives). The NST is easily identified in these slices due to its lack of myelin; 4–5 slices containing NST were collected from each animal and placed in normal Krebs' solution (recipe below) which was bubbled with 95% O_2/5% CO_2 and maintained at a constant temperature of 29°C. Slices were allowed to equilibrate to these conditions for an hour prior to imaging.

In vitro DRUGS AND SOLUTIONS

All solutions were freshly prepared on the day of the experiment. The cutting solution contained 110 mM choline chloride, 25 mM $NaHCO_3$, 2.5 mM KCl, 7 mM $MgSO_4$–7H2O, 1.25 mM NaH_2PO_4, 10 mM glucose, and 0.5 mM $CaCl_2$–$2H_2O$. The normal Krebs' solution contained 124 mM NaCl, 25 mM $NaHCO_3$, 3.0 mM KCl, 1 mM $MgSO_4$–$7H_2O$, 1.5 mM NaH_2PO_4, 5 mM glucose, and 1.5 mM $CaCl_2$–$2H_2O$. Composition of the "low glucose challenge" solutions was identical to the normal Krebs' solution except that the concentration of glucose was decreased from 5 to 2.5 mM, 1 mM, or 0.5 mM. Given that extracellular brain glucose levels are ~30% that of plasma glucose (Silver and Erecinska, 1994), the range of normal extracellular brain glucose levels runs between 0.5 and 2.5 mM (Song et al., 2001). However, brain areas such as the arcuate nucleus of the hypothalamus or the NST, which border circumventricular organs, are predicted to be exposed to glucose levels normally seen in the CSF (3.4 mM) or serum (5.5 mM) (Levin et al., 2004). Therefore, we include 5 mM glucose as our "normal" glucose concentration for comparisons.

The "glucoprivic challenge" solution consisted of 5 mM 2-deoxy-D-glucose (2-DG; Sigma-Aldrich, St. Louis, MO) dissolved in normal 5 mM glucose Krebs' solution. The osmolarity of

the normal Krebs', low glucose challenge, and glucoprivic challenge solutions were adjusted to 300 ± 3 mOsm with sucrose. Tetrodotoxin (1 μM TTX; Sigma-Aldrich, St Louis, MO) was included in some low glucose challenge solutions. Bath application of TTX has been shown to block approximately 95% of the direct neuronal activation of NST astrocytes (McDougal et al., 2011).

LIVE CELL CALCIUM IMAGING

Slices were transferred to a custom imaging chamber (Rogers and Hermann, 2012b); perfused at a rate of 2.5 mL/min with normal Krebs' maintained at a temperature of 32°C. Slices were imaged with a Nikon F1 fixed stage upright microscope equipped with a Nikon Fast Scan laser confocal head and a Luca EMCCD camera (Andor Technology, South Windsor, CT). Co-injection of CAG and SR101 allows for discrimination of astrocytes and neurons at the cellular level by comparing images captured using the 488 and 561 nm laser lines (McDougal et al., 2011). That is, at 488 nm, both astrocytes and neurons pre-labeled with CAG will appear green; at 561 nm, all astrocytes will also appear red. A single, dual exposure image was collected just prior to and following each experimental trial in order to confirm the cell types being recorded (**Figure 1**).

Changes in intracellular calcium concentrations within CAG pre-labeled NST-astrocytes and NST-neurons in response to different stimuli were recorded using the 488 nm laser line to excite the CAG. Increases in intracellular calcium concentrations are reflected as an increase in fluorescence and is indicative of increased cellular activity. During experimental trials, time-lapsed images of mixed fields of NST-astrocytes and neurons were monitored for their responses to low glucose or glucoprivic conditions.

EXPERIMENTAL DESIGN

Each slice was exposed to a single "experimental trial" which consisted of three perfusion conditions of equal duration (i.e., 10 min for each condition). Slices were perfused with normal Krebs' containing 5 mM glucose during the initial and final blocks of time. The intervening block was the experimental condition [e.g., "time control" consisting of continued perfusion with 5 mM glucose Krebs', low glucose (i.e., 0.5, 1.0, or 2.5 mM) or glucoprivic challenge (i.e., 5 mM 2-DG with 5 mM glucose Krebs')]. Thus, each cell functioned as its own control and transitional differences in activity due to changes in available glucose (i.e., decreasing or increasing) could also be monitored.

In order to rule out the possibility that neuronal synaptic input to glia was responsible for the astrocytic responses to low-glucose conditions, tetrodotoxin (TTX) was used to block action potential-mediated communication between neurons and astrocytes (McDougal et al., 2011). For this study, we specifically chose the 1 mM glucose challenge, to ensure that the neurons would not be compromised by very low glucose. In these experiments, TTX (1 μM) was present during all three perfusion periods [i.e., normal (5 mM), low glucose challenge (1 mM), and normal (5 mM) glucose]. The responses of cells during the low glucose challenge plus TTX were then compared to responses of cells exposed to an identical experimental trial that did not use TTX, i.e., identical blocks of 0.5, 1 and 5 mM profusion conditions without TTX.

Time-lapse images were analyzed using Nikon NIS-Elements software. Each cell in a field was delineated as a region of interest (ROI) and the average intensity of all pixels within each ROI was calculated for each time point (**Figure 1**). These data were exported to Microsoft Excel for analysis offline.

Relative changes in intracellular calcium in response to all stimulation paradigms were quantified as percent changes in fluorescence: $(\Delta F/F)\%$, where F is the baseline fluorescence intensity within an area of interest (e.g., the outline of an SR101-labeled astrocyte) before stimulation, and ΔF is the change from this value resulting from stimulus-induced cellular activity (Helmchen, 2000). Background fluorescence (i.e., non-responsive areas in same field) was subtracted from both F and ΔF. An individual cell was considered to have responded to a given stimulus if the stimulus induced a peak change in $(\Delta F/F)\% > 5\%$ (O'Malley et al., 2006; Rogers et al., 2006a,b; Hermann et al., 2009; McDougal et al., 2011).

Parameters including average baseline fluorescence intensity, peak intensity, as well as the onset of the response to the low glucose or glucoprivic challenge were determined for each ROI. These values were used to calculate: (a) latency to onset of response, (b) peak response magnitude (percent increase in intensity from baseline), (c) response offset (time at which the response magnitude decayed to $1/e$ of the peak value; ∼37%), and (d) response magnitude (area under the curve from response onset to response offset) for each ROI. In order to verify the macro-defined values, each was displayed graphically on a line plot of intensity vs. time and visually inspected for accuracy.

The criteria of low-glucose (or 2DG) responder types:

- *Positive*: Peak response > 5% and AUC > 175 $(\Delta F/F)\%$ minute and $\Delta F/F$ values returned to $1/e$ of peak (∼37%) before the end of the trial.
- *Negative*: Peak response < –5% and AUC< −175 $(\Delta F/F)\%$ minute
- *Sustained activation*: Peak response > 5% and $\Delta F/F$ values failed to return to $1/e$ of peak (∼37%) before the end of the trial. AUC is undefined in these cells because there is no "stop time" which is defined as the time at which $\Delta F/F$ values returned to $1/e$ of peak (∼37%).
- *Non-responders*: Any cell which did not meet the above criteria.

DATA ANALYSIS

The cell type (i.e., astrocyte or neuron) represented by each ROI was determined by the presence or absence of SR101 staining. The average values of three separate response parameters (peak, latency, and response magnitude) were determined for each cell type in each experimental condition, and then compared statistically. Astrocytic response parameters across the three concentrations of glucose were compared to neuronal response parameters using two-way analysis of variance (i.e., cell type vs. concentration of glucose). Separate analyses were made of the average response parameters of astrocytes vs. neurons to a glucoprivic condition (i.e., 5 mM glucose plus 5 mM 2-DG) using unpaired t-tests.

Studies using TTX to determine if astrocytic responses were secondary to neuronal activation used unpaired *t*-tests to evaluate cellular response parameters of astrocytes or neurons during the 1 mM glucose challenge with vs. without TTX in the perfusion solution. All statistical analyses were performed using GraphPad Prism software (GraphPad Software, La Jolla, CA); *p*-values < 0.05 were considered statistically significant.

Table 1 | Classification of cellular response patterns to low glucose (top) or glucoprivic (bottom) challenges.

	Low glucose positive (%)	Low glucose negative (%)	Low glucose sustained (%)	Low glucose NR (%)
Astrocytes (263 total)	39	13	1	47
Neurons (160 total)	37	11	1	51
	2DG positive (%)	**2DG negative (%)**	**2DG sustained (%)**	**2DG NR (%)**
Astrocytes (118 total)	42	8	3	47
Neurons (81 total)	26	16	6	52

RESULTS

A SUBSET OF NST-ASTROCYTES AND NEURONS RESPOND TO LOW GLUCOSE CHALLENGE

Brainstem slices challenged by conditions of low glucose availability (i.e., bath application of Krebs' solution containing 0.5, 1.0, or 2.5 mM glucose) showed fluxes in intracellular calcium levels in both NST-astrocytes and neurons. The cellular responses were measured by changes in the fluorescent intensity of CAG relative to individual baseline levels. The relative changes in cytoplasmic calcium were expressed as percent changes in fluorescence $[(\Delta F/F)\%]$ of the CAG reporter dye, where F is the intensity of the baseline fluorescence signal before stimulation, and ΔF is the difference between the peak fluorescence intensity and the baseline signal (**Figures 2**, **4**, **5**).

Both NST-astrocytes and neurons displayed one of four distinct response patterns as a result of exposure to each low glucose challenge (**Table 1**). The most prevalent response pattern was the "non-responder" which showed no response to conditions of low glucose availability (47% of astrocytes; 51% of neurons). The second largest category encountered was a "low glucose positive"

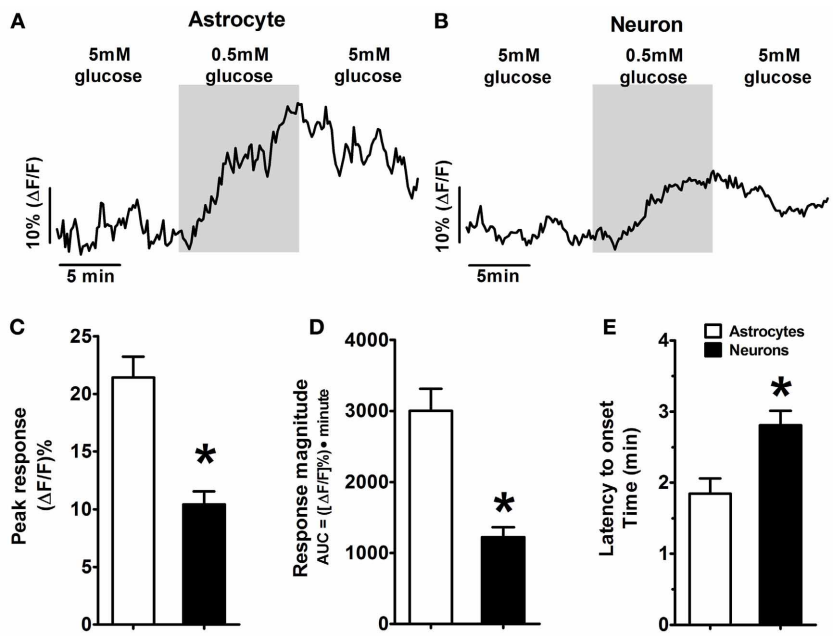

FIGURE 2 | Example of response patterns of low glucose-positive astrocytes and neurons in the hindbrain slice preparation to low glucose challenge. As seen in **Figure 1**, mixed fields of NST-astrocytes and neurons were recorded using confocal live cell calcium imaging. Changes in intracellular calcium levels were reflected as changes in intensity of the fluorescent calcium indicator dye, Calcium Green 1-AM. Both low glucose-positive **(A)** astrocytes and **(B)** neurons were activated in response to a change in the extracellular glucose concentration from 5 to 0.5 mM; this activation returned toward baseline levels following return to 5 mM glucose. [Traces in **(A,B)** are the average response of five representative low glucose positive astrocytes and neurons, respectively]. Two-Way ANOVA: **(C)** Peak response and **(D)** response magnitude demonstrated significant main effects attributed to the cell type ($p < 0.05$) as well as significant main effects attributed to the concentration of glucose ($p < 0.05$) (see also **Figure 3**). These main effects are qualified due to the significant interactions between cell types and glucose concentrations. Thus, NST-astrocytes were more responsive than NST-neurons to low glucose conditions particularly at the 0.5 mM concentration. **(E)** Latency to onset of response to low glucose also demonstrated a significant main effect attributed to cell type ($p < 0.05$); astrocytes responded at 1.7 ± 0.2 min (mean ± s.e.m.) compared to neurons at 2.6 ± 0.2 min. $^*P < 0.05$.

response pattern where cells showed an increase in intracellular calcium concentrations when exposed to low glucose and baseline levels of intracellular calcium concentrations returned following the return to 5 mM glucose Krebs' solution (39% of astrocytes; 37% of neurons) (**Figures 2A,B**; **Table 1**). The remaining cells responded either with a decrease in intracellular calcium levels and were characterized as "low glucose negative" (13% of astrocytes; 11% of neurons) or displayed an increase in intracellular calcium signaling which failed to return to baseline levels following the return to 5 mM glucose levels. This last group is referred to as "sustained activation" (1% of astrocytes; 1% of neurons; **Table 1**).

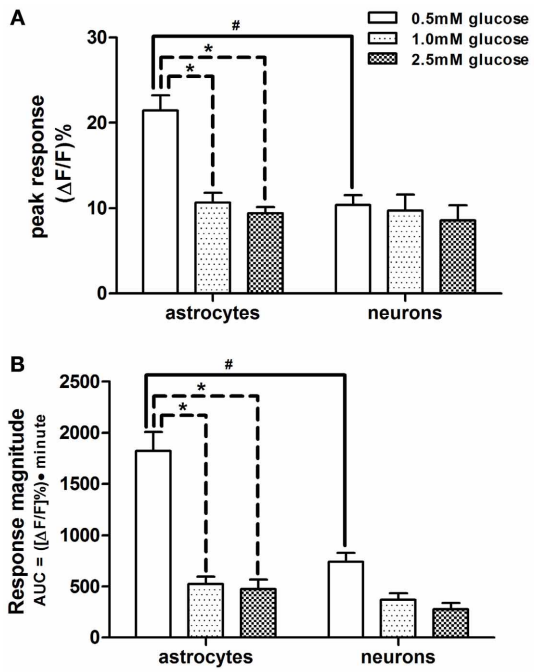

FIGURE 3 | Comparison of response parameters of NST-astrocytes and -neurons to low glucose conditions. Subsets of both astrocytes and neurons responded with increased activation, as seen by their change in fluorescence, when exposed to lower glucose concentrations in the perfusion solution. Two-Way ANOVA of the peak and magnitude of astrocytic and neuronal responses to low glucose conditions revealed that astrocytes were more responsive than neurons in **(A)** peak response and **(B)** response magnitude, i.e., area under the curve [significant main effect of cell type; $F_{(1,\ 159)} = 8.36$ and 12.57, respectively; $p < 0.05$]. There were significant main effects attributed to the concentration of glucose [$F_{(2,\ 159)} = 8.40$ and 18.57; respectively; $p < 0.05$]. These main effects are qualified due to the significant interactions between cell types and glucose concentrations [$F_{(2,\ 159)} = 5.24$ and 4.99, respectively; $p < 0.05$]. Bonferroni *post-hoc t*-tests demonstrated that astrocytes and neurons differ significantly in these response parameters when 0.5 mM glucose was in the perfusion bath; #$p < 0.05$. In astrocytes, these response parameters at the 0.5 mM glucose level where significantly different from those at the 1.0 and 2.5 mM glucose levels; *$p < 0.05$.

RESPONSE TO LOW GLUCOSE CHALLENGE DIFFERED BASED ON CELL TYPE AND GLUCOSE CONCENTRATION

Three response parameters were measured in "low glucose positive" astrocytes and neurons following exposure to each low glucose challenge condition (0.5, 1.0, or 2.5 mM); see **Figure 3** and **Table 2**. These parameters included: (1) response latency (time between onset of challenge and response onset), (2) response magnitude (area under the curve from response onset to response offset), and (3) peak response (percent increase in CAG intensity from baseline). Two-Way ANOVA revealed that latency to onset of response demonstrated a significant main effect attributed to cell type [$F_{(1,\ 111)} = 6.38$, $p < 0.05$]. Latency to onset of response to low glucose for astrocytes was 1.7 ± 0.2 min (mean $\pm$ SEM) compared to neurons at 2.6 ± 0.2 min. Peak response and response magnitude also demonstrated significant main effects attributed to the cell type [$F_{(1,\ 159)} = 8.36$ and 12.57, respectively; $p < 0.05$] as well as significant main effects attributed to the concentration of glucose [$F_{(2,\ 159)} = 8.40$ and 18.57; respectively; $p < 0.05$]. These main effects are qualified due to the significant interactions between cell types and glucose concentrations [$F_{(2,\ 159)} = 5.24$ and 4.99, respectively; $p < 0.05$]. Thus, astrocytes were more responsive than neurons to low glucose conditions particularly at the 0.5 mM concentration (**Figure 3**).

Bonferroni *post-hoc t*-tests showed that astrocytes and neurons differ in these response parameters to 0.5 mM glucose in the perfusion bath (**Figure 2**). Additionally, astrocytes demonstrated significantly larger peak responses and response magnitudes to 0.5 mM glucose compared to either 1.0 or 2.5 mM glucose challenges (**Figure 3**).

A SUBSET OF NST-ASTROCYTES AND NEURONS RESPOND TO GLUCOPRIVIC CHALLENGE

NST-astrocytes and neurons showed similar response patterns during glucoprivic challenge where 5 mM 2-DG was included in the 5 mM glucose-Krebs' solution (**Figure 4**). Most astrocytes (47%) and neurons (52%) were "non-responders" (**Table 1**). The

Table 2 | Response parameters of NST astrocytes and neurons responsive to low-glucose or 2DG conditions.

Condition	Peak response(DF/F)%		Magnitude of response (Area under the curve = change over time)		*N*	
	Astrocytes	Neurons	Astrocytes	Neurons	Astrocytes	Neurons
5 mM 2DG	15.5 ± 1.1	14.0 ± 1.0	2329 ± 228	2093 ± 229	56	21
0.5 mM glucose	21.4 ± 1.8	10.4 ± 1.1	3005 ± 308	1224 ± 140	46	33
1.0 mM glucose	10.1 ± 1.1	9.3 ± 1.8	678 ± 124	391 ± 60	35	17
2.5 mM glucose	8.4 ± 0.7	7.8 ± 1.5	704 ± 139	391 ± 94	29	12

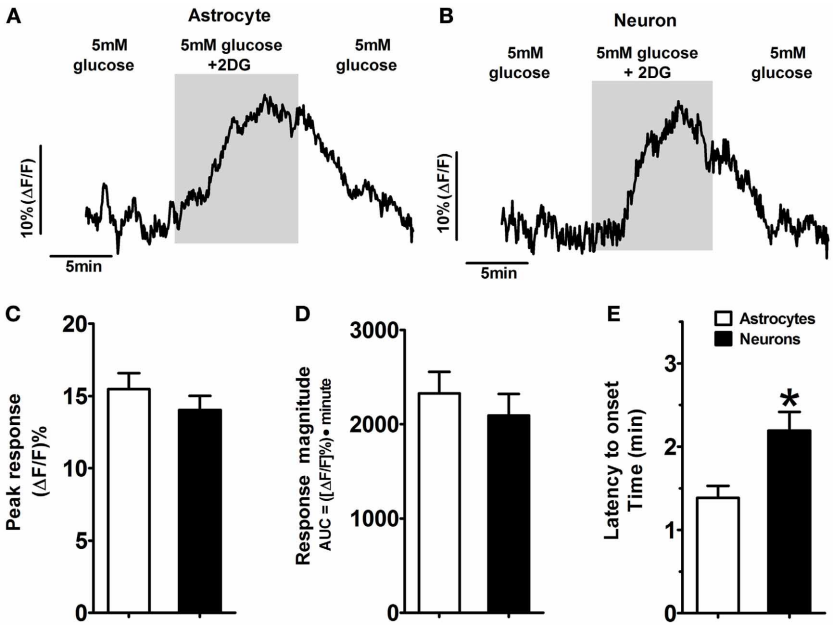

FIGURE 4 | Activated response patterns of astrocytes and neurons in the hindbrain slice preparation to glucoprivic challenge (i.e., 2-DG-positive). Approximately 40% of NST-astrocytes and 25% of NST-neurons responded to a glucoprivic solution consisting of 5 mM 2-Deoxy-D-glucose (2-DG) dissolved in media containing normal (5 mM) glucose concentrations with an increase in activity (**Tables 1**, **2**). Examples of 2-DG-positive astrocytes and neurons activated in response to the glucoprivic challenge are shown [Traces in **(A,B)** are the average response of five representative 2-DG-positive astrocytes and neurons, respectively]. The peak responses **(C)** and response magnitudes **(D)** were similar in both astrocytes and neurons. However, these two cell types differed in time to onset of response **(E)**. NST-astrocytes averaged 1.4 ± 0.1 min compared to the onset of NST-neuronal response at 2.2 ± 0.2 min ($^*p < 0.05$).

next largest class was "2-DG positive" which displayed an increase in intracellular calcium signaling during exposure to this glucoprivic condition that returned to baseline following washout (42% of astrocytes; 26% of neurons). The remainder of cells could be characterized as either "2-DG negative" (8% of astrocytes; 16% of neurons) or "sustained activation" (3% of astrocytes; 6% of neurons). Unpaired *t*-test comparisons revealed that astrocytes had significantly shorter latencies to response onset compared to neurons [1.4 ± 0.1 min vs. 2.2 ± 0.2 min; $t_{(73)} = 3.00$; $p = 0.0037$]. There were no differences in peak response (15.5 ± 1.1% vs. 14.0 ± 1.0%; astrocytes vs. neurons) or response magnitude (2329 ± 228 vs. 2093 ± 229) between astrocytes and neurons during glucoprivic challenge (**Table 2**).

LOW GLUCOSE SIGNALING IN NST-ASTROCYTES IS INDEPENDENT OF NEURONAL SIGNALING

In order to rule out the possibility that neuronal synaptic input to glia was responsible for the astrocytic responses to low-glucose conditions, TTX was used to block action potential-mediated communication between neurons and astrocytes (**Figure 5**). Astrocytic peak responsiveness to a 1mM low glucose challenge was unaffected by TTX (15.3 ± 0.9% vs. 17.5 ± 1.7%), although response magnitude was somewhat lower than control levels (991 ± 102 vs. 763 ± 116; **Figures 5A,C,D**). The slight reduction in the size of the astrocytic responses in the presence of TTX likely represents a loss of tonic neuronal activation of NST-astrocytes independent of glucose availability, possibly mediated by glutamate release from vagal afferents (McDougal et al., 2011).

In contrast, neuronal peak response and response magnitude during the same low glucose challenge were significantly reduced by TTX [peak response: 9.0 + 1.0% vs. 6.2 + 0.6%; $t_{(17)} = 2.422$, $p = 0.013$; magnitude: 652 ± 135 vs. 156 ± 37; $t_{(17)} = 3.043$, $p = 0.004$ (**Figures 5B,E,F**)]. NST neuronal calcium signaling in response to low glucose challenge may be dependent on other neuronal inputs or on modulation of the voltage-dependent sodium conductance.

DISCUSSION

The dorsal medulla and NST have long been associated with the central detection of the glucose availability and the control of the glycemic state (Bernard, 1855; Marty et al., 2007; Grill and Hayes, 2012). Recent evidence is emerging in support of astrocytic involvement in glucose homeostasis (Young et al., 2000; Guillod-Maximin et al., 2004; Marty et al., 2005). Our present report provides evidence that astrocytes in the NST respond to changes in glucose availability. Following exposure to conditions of low glucose, a subset of NST-astrocytes and neurons exhibit an increase in intracellular calcium signaling, this is reversed following restoration of normal glucose availability. Both the peak and magnitude of the astrocytic response varied across different levels of low glucose availability. The size of the neuronal response across the different glucose concentrations did not vary significantly. In comparison to adjacent

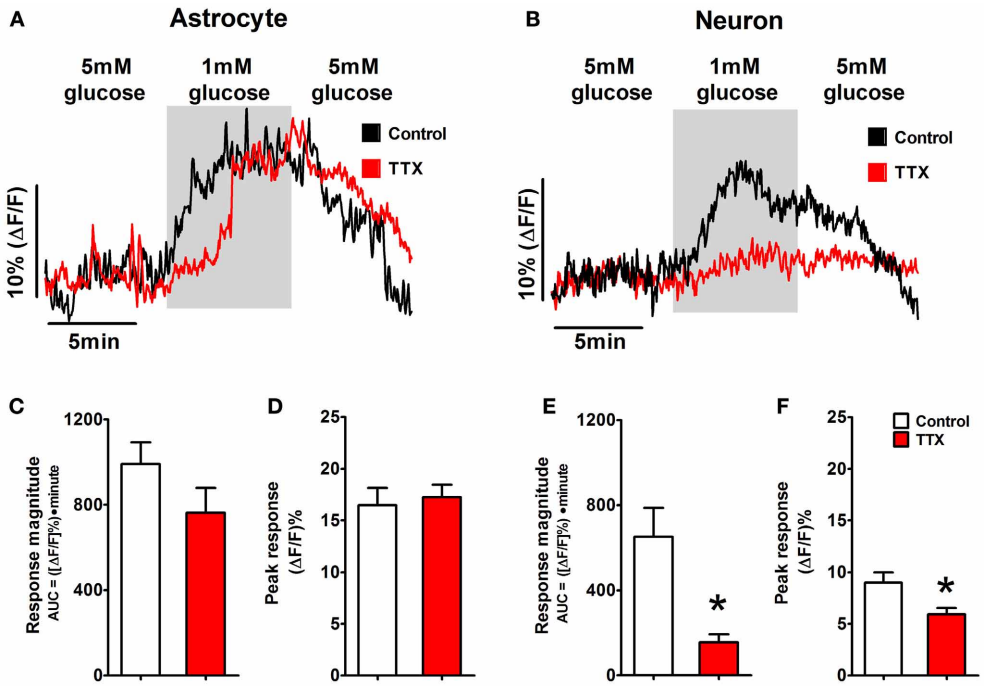

FIGURE 5 | Astrocytic glucodetection is independent of neuronal glucodetection. Mixed fields of NST-astrocytes and neurons were exposed to 1 mM glucose concentrations with and without the presence of TTX in the perfusion bath. **(A)** The response of NST-astrocytes to a low glucose challenge is shown by black trace. The presence of 1 μM TTX did not effectively alter the astrocytic response (red trace). In contrast, **(B)** the response of NST-neurons to a 1mM low glucose challenge was nearly abolished in the presence of bath TTX (black trace = control condition; red trace = TTX condition). Specifically, TTX did not produce any statistically significant changes in astrocytic **(C)** response magnitude or **(D)** peak response to low glucose conditions. In contrast, TTX caused a statistically significant reduction in both neuronal response magnitude **(E)** and peak responsiveness **(F)** when compared to control neuronal responses to low glucose. These results suggest that activation of NST-astrocytes by low glucose challenge is independent of neuronal gluco-sensation. NST neuronal calcium signaling in response to low glucose challenge, on the other hand, may be dependent on other neuronal inputs or on modulation of the voltage-dependent sodium conductance. [$*p < 0.05$; unpaired *t*-test comparing response parameters in control vs. TTX condition. Traces in **(A,B)** are the average response of five representative low glucose positive astrocytes and neurons, respectively.]

neurons, astrocytes displayed larger peak responses and response magnitudes, with a reduced latency to respond, following exposure to 0.5mM glucose concentrations. Note that the activation of astrocytes by reduced glucose was not a smooth linear function; increased activation occurred abruptly at 0.5 mM glucose. This behavior may be a reflection of the operation of an emergency low threshold detection mechanism of the sort driving counter-regulation in response to hypoglycemia (Song et al., 2001; Marty et al., 2007). Furthermore, this astrocytic response to low glucose challenge was independent of neuronal activation, as it was preserved during bath application of TTX. Note that bath application of TTX nearly eliminated the neuronal response to the same low glucose challenge. This suggests that low glucose-mediated increases in neuronal cytoplasmic calcium are produced as a consequence of action potential discharge (Gobel and Helmchen, 2007). In addition, a subset of NST-astrocytes and neurons exhibited an increase in intracellular calcium signaling in response to bath application of the glucoprivic compound 2-DG (5 mM). The onset of this response to glucoprivation was more rapid in astrocytes as compared to adjacent neurons. However, the latencies we observed for astrocytes and neurons are similar to those reported previously for glucose sensitive cells in the hypothalamus or hindbrain (Song et al., 2001; Kang et al., 2004; Balfour et al., 2006). These observations suggest that NST-astrocytes are important sensors of low glucose levels, and that the chemodetection of glucose availability by NST-astrocytes may play an important role in the autonomic regulation of glucose homeostasis.

Astrocyte chemodetection is emerging as an important means by which the brain mediates autonomic homeostasis. Astrocytes in the ventral medulla increase cytoplasmic calcium in response to elevated pCO_2. This increase in glial calcium triggers a gliotransmission mechanism that, in this instance, causes the release of ATP onto adjacent respiratory rhythmogenic neurons (Gourine et al., 2010; Marina et al., 2013). Our own work has shown that astrocytes in the NST are activated by proteinase activated receptor (PAR) agonists and, in turn, release glutamate onto adjacent NST neurons (Hermann et al., 2009). In addition to glucoregulatory functions, the NST also suppresses gastric motility through vago-vagal reflex connections with parasympathetic motor neurons (Rogers and Hermann, 2012a). This mechanism may explain in part why bleeding trauma and burn injuries (both conditions

generate large amounts of PAR-activating thrombin) are associated with profound gastrointestinal stasis (Hermann et al., 2009). It remains to be determined whether similar glial-neural interactions are present between glucosensitive astrocytes and NST neurons.

In addition, the mechanism by which a *reduction* in glucose availability signals an *increase* in cytoplasmic calcium in the NST-astrocyte also remains indeterminate. While astrocytic expression of GLUT2 appears necessary for proper glucose counter-regulation (Marty et al., 2005), the transduction mechanisms often coupled to GLUT2 produce changes in calcium that run in the *opposite direction* to that observed for astrocytes. For example, pancreatic beta cells respond with an increase in intracellular calcium levels in response to *increasing* extracellular glucose. Here, glucose is transported through the GLUT2 transporter and metabolized via glycolysis and the tricarboxcylic acid cycle to CO_2, producing ATP. Increased cellular ATP energy charge acts to phosphorylate and inactivate K_{ATP} channels, leading to depolarization, activation of voltage gated calcium channels and ending in excitation—secretion coupling (Schuit et al., 2001; Holsbeeks et al., 2004; Levin et al., 2004).

However, others have also reported that glucose restriction in cultured astrocytes causes an *increase* in astrocytic cytoplasmic calcium signals (Arnold, 2005). Similar to our present observations, this increase in cytoplasmic calcium is reversed with the restoration of normal levels of glucose in the perfusion bath. There is evidence suggesting that astrocytes are highly dependent on glycolysis for ATP production; removal of glucose or blocking glucose utilization may rapidly starve astrocytes of glucose for ATP production (Kahlert and Reiser, 2000). With impaired glycolysis and subsequent low ATP following low extracellular glucose availability, the calcium-ATPase pump in the endoplasmic reticulum (ER) of astrocytes fails and ER calcium is released to the cytoplasm (Kahlert and Reiser, 2000; Arnold, 2005). While these results are consistent with our observations in the slice preparation, it is not clear if this mechanism is actually responsible for the cytoplasmic calcium signal seen by our laboratory in *in situ* NST-astrocytes. For example, the response time for astrocytes in our NST slice preparation is about five-fold faster than that reported for cultured hippocampal astrocytes.

One possibility for the acceleration of this mechanism relative to cultured astrocytes would be the expression of GLUT2 and glucokinase (GK) by glucosensitive NST-astrocytes. Glial expression of both GLUT2 and GK has been reported previously (Garcia et al., 2003; Arluison et al., 2004; Young and McKenzie, 2004; Millan et al., 2010), as well as the specific expression of GLUT2 by a subset of NST-astrocytes (Leloup et al., 1994). Co-expression of these proteins would permit cytoplasmic glucose to flow backward through the GLUT2 transporter following a reduction in extracellular glucose below intracellular glucose concentrations, thus speeding the elimination of fuel for glycolysis, and therefore accelerating ER calcium release. Further studies utilizing single cell qPCR could be employed to directly investigate whether GLUT2 or GK is preferentially expressed by glucosensitive NST-astrocytes as compared to non-glucoresponsive NST astrocytes.

Another possibility which could account for the more rapid astrocytic cytoplasmic calcium signals in our preparation is that NST-astrocytes may contain a much more active low-glucose detection mechanism via direct signaling of low glucose availability by GLUT2. GLUT2 is the only mammalian glucose transporter known to act as a "transceptor," i.e., a protein which functions as both a transporter and receptor. The receptor function of mammalian GLUT2 is mediated by the large intracellular loop between the 6th and 7th transmembrane domains (Guillemain et al., 2000). Transgenic mice generated to knock down a GLUT2-intracellular loop domain yielded animals that demonstrated an inability to detect glucose but left the GLUT2-dependent glucose transport unaffected (Stolarczyk et al., 2007, 2010). Depression of glucose detection in these animals resulted in increased daily food intake due to increased meal sizes.

The transporter function of GLUT2 has also been linked to the activation of hepatic transcription factor, a carbohydrate response-element binding protein (Uyeda and Repa, 2006). However, it seems unlikely that similar GLUT2-mediated transcriptional regulation in NST-astrocytes could bring about the large and rapid changes in intracellular calcium signaling we observed in response to low glucose availability. Instead, it seems more likely that there may be a direct interaction between the intracellular loop domain of GLUT2 and signaling pathways present in NST-astrocytes; although, at present, there is no information available as to how it might function.

ACKNOWLEDGMENTS

This work was supported by NIH grants GM103528, NS52142, DK56373, HD47643, and NS60664. A preliminary report of some of this work was presented at the 1st Joint ISAN/AAS meeting in Buzios, Brazil. The symposium review appeared in Autonomic Neuroscience: Basic and Clinical (2013, 175:61–69).

REFERENCES

Adachi, A., Kobashi, M., and Funahashi, M. (1995). Glucose-responsive neurons in the brainstem. *Obes. Res.* 3(Suppl. 5), 735S–740S. doi: 10.1002/j.1550-8528.1995.tb00493.x

Andrew, S. F., Dinh, T. T., and Ritter, S. (2007). Localized glucoprivation of hindbrain sites elicits corticosterone and glucagon secretion. *Am. J. Physiol. Regul. Integr. Comp. Physiol.* 292, R1792–1798. doi: 10.1152/ajpregu.00777.2006

Arluison, M., Quignon, M., Nguyen, P., Thorens, B., Leloup, C., and Penicaud, L. (2004). Distribution and anatomical localization of the glucose transporter 2 (GLUT2) in the adult rat brain–an immunohistochemical study. *J. Chem. Neuroanat.* 28, 117–136. doi: 10.1016/j.jchemneu.2004.05.009

Arnold, S. (2005). Estrogen suppresses the impact of glucose deprivation on astrocytic calcium levels and signaling independently of the nuclear estrogen receptor. *Neurobiol. Dis.* 20, 82–92. doi: 10.1016/j.nbd.2005.02.002

Balfour, R. H., Hansen, A. M., and Trapp, S. (2006). Neuronal responses to transient hypoglycaemia in the dorsal vagal complex of the rat brainstem. *J. Physiol.* 570, 469–484. doi: 10.1113/jphysiol.2005.098822

Bernard, C. (1855). *Lecons de Physiologie Experimentale Appliques á la Medecine*. Paris: Bailliere.

Biag, J., Huang, Y., Gou, L., Hintiryan, H., Askarinam, A., Hahn, J. D., et al. (2012). Cyto- and chemoarchitecture of the hypothalamic paraventricular nucleus in the C57BL/6J male mouse: a study of immunostaining and multiple fluorescent tract tracing. *J. Comp. Neurol.* 520, 6–33. doi: 10.1002/cne.22698

Blessing, W. W. (1997). "Anatomy of the lower brainstem," in *The Lower Brainstem and Bodily Homeostasis*, (Oxford: Oxford University Press), 29–100.

Briski, K. P., and Marshall, E. S. (2000). Caudal brainstem Fos expression is restricted to periventricular catecholamine neuron-containing loci following

intraventricular administration of 2-deoxy-D-glucose. *Exp. Brain Res.* 133, 547–551. doi: 10.1007/s002210000448

Burcelin, R., and Thorens, B. (2001). Evidence that extrapancreatic GLUT2-dependent glucose sensors control glucagon secretion. *Diabetes* 50, 1282–1289. doi: 10.2337/diabetes.50.6.1282

Cottrell, G. T., and Ferguson, A. V. (2004). Sensory circumventricular organs: central roles in integrated autonomic regulation. *Regul. Pept.* 117, 11–23. doi: 10.1016/j.regpep.2003.09.004

Dallaporta, M., Himmi, T., Perrin, J., and Orsini, J. C. (1999). Solitary tract nucleus sensitivity to moderate changes in glucose level. *Neuroreport* 10, 2657–2660. doi: 10.1097/00001756-199908200-00040

Dodd, G. T., Williams, S. R., and Luckman, S. M. (2010). Functional magnetic resonance imaging and c-Fos mapping in rats following a glucoprivic dose of 2-deoxy-D-glucose. *J. Neurochem.* 113, 1123–1132. doi: 10.1111/j.1471-4159.2010.06671.x

Garcia, M., Millan, C., Balmaceda-Aguilera, C., Castro, T., Pastor, P., Montecinos, H., et al. (2003). Hypothalamic ependymal-glial cells express the glucose transporter GLUT2, a protein involved in glucose sensing. *J. Neurochem.* 86, 709–724. doi: 10.1046/j.1471-4159.2003.01892.x

Geerling, J. C., Shin, J. W., Chimenti, P. C., and Loewy, A. D. (2010). Paraventricular hypothalamic nucleus: axonal projections to the brainstem. *J. Comp. Neurol.* 518, 1460–1499. doi: 10.1002/cne.22283

Gobel, W., and Helmchen, F. (2007). *In vivo* calcium imaging of neural network function. *Physiology (Bethesda).* 22, 358–365. doi: 10.1152/physiol.00032.2007

Gourine, A. V., Kasymov, V., Marina, N., Tang, F., Figueiredo, M. F., Lane, S., et al. (2010). Astrocytes control breathing through pH-dependent release of ATP. *Science* 329, 571–575. doi: 10.1126/science.1190721

Grabauskas, G., Song, I., Zhou, S., and Owyang, C. (2010). Electrophysiological identification of glucose-sensing neurons in rat nodose ganglia. *J. Physiol.* 588, 617–632. doi: 10.1113/jphysiol.2009.182147

Grill, H. J., and Hayes, M. R. (2012). Hindbrain neurons as an essential hub in the neuroanatomically distributed control of energy balance. *Cell Metab.* 16, 296–309. doi: 10.1016/j.cmet.2012.06.015

Gross, P. M., Wall, K. M., Pang, J. J., Shaver, S. W., and Wainman, D. S. (1990). Microvascular specializations promoting rapid interstitial solute dispersion in nucleus tractus solitarius. *Am. J. Physiol.* 259, R1131–R1138.

Guillemain, G., Loizeau, M., Pincon-Raymond, M., Girard, J., and Leturque, A. (2000). The large intracytoplasmic loop of the glucose transporter GLUT2 is involved in glucose signaling in hepatic cells. *J Cell Sci* 113(Pt 5), 841–847.

Guillod-Maximin, E., Lorsignol, A., Alquier, T., and Penicaud, L. (2004). Acute intracarotid glucose injection towards the brain induces specific c-fos activation in hypothalamic nuclei: involvement of astrocytes in cerebral glucose-sensing in rats. *J. Neuroendocrinol.* 16, 464–471. doi: 10.1111/j.1365-2826.2004.01185.x

Helmchen, F. (2000). "Calibration of fluorescent calcium indicators," in *Imaging Neurons: A Laboratory Manual,* eds R. Yuste, F. Lanni, and A. Konnerth (Cold Spring Harbor, NY: Cold Spring Harbor Laboratory Press), 32.31–32.39.

Hermann, G. E., and Rogers, R. C. (2009). TNF activates astrocytes and catecholaminergic neurons in the solitary nucleus: implications for autonomic control. *Brain Res.* 1273, 72–82. doi: 10.1016/j.brainres.2009.03.059

Hermann, G. E., Van Meter, M. J., Rood, J. C., and Rogers, R. C. (2009). Proteinase-activated receptors in the nucleus of the solitary tract: evidence for glial-neural interactions in autonomic control of the stomach. *J. Neurosci.* 29, 9292–9300. doi: 10.1523/JNEUROSCI.6063-08.2009

Himmi, T., Dallaporta, M., Perrin, J., and Orsini, J. C. (1996). Neuronal responses to delta 9-tetrahydrocannabinol in the solitary tract nucleus. *Eur. J. Pharmacol.* 312, 273–279. doi: 10.1016/0014-2999(96)00490-6

Holsbeeks, I., Lagatie, O., Van Nuland, A., Van De Velde, S., and Thevelein, J. M. (2004). The eukaryotic plasma membrane as a nutrient-sensing device. *Trends Biochem. Sci.* 29, 556–564. doi: 10.1016/j.tibs.2004.08.010

Kahlert, S., and Reiser, G. (2000). Requirement of glycolytic and mitochondrial energy supply for loading of Ca(2+) stores and InsP(3)-mediated Ca(2+) signaling in rat hippocampus astrocytes. *J. Neurosci. Res.* 61, 409–420. doi: 10.1002/1097-4547(20000815)61:4<409::AID-JNR7>3.0.CO;2-M

Kang, L., Routh, V. H., Kuzhikandathil, E. V., Gaspers, L. D., and Levin, B. E. (2004). Physiological and molecular characteristics of rat hypothalamic ventromedial nucleus glucosensing neurons. *Diabetes* 53, 549–559. doi: 10.2337/diabetes.53.3.549

Kasymov, V., Larina, O., Castaldo, C., Marina, N., Patrushev, M., Kasparov, S., et al. (2013). Differential sensitivity of brainstem versus cortical astrocytes to changes in pH reveals functional regional specialization of astroglia. *J. Neurosci.* 33, 435–441. doi: 10.1523/JNEUROSCI.2813-12.2013

Leloup, C., Arluison, M., Lepetit, N., Cartier, N., Marfaing-Jallat, P., Ferre, P., et al. (1994). Glucose transporter 2 (GLUT 2): expression in specific brain nuclei. *Brain Res.* 638, 221–226. doi: 10.1016/0006-8993(94)90653-X

Levin, B. E., Routh, V. H., Kang, L., Sanders, N. M., and Dunn-Meynell, A. A. (2004). Neuronal glucosensing: what do we know after 50 years? *Diabetes* 53, 2521–2528. doi: 10.2337/diabetes.53.10.2521

Marina, N., Tang, F., Figueiredo, M., Mastitskaya, S., Kasimov, V., Mohamed-Ali, V., et al. (2013). Purinergic signalling in the rostral ventro-lateral medulla controls sympathetic drive and contributes to the progression of heart failure following myocardial infarction in rats. *Basic Res. Cardiol.* 108, 317. doi: 10.1007/s00395-012-0317-x

Marty, N., Dallaporta, M., Foretz, M., Emery, M., Tarussio, D., Bady, I., et al. (2005). Regulation of glucagon secretion by glucose transporter type 2 (glut2) and astrocyte-dependent glucose sensors. *J. Clin. Invest.* 115, 3545–3553. doi: 10.1172/JCI26309

Marty, N., Dallaporta, M., and Thorens, B. (2007). Brain glucose sensing, counterregulation, and energy homeostasis. *Physiology (Bethesda).* 22, 241–251. doi: 10.1152/physiol.00010.2007

McDougal, D. H., Hermann, G. E., and Rogers, R. C. (2011). Vagal afferent stimulation activates astrocytes in the nucleus of the solitary tract via AMPA receptors: evidence of an atypical neural-glial interaction in the brainstem. *J. Neurosci.* 31, 14037–14045. doi: 10.1523/JNEUROSCI.2855-11.2011

Millan, C., Martinez, F., Cortes-Campos, C., Lizama, I., Yanez, M. J., Llanos, P., et al. (2010). Glial glucokinase expression in adult and post-natal development of the hypothalamic region. *ASN Neuro* 2, e00035. doi: 10.1042/AN20090059

Mizuno, Y., and Oomura, Y. (1984). Glucose responding neurons in the nucleus tractus solitarius of the rat: *in vitro* study. *Brain Res.* 307, 109–116. doi: 10.1016/0006-8993(84)90466-9

Niijima, A. (1984). The effect of D-glucose on the firing rate of glucose-sensitive vagal afferents in the liver in comparison with the effect of 2-deoxy-D-glucose. *J. Auton. Nerv. Syst.* 10, 255–260. doi: 10.1016/0165-1838(84)90021-3

Nimmerjahn, A., Kirchhoff, F., Kerr, J. N., and Helmchen, F. (2004). Sulforhodamine 101 as a specific marker of astroglia in the neocortex *in vivo*. *Nat. Methods* 1, 31–37. doi: 10.1038/nmeth706

O'Malley, D., Reimann, F., Simpson, A. K., and Gribble, F. M. (2006). Sodium-coupled glucose cotransporters contribute to hypothalamic glucose sensing. *Diabetes* 55, 3381–3386. doi: 10.2337/db06-0531

Ritter, S., Dinh, T. T., and Zhang, Y. (2000). Localization of hindbrain glucoreceptive sites controlling food intake and blood glucose. *Brain Res.* 856, 37–47. doi: 10.1016/S0006-8993(99)02327-6

Ritter, S., Llewellyn-Smith, I., and Dinh, T. T. (1998). Subgroups of hindbrain catecholamine neurons are selectively activated by 2-deoxy-D-glucose induced metabolic challenge. *Brain Res.* 805, 41–54. doi: 10.1016/S0006-8993(98)00655-6

Rogers, R. C., and Hermann, G. E. (2012a). "Brainstem control of gastric function," in *Physiology of the Gastrointestinal Tract, 4th Edn.,* ed L. R. Johnson (San Diego, CA: Elsevier Academic Press), 861–892. doi: 10.1016/B978-0-12-382026-6.00031-2

Rogers, R. C., and Hermann, G. E. (2012b). Tumor necrosis factor activation of vagal afferent terminal calcium is blocked by cannabinoids. *J. Neurosci.* 32, 5237–5241. doi: 10.1523/JNEUROSCI.6220-11.2012

Rogers, R. C., Nasse, J. S., and Hermann, G. E. (2006a). Live-cell imaging methods for the study of vagal afferents within the nucleus of the solitary tract. *J. Neurosci. Methods* 150, 47–58. doi: 10.1016/j.jneumeth.2005.05.020

Rogers, R. C., Van Meter, M. J., and Hermann, G. E. (2006b). Tumor necrosis factor potentiates central vagal afferent signaling by modulating ryanodine channels. *J. Neurosci.* 26, 12642–12646. doi: 10.1523/JNEUROSCI.3530-06.2006

Sanders, N. M., and Ritter, S. (2000). Repeated 2-deoxy-D-glucose-induced glucoprivation attenuates Fos expression and glucoregulatory responses during subsequent glucoprivation. *Diabetes* 49, 1865–1874. doi: 10.2337/diabetes.49.11.1865

Schuit, F. C., Huypens, P., Heimberg, H., and Pipeleers, D. G. (2001). Glucose sensing in pancreatic beta-cells: a model for the study of other glucose-regulated cells in gut, pancreas, and hypothalamus. *Diabetes* 50, 1–11. doi: 10.2337/diabetes.50.1.1

Silver, I. A., and Erecinska, M. (1994). Extracellular glucose concentration in mammalian brain: continuous monitoring of changes during increased neuronal activity and upon limitation in oxygen supply in normo-, hypo-, and hyperglycemic animals. *J. Neurosci.* 14, 5068–5076.

Song, Z., Levin, B. E., McArdle, J. J., Bakhos, N., and Routh, V. H. (2001). Convergence of pre- and postsynaptic influences on glucosensing neurons in the ventromedial hypothalamic nucleus. *Diabetes* 50, 2673–2681. doi: 10.2337/diabetes.50.12.2673

Stolarczyk, E., Guissard, C., Michau, A., Even, P. C., Grosfeld, A., Serradas, P., et al. (2010). Detection of extracellular glucose by GLUT2 contributes to hypothalamic control of food intake. *Am. J. Physiol. Endocrinol. Metab.* 298, E1078–E1087. doi: 10.1152/ajpendo.00737.2009

Stolarczyk, E., Le Gall, M., Even, P., Houllier, A., Serradas, P., Brot-Laroche, E., et al. (2007). Loss of sugar detection by GLUT2 affects glucose homeostasis in mice. *PLoS ONE* 2:e1288. doi: 10.1371/journal.pone.0001288

Uyeda, K., and Repa, J. J. (2006). Carbohydrate response element binding protein, ChREBP, a transcription factor coupling hepatic glucose utilization and lipid synthesis. *Cell Metab.* 4, 107–110. doi: 10.1016/j.cmet.2006.06.008

Watts, A. G., and Donovan, C. M. (2010). Sweet talk in the brain: glucosensing, neural networks, and hypoglycemic counterregulation. *Front. Neuroendocrinol.* 31:32–43. doi: 10.1016/j.yfrne.2009.10.006

Yettefti, K., Orsini, J. C., El Ouazzani, T., Himmi, T., Boyer, A., and Perrin, J. (1995). Sensitivity of nucleus tractus solitarius neurons to induced moderate hyperglycemia, with special reference to catecholaminergic regions. *J. Auton. Nerv. Syst.* 51, 191–197. doi: 10.1016/0165-1838(94)00130-C

Yettefti, K., Orsini, J. C., and Perrin, J. (1997). Characteristics of glycemia-sensitive neurons in the nucleus tractus solitarii: possible involvement in nutritional regulation. *Physiol. Behav.* 61, 93–100. doi: 10.1016/S0031-9384(96)00358-7

Young, J. K., Baker, J. H., and Montes, M. I. (2000). The brain response to 2-deoxy glucose is blocked by a glial drug. *Pharmacol. Biochem. Behav.* 67, 233–239. doi: 10.1016/S0091-3057(00)00315-4

Young, J. K., and McKenzie, J. C. (2004). GLUT2 immunoreactivity in gomori-positive astrocytes of the hypothalamus. *J. Histochem. Cytochem.* 52, 1519–1524. doi: 10.1369/jhc.4A6375.2004

Conflict of Interest Statement: The authors declare that the research was conducted in the absence of any commercial or financial relationships that could be construed as a potential conflict of interest.

Received: 03 September 2013; accepted: 04 December 2013; published online: 20 December 2013.

*Citation: McDougal DH, Hermann GE and Rogers RC (2013) Astrocytes in the nucleus of the solitary tract are activated by low glucose or glucoprivation: evidence for glial involvement in glucose homeostasis. Front. Neurosci. **7**:249. doi: 10.3389/fnins.2013.00249*

This article was submitted to Autonomic Neuroscience, a section of the journal Frontiers in Neuroscience.

frontiers in
NEUROSCIENCE

ORIGINAL RESEARCH ARTICLE
published: 10 January 2014
doi: 10.3389/fnins.2013.00270

Regulation of neurons in the dorsal motor nucleus of the vagus by SIRT1

Yanyan Jiang*[1,2] *and Andrea Zsombok*[1,2]

[1] *Neuroscience Program, School of Science and Engineering, Tulane University, New Orleans, LA, USA*
[2] *Department of Physiology, School of Medicine, Tulane University, New Orleans, LA, USA*

Edited by:
Stuart McDougall, University of Melbourne, Australia

Reviewed by:
L. Ashley Blackshaw, University of Adelaide, Australia
David Linden, Mayo Clinic, USA

****Correspondence:***
Andrea Zsombok, Department of Physiology, School of Medicine, Tulane University, 1430 Tulane Ave., SL-39, New Orleans, LA 70112, USA
e-mail: azsombo@tulane.edu

Neurons in the dorsal motor nucleus of the vagus (DMV) play a critical role in the regulation of autonomic functions. Previous studies indicated that central activation of sirtuin 1 (SIRT1) has beneficial effects on homeostasis, most likely via modulation of the autonomic output. Sirtuins are NAD^+-dependent deacetylases and have been associated with longevity. SIRT1 is one of the best-characterized sirtuins expressed in mammals, and may be involved in the regulation of metabolism. Resveratrol, a SIRT1 activator reduced hyperglycemia likely through activation of vagal output; however, the cellular mechanisms of action have not been determined. In this study, whole-cell patch-clamp electrophysiology on acute brainstem slices was used to test the hypothesis that activation of SIRT1 with resveratrol enhances neurotransmission in DMV neurons. Application of resveratrol increased the frequency of spontaneous excitatory postsynaptic currents (sEPSC). This effect was K_{ATP} channel-dependent and was prevented with pre-application of SIRT1 inhibitor, EX527. Resveratrol also increased miniature EPSC (mEPSC) frequency without change in amplitude. Furthermore, our data demonstrated that resveratrol regulates excitatory neurotransmission in a PI3 kinase-dependent manner, since wortmannin, a PI3K inhibitor prevented the increase of mEPSC frequency caused by resveratrol. In conclusion, our data demonstrate that resveratrol via SIRT1 increases excitatory neurotransmission to DMV neurons. These observations suggest that activation of SIRT1 may regulate the function of subdiaphragmatic organs through controlling the activity of parasympathetic DMV neurons.

Keywords: resveratrol, SIRT1, ATP-sensitive potassium channel, PI3-kinase, dorsal motor nucleus of vagus, patch-clamp

INTRODUCTION

Neurons within the dorsal motor nucleus of the vagus (DMV) are parasympathetic motor neurons as they project to the periphery and regulate the tone to most of the subdiaphragmatic organs and thus, regulate feeding, digestion, energy, and glucose homeostasis (Laughton and Powley, 1987; Berthoud, 2008). The activity of DMV neurons is largely controlled by local circuits and by inputs from other brain regions including the hypothalamus (Saper et al., 1976; Swanson and Sawchenko, 1980; Zsombok and Smith, 2009). Hormones, metabolic signals, gastrointestinal signals, or pharmacological agents have the potential to alter the activity of DMV neurons and thereby modulate the parasympathetic outflow to the organs. Therefore, there is a continuous search to identify potential therapeutic agents that alter synaptic activity and thus, influence the function of the visceral organs.

Sirtuins are NAD^+-dependent histone deacetylases that are highly conserved throughout the evolution (Imai et al., 2000; Michan and Sinclair, 2007). Sirtuins play protective roles promoting the survival of the organism and it has been suggested that they may serve as the molecular link between calorie restriction and prolonged lifespan following dietary restrictions (Cohen et al., 2004; Michan and Sinclair, 2007; Haigis and Sinclair, 2010; Satoh et al., 2010; Coppari, 2012). Sirtuin 1 (SIRT1) is one of the best characterized sirtuins and plays a pivotal role in adaptive responses to high-energy states and hypercaloric diets (Haigis and Sinclair, 2010). Liver-specific deletion of SIRT1 impairs lipid metabolism and reduces glucose production (Erion et al., 2009; Purushotham et al., 2009). In pancreatic beta cells, SIRT1 increases insulin secretion through reduction of uncoupling protein 2 (UCP2) (Moynihan et al., 2005). In addition to its peripheral action, activation of SIRT1 in the brain improves diet-induced diabetes (Ramadori et al., 2009). Central administration of resveratrol, a SIRT1 activator can normalize diet-induced hyperglycemia and mediate anti-diabetic actions (Ramadori et al., 2009). On the other hand, fasting increases SIRT1 levels in the hypothalamus, and blockade of SIRT1 in the hypothalamus decreases food intake and body weight (Ramadori et al., 2008; Cakir et al., 2009). Resveratrol administration into the hypothalamus also improved insulin sensitivity and hepatic vagotomy significantly attenuated this effect (Knight et al., 2011). Despite that the expression of SIRT1 has been shown in brain areas involved in energy and glucose homeostasis, including the hypothalamus and the dorsal vagal complex of the brainstem (Ramadori et al., 2008) and the *in vivo* studies suggested its beneficial effects, the synaptic mechanism underlying the actions of resveratrol in the brain remained to be determined.

In this study, we used whole-cell patch-clamp electrophysiology from DMV neurons to test the hypothesis that activation of SIRT1 with resveratrol enhances neurotransmission in DMV neurons. Our data demonstrate that resveratrol increased spontaneous and miniature excitatory neurotransmission through modulation of ATP-sensitive K^+ channels (K_{ATP}) in a PI3-kinase-dependent manner.

METHODS

ANIMALS

Male CD1 mice (6–8 weeks; Harlan Laboratories, Indianapolis, IN) were used for these experiments. Animals were housed in a vivarium under 12-h light, 12-h dark cycle with food and water available *ad libitum*. Experiments were performed under the guideline of National Institute of Health Guide for the Care and Use of Laboratory Animals and approved by Tulane University's Institutional Animal Care and Use Committee.

BRAIN SLICES PREPARATION

Acute brainstem slices containing the DMV were prepared as previously described (Williams et al., 2007; Zsombok et al., 2011). Under deep anesthesia, mice were decapitated and the brain was removed and immersed in ice-cold oxygenated artificial cerebrospinal fluid (aCSF) containing the following (in mM): 124 NaCl, 26 $NaHCO_3$, 1.4 NaH_2PO_4, 11 glucose, 3 KCl, 1.3 $MgCl_2$, 1.5 $CaCl_2$, pH 7.3–7.4. Transverse brainstem slices (300 μm) were cut with a vibratome (Leica), and then the slices were transferred to a holding chamber containing aCSF (34–36°C, ∼1 h) before being transferred to a recording chamber mounted on a fixed stage under an upright microscope (Nikon FN1).

WHOLE-CELL PATCH-CLAMP RECORDINGS

Whole-cell patch-clamp recordings were performed at 34–36°C. Neurons were identified under 40x water-immersion objective (N.A = 0.8) using infrared illumination and differential interference contrast optics (IR-DIC). For whole-cell patch-clamp recordings, electrodes (2–5 MΩ) were filled with a solution containing the following (in mM): 130 K^+ gluconate, 10 HEPES, 5 EGTA, 1 NaCl, 1 $MgCl_2$, 1 $CaCl_2$, 3 KOH, 2–3 Mg-ATP, pH 7.3–7.4. Excitatory postsynaptic currents (EPSCs) were examined at a holding potential of −60 mV. Electrophysiological signals were recorded using an Axoclamp 700B amplifier (Molecular Devices) and acquired by pClamp 10 (Molecular Devices). Synaptic currents were analyzed offline using pClamp 10 and MiniAnalysis (Synaptosoft).

DRUG APPLICATION

Tetrodotoxin (TTX, 1 μM, Tocris Bioscience) was used in the bath solution in specific experiments to block action potential and monitor miniature EPSCs (mEPSCs). The SIRT1 activator resveratrol (1–500 μM, Tocris Bioscience) and the selective SIRT1 inhibitor EX527 (500 nM, Tocris Bioscience) were dissolved in ethanol and diluted in aCSF (final concentration of ethanol <0.1% by volume). The ATP-sensitive K^+ channel blocker glibenclamide (1 μM, Tocris Bioscience), and a PI3-kinase inhibitor wortmannin (1 μM, Tocris Bioscience) were dissolved in DMSO and diluted in aCSF (final DMSO concentration <0.01%).

STATISTICAL ANALYSIS

Continuous recordings of EPSCs have been conducted before and after application of the drugs and the data were analyzed in 2 min epochs. We observed the maximum effect of resveratrol ∼6–8 min following bath application and we have used this time point in bar-graphs. The effect of activators and inhibitors on spontaneous and mEPSC frequency and amplitude were analyzed within individual cells using the Kolmogorov-Smirnov test by comparing 2 min epochs before and 6–8 min after drug application. The effects of drug applications across the neuron groups were analyzed using a paired two-tailed Student's *t*-test. For all analysis, probability values over the 95% confidence level ($p < 0.05$) were considered significant. Numbers were reported as mean ± standard error (SEM).

RESULTS

RESVERATROL INCREASED SPONTANEOUS EXCITATORY NEUROTRANSMISSION

Previous *in vivo* findings revealed that the beneficial effect of central administration of resveratrol is modulated by the autonomic nervous system. Hepatic vagotomy attenuated this effect (Knight et al., 2011) suggesting the involvement of synaptic mechanisms at the level of DMV. Here, we have assessed the excitatory control of DMV neurons following SIRT1 activation with resveratrol. Recordings of spontaneous EPSC (sEPSCs) were conducted at −60 mV. The average frequency of sEPSCs was 3.5 ± 0.7 Hz (range from 0.7 to 6.5 Hz, $n = 8$). After bath application of 100 μM resveratrol the frequency of sEPSCs significantly increased to 4.2 ± 0.8 Hz (range from 0.8 to 8.2 Hz, $n = 8$, $p < 0.05$) (**Figures 1A–C**). The average amplitude of sEPSCs was 13.2 ± 1.4 pA (range from 7.5 to 19.2 pA) before and 10.3 ± 0.6 pA (range from 8.0 to 13.7 pA) after application of resveratrol ($n = 8$, $p < 0.05$).

To verify that the increased sEPSC frequency is due to SIRT1 activation we pre-incubated the slices with a selective SIRT1 inhibitor, EX527 (500 nM). The average frequency of sEPSCs was 5.9 ± 1.3 Hz (range from 1.1 to 10.1 Hz, $n = 7$) before and 5.8 ± 1.3 Hz (range from 0.6 to 11.9 Hz) after application of EX527 indicating no change in sEPSC frequency in the presence of EX527 ($p > 0.05$). Furthermore, application of resveratrol (100 μM) in the presence of EX527 did not increase sEPSC frequency (5.1 ± 1.0 Hz, range from 0.5 to 8.5 Hz, $n = 7$, $p > 0.05$) (**Figure 1D**). The amplitude of sEPSCs was 15.6 ± 1.7 pA in aCSF, 12.6 ± 1.8 pA in the presence of EX527 and 11.9 ± 2.7 pA after resveratrol application ($n = 7$, $p > 0.05$) (**Figure 1E**). Together, our data indicate that resveratrol through SIRT1 activation significantly increased spontaneous excitatory neurotransmission in DMV neurons.

RESVERATROL INCREASED MINIATURE EXCITATORY SYNAPTIC NEUROTRANSMISSION

Recordings of miniature EPSCs were conducted in the presence of TTX (1 μM) to block action potential dependent neurotransmitter release. The average frequency of mEPSCs was 2.1 ± 0.5 Hz

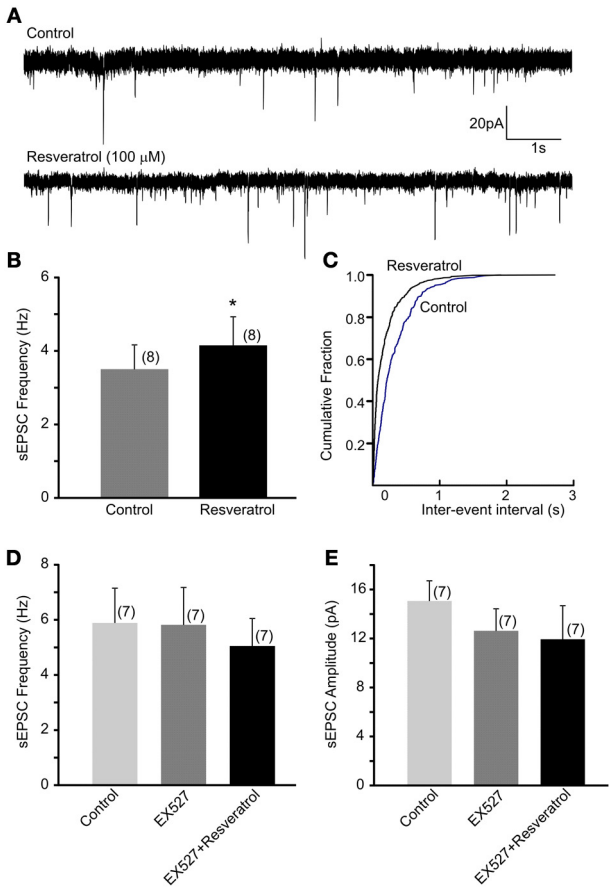

FIGURE 1 | Resveratrol increased spontaneous excitatory neurotransmission through SIRT1 activation in neurons of the dorsal motor nucleus of the vagus (DMV). (A) Continuous whole-cell patch-clamp recordings of spontaneous EPSCs (sEPSCs) at holding potential of −60 mV before (upper trace) and after (lower trace) resveratrol application. **(B)** Combined data showing increased frequency of sEPSCs following resveratrol application. *Significance ($p < 0.05$). **(C)** Cumulative event probability plot of inter-event interval distribution in the recording shown in **(A)**. **(D)** Mean group data showing that in the presence of a selective SIRT1 inhibitor EX527 resveratrol failed to increase sEPSC frequency in DMV neurons. **(E)** Combined data showing no significant change in amplitude of sEPSCs following resveratrol application in the presence of EX527.

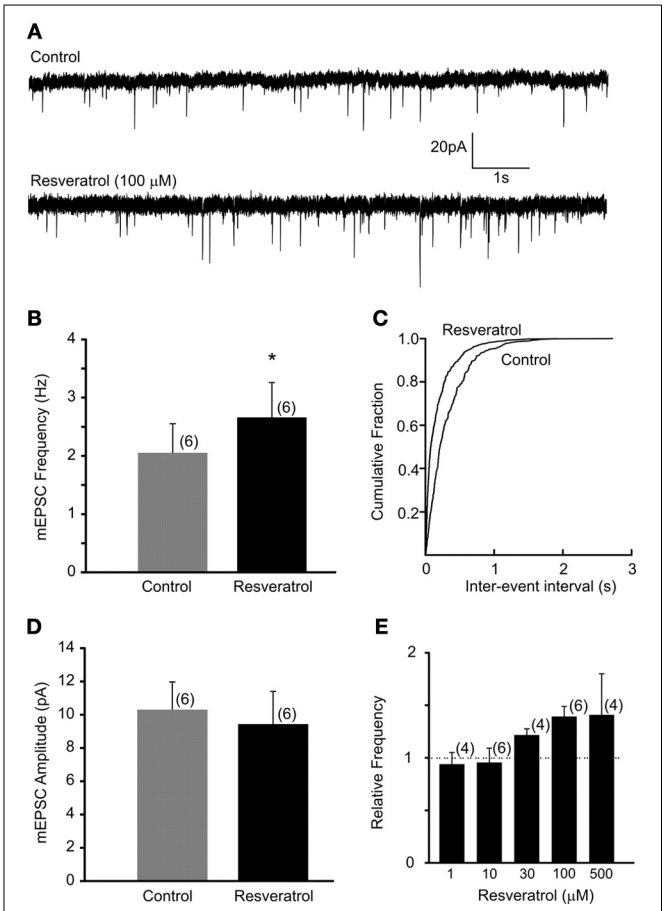

FIGURE 2 | Resveratrol enhanced miniature excitatory neurotransmission in DMV neurons. (A) Voltage-clamp recordings of mEPSCs from a DMV neuron before (upper trace) and after (lower trace) resveratrol application. ($V_m = -60$ mV). **(B)** Combined data demonstrating that resveratrol increased mEPSC frequency. *Significance ($p < 0.05$). **(C)** Cumulative event probability plot of inter-event interval distribution in the recording shown in **(A)**. **(D)** Mean group data showing that resveratrol did not alter the amplitude of mEPSCs. **(E)** Histogram showing the concentration dependence of the response to resveratrol in DMV neurons. Number of replicates indicated at each concentration in parentheses.

(range from 0.4 to 3.5 Hz, $n = 6$). Bath application of resveratrol (100 μM) significantly increased the frequency of mEPSCs to 2.7 ± 0.6 Hz (range from 0.6 to 4.6 Hz, $n = 6$, $p < 0.05$) without altering the amplitude (10.3 ± 1.7 vs. 9.4 ± 2.0 pA, $n = 6$, $p > 0.05$) (**Figure 2**). These data demonstrate that resveratrol via SIRT1 activation increased mEPSC frequency and suggest presynaptic site of action.

Previous studies used resveratrol in a variety of concentrations suggesting that resveratrol may alter synaptic transmission in dose-dependent manner. Therefore, we conducted additional experiments using resveratrol from 1 to 500 μM. Our data demonstrated that resveratrol did not alter the frequency of mEPSCs at concentration of 1 and 10 μM in the recorded DMV neurons ($p > 0.05$) (**Figure 2E**). Application of 30 μM resveratrol increased the frequency of mEPSCs from 4.0 ± 0.4 (range from 3.3 to 4.5 Hz) to 4.8 ± 0.3 Hz (range from 4.1 to 5.3 Hz, $n = 4$, $p < 0.05$) (**Figure 2E**). Application of 500 μM of resveratrol increased mEPSC frequency from 2.4 ± 0.8 (range from 0.9 to 3.8 Hz) to 3.3 ± 0.6 Hz (range from 2.2 to 4.4 Hz, $n = 4$) (**Figure 2E**).

MECHANISM OF EFFECT ON SYNAPTIC TRANSMISSION

Previous *in vivo* and cell culture studies suggested that resveratrol may alter ATP-sensitive K^+ channels (Chen et al., 2007; Knight et al., 2011). To investigate whether K_{ATP} channels are involved in the regulation of excitatory neurotransmission following resveratrol administration we have used a K_{ATP} channel blocker glibenclamide and investigated its effect on the resveratrol induced increase of EPSC frequency. Slices were incubated in aCSF

containing glibenclamide (1 μM) for 30 min to block K_{ATP} channels, and then recordings were conducted. The average frequency of spontaneous EPSCs in the presence of glibenclamide (1 μM) was 3.7 ± 0.7 Hz (range from 1.1 to 7.9 Hz, $n = 9$). Application of resveratrol (100 μM) in the presence of glibenclamide did not increase sEPSC frequency (3.9 ± 0.7 Hz, $n = 9$, $p > 0.05$; not shown). The average frequency of mEPSCs in the presence of glibenclamide was 2.6 ± 0.6 Hz (range from 0.9 to 4.4 Hz, $n = 6$). In the presence of glibenclamide application of resveratrol failed to increase mEPSC frequency (2.6 ± 0.6 Hz, range from 0.9 to 4.9 Hz, $n = 6$, $p > 0.05$) (**Figures 3A,C**). Resveratrol did not have effect on the amplitude of mEPSCs (10.6 ± 2.2 vs. 9.3 ± 2.0 pA, $p > 0.05$) (**Figure 3D**). Our data suggest that resveratrol acts to increase synaptic transmission through K_{ATP} channels. In addition, we have conducted experiments to determine the effect of glibenclamide alone on mEPSC frequency. The average frequency of mEPSCs was 3.9 ± 0.5 Hz (range from 2.0 to 6.2 Hz) before and 4.8 ± 0.7 Hz (range from 2.9 to 7.2 Hz; $n = 6$; $p < 0.05$) after application of glibenclamide. These data demonstrate the modulation of excitatory neurotransmission by K_{ATP} channel.

Next, DMV neurons were exposed to wortmannin, a PI3-kinase inhibitor for 30 min to determine whether the resveratrol induced increase of excitatory neurotransmission is PI3-kinase dependent. Slices were perfused with wortmannin (1 μM) and mEPSCs were recorded. The average frequency of mEPSCs in the presence of wortmannin was 4.0 ± 0.8 Hz (range from 1.9 to 7.8 Hz, $n = 8$) while 4.1 ± 1.0 Hz (range from 1.2 to 8.7 Hz) after resveratrol application ($p > 0.05$) (**Figures 3B,E,F**). These findings demonstrate that the PI3-kinase pathway is involved in the resveratrol induced increase of EPSC frequency. The average amplitude of mEPSCs was 15.9 ± 3.3 (range from 7.2 to 29.5 pA, $n = 8$) and 11.7 ± 2.2 pA (range from 5.5 to 21.2 pA, $p < 0.05$) after resveratrol administration.

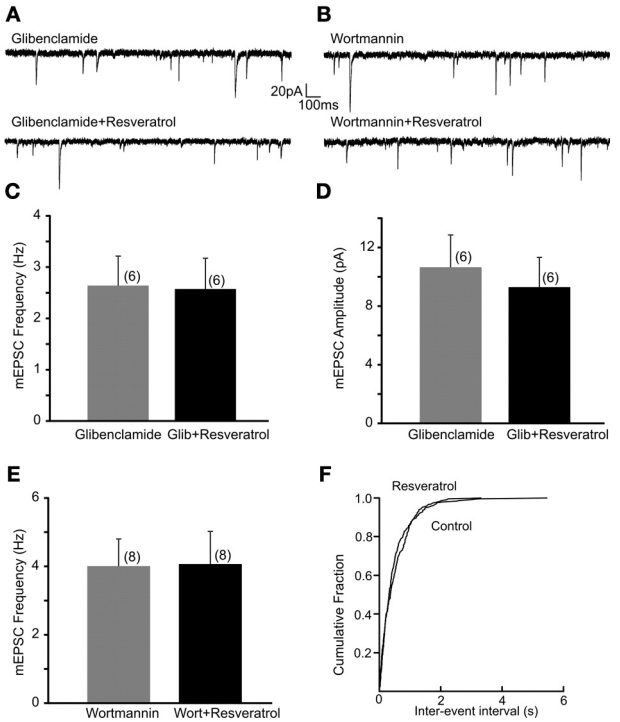

FIGURE 3 | Resveratrol increased excitatory neurotransmission through PI3-kinase activated K_{ATP} channels. (A) Continuous whole-cell patch-clamp recordings of mEPSCs before (upper trace) and after (lower trace) resveratrol (100 μM) application in the presence of glibenclamide (1 μM). **(B)** Voltage-clamp recordings showing mEPSCs recordings before (upper trace) and after (lower trace) resveratrol application in the presence of wortmannin (1 μM). **(C)** Combined data demonstrating that resveratrol failed to increase mEPSC frequency in the presence of glibenclamide. **(D)** Combined data indicating no change in amplitude of mEPSCs after resveratrol application in the presence of glibenclamide. **(E)** Combined data showing that resveratrol failed to increase mEPSC frequency in the presence of wortmannin. **(F)** Cumulative event probability plot of inter-event interval distribution in the recording shown in **(B)**.

RESVERATROL DID NOT ALTER THE MEMBRANE POTENTIAL OR INPUT RESISTANCE OF DMV NEURONS

Since resveratrol altered synaptic neurotransmission through K_{ATP} channels we determined the effect of resveratrol on membrane potential and input resistance. The resting membrane potential of recorded DMV neurons was −45.9 ± 1.7 mV (range from −39.7 to −50.4 mV, $n = 6$). Application of resveratrol did not result in a significant change of membrane potential (−46.2 ± 1.1 mV, range from −42.3 to −49.5 mV, $n = 6$, $p > 0.05$). The input resistance of DMV neurons was not different before and after resveratrol application (0.9 ± 0.09 vs. 1.1 ± 0.1 GΩ). These data suggest that despite resveratrol effects on K_{ATP} channels, it does not alter membrane potential or input resistance of the recorded DMV neurons, further indicating presynaptic mechanisms.

DISCUSSION

In this study we present novel evidence for synaptic regulation of DMV neurons by resveratrol. The following major findings have emerged from this investigation: (1) resveratrol increases spontaneous and mEPSC frequency via SIRT1 activation; (2) resveratrol modulates excitatory neurotransmission through PI3-kinase activated K_{ATP} channels; and (3) resveratrol did not alter membrane potential and input resistance, implying presynaptic mechanism of action.

The increasing prevalence of diabetes, obesity and metabolic syndrome results in a need to identify potential therapeutic targets for the management of these devastating diseases. SIRT1 has been considered as a potential therapeutic target for a variety of diseases including metabolic disorders (Haigis and Sinclair, 2010). Resveratrol, a natural compound found in grapes and red wine has been shown as an effective SIRT1 activator (Howitz et al., 2003). Numerous studies conducted on animals demonstrated that resveratrol improves glucose metabolism (Baur and Sinclair, 2006; Baur et al., 2006; Barger et al., 2008; Andersen et al., 2011; Kang et al., 2012; Marchal et al., 2012), reduces inflammation (Rivera et al., 2009), reverses non-alcoholic fatty liver disease (Bujanda et al., 2008) and prevents obesity (Dal-Pan et al., 2010). On the other hand the results of clinical studies using resveratrol are controversial. It has

been reported that oral administration of resveratrol improves mean hemoglobin A1C, systolic blood pressure, total cholesterol, and protein in type 2 diabetic patients (Bhatt et al., 2012). In contrast, a more recent study using high-dose resveratrol supplementation in obese men reported no effect on endogenous glucose production, blood pressure, energy expenditure, fat mass or inflammatory and metabolic biomarkers (Poulsen et al., 2013) raising debates about the effectiveness of resveratrol as a dietary supplement in humans; however, additional studies with more subjects would be necessary to make conclusion.

In addition to the overall effect of resveratrol, the question regarding peripheral or central mechanisms of resveratrol also has been investigated. SIRT1 protein expression has been detected with Western blot analysis in the rat hypothalamus markedly in the arcuate, ventromedial, dorsomedial hypothalamus, and paraventricular nucleus (Knight et al., 2011). This is consistent with *in situ* hybridization and immunohistochemical studies performed on mice that showed marked expression of SIRT1 mRNA and protein in metabolically relevant brain areas including the above mentioned sites (Ramadori et al., 2008; Sasaki et al., 2010). The Ramadori et al. study also demonstrated high expression in the brainstem including the area postrema and the nucleus of the solitary tract (NTS) suggesting SIRT1 expression throughout the neuroaxis involved in energy and glucose homeostasis (Ramadori et al., 2008). Administration of resveratrol into the brain improved insulin sensitivity and normalized hyperglycemia (Ramadori et al., 2009; Knight et al., 2011); however, the underlying synaptic mechanisms are not fully understood. Our study demonstrated that resveratrol, a SIRT1 activator increased excitatory neurotransmission to parasympathetic DMV neurons. Our findings also revealed that the resveratrol effect requires the involvement of K_{ATP} channel and the PI3-kinase pathway.

Glutamate, the main excitatory neurotransmitter is released in the DMV from inputs arriving from many different brain areas including the hypothalamus and the NTS (Travagli et al., 1991; Jiang et al., 2003; Davis et al., 2004). *In vitro* application of resveratrol increased the frequency of both spontaneous and mEPSCs in the DMV indicating a presynaptic action of resveratrol. Our observations also revealed that resveratrol alters EPSC frequency of DMV neurons in dose-dependent manner. The resveratrol induced frequency increase of EPSCs was prevented in the presence of a SIRT1 inhibitor EX527. EX527 is a selective inhibitor of SIRT1 that does not inhibit other sirtuins or histone deacethylase, therefore, our data verified that resveratrol exerts its effect through SIRT1 activation.

Previous studies established that resveratrol alters ion channels by various mechanisms depending on the cell types. Resveratrol activates BK channels in endothelial cells (Li et al., 2000), inhibits I_K channels in cultured rat hippocampal neurons (Gao et al., 2006; Dong et al., 2013) and inhibits TRP channels in HEK and dorsal root ganglia cells (Yu et al., 2013). The involvement of K_{ATP} channels also has been demonstrated (Chen et al., 2007). This study by Chen revealed that resveratrol significantly inhibits K_{ATP} channels and voltage-gated K^+ currents in order to depolarize the membrane and increase insulin secretion from pancreatic beta cells. Similarly, the *in vivo* work of Knight and co-workers indicated that the effect of resveratrol was inhibited in the presence of a K_{ATP} channel blocker, glibenclamide (Knight et al., 2011). Our data also suggest that resveratrol increases excitatory neurotransmission in the DMV through K_{ATP} channels (**Figure 4**). Pre-incubation of the brainstem slices with glibenclamide prevented the resveratrol-dependent increase of mEPSC frequency, suggesting the involvement of K_{ATP} channels. Furthermore, application of glibenclamide alone resulted in an increase of mEPSC frequency, indicating that blocking K_{ATP} channels modulates pre-synaptic neurotransmitter release. K_{ATP} channels have been shown to modulate synaptic neurotransmission in the brainstem (Ferreira et al., 2001; Williams and Smith, 2006; Williams et al., 2007). Previous electrophysiological studies demonstrated that tolbutamide, another K_{ATP} channel blocker depolarizes NTS neurons, suggesting the presence of K_{ATP} channels in brainstem NTS neurons (Williams and Smith, 2006). Depolarization of NTS neurons could lead to increased neurotransmitter release to DMV neurons. Furthermore, the effect of K_{ATP} channel opener diazoxide alone has been shown to reduce mEPSC frequency in DMV neurons, demonstrating that K_{ATP} channels are able to modulate glutamate release at the presynaptic terminals (Williams et al., 2007). Another cellular observation demonstrated that glibenclamide mimics the actions of elevated glucose levels on the amplitude of evoked PSCs in DMV neurons, while diazoxide, a K_{ATP} opener had opposite effect (Ferreira et al., 2001). These experiments also suggest a presynaptic site of action and indicate modulation of neurotransmission by K_{ATP} channels.

The involvement of PI3K in K_{ATP}-dependent mechanisms is known. Furthermore, it also has been demonstrated that PI3K is involved in SIRT1 activation (Frojdo et al., 2011). Therefore, we also pre-incubated the slices with wortmannin

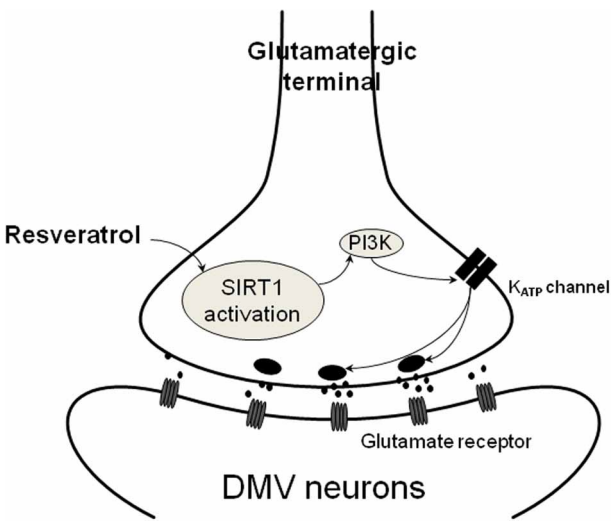

FIGURE 4 | Schematic illustration of resveratrol action on presynaptic terminals. SIRT1 activation with resveratrol results in increased glutamate release from presynaptic terminals. This mechanism depends on PI3-kinase dependent closure of K_{ATP} channels leading to depolarization and increased neurotransmitter release.

then applied resveratrol and found that wortmannin blunted the resveratrol-dependent increase of EPSC frequency. Previous electrophysiological studies used wortmannin from 10 nM to 3 μM concentration (Williams et al., 2007; Gao et al., 2012). In our experiments we used 1 μM of wortmannin for 30 min, which diminished the effect of resveratrol. It has been shown that this concentration of wortmannin inhibits the mammalian target of rapamycin (mTOR) (Brunn et al., 1996), therefore, there is a possibility that in addition to PI3K, the mTOR signaling is modulated by resveratrol. However, this scenario is unlikely, because a recent study demonstrated that less than 72 h treatment with rapamycin, a specific inhibitor of mTOR did not alter the electrophysiological properties of neurons (Weston et al., 2012). It also has been demonstrated that 3-week long inhibition of mTOR with rapamycin increases the excitability of hypothalamic neurons via K_{ATP} channel (Yang et al., 2012), suggesting that changing the electrophysiological properties of neurons via the mTOR signaling requires longer duration. In our experiments resveratrol increased EPSC frequency within 10 min, therefore, it is unlikely that the observed electrophysiological response involves the mTOR signaling; however, additional studies would be necessary to make conclusion regarding the interaction between resveratrol and mTOR signaling. It has been observed in hypothalamic cells that the presence of PI3K inhibitor *per se* reduced the phosphorylation of protein kinase B (PKB) and glycogen synthase kinase 3 (GSK3) levels, indicating that PI3K is active to a limited degree in neurons of the arcuate nucleus, and it also prevented the leptin and insulin induced phosphorylation of PKB and GSK3 (Mirshamsi et al., 2004). Furthermore, inhibiting PI3K has been shown to decrease insulin-stimulated phosphorylation of MAPK (Mirshamsi et al., 2004), and blocking PI3K can also inhibit insulin induced increase of MAPK activity in adipose tissue (Sajan et al., 1999). It also has been described that inhibition of PI3K reduced the effect of leptin or insulin on K_{ATP} channels (Mirshamsi et al., 2004). Moreover, inhibition of PI3K prevented the leptin caused increase of phosphatidylinositol 3,4,5-triphosphate. PtdIns activates K_{ATP} channels, probably not through direct binding (Harvey et al., 2000; Mirshamsi et al., 2004), but actin remodeling. Furthermore, direct interplay between SIRT1 and insulin signaling pathway including PI3K has been demonstrated in muscle (Frojdo et al., 2011). Downregulation of SIRT1 expression levels diminished insulin-stimulated PKB phosphorylation and overexpression increased insulin-stimulated PKB phosphorylation. SIRT1 positively modulated the activity of upstream components of insulin pathway and SIRT1 interacted with tyrosin phosphorylated proteins and with the PI3K-p85alpha (Frojdo et al., 2011). In addition, it has been shown that resveratrol also could directly modulate the sulfonylurea receptor 1 (SUR1) of K_{ATP} channels (Hambrock et al., 2007), indicating a possible direct link between resveratrol and binding to SUR1. In summary, the evaluation of interactions among the above mentioned intracellular pathways remains to be determined and could be the subject of future studies.

Together, these data indicate that pre-application of glibenclamide or wortmannin prevented the resveratrol induced increase of EPSC frequency that might imply a PI3-kinase activated K_{ATP} channel in response. Previous data demonstrated that the resveratrol effect depends on K_{ATP} channels and hepatic vagotomy significantly attenuated this effect (Knight et al., 2011), indicating the involvement of the parasympathetic nervous system. Our data confirmed that resveratrol is able to modulate neurotransmission to DMV neurons. The synaptic effects of resveratrol appear to be due to increased glutamate release, likely via closing K_{ATP} channels, from synaptic terminals contacting DMV neurons (**Figure 4**). Based on the high expression of SIRT1 mRNA detected in the NTS, one possible origin of the synaptic terminals is the NTS. Another possibility is the hypothalamus (Ramadori et al., 2008; Sasaki et al., 2010). Both brain areas are known to send projections to the DMV (Swanson and Sawchenko, 1980; Travagli et al., 1991) and thereby involved in the modulation of parasympathetic output to the subdiaphragmatic organs.

Our findings identified a potential cellular mechanism underlying the effect of resveratrol administration into the brain. Considering the described anti-diabetic effects of central resveratrol administration and that vagotomy attenuated this effect (Ramadori et al., 2009; Knight et al., 2011) we can speculate that modulating the synaptic activity of DMV neurons underlies the effect of resveratrol on the autonomic nervous system.

AUTHOR CONTRIBUTIONS

Yanyan Jiang conducted experiments and contributed to the manuscripts preparation; Andrea Zsombok designed the experiments and prepared the manuscript.

ACKNOWLEDGMENTS

This work was supported by grants from the NIH Tulane Aging COBRE Pilot Project (P20GM103629) and Tulane University Neuroscience Bridge Grant for Andrea Zsombok.

REFERENCES

Andersen, G., Burkon, A., Sulzmaier, F. J., Walker, J. M., Leckband, G., Fuhst, R., et al. (2011). High dose of dietary resveratrol enhances insulin sensitivity in healthy rats but does not lead to metabolite concentrations effective for SIRT1 expression. *Mol. Nutr. Food Res.* 55, 1197–1206. doi: 10.1002/mnfr.201100292

Barger, J. L., Kayo, T., Vann, J. M., Arias, E. B., Wang, J., Hacker, T. A., et al. (2008). A low dose of dietary resveratrol partially mimics caloric restriction and retards aging parameters in mice. *PLoS ONE* 3:e2264. doi: 10.1371/journal.pone.0002264

Baur, J. A., Pearson, K. J., Price, N. L., Jamieson, H. A., Lerin, C., Kalra, A., et al. (2006). Resveratrol improves health and survival of mice on a high-calorie diet. *Nature* 444, 337–342. doi: 10.1038/nature05354

Baur, J. A., and Sinclair, D. A. (2006). Therapeutic potential of resveratrol: the *in vivo* evidence. *Nat. Rev. Drug Discov.* 5, 493–506. doi: 10.1038/nrd2060

Berthoud, H. R. (2008). The vagus nerve, food intake and obesity. *Regul. Pept.* 149, 15–25. doi: 10.1016/j.regpep.2007.08.024

Bhatt, J. K., Thomas, S., and Nanjan, M. J. (2012). Resveratrol supplementation improves glycemic control in type 2 diabetes mellitus. *Nutr. Res.* 32, 537–541. doi: 10.1016/j.nutres.2012.06.003

Brunn, G. J., Williams, J., Sabers, C., Wiederrecht, G., Lawrence, J. C. Jr., and Abraham, R. T. (1996). Direct inhibition of the signaling functions of the mammalian target of rapamycin by the phosphoinositide 3-kinase inhibitors, wortmannin and LY294002. *EMBO J.* 15, 5256–5267.

Bujanda, L., Hijona, E., Larzabal, M., Beraza, M., Aldazabal, P., Garcia-Urkia, N., et al. (2008). Resveratrol inhibits non-alcoholic fatty liver disease in rats. *BMC Gastroenterol.* 8:40. doi: 10.1186/1471-230X-8-40

Cakir, I., Perello, M., Lansari, O., Messier, N. J., Vaslet, C. A., and Nillni, E. A. (2009). Hypothalamic Sirt1 regulates food intake in a rodent model system. *PLoS ONE* 4:e8322. doi: 10.1371/journal.pone.0008322

Chen, W. P., Chi, T. C., Chuang, L. M., and Su, M. J. (2007). Resveratrol enhances insulin secretion by blocking K(ATP) and K(V) channels of beta cells. *Eur. J. Pharmacol.* 568, 269–277. doi: 10.1016/j.ejphar.2007.04.062

Cohen, H. Y., Miller, C., Bitterman, K. J., Wall, N. R., Hekking, B., Kessler, B., et al. (2004). Calorie restriction promotes mammalian cell survival by inducing the SIRT1 deacetylase. *Science* 305, 390–392. doi: 10.1126/science.1099196

Coppari, R. (2012). Metabolic actions of hypothalamic SIRT1. *Trends Endocrinol. Metab.* 23, 179–185. doi: 10.1016/j.tem.2012.01.002

Dal-Pan, A., Blanc, S., and Aujard, F. (2010). Resveratrol suppresses body mass gain in a seasonal non-human primate model of obesity. *BMC Physiol.* 10:11. doi: 10.1186/1472-6793-10-11

Davis, S. F., Derbenev, A. V., Williams, K. W., Glatzer, N. R., and Smith, B. N. (2004). Excitatory and inhibitory local circuit input to the rat dorsal motor nucleus of the vagus originating from the nucleus tractus solitarius. *Brain Res.* 1017, 208–217. doi: 10.1016/j.brainres.2004.05.049

Dong, W. H., Chen, J. C., He, Y. L., Xu, J. J., and Mei, Y. A. (2013). Resveratrol inhibits Kv2.2 currents through the estrogen receptor GPR30-mediated PKC pathway. *Am. J. Physiol. Cell. Physiol.* 305, C547–C557. doi: 10.1152/ajpcell.00146.2013

Erion, D. M., Yonemitsu, S., Nie, Y., Nagai, Y., Gillum, M. P., Hsiao, J. J., et al. (2009). SirT1 knockdown in liver decreases basal hepatic glucose production and increases hepatic insulin responsiveness in diabetic rats. *Proc. Natl. Acad. Sci. U.S.A.* 106, 11288–11293. doi: 10.1073/pnas.0812931106

Ferreira, M. Jr., Browning, K. N., Sahibzada, N., Verbalis, J. G., Gillis, R. A., and Travagli, R. A. (2001). Glucose effects on gastric motility and tone evoked from the rat dorsal vagal complex. *J. Physiol.* 536, 141–152. doi: 10.1111/j.1469-7793.2001.t01-1-00141.x

Frojdo, S., Durand, C., Molin, L., Carey, A. L., El-Osta, A., Kingwell, B. A., et al. (2011). Phosphoinositide 3-kinase as a novel functional target for the regulation of the insulin signaling pathway by SIRT1. *Mol. Cell Endocrinol.* 335, 166–176. doi: 10.1016/j.mce.2011.01.008

Gao, H., Miyata, K., Bhaskaran, M. D., Derbenev, A. V., and Zsombok, A. (2012). Transient receptor potential vanilloid type 1-dependent regulation of liver-related neurons in the paraventricular nucleus of the hypothalamus diminished in the type 1 diabetic mouse. *Diabetes* 61, 1381–1390. doi: 10.2337/db11-0820

Gao, Z. B., Chen, X. Q., and Hu, G. Y. (2006). Inhibition of excitatory synaptic transmission by trans-resveratrol in rat hippocampus. *Brain Res.* 1111, 41–47. doi: 10.1016/j.brainres.2006.06.096

Haigis, M. C., and Sinclair, D. A. (2010). Mammalian sirtuins: biological insights and disease relevance. *Annu. Rev. Pathol.* 5, 253–295. doi: 10.1146/annurev.pathol.4.110807.092250

Hambrock, A., de Oliveira Franz, C. B., Hiller, S., Grenz, A., Ackermann, S., Schulze, D. U., et al. (2007). Resveratrol binds to the sulfonylurea receptor (SUR) and induces apoptosis in a SUR subtype-specific manner. *J. Biol. Chem.* 282, 3347–3356. doi: 10.1074/jbc.M608216200

Harvey, J., McKay, N. G., Walker, K. S., Van der Kaay, J., Downes, C. P., and Ashford, M. L. (2000). Essential role of phosphoinositide 3-kinase in leptin-induced K(ATP) channel activation in the rat CRI-G1 insulinoma cell line. *J. Biol. Chem.* 275, 4660–4669. doi: 10.1074/jbc.275.7.4660

Howitz, K. T., Bitterman, K. J., Cohen, H. Y., Lamming, D. W., Lavu, S., Wood, J. G., et al. (2003). Small molecule activators of sirtuins extend Saccharomyces cerevisiae lifespan. *Nature* 425, 191–196. doi: 10.1038/nature01960

Imai, S., Armstrong, C. M., Kaeberlein, M., and Guarente, L. (2000). Transcriptional silencing and longevity protein Sir2 is an NAD-dependent histone deacetylase. *Nature* 403, 795–800. doi: 10.1038/35001622

Jiang, C., Fogel, R., and Zhang, X. (2003). Lateral hypothalamus modulates gut-sensitive neurons in the dorsal vagal complex. *Brain Res.* 980, 31–47. doi: 10.1016/S0006-8993(03)02844-0

Kang, W., Hong, H. J., Guan, J., Kim, D. G., Yang, E. J., Koh, G., et al. (2012). Resveratrol improves insulin signaling in a tissue-specific manner under insulin-resistant conditions only: *in vitro* and *in vivo* experiments in rodents. *Metabolism* 61, 424–433. doi: 10.1016/j.metabol.2011.08.003

Knight, C. M., Gutierrez-Juarez, R., Lam, T. K., Arrieta-Cruz, I., Huang, L., Schwartz, G., et al. (2011). Mediobasal hypothalamic SIRT1 is essential for resveratrol's effects on insulin action in rats. *Diabetes* 60, 2691–2700. doi: 10.2337/db10-0987

Laughton, W. B., and Powley, T. L. (1987). Localization of efferent function in the dorsal motor nucleus of the vagus. *Am. J. Physiol.* 252, R13–R25.

Li, H. F., Chen, S. A., and Wu, S. N. (2000). Evidence for the stimulatory effect of resveratrol on Ca(2+)-activated K+ current in vascular endothelial cells. *Cardiovasc. Res.* 45, 1035–1045. doi: 10.1016/S0008-6363(99)00397-1

Marchal, J., Blanc, S., Epelbaum, J., Aujard, F., and Pifferi, F. (2012). Effects of chronic calorie restriction or dietary resveratrol supplementation on insulin sensitivity markers in a primate, Microcebus murinus. *PLoS ONE* 7:e34289. doi: 10.1371/journal.pone.0034289

Michan, S., and Sinclair, D. (2007). Sirtuins in mammals: insights into their biological function. *Biochem. J.* 404, 1–13. doi: 10.1042/BJ20070140

Mirshamsi, S., Laidlaw, H. A., Ning, K., Anderson, E., Burgess, L. A., Gray, A., et al. (2004). Leptin and insulin stimulation of signalling pathways in arcuate nucleus neurones: PI3K dependent actin reorganization and KATP channel activation. *BMC Neurosci.* 5:54. doi: 10.1186/1471-2202-5-54

Moynihan, K. A., Grimm, A. A., Plueger, M. M., Bernal-Mizrachi, E., Ford, E., Cras-Meneur, C., et al. (2005). Increased dosage of mammalian Sir2 in pancreatic beta cells enhances glucose-stimulated insulin secretion in mice. *Cell Metab.* 2, 105–117. doi: 10.1016/j.cmet.2005.07.001

Poulsen, M. M., Vestergaard, P. F., Clasen, B. F., Radko, Y., Christensen, L. P., Stodkilde-Jorgensen, H., et al. (2013). High-dose resveratrol supplementation in obese men: an investigator-initiated, randomized, placebo-controlled clinical trial of substrate metabolism, insulin sensitivity, and body composition. *Diabetes* 62, 1186–1195. doi: 10.2337/db12-0975

Purushotham, A., Schug, T. T., Xu, Q., Surapureddi, S., Guo, X., and Li, X. (2009). Hepatocyte-specific deletion of SIRT1 alters fatty acid metabolism and results in hepatic steatosis and inflammation. *Cell Metab.* 9, 327–338. doi: 10.1016/j.cmet.2009.02.006

Ramadori, G., Gautron, L., Fujikawa, T., Vianna, C. R., Elmquist, J. K., and Coppari, R. (2009). Central administration of resveratrol improves diet-induced diabetes. *Endocrinology* 150, 5326–5333. doi: 10.1210/en.2009-0528

Ramadori, G., Lee, C. E., Bookout, A. L., Lee, S., Williams, K. W., Anderson, J., et al. (2008). Brain SIRT1: anatomical distribution and regulation by energy availability. *J. Neurosci.* 28, 9989–9996. doi: 10.1523/JNEUROSCI.3257-08.2008

Rivera, L., Moron, R., Zarzuelo, A., and Galisteo, M. (2009). Long-term resveratrol administration reduces metabolic disturbances and lowers blood pressure in obese Zucker rats. *Biochem. Pharmacol.* 77, 1053–1063. doi: 10.1016/j.bcp.2008.11.027

Sajan, M. P., Standaert, M. L., Bandyopadhyay, G., Quon, M. J., Burke, T. R. Jr., and Farese, R. V. (1999). Protein kinase C-zeta and phosphoinositide-dependent protein kinase-1 are required for insulin-induced activation of ERK in rat adipocytes. *J. Biol. Chem.* 274, 30495–30500. doi: 10.1074/jbc.274.43.30495

Saper, C. B., Loewy, A. D., Swanson, L. W., and Cowan, W. M. (1976). Direct hypothalamo-autonomic connections. *Brain Res.* 117, 305–312. doi: 10.1016/0006-8993(76)90738-1

Sasaki, T., Kim, H. J., Kobayashi, M., Kitamura, Y. I., Yokota-Hashimoto, H., Shiuchi, T., et al. (2010). Induction of hypothalamic Sirt1 leads to cessation of feeding via agouti-related peptide. *Endocrinology* 151, 2556–2566. doi: 10.1210/en.2009-1319

Satoh, A., Brace, C. S., Ben-Josef, G., West, T., Wozniak, D. F., Holtzman, D. M., et al. (2010). SIRT1 promotes the central adaptive response to diet restriction through activation of the dorsomedial and lateral nuclei of the hypothalamus. *J. Neurosci.* 30, 10220–10232. doi: 10.1523/JNEUROSCI.1385-10.2010

Swanson, L. W., and Sawchenko, P. E. (1980). Paraventricular nucleus: a site for the integration of neuroendocrine and autonomic mechanisms. *Neuroendocrinology* 31, 410–417. doi: 10.1159/000123111

Travagli, R. A., Gillis, R. A., Rossiter, C. D., and Vicini, S. (1991). Glutamate and GABA-mediated synaptic currents in neurons of the rat dorsal motor nucleus of the vagus. *Am. J. Physiol.* 260, G531–G536.

Weston, M. C., Chen, H., and Swann, J. W. (2012). Multiple roles for mammalian target of rapamycin signaling in both glutamatergic and GABAergic synaptic transmission. *J. Neurosci.* 32, 11441–11452. doi: 10.1523/JNEUROSCI.1283-12.2012

Williams, K. W., and Smith, B. N. (2006). Rapid inhibition of neural excitability in the nucleus tractus solitarii by leptin: implications for ingestive behaviour. *J. Physiol.* 573, 395–412. doi: 10.1113/jphysiol.2006.106336

Williams, K. W., Zsombok, A., and Smith, B. N. (2007). Rapid inhibition of neurons in the dorsal motor nucleus of the vagus by leptin. *Endocrinology* 148, 1868–1881. doi: 10.1210/en.2006-1098

Yang, S. B., Tien, A. C., Boddupalli, G., Xu, A. W., Jan, Y. N., and Jan, L. Y. (2012). Rapamycin ameliorates age-dependent obesity associated with increased mTOR signaling in hypothalamic POMC neurons. *Neuron* 75, 425–436. doi: 10.1016/j.neuron.2012.03.043

Yu, L., Wang, S., Kogure, Y., Yamamoto, S., Noguchi, K., and Dai, Y. (2013). Modulation of TRP channels by resveratrol and other stilbenoids. *Mol. Pain* 9, 3. doi: 10.1186/1744-8069-9-3

Zsombok, A., Bhaskaran, M. D., Gao, H., Derbenev, A. V., and Smith, B. N. (2011). Functional plasticity of central TRPV1 receptors in brainstem dorsal vagal complex circuits of streptozotocin-treated hyperglycemic mice. *J. Neurosci.* 31, 14024–14031. doi: 10.1523/JNEUROSCI.2081-11.2011

Zsombok, A., and Smith, B. N. (2009). Plasticity of central autonomic neural circuits in diabetes. *Biochim. Biophys. Acta* 1792, 423–431. doi: 10.1016/j.bbadis.2008.12.001

Conflict of Interest Statement: The authors declare that the research was conducted in the absence of any commercial or financial relationships that could be construed as a potential conflict of interest.

Received: 27 August 2013; accepted: 20 December 2013; published online: 10 January 2014.

Citation: Jiang Y and Zsombok A (2014) Regulation of neurons in the dorsal motor nucleus of the vagus by SIRT1. Front. Neurosci. 7:270. doi: 10.3389/fnins.2013.00270

This article was submitted to Autonomic Neuroscience, a section of the journal Frontiers in Neuroscience.

frontiers in
NEUROSCIENCE

ORIGINAL RESEARCH ARTICLE
published: 31 January 2014
doi: 10.3389/fnins.2014.00006

Isolation of TRPV1 independent mechanisms of spontaneous and asynchronous glutamate release at primary afferent to NTS synapses

Axel J. Fenwick†, Shaw-wen Wu† and James H. Peters*

Department of Integrative Physiology and Neuroscience, Washington State University, Pullman, WA, USA

Edited by:
Stuart McDougall, University of Melbourne, Australia

Reviewed by:
Andrei V. Derbenev, Tulane University School of Medicine, USA
Stuart McDougall, University of Melbourne, Australia
Daniel Weinreich, University of Maryland School of Medicine, USA

***Correspondence:**
James H. Peters, Department of Integrated Physiology and Neuroscience, Washington State University, 1815 Ferdinand's Lane, Pullman, WA 99164, USA
e-mail: jamespeters@vetmed.wsu.edu
† These authors have contributed equally to this work.

Cranial visceral afferents contained within the solitary tract (ST) contact second-order neurons in the nucleus of the solitary tract (NTS) and release the excitatory amino acid glutamate via three distinct exocytosis pathways; synchronous, asynchronous, and spontaneous release. The presence of TRPV1 in the central terminals of a majority of ST afferents conveys activity-dependent asynchronous glutamate release and provides a temperature sensitive calcium conductance which largely determines the rate of spontaneous vesicle fusion. TRPV1 is present in unmyelinated C-fiber afferents and these facilitated forms of glutamate release may underlie the relative strength of C-fibers in activating autonomic reflex pathways. However, pharmacological blockade of TRPV1 signaling eliminates only ∼50% of the asynchronous profile and attenuates the temperature sensitivity of spontaneous release indicating additional thermosensitive calcium influx pathways may exist which mediate these forms of vesicle release. In the present study we isolate the contribution of TRPV1 independent forms of glutamate release at ST-NTS synapses. We found ST afferent innervation at NTS neurons and synchronous vesicle release from TRPV1 KO mice was not different to control animals; however, only half of TRPV1 KO ST afferents completely lacked asynchronous glutamate release. Further, temperature driven spontaneous rates of vesicle release were not different from 33 to 37°C between control and TRPV1 KO afferents. These findings suggest additional temperature dependent mechanisms controlling asynchronous and thermosensitive spontaneous release at physiological temperatures, possibly mediated by additional thermosensitive TRP channels in primary afferent terminals.

Keywords: vagus, solitary tract, vesicle release, synaptic, calcium, autonomic reflexes, TRPV3, TRPM3

INTRODUCTION

Primary vagal afferent neurons provide a direct neural pathway through which the ongoing status of visceral organ systems (including the heart, lungs, and gastrointestinal tract) is conveyed to the brain (Loewy, 1990). Vagal afferents contact neurons within the nucleus of the solitary tract (NTS) to initiate homeostatic reflex pathways and inform the relevant forebrain projecting neurocircuitry on the ongoing peripheral status (Saper, 2002). The range of information types, time-frames, and relative physiological urgencies conveyed by vagal afferents is remarkable. As a result information transfer must be at one time reliable and precise while maintaining plasticity to match autonomic function to the physiological state. Vagal afferents release the fast excitatory neurotransmitter glutamate via three distinct pathways: synchronous, asynchronous, and spontaneous (Andresen et al., 2012b). Synchronous glutamate release is a tightly regulated process by which an action potential evokes a coordinated release of multiple glutamate vesicles into the synaptic cleft to ensure high-fidelity signaling between neurons. In contrast, asynchronous glutamate release is a loosely timed process by which an action potential evokes a release of glutamate that is delayed in response to the action potential. Equally significant is spontaneous glutamate release, by which neurotransmitter is released independent of action potential depolarization of the terminal. We predict that the interplay between multiple complementary vesicle release pathways allows for robust/precise information transfer which is also adaptable and plastic to changing physiological states.

Centrally, vagal afferent neurons merge with the facial (VII) and glossopharyngeal (IX) nerves to form the solitary tract (ST) bundle and innervate second-order NTS neurons (Loewy, 1990). ST-NTS synapses are a strong high probability of release (P_r) synapse where action potential invasion of the central terminals leads to the coordinated synchronous release of multiple vesicles (Bailey et al., 2006b; Peters et al., 2008). Synchronous vesicle release provides a large excitatory drive from the afferent to the postsynaptic neuron and ensures high fidelity synaptic throughput (Bailey et al., 2006a). While synchronous release is large initially, during trains of action-potentials at physiological frequencies it rapidly falls off due to vesicle release outpacing vesicle mobilization to the membrane; a process called frequency dependent depression (FDD) (Chen et al., 1999; Doyle and Andresen, 2001). The presence of the transient receptor potential vanilloid type 1 (TRPV1) ion channel in the central terminals of most ST afferents conveys activity-dependent asynchronous glutamate

release prolonging the period of action potential driven release (from milliseconds to seconds) and extending the postsynaptic excitatory period despite FDD of synchronous release (Peters et al., 2010). TRPV1 also provides a temperature sensitive calcium conductance which largely determines the rate of spontaneous vesicle fusion (Shoudai et al., 2010). Further, convergent vagal afferent innervation onto NTS neurons is segregated based on the presence or absence of TRPV1 and asynchronous vesicle release (Peters et al., 2011). Because TRPV1 is present in unmyelinated C-fiber afferents these facilitated forms of glutamate release may underlie the relative strength of C-fibers in activating autonomic reflex pathways (Peters et al., 2010; Andresen et al., 2012b).

The current experiments aim to further determine the contribution of TRPV1 in synaptic communication at ST-NTS synapses. As previously reported pharmacological blockade of TRPV1 signaling eliminates only ∼50% of the asynchronous profile (Peters et al., 2010) and attenuates the temperature sensitivity of spontaneous release (Shoudai et al., 2010) indicating additional thermosensitive calcium influx pathways may exist to mediate these forms of vesicle release. In the present study we utilize mice genetically lacking the TRPV1 ion channel (TRPV1 KO) and characterize synchronous, asynchronous, and spontaneous vesicle release pathways as well as afferent innervation patterns independent of TRPV1. In addition we provide evidence that alternative thermo-TRP channels are functionally expressed in primary vagal afferent neurons.

METHODS

ANIMALS

Male Sprague Dawley rats (120–250 g, Simonsen Laboratories), male C57BL/6 mice (20–30 g), and male TRPV1$^{-/-}$ knockout mice (20–30 g) (B6.129X1-*Trpv1*^{tm1Jul}/J, Jackson Laboratories) were used under procedures approved by the IACUC at Washington State University. The TRPV1 gene product was confirmed as present (wild type, WT) or lacking (TRPV1$^{-/-}$) via PCR amplification of genomic DNA and with RT-PCR on collected nodose ganglia. Animals were housed under 12 h light/12 h dark conditions and fed standard pellet chow *ad libitum*.

MOLECULAR BIOLOGY

Wild-type and homozygous TRPV1 null mice were purchased from Jackson Laboratory and genotyped according to protocol for separated PCR. Genomic DNA was isolated from tail fragments using NaOH extraction. cDNA was obtained from RNA isolated from nodose ganglia mice. RNA (purified using the Qiagen RNEasy Kit and the QIACube robotic workstation) was converted into cDNA using the Ambion DNA-free Kit and QuantiTect Reverse Transcription Kit. Primers and cycling parameters used to detect WT TRPV1 fragments from genomic DNA and cDNA were obtained from the Jackson Laboratory website for genotyping using separated PCR: forward—CCT GCT CAA CAT GCT CAT TG; reverse—TCC TCA TGC ACT TCA GGA AA. Expected sizes for Wild-type TRPV1 fragments are 984 bp for genomic DNA and 134 bp for cDNA.

HORIZONTAL BRAINSTEM SLICE PREPARATION

Experiments utilizing brainstem slices were performed on WT and TRPV1$^{-/-}$ mice anesthetized with isoflurane as previously described (Doyle et al., 2004). The medulla was removed and placed in ice-cold artificial cerebral spinal fluid (aCSF) containing (mM): 125 NaCl, 3 KCl, 1.2 KH_2PO_4, 1.2 $MgSO_4$, 25 $NaHCO_3$, 10 dextrose, and 2 $CaCl_2$, bubbled with 95% O_2–5% CO_2. Once chilled, the tissue block was trimmed to remove the remaining cerebellum and a wedge was taken from the ventral surface. This ventral wedge cut, which was tangent to midline, causes the brainstem block to sit slightly to the right when horizontal and orients the ST axons with the NTS in a common plane for cutting. The tissue block was then mounted horizontally to a pedestal and submerged in cold aCSF on a vibrating microtome (VT1000S; Leica Microsystems Inc., Bannockburn, IL). Approximately 300 μm was removed from the dorsal surface and then a single 250 μm thick horizontal slice was collected that contained the ST together with the neuronal cell bodies of the medial NTS region. Slices were cut with a sapphire knife (Delaware Diamond Knives, Wilmington, DE). Slices were submerged in aCSF and secured with a fine polyethylene mesh in a perfusion chamber with continuous perfusion of aCSF bubbled with 95% O_2–5% CO_2 at 32–35°C and 300 mOsm.

WHOLE CELL PATCH-CLAMP RECORDINGS

Recorded neurons were located medial to the ST and within 200 μm rostral or caudal of obex. Recording electrodes (2.8–3.8 MΩ) were filled with an intracellular solution containing (mM): 6 NaCl, 4 NaOH, 130 K-gluconate, 11 EGTA, 1 $CaCl_2$, 1 $MgCl_2$, 10 HEPES, 2 Na_2ATP, and 0.2 Na_2GTP. The intracellular solution was pH 7.4 and 296 mOsm. All neurons were studied under voltage clamp conditions with an Axopatch 200A or MultiClamp 700A amplifier (Molecular Devices, Union City, CA) and held at $V_H = -60$ mV using pipettes in whole cell patch configuration. Signals were filtered at 3 kHz and sampled at 30 kHz using p-Clamp software (version 10, Molecular Devices). Liquid junction potentials were not corrected.

FUNCTIONAL IDENTIFICATION OF SECOND-ORDER NTS NEURONS

In order to selectively activate ST afferent fibers a concentric bipolar stimulating electrode (200 μm outer tip diameter; Frederick Haer Co., Bowdoinham, ME) was placed on distal portions of the visible ST rostral to the recording region. Current shocks to the ST occurred every 6 s (shock duration 60 μs) using a Master-8 isolated stimulator (A.M.P.I., Jerusalem, Israel). Suprathreshold shocks resulted in long latency excitatory postsynaptic currents (EPSCs) resulting from the synchronous release of multiple glutamate vesicles activating postsynaptic α-amino-3-hydroxyl-5-methyl-4-isoxazole-propionate (AMPA) glutamate receptors under these recording conditions. Latency was measured as the time between the ST shock artifact and the onset of the resulting synchronous EPSC. Synaptic "jitter" was calculated as the standard deviation of ST-EPSC latencies for 30–40 trials within each neuron. Jitters of <200 μs functionally identify monosynaptic afferent inputs onto the recorded NTS neuron (Doyle and Andresen, 2001). The TRPV1 selective agonist capsaicin (CAP) was applied to identify ST afferents as possessing TRPV1 or not. Specifically, CAP exposure dramatically increases the frequency of sEPSCs and decreases the evoked synchronous ST-EPSCs in brainstem slices (Peters et al., 2011). CAP exposure on dissociated

nodose neurons produces a large increase in cytosolic calcium (**Figure 8**).

STATISTICAL ANALYSIS OF SYNAPTIC RESPONSES

Digitized waveforms of synaptic events were analyzed using an event detection and analysis program (MiniAnalysis, Synaptosoft, Decatur, GA) for all quantal synaptic currents and Clampfit 10 (Molecular Devices) for all ST-stimulated currents. All events >10 pA were counted for frequency values. Fitting of quantal EPSC amplitudes and decay kinetics (90–10%) was performed using a fitting protocol (MiniAnalysis) on >100 discrete events. To quantify the number of events released asynchronously following ST stimulation we summed the total number of quantal events for 4 s following the synchronous EPSCs from across 50 trials. In order to account for the ongoing spontaneous release we subtracted the number of quantal events for the same period of time during unstimulated conditions. For statistical comparisons *T*-tests, Mann Whitney Rank Sum test, and linear regression analysis were used when appropriate (Systat Software Inc., San Jose, CA). For group comparisons $p < 0.05$ was considered statistically significant.

NODOSE GANGLIA ISOLATIONS AND PRIMARY NEURONAL CULTURES

Nodose ganglia were isolated bilaterally from rats and mice under a deep plane of anesthesia (Ketamine, 25 mg/100 g; with Xylazine, 2.5 mg/100 g) using aseptic surgical conditions based on methods previously reported (Lancaster and Weinreich, 2001; Simasko et al., 2002). Following a midline incision in the neck the musculature was retracted and blunt dissection techniques were used to dissociate the vagal trunk from the common carotid artery. High-magnification optics (10–100x dissecting scope; Leica Microsystems, Buffalo Grove, IL) were utilized to help visualize the nodose ganglia and facilitate complete removal. Once isolated, nodose ganglia were digested in Ca^{2+}/Mg^{2+}free Hank's Balanced Salt Solution containing 1 mg/mL of both Dispase II (Hoffmann- La Roche) and Collagenase Type 1A (Sigma Aldrich) (120 min at 37°C in 95% air/5% CO_2). Neurons were dispersed by gentle trituration through silicanized pipettes, and then washed in Dulbecco's Modified Eagle's Medium (DMEM) supplemented with 10% fetal bovine serum (FBS) and 1% penicillin-streptomycin. Dispersed cells were plated onto poly-lysine coated coverslips and maintained in DMEM+10% FBS (37°C in 95% air/5% CO_2). Measurements were made within 24 h of isolation.

RATIOMETRIC FLUORESCENT CALCIUM MEASUREMENTS

Intracellular calcium measurements were made with the fluorescent Ca^{2+} indicator Fura-2 AM (Molecular Probes, Eugene, OR). Manipulations were made at room temperature in a physiological saline bath (in mM: 140 NaCl, 5 KCl, 2 $CaCl_2$, 1 $MgCl_2$, 6 glucose, 10 HEPES with pH adjusted to 7.4 with NaOH). High K^+ bath (HiK) had 55 mM KCl with an equimolar reduction of NaCl to 90 mM. Neurons on coverslips were loaded with 1 μM Fura-2-AM for 1 h followed by a 15 min wash for de-esterification. Coverslips were mounted into an open chamber and constantly perfused with physiological bath. Neurons containing Fura-2 were alternatively excited with 340 and 380 nm light with fluorescence monitored at 510 nm. Data points were collected with MetaFluor software at 6 s time points. Ratios of fluorescence intensity were converted to Ca^{2+} concentrations with a standard curve.

STATISTICAL ANALYSIS FOR CALCIUM IMAGING EXPERIMENTS

For each experiment data were collected from 2 to 3 nodose ganglion cell cultures. Protocols were designed to be within subject and analyzed using repeated measures ANOVA followed by *post-hoc* comparisons against control. Parameters of dose-response relationships (EC_{50}, slope, maximum) were determined by sigmoid fit of the data. For antagonist studies (ruthenium red) all neurons received each treatment and were compared using within subject *t*-tests. Data are expressed as the average ± s.e.m. Statistical analysis was performed using SigmaStat software (Systat Software Inc., San Jose, CA).

RESULTS

Action potential invasion of vagal afferent terminals produces synchronous release of multiple glutamate vesicles via opening of N-type voltage activated calcium channels (Mendelowitz et al., 1995). While TRPV1 activation increases terminal calcium and vesicle mobilization, it is not reported to contribute to synchronous vesicle release (Peters et al., 2010). As such we predict that genetic deletion of TRPV1 will leave evoked synchronous ST EPSCs intact. To confirm that TRPV1 gene expression was eliminated, we probed the gene product from genomic DNA and RNA expression within the nodose ganglia (**Figure 1A**). We also functionally confirmed the loss of TRPV1 by CAP induced increases in frequency of spontaneous EPSCs which were absent in $TRPV1^{-/-}$ synapses (**Figure 1B**). The horizontal brainstem slice permits selective activation of the ST bundle by placement of a concentric bipolar stimulating electrode distant (1–3 mm) from the recorded neurons (Doyle et al., 2004). Using graded stimulation intensities we are able to recruit single or multiple ST afferents discretely (McDougall et al., 2009; Peters et al., 2011). We found that the amplitude of solitary tract evoked EPSCs (ST-EPSCs) from single ST afferent contacts were not statistically different between control and TRPV1 KO animals (control: 150 ± 47 pA vs. $TRPV1^{-/-}$: 158 ± 53 pA, $N = 6$ and 13 respectively, $P = 0.93$, *T*-test) (**Figure 1**). The latency to event onset is an approximate measure of conduction velocity and was also not different between groups (control: 3.58 ± 0.35 ms vs. $TRPV1^{-/-}$: 3.82 ± 0.24 ms, $N = 6$ and 13 respectively, $P = 0.56$, *T*-test) (**Figure 1B**); indicating the afferent fibers activated have the same degree of myelination. The variability, or "jitter," in latency is used as a verified functional determinate of connectivity with jitter measurements under 200 μs indicating direct monosynaptic ST afferent innervation of the recorded neurons (control: 101 ± 17 μs vs. $TRPV1^{-/-}$: 108 ± 11 μs, $N = 6$ and 13 respectively, $P = 0.74$, *T*-test) (**Figure 1C**).

On average, ST-EPSC amplitude and variability (amplitude co-variance, Cv) were also not different between control and TRPV1 KO afferents (control: 5.58 ± 1.54% vs. $TRPV1^{-/-}$: 6.34 ± 1.92%, $N = 6$ and 13 respectively, $P = 0.96$, *T*-test) (**Figure 1E**); suggesting similar numbers of synaptic release sites (N) and probability of vesicle release (P_r). To compare potential differences in synaptic performance between these two groups

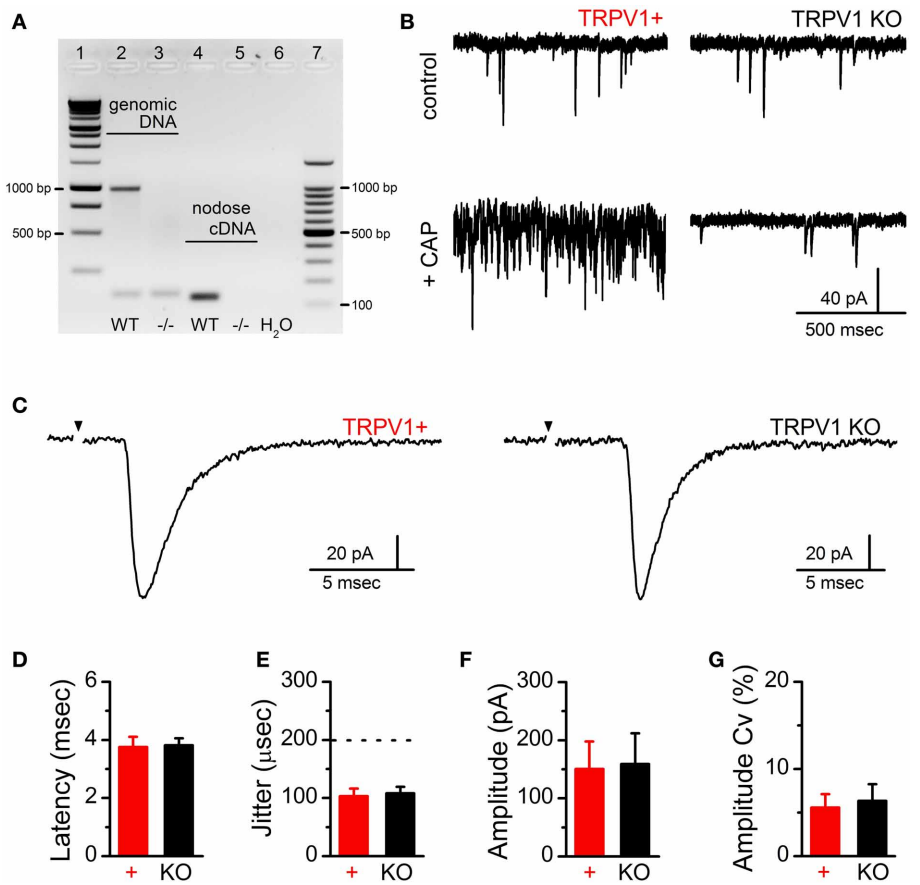

FIGURE 1 | Confirmation of TRPV1 deletion and comparison of ST-evoked synchronous glutamate release between primary afferent contacts onto second-order NTS neurons from control and TRPV1 KO animals. (A) Gel electrophoresis showing the TRPV1 specific genomic DNA (predicted band at 984 bp) and nodose cDNA (predicted band at 134 bp) amplicon from control and TRPV1 KO mice. **(B)** Currents traces showing sEPSC frequency in control bath (upper panels) and following CAP (100 nM) exposure (lower panels) from TRPV1+ (left) and TRPV1 KO afferents. **(C)** Current traces comparing ST-evoked synchronous glutamate release from single ST afferent inputs confirmed to express TRPV1 (CAP sensitive) or from TRPV1 KO mice. Traces are of individual sweeps with the black arrow indicating the time of ST activation. The stimulus artifacts have been removed. There were no significant differences between control ($n = 6$) and TRPV1 KO ($n = 13$) ST afferent inputs with regards to the average latency to EPSC onset **(D)** or synaptic "jitter" (the dotted line indicates the threshold below which inputs are considered monosynaptic) **(E)** ($P = 0.56$ and $P = 0.74$ respectively, unpaired *t*-tests); demonstrating monosynaptic innervation from ST afferents likely expressing similar degrees of myelination. Further, neither the amplitude **(F)** nor coefficient of amplitude variation (Cv) **(G)** of single ST-EPSCs were significantly different ($P = 0.93$ and $P = 0.95$ respectively, unpaired *t*-tests); consistent with similar numbers of vesicle release sites (N) and release probability (P_r).

we delivered trains of ST stimulations (5 shocks at 50 Hz) and compared the initial paired-pulse ratio (PPR) and frequency dependent depression (FDD) (**Figure 2**). The PPR between control and TRPV1 KO was not different, consistent with similar initial P_r (control: 0.53 ± 0.06 vs. TRPV1$^{-/-}$: 0.44 ± 0.04, $N = 6$ and 13 respectively, $P = 0.08$, *T*-test) (**Figure 2B**). Initial FDD reflects depletion of the readily releasable pool of vesicles followed by the steady-state equilibrium between vesicle mobilization and release (**Figure 2C**). Loss of TRPV1 did not significantly alter either of these parameters ($P = 0.93$, ANOVA).

Increasing shock intensity on the ST bundle routinely activates multiple direct afferent inputs. Convergent inputs are discriminated based on threshold of activation for each recruited ST-EPSC, latency to ST-EPSC onset, and cumulative amplitude of the multiple ST-EPSCs (i.e., max current change from 1 input alone, 1 + 2 inputs, 1 + 2 + 3 inputs, etc.) (**Figure 3A**) (McDougall et al., 2009; Peters et al., 2011). Using the systematic stimulus recruitment analysis a functional map of the number of direct ST afferent inputs innervating each medial NTS neuron was generated and compared between control and TRPV1 KO recordings (**Figures 3B,C**). Comparison of innervation patterns across neurons revealed no significant difference in the ST afferent innervation patterns between control and TRPV1 KO animals ($P = 0.63$, Wilcoxon ranked sum test).

Action-potential invasion of the central terminals of ST afferents produces rapid synchronous vesicle mobilization followed by prolonged TRPV1 dependent asynchronous vesicle release in rats (Peters et al., 2010). Both of these release pathways are also present in ST afferents from mice however the asynchronous profile in mice decays with a single exponential time constant as

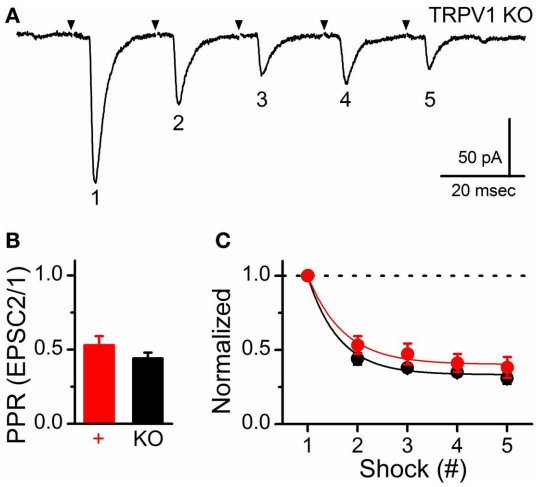

FIGURE 2 | Conserved synaptic performance during trains of ST shocks between control and TRPV1 KO afferents. (A) Representative current trace showing decreasing ST-evoked EPSCs during a train of ST shocks (5 shocks at 50 Hz). Traces are of individual sweeps with the black arrow indicating the time of ST activation. The stimulus artifacts have been removed. This frequency dependent depression (FDD) is a result of a high initial probability of vesicle release (P_r) and relatively fast stimulations releasing vesicles faster than they can be mobilized to the membrane. **(B)** The paired-pulse ratio (PPR) comparison between evoked EPSC2 to EPSC1 (20 ms interval) showed no significant difference between groups ($P = 0.08$, unpaired t-test); consistent with similar initial P_r. **(C)** The train a stimulations produced nearly identical frequency dependent depression (FDD) profiles that were not different between groups ($P = 0.93$, ANOVA). Dashed line provides reference to initial EPSC1 amplitude.

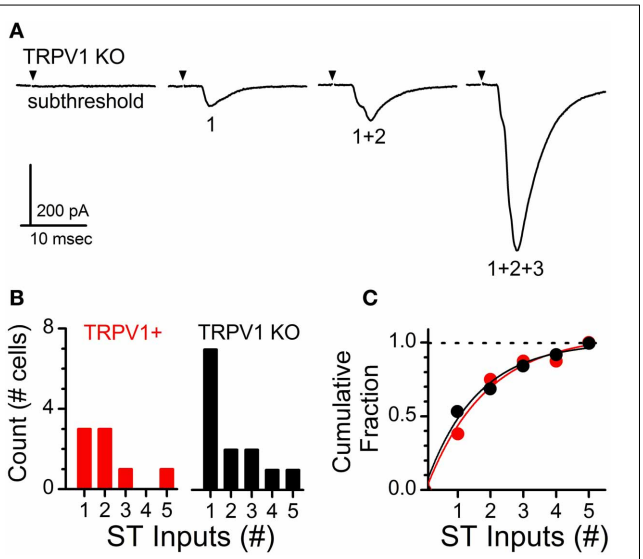

FIGURE 3 | Analysis of primary afferent innervation patterns onto second-order NTS neurons from control and TRPV1 KO animals. (A) Current traces showing increasing stimulus intensity recruiting a single contact followed by multiple convergent ST afferent inputs. Traces are of individual sweeps with the black arrow indicating the time of ST activation. The stimulus artifacts have been removed. Activation of multiple inputs produces a compound waveform; with individual inputs discriminated by shock intensity at activation, latency, and amplitude. **(B)** Histogram detailing the total number direct ST inputs across recorded neurons from each group. **(C)** Cumulative proportion showing no significant difference in the percentage of neurons receiving 1 or >1 inputs between control and TRPV1 KO animals ($P = 0.63$, Wilcoxon ranked sum test). Dashed line provides reference to 1.0 on the vertical axis.

compared to a biexponential decay in the rat and as a result the synchronous to asynchronous ratio is increased. Nevertheless, activation of TRPV1+ ST afferents in mice produces a reliable asynchronous release that peaks rapidly and decays over a period of hundreds of milliseconds and is proportional to the size of the evoked ST-EPSC ($n = 11$ inputs, $R^2 = 0.48$, slope $= 1.34 \pm 0.47$ sync/async ratio) (**Figures 4A**, upper/lower panels, and **D**). As in the rat, convergent ST inputs segregate based on the presence or absence of TRPV1 and asynchronous release pathway. As a result all convergent inputs onto a second-order NTS neuron either possess asynchronous release or not (**Figure 4D**). In TRPV1 KO animals nearly half of recorded neurons (6 of 13) received direct ST afferent innervation with no asynchronous release ($n = 8$ inputs, $R^2 = 0.58$, slope $= 0.42 \pm 0.14$ sync/async ratio) (**Figures 4B**, upper/lower panels, and **E**) while the remaining neurons received afferent innervation with asynchronous release indistinguishable from the control animals ($n = 15$ inputs, $R^2 = 0.92$, slope $=$ 1.75 ± 0.14 sync/async ratio) (**Figures 4C**, upper/lower panels, and **F**). Further, recruitment of multiple direct inputs either completely lacked or possessed asynchronous release (**Figures 4E,F**). These results were surprising for several reasons; first we would have predicted that asynchronous release would have been attenuated and not completely lacking or completely present; and second, ST afferent innervation is still segregated based off the presence or absence of asynchronous release.

At ST-NTS synapses ongoing spontaneous vesicle fusion and release is steeply temperature dependent and suspected to be directly controlled by TRPV1 (Shoudai et al., 2010). As such we may expect differences in spontaneous release between control and TRPV1 KO animals. Initially, we compared the steady-state frequency of sEPSCs from control and TRPV1 KO animals at a constant warm recording temperature (33°C) and found no significant difference (control: 4.43 ± 1.04 Hz vs. TRPV1$^{-/-}$: 4.17 ± 1.17 Hz, $N = 8$ and 13 respectively, $P = 0.57$, unpaired T-test) (**Figure 5**). While there exists a wide range of sEPSC frequencies neither the distributions nor the average frequencies were statistically different between groups (**Figures 5B,C**). This observation suggests that at warm temperatures at least the rate of spontaneous vesicle release is maintained independent of TRPV1. Detailed fitting analysis of the quantal EPSCs also found no differences in event amplitude(control: 37 ± 5 pA vs. TRPV1$^{-/-}$: 32 ± 3 pA, $P = 0.59$, T-test), decay (tau) (control: 2.04 ± 0.24 ms vs. TRPV1$^{-/-}$: 2.52 ± 0.27 ms, $P = 0.17$, T-test), or total charge transfer (control: 114 ± 16 pA*ms vs. TRPV1$^{-/-}$: 105 ± 7 pA*ms, $P = 0.98$, T-test) (**Figure 6**). These findings are consistent with similar vesicle neurotransmitter content, postsynaptic receptor expression and position on the recorded neurons (distal vs. proximal to the soma). Varying bath temperature from 25 to 39°C revealed that frequency of spontaneous release was still temperature dependent from controls ($N = 4$, $P = 0.005$, Friedman repeated measures ANOVA) and TRPV1$^{-/-}$ ($N = 5$, $P < 0.001$, Friedman repeated measure ANOVA) animals; but not statistically different between control and TRPV1$^{-/-}$ animals

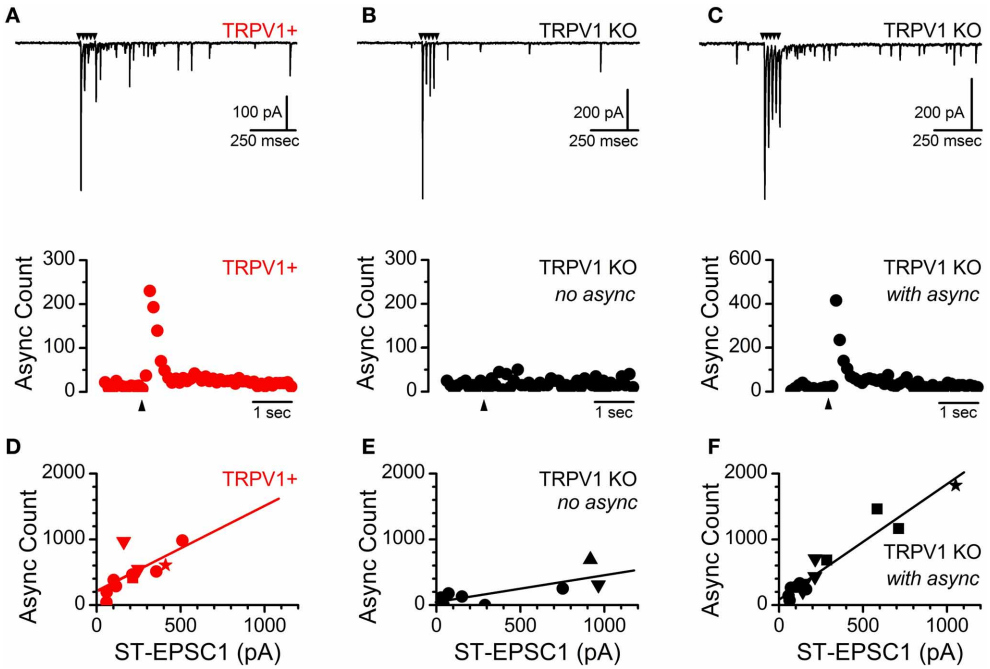

FIGURE 4 | Identification of a subpopulation of ST afferents from TRPV1 KO mice which maintain activity dependent asynchronous glutamate release. (**A**, upper) Current trace showing ST driven synchronous and asynchronous release from an identified TRPV1+ afferents in control mice. (**A**, lower) Histogram of summed asynchronous quantal glutamate events from across 50 trials. Black arrows indicate time of ST shock in all panels. (**B**, upper/lower) Nearly half (6 of 13) of all neurons recorded from TRPV1 KO ST afferents showed no asynchronous release regardless of the size or number of direct ST inputs. **(C**, upper**)** A significant population of TRPV1 KO afferents still mobilized vesicles via the asynchronous release pathway; with the magnitude and duration of additional release similar to the TRPV1+ afferents from control animals **(C**, lower**)**. **(D)** The total number of asynchronously released vesicles positively correlates with the size of the evoked ST-EPSC ($n = 11$ inputs, $R^2 = 0.48$, slope = 1.34 ± 0.47) from control TRPV1+ afferents. **(E)** TRPV1 KO afferents with no asynchronous release show only a weak relationship between EPSC1 amplitude and additional quantal events ($n = 8$ inputs, $R^2 = 0.58$, slope = 0.42 ± 0.14). **(F)** From TRPV1 KO afferents with asynchronous release the magnitude of the release was strongly correlated with the size of the evoked synchronous EPSC ($n = 15$ inputs, $R^2 = 0.92$, slope = 1.75 ± 0.14). The synchronous to asynchronous relationship is maintained across multiple inputs and the data have been fit including convergent ST contacts: 1st = circle, 2nd = down triangle, 3rd = square, 4th = star, and 5th = upward triangle. These data suggest an additional mechanism of mobilizing asynchronous glutamate vesicles is present in a subpopulation of ST afferents.

($P = 0.82$, Two-Way ANOVA) (**Figure 7**). Together these findings indicate that TRPV1 may be involved in driving spontaneous fusion at very high temperatures (>40°C) while additional temperature sensitive mechanisms appear to be maintaining release at lower, physiological temperatures.

The findings so far suggest a more nuanced contribution of TRPV1 to synaptic glutamate release and indicate the presence of additional temperature dependent controls of quantal vesicle release. Because spontaneous release was maintained across warm temperatures and is known to be calcium dependent (Smith et al., 2012) we hypothesized that additional thermosensitive TRP channels are expressed in vagal primary afferents. Only a few thermosensitive TRP channels have temperature activation thresholds in the warm range including TRPV3 and TRPM3 (Ramsey et al., 2006). To begin to determine if these channels are present and functional we utilized fluorescent calcium imaging of cultured nodose ganglion neurons from control rats and TRPV1$^{-/-}$ mice (**Figure 8**). TRPV3 has no described selective agonist but can be activated by the TRPM8 agonist menthol at high concentrations ($N = 7$, $P < 0.001$, Kruskal-Wallis One-Way ANOVA) (Macpherson et al., 2006). TRPV3 mediated responses were differentiated from TRPM8 based on threshold to activation and blockade by bath application of ruthenium red (menthol 1 mM: 106 ± 21 nM vs. menthol + RuR: 37 ± 5 nM, $N = 9$, $P = 0.006$, paired T-Test) (**Figure 8A**, upper and lower panels). We also screened the TRPV3 agonist ethyl vanillin on cultured vagal afferents from TRPV1$^{-/-}$ mice and found that it concentration-dependently increased cytosolic calcium in a subpopulation of neurons (ethyl vanillin 0.01, 0.1, 0.3, 1, 3 mM: $N = 5$, $P = 0.002$, One-Way repeated measure ANOVA) (**Figure 8B**, upper and lower panels); suggesting TRPV3 expression is maintained independent of TRPV1. The ion channel TRPM3, on the other hand, is selectively activated by the steroid pregnenolone sulfate (pregnenolone sulfate 0.1, 1, 3, 1, 10, 30 μM: 1 ± 1, 4 ± 2, 11 ± 6, 54 ± 15, 106 ± 19 nM respectively, $N = 8$, $P < 0.001$, One-Way repeated measure ANOVA) (**Figure 8C**) (Wagner et al., 2008). Pregnenolone sulfate activated a subpopulation of cultured afferents from rats and TRPV1$^{-/-}$ mice (115 ± 67, $N = 3$, $P = 0.11$) (**Figure 8C**). In both experiments responsive neurons were also activated by the TRPV1 agonist capsaicin (data not shown) showing co-segregation of TRPV3 and TRPM3 with TRPV1. CAP exposure in the TRPV1$^{-/-}$ neurons

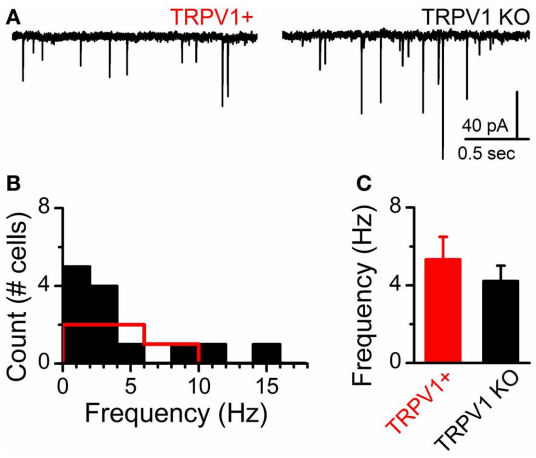

FIGURE 5 | Comparison of sEPSCs frequency onto NTS neurons from control (TRPV1+) and TRPV1 KO mice. (A) Current traces ($V_m = -60$ mV) of sEPSCs onto NTS neurons with each type of identified direct ST afferent contact. Temperature was held constant at 33°F. **(B)** Histogram of average sEPSC frequency across neurons (TRPV1+: $n = 8$ neurons, red and TRPV1 KO: $n = 13$ neurons, black). **(C)** The distribution of sEPSC frequencies was not statistically different between neurons receiving TRPV1+ and TRPV1 KO contacts ($P = 0.57$, unpaired t-test).

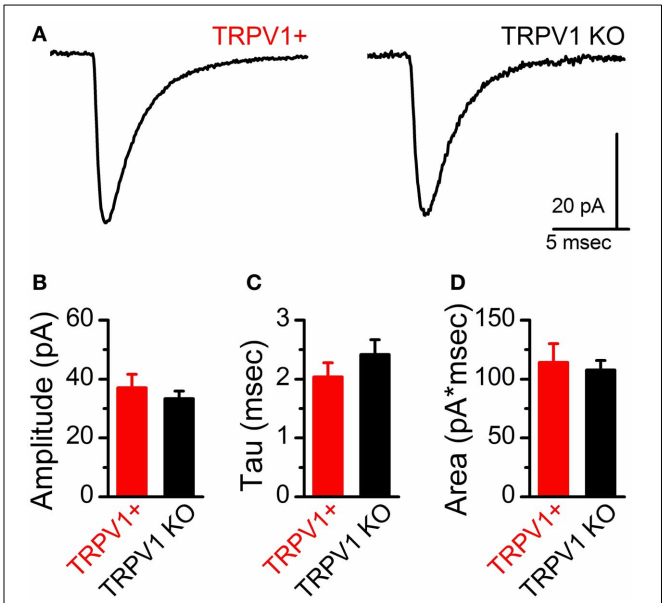

FIGURE 6 | No difference in spontaneous EPSC waveforms between control and TRPV KO ST afferents. (A) Representative average sEPSCs from control and TRPV1 KO afferents. Waveforms are the average of 100 events. Statistical comparison of sEPSC amplitude **(B)** and decay kinetics **(**Tau, **C)** and integrated current **(**Area, **D)** were not significantly different between TRPV1+ and TRPV1 KO afferents ($P = 0.46$, 0.71, and 0.31 respectively, unpaired t-tests).

failed to increase cytosolic calcium confirming deletion of the TPRV1 gene.

DISCUSSION

The major findings of these experiments confirm that TRPV1 is important in asynchronous vesicle release pathways at ST-NTS synapses but suggest that additional thermosensitive TRP channels are present in the presynaptic primary afferent neurons and may be contributing to the remaining asynchronous release and temperature driven spontaneous glutamate release. The fact that convergent primary afferent innervation remains completely segregated based on the presence or absence of asynchronous vesicle release, independent of TRPV1 expression, indicates a particular importance for asynchronous neurotransmission in ST-NTS synaptic organization. The maintenance of overall synaptic innervation patterns and action-potential driven synchronous vesicle release from TRPV1 KO afferents suggest that TRPV1 signaling and its impact on quantal glutamate release are not essential for development of this circuitry. Rather, TRPV1, likely in concert with other thermosensitive TRP channels, provides precise and nuanced control mechanism of quantal glutamate release pathways.

ACTION-POTENTIAL EVOKED SYNCHRONOUS RELEASE IS CONSERVED IN TRPV1 KO AFFERENTS

Neither primary afferent innervation patterns, action-potential driven synchronous release, nor vesicle mobilization to the readily releasable pool during trains of stimulations were different in TRPV1 KO afferents compared to control animals. Considering TRPV1 is expressed in the majority (70–80%) of visceral afferent neurons forming synapses onto second-order NTS neurons (Andresen et al., 2012b) and provides a large calcium influx pathway, we were surprised that none of these parameters were altered. In particular during trains of action-potentials, where terminal calcium waves accumulate and TRPV1 is likely being activated by voltage and other factors such as anandamide generation and activation of protein kinase C (PKC) (Premkumar and Ahern, 2000; Di Marzo et al., 2001; Studer and McNaughton, 2010), showed no difference in the vesicle mobilization. Other use dependent calcium influx pathways, such as activation of presynaptic NMDA type glutamate receptors are known to facilitate synapsin phosphorylation (Campos et al., 2013); a key step in vesicle shuttling to the readily releasable pool (Cesca et al., 2010). The current findings are consistent with the concept that calcium influx into the presynaptic terminal is very precisely controlled and that different calcium influx pathways participate in distinct cellular processes (Kavalali et al., 2011). It appears that TRPV1 derived calcium has little to do with synchronous release pathways and is specialized to impact quantal vesicle mobilization via spontaneous and asynchronous release pathways (Andresen et al., 2012a).

THE COMPLETE PRESENCE OR ABSENCE OF ASYNCHRONOUS RELEASE FROM TRPV1 KO AFFERENTS

The presence of TRPV1 predicts robust action-potential driven asynchronous release (Peters et al., 2010). Pharmacological blockade of TRPV1 attenuates the asynchronous release pathway (Peters et al., 2010) and suggests that TRPV1 genetic deletion should diminish asynchronous release for a given synapse.

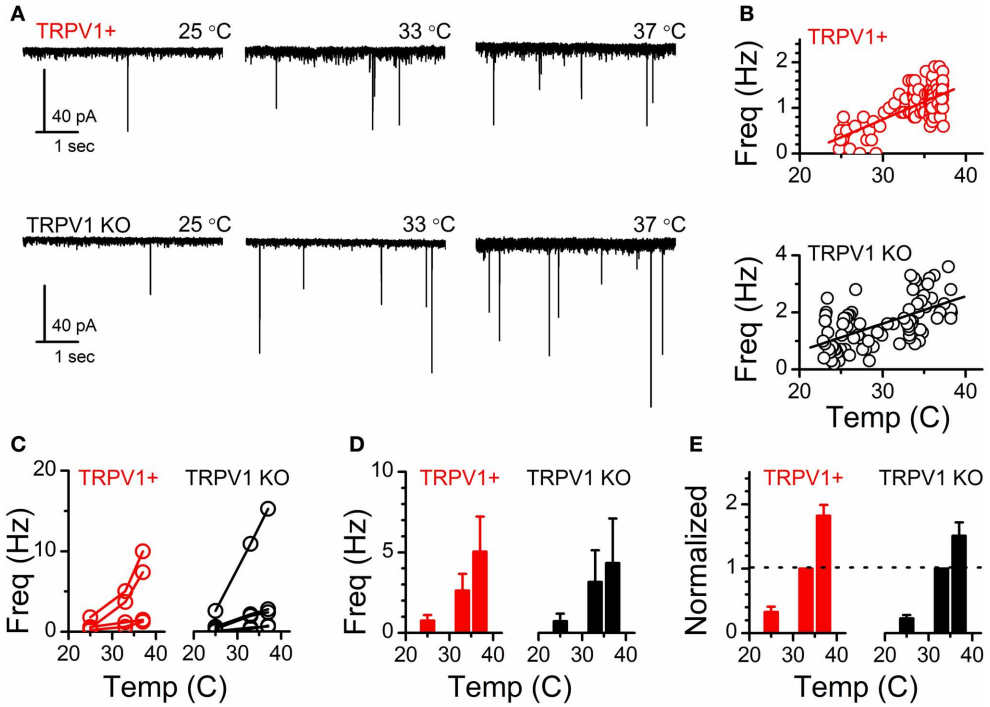

FIGURE 7 | Temperature driven changes in sEPSC frequency across the physiological range are not different from TRPV1 KO afferents. **(A)** Current traces of temperature driven increase in sEPSC frequency from TRPV1+ and TRPV1 KO mice. **(B)** Scatter-plot showing binned average frequency (10 s bins) across changing temperatures from the TRPV1+ and TRPV1 KO neurons shown in **(A)**. **(C)** Frequency of sEPSCs at each temperature from individual recorded neurons from TRPV1+ and TRPV1 KO animals. Lines connect frequencies at each temperature for an individual neuron. **(D)** Average sEPSC frequencies across neurons at each of the steady state temperatures. **(E)** Changes in frequency normalized to frequency recorded at 33°C. The frequency of spontaneous release is still temperature driven in the absences of TRPV1.

Surprisingly, the present work comparing ST-NTS synapses between control and TRPV1 KO animals revealed that afferents genetically lacking TRPV1 either completely lacked asynchronous release or completely maintained it (**Figure 4**). The characterization of the inputs lacking asynchronous release suggest that they are not simply an improbable collection of neurons that happen to have all A-fiber afferent inputs, based on their conduction velocity (latency), size of quantal events, and distribution within the medial NTS (Peters et al., 2010, 2011). Rather, they may represent the afferents wherein the asynchronous release would have been maintained entirely by the presence of TRPV1 and those with the remaining asynchronous release have redundant use dependent calcium influx pathways, such as the alternative TRP channels (TRPV3 and TRPM3) characterized in **Figure 8**. Convergent ST afferent innervation is segregated based on the presence or absence of TRPV1 and asynchronous release in control animals (Peters et al., 2011). Surprisingly TRPV1 KO afferents maintained this relationship. Wherein ST afferents without asynchronous release converged onto common neurons, those with asynchronous release converged onto a separate population of NTS neurons. This observation suggests that the presence or absence of the asynchronous vesicle release pathway may determine of convergent afferent organization into the NTS.

TEMPERATURE DRIVEN SPONTANEOUS GLUTAMATE RELEASE AND THE PRESENCE OF ALTERNATIVE THERMOSENSITIVE TRP CHANNELS

Spontaneous vesicle release is a stochastic process largely driven by temperature sensitive calcium conductances at ST-NTS synapses (Shoudai et al., 2010). The presence of TRPV1 in ST primary afferents predicts relatively high spontaneous frequency; while pharmacological antagonism of TRPV1 reduces overall temperature sensitivity of the spontaneous release pathway particularly at the highest temperatures recorded (∼40°C) (Peters et al., 2010; Shoudai et al., 2010). In TRPV1 KO animals we found that frequency of spontaneous release was indistinguishable from control animals (**Figure 5**). Further, temperature ramps revealed statistically significant increases in spontaneous frequency from 33 to 37°C that was not different between control and TRPV1$^{-/-}$ animals (**Figure 7**). The observation that spontaneous frequency is maintained at warm temperatures and still reactive to temperature steps from 25 to 37°C indicates that additional temperature sensitive mechanisms are intact in the TRPV1 KO afferents. These temperature driven changes may be relevant in detecting a number of physiological processes that alter internal temperatures such as post prandial thermogenesis (Griggio et al., 1991), circadian temperature changes (Buhr et al., 2010), or infection. Our preliminary pharmacological findings demonstrating functional expression of TRPV3 and TRPM3 provide evidence for plausible candidate ion channels to maintain the temperature

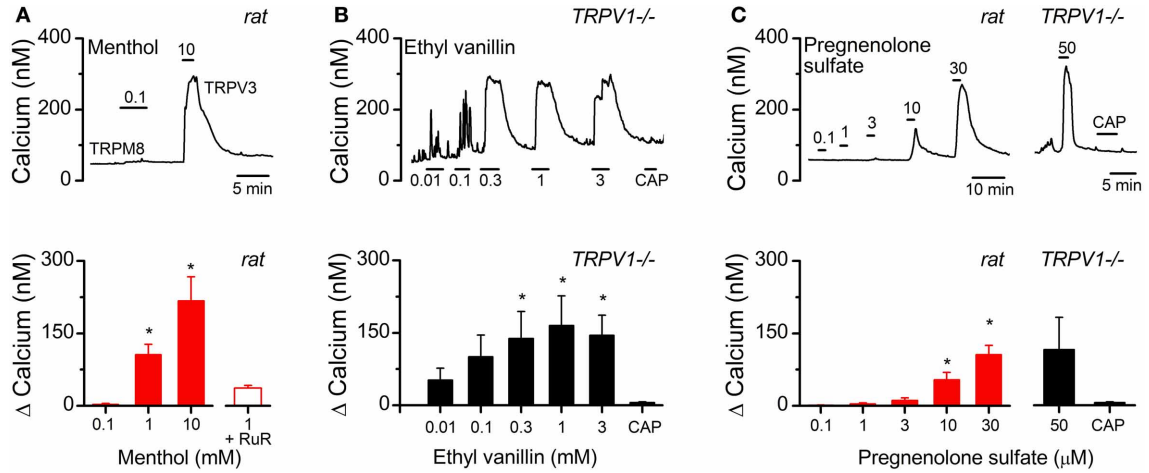

FIGURE 8 | Functional evidence suggesting alternative thermo-TRP channels present in vagal afferents. (A, upper panel) Representative calcium trace from cultured vagal afferent cell bodies showing menthol fails to activate at concentrations selective for TRPM8, but produce large calcium transients at concentrations known to activate TRPV3. **(A**, lower panel**)** Average concentration response relationship for menthol induced increases in cytosolic calcium ($N = 7$, $P < 0.001$, ANOVA). Menthol induced calcium increases were significantly reduced with RuR ($N = 9$, $P < 0.001$, paired *t*-test) also consistent with TRPV3 activation. **(B**, upper panel**)** Calcium trace showing the concentration-dependent increase in cytosolic calcium by the TRPV3 agonist ethyl vanillin in cultured vagal afferents taken from TRPV1$^{-/-}$ mice. CAP exposure failed to elicit a response as predicted. **(B**, lower panel**)** Average concentration response relationship for ethyl vanillin induced increases in cytosolic calcium ($N = 5$, $P = 0.002$, ANOVA). **(C**, upper panel**)** Left: Calcium trace showing the TRPM3 agonist pregnenolone sulfate concentration-dependently activated a subpopulation of CAP-sensitive vagal afferent neurons. Right: This response was maintained in afferents taken from TRPV1$^{-/-}$ mice. **(C**, lower panel**)** Average change in intracellular calcium across concentrations from pregnenolone sulfate responsive neurons from rat ($N = 8$, $P < 0.001$, ANOVA) and TRPV1$^{-/-}$ mice ($N = 3$, $P < 0.01$, paired *T*-test). Statistical significance is indicated by an asterisk (*).

driven spontaneous release at warm physiological temperatures. However, the specific roles of these candidate channels in the control of synaptic glutamate release remains to be determined.

Together these findings suggest additional temperature dependent mechanisms controlling asynchronous and thermosensitive spontaneous release at physiological temperatures, possibly mediated by additional thermosensitive TRP channels in primary afferent terminals. Because a major portion of the synaptic charge transfer is carried by glutamate released via spontaneous and asynchronous release pathways these central thermo-sensitive TRP channels are likely critical in the control of autonomic reflex generation and neuronal processing originating via cranial visceral afferents.

GRANTS

Supported by a grant from the National Institutes of Health, DK092651.

ACKNOWLEDGMENTS

We would like to thank Jonathon E. M. Lindberg and BreeAnne Peterson for their assistance and development of this manuscript.

REFERENCES

Andresen, M. C., Fawley, J. A., and Hofmann, M. E. (2012a). Peptide and lipid modulation of glutamatergic afferent synaptic transmission in the solitary tract nucleus. *Front. Neurosci.* 6:191. doi: 10.3389/fnins.2012.00191

Andresen, M. C., Hofmann, M. E., and Fawley, J. A. (2012b). The unsilent majority-TRPV1 drives "spontaneous" transmission of unmyelinated primary afferents within cardiorespiratory NTS. *Am. J. Physiol. Regul. Integr. Comp. Physiol.* 303, R1207–R1216. doi: 10.1152/ajpregu.00398.2012

Bailey, T. W., Hermes, S. M., Andresen, M. C., and Aicher, S. A. (2006a). Cranial visceral afferent pathways through the nucleus of the solitary tract to caudal ventrolateral medulla or paraventricular hypothalamus: target-specific synaptic reliability and convergence patterns. *J. Neurosci.* 26, 11893–11902. doi: 10.1523/JNEUROSCI.2044-06.2006

Bailey, T. W., Jin, Y.-H., Doyle, M. W., Smith, S. M., and Andresen, M. C. (2006b). Vasopressin inhibits glutamate release via two distinct modes in the brainstem. *J. Neurosci.* 26, 6131–6142. doi: 10.1523/JNEUROSCI.5176-05.2006

Buhr, E. D., Yoo, S. H., and Takahashi, J. S. (2010). Temperature as a universal resetting cue for mammalian circadian oscillators. *Science* 330, 379–385. doi: 10.1126/science.1195262

Campos, C. A., Shiina, H., Silvas, M., Page, S., and Ritter, R. C. (2013). Vagal afferent NMDA receptors modulate CCK-induced reduction of food intake through synapsin I phosphorylation in adult male rats. *Endocrinology* 154, 2613–2625. doi: 10.1210/en.2013-1062

Cesca, F., Baldelli, P., Valtorta, F., and Benfenati, F. (2010). The synapsins: key actors of synapse function and plasticity. *Prog. Neurobiol.* 91, 313–348. doi: 10.1016/j.pneurobio.2010.04.006

Chen, C. Y., Horowitz, J. M., and Bonham, A. C. (1999). A presynaptic mechanism contributes to depression of autonomic signal transmission in NTS. *Am. J. Physiol.* 277, H1350–H1360.

Di Marzo, V., Bisogno, T., and De Petrocellis, L. (2001). Anandamide: some like it hot. *Trends Pharmacol. Sci.* 22, 346–349. doi: 10.1016/S0165-6147(00)01712-0

Doyle, M. W., and Andresen, M. C. (2001). Reliability of monosynaptic transmission in brain stem neurons *in vitro*. *J. Neurophysiol.* 85, 2213–2223. doi: 10.1113/jphysiol.2010.190611

Doyle, M. W., Bailey, T. W., Jin, Y.-H., Appleyard, S. M., Low, M. J., and Andresen, M. C. (2004). Strategies for cellular identification in nucleus tractus solitarius slices. *J. Neurosci. Methods* 37, 37–48. doi: 10.1016/j.jneumeth.2004.02.007

Griggio, M. A., Richard, D., and Leblanc, J. (1991). The involvement of the sympathetic nervous system in meal-induced thermogenesis in mice. *Int. J. Obes.* 15, 711–715.

Kavalali, E. T., Chung, C., Khvotchev, M., Leitz, J., Nosyreva, E., Raingo, J., et al. (2011). Spontaneous neurotransmission: an independent pathway for

neuronal signaling? *Physiology (Bethesda)* 26, 45–53. doi: 10.1152/physiol.00040.2010

Lancaster, E., and Weinreich, D. (2001). Sodium currents in vagotomized primary afferent neurones of the rat. *J. Physiol.* 536, 445–458. doi: 10.1111/j.1469-7793.2001.0445c.xd

Loewy, A. D. (1990). "Central autonomic pathways," in *Central Regulation of Autonomic Functions*, eds A. D. Loewy and K. M. Spyer (New York, NY: Oxford), 88–103.

Macpherson, L. J., Hwang, S. W., Miyamoto, T., Dubin, A. E., Patapoutian, A., and Story, G. M. (2006). More than cool: promiscuous relationships of menthol and other sensory compounds. *Mol. Cell. Neurosci.* 32, 335–343. doi: 10.1016/j.mcn.2006.05.005

McDougall, S. J., Peters, J. H., and Andresen, M. C. (2009). Convergence of cranial visceral afferents within the solitary tract nucleus. *J. Neurosci.* 29, 12886–12895. doi: 10.1523/JNEUROSCI.3491-09.2009

Mendelowitz, D., Yang, M., Reynolds, P. J., and Andresen, M. C. (1995). Heterogeneous functional expression of calcium channels at sensory and synaptic regions in nodose neurons. *J. Neurophysiol.* 73, 872–875.

Peters, J. H., McDougall, S. J., Fawley, J. A., and Andresen, M. C. (2011). TRPV1 marks synaptic segregation of multiple convergent afferents at the rat medial solitary tract nucleus. *PLoS ONE* 6:e25015. doi: 10.1371/journal.pone.0025015

Peters, J. H., McDougall, S. J., Fawley, J. A., Smith, S. M., and Andresen, M. C. (2010). Primary afferent activation of thermosensitive TRPV1 triggers asynchronous glutamate release at central neurons. *Neuron* 65, 657–669. doi: 10.1016/j.neuron.2010.02.017

Peters, J. H., McDougall, S. J., Kellett, D. O., Jordan, D., Llewellyn-Smith, I. J., and Andresen, M. C. (2008). Oxytocin enhances cranial visceral afferent synaptic transmission to the solitary tract nucleus. *J. Neurosci.* 28, 11731–11740. doi: 10.1523/JNEUROSCI.3419-08.2008

Premkumar, L. S., and Ahern, G. P. (2000). Induction of vanilloid receptor channel activity by protein kinase C. *Nature* 408, 985–990. doi: 10.1038/35050121

Ramsey, I. S., Delling, M., and Clapham, D. E. (2006). An introduction to trp channels. *Annu. Rev. Physiol.* 68, 619–647. doi: 10.1146/annurev.physiol.68.040204.100431

Saper, C. B. (2002). The central autonomic nervous system: conscious visceral perception and autonomic pattern generation. *Annu. Rev. Neurosci.* 25, 433–469. doi: 10.1146/annurev.neuro.25.032502.111311

Shoudai, K., Peters, J. H., McDougall, S. J., Fawley, J. A., and Andresen, M. C. (2010). Thermally active TRPV1 tonically drives central spontaneous glutamate release. *J. Neurosci.* 30, 14470–14475. doi: 10.1523/JNEUROSCI.2557-10.2010

Simasko, S. M., Wiens, J., Karpiel, A., Covasa, M., and Ritter, R. C. (2002). Cholecystokinin increases cytosolic calcium in a subpopulation of cultured vagal afferent neurons. *Am. J. Physiol. Regul. Integr. Comp. Physiol.* 283, R1303–R1313. doi: 10.1152/ajpregu.00050.2002

Smith, S. M., Chen, W., Vyleta, N. P., Williams, C., Lee, C. H., Phillips, C., et al. (2012). Calcium regulation of spontaneous and asynchronous neurotransmitter release. *Cell Calcium* 52, 226–233. doi: 10.1016/j.ceca.2012.06.001

Studer, M., and McNaughton, P. A. (2010). Modulation of single-channel properties of TRPV1 by phosphorylation. *J. Physiol.* 588, 3743–3756. doi: 10.1113/jphysiol.2010.190611

Wagner, T. F., Loch, S., Lambert, S., Straub, I., Mannebach, S., Mathar, I., et al. (2008). Transient receptor potential M3 channels are ionotropic steroid receptors in pancreatic beta cells. *Nat. Cell Biol.* 10, 1421–1430. doi: 10.1038/ncb1801

Conflict of Interest Statement: The authors declare that the research was conducted in the absence of any commercial or financial relationships that could be construed as a potential conflict of interest.

Received: 30 September 2013; accepted: 09 January 2014; published online: 31 January 2014.

Citation: Fenwick AJ, Wu S-w and Peters JH (2014) Isolation of TRPV1 independent mechanisms of spontaneous and asynchronous glutamate release at primary afferent to NTS synapses. Front. Neurosci. ***8****:6. doi: 10.3389/fnins.2014.00006*

This article was submitted to Autonomic Neuroscience, a section of the journal Frontiers in Neuroscience.

frontiers in
NEUROSCIENCE

ORIGINAL RESEARCH ARTICLE
published: 13 December 2013
doi: 10.3389/fnins.2013.00238

TRPV1-dependent regulation of synaptic activity in the mouse dorsal motor nucleus of the vagus nerve

***Imran J. Anwar*[1] *and Andrei V. Derbenev*[1,2]*

[1] *Neuroscience Program, Tulane University, New Orleans, LA, USA*
[2] *Department of Physiology, Health Sciences Center, Tulane University, New Orleans, LA, USA*

Edited by:
Stuart McDougall, University of Melbourne, Australia

Reviewed by:
Kirsteen Browning, Penn State College of Medicine, USA
Ruben Stepanyan, Case Western Reserve University, USA

***Correspondence:**
Andrei V. Derbenev, Department of Physiology, Tulane University School of Medicine, 1430 Tulane Ave. SL-39, New Orleans, LA 70112, USA
e-mail: aderben@tulane.edu

The dorsal motor nucleus of the vagus (DMV) is a key integrative point of the parasympathetic neuronal network localized in the dorsal vagal complex. Activity of neurons in the DMV is closely regulated by synaptic inputs, and regulation of excitatory and inhibitory synapsis by transient receptor potential vanilloid type 1 (TRPV1) has been demonstrated. Activation of TRPV1 by heat, protons, endovanilloids, endocannabinoids, and inflammatory mediators is well established. In our study we hypothesized that TRPV1 contributes to the synaptic transmission of DMV neurons at physiological range of temperature without additional stimuli. Using whole-cell patch-clamp recordings we evaluated the effect of a rapid increase of temperature on excitatory and inhibitory neurotransmission and the contribution of TRPV1 to this response. Rapid increase of temperature from 25 to 37°C increased the frequency of miniature excitatory post-synaptic currents (mEPSC) by 351.7%. The frequency of miniature inhibitory post-synaptic currents (mIPSC) also increased by 184.7%. 5′-iodoresiniferatoxin (5′-iRFT), a selective TRPV1 antagonist, prevented the increase of mEPSC and mIPSC frequency. In summary, our data demonstrate that at physiological range of temperature TRPV1 contributes to presynaptic neurotransmission of DMV neurons.

Keywords: TRPV1, dorsal motor nucleus of the vagus, whole-cell patch-clamp recording, miniature postsynaptic currents

INTRODUCTION

The dorsal vagal complex (DVC) is a main parasympathetic autonomic center. It encompasses the nucleus of the solitary tract (NTS), the dorsal motor nucleus of the vagus nerve (DMV), and the area postrema (AP) (Bailey, 2008). The NTS receives inputs from cranial visceral afferents that carry viscerosensory information. The interneurons in the NTS send outputs to various targets, including the DMV (Travagli et al., 1991; Travagli and Rogers, 2001; Davis et al., 2003, 2004; Glatzer and Smith, 2005). The DMV sends vagal projections to postganglionic neurons innervating subdiaphragmatic organs (Browning and Travagli, 2011), thereby regulating the function of the gastrointestinal tract, the cardiovascular system, and the respiratory system (Bauer et al., 2005; Shoudai et al., 2010; Cavanaugh et al., 2011; Zsombok et al., 2011b).

The transient receptor potential vanilloid type 1 (TRPV1) is a non-selective cation channel that displays high permeability to divalent cations such as Ca^{2+} and Mg^{2+} (Caterina et al., 1997; Tominaga et al., 1998; Venkatachalam and Montell, 2007). TRPV1 is activated by heat, protons, endovanilloids, endocannabinoids, and inflammatory mediators (Bevan and Yeats, 1991; Caterina et al., 1997; Tominaga et al., 1998; Zygmunt et al., 1999; Terenzi et al., 2013). In the peripheral nervous system, it has been shown that TRPV1 contributes to pain, thermosensation, chemosensation, and inflammatory responses (Bessac and Jordt, 2008; Gavva et al., 2008; Patwardhan et al., 2010). While the contribution of TRPV1 to physiological responses has been thoroughly investigated in the peripheral nervous system, less information is known about TRPV1-dependent regulation of synaptic transmission in the central nervous system (CNS). TRPV1 expression in the CNS is restricted to specific areas. TRPV1 is expressed in the cerebral cortex, the hypothalamus, the brainstem and the hindbrain, as shown by different methods (Cristino et al., 2006; Derbenev et al., 2006; Pingle et al., 2007; Cavanaugh et al., 2011; Zsombok et al., 2011b; Gao et al., 2012).

Previous studies demonstrated the functional properties of TRPV1 in the DVC (Derbenev et al., 2006; Peters et al., 2010, 2011; Shoudai et al., 2010; Cavanaugh et al., 2011; Fawley et al., 2011; Zsombok et al., 2011b). TRPV1 drives synaptic activity of cranial visceral afferents providing continuous inputs to the NTS independently of afferent activity (Peters et al., 2010; Shoudai et al., 2010). Furthermore, TRPV1 enhances neurotransmitters release to DMV neurons. Activation of TRPV1 by capsaicin, an exogenous agonist, produces a robust increase of both miniature excitatory postsynaptic current (mEPSC) frequency and miniature inhibitory postsynaptic current (mIPSC) frequency in DMV neurons demonstrating that TRPV1 activation increases synaptic activity in the DVC (Derbenev et al., 2006).

Thermal activation of TRPV1 has also been demonstrated. TRPV1 has a heat activation threshold of ∼43°C *in vitro* (Caterina et al., 1997; Tominaga et al., 1998; Premkumar and Ahern, 2000; Gavva et al., 2007; Grandl et al., 2010; Shoudai et al., 2010). Due to the polymodal characteristics of TRPV1, the heat activation threshold can be reduced by a variety

of processes, including PKC phosphorylation, proton activation and repeated exposure to heat (Ji et al., 2002; Moriyama et al., 2005; Jay, 2007). Lowering the heat activation threshold could allow TRPV1 to be potentiated at physiological temperatures (~37°C). Based on the above-mentioned observations, we hypothesized that TRPV1 is active at physiological range of temperatures and enhances synaptic activity to DMV neurons. To test this, we conducted patch-clamp recordings where the temperature was increased from 25 to 37°C to demonstrate thermal activation of TRPV1 in the DMV. Our data revealed that at 37°C, the frequency of mEPSCs and the frequency of mIPSCs increased as compared to recordings conducted at 25°C. Upon further examination, we found that the potentiation of excitatory and inhibitory neurotransmission to DMV neurons was a result of thermal activation of presynaptic TRPV1 receptors. Our results indicate that TRPV1 regulates synaptic inputs to DMV neurons at physiological temperatures.

MATERIALS AND METHODS

Experiments were performed on male CD1 mice (7–8 weeks old; Harlan) following the National Institutes of Health Guide for the Care and Use of Laboratory Animals and were approved by Tulane University's Institutional Animal Care and Use Committee.

BRAINSTEM SLICE PREPARATION

Transverse brainstem slices were prepared from male mice as described previously (Zsombok et al., 2011a). Mice were deeply anesthetized by isoflurane inhalation and sacrificed by decapitation while anesthetized. Brains were rapidly removed and immersed in ice-cold (0–4°C) oxygenated artificial cerebrospinal fluid (ACSF) containing the following: 124 mM NaCl, 3 mM KCl, 26 mM $NaHCO_3$, 1.4 mM NaH_2PO_4, 11 mM glucose, 1.3 mM $CaCl_2$, and, 1.3 mM $MgCl_2$. The pH was adjusted to physiological ranges (7.3–7.4), with an osmolality of 290–310 mOsm/kg. Transverse brainstem slices (300 μm) containing the DMV were made using a vibrating microtome (Vibratome Series 1000; Technical Products). Slices were maintained in an oxygenated bath solution at 35°C for at least 1 h before performing experiments. Slices were then transferred to a recording chamber mounted on a fixed stage under an upright microscope (Nikon FN1).

WHOLE-CELL PATCH-CLAMP RECORDINGS

DMV neurons were visually identified in coronal brainstem slices and were patch-clamped with a glass pipette with series resistance between 2 to 4 MΩ. The electrodes were filled with a solution containing the following: 130 mM Cs^+-gluconate, 1 mM NaCl, 5 mM EGTA, 10 mM HEPES, 1 mM $MgCl_2$, 1 mM $CaCl_2$, 3 mM CsOH, 2-4 mM Mg-ATP, buffered to pH = 7.3–7.4 (with CsOH). Electrophysiological signals were low-pass filtered at 2–5 kHz, digitized at 88 kHz, recorded using an Axopatch 700 B amplifier (Molecular Devices). Excitatory post-synaptic currents (EPSCs) were examined at a holding potential of −60 mV while inhibitory post-synaptic currents (IPSCs) were recorded at a holding potential of 0 mV.

TEMPERATURE SETTING AND PROTOCOL

The temperature was monitored by an extracellular probe placed in the chamber 1 cm apart from the slice. The probe was placed upstream from the slice, close to where the ACSF entered the chamber. Therefore the temperature changes reflected by the probe occurred with a slight delay at the level of the brain slice. A Koolance device (Warner instrument) was used to heat the ACSF entering the chamber, allowing for the precise control of the temperature inside the chamber. In control conditions, DMV neurons were maintained at 25°C. To investigate the temperature-dependent contribution of TRPV1 to the synaptic transmission, recordings were made while the ACSF was gradually heated up to 37°C. Then, the temperature was decreased back to 25°C.

DRUG APPLICATION

Recordings were performed with tetrodotoxin (1 μM; TTX; Tocris Bioscience) in ACSF to block action potentials and monitor mEPSCs or mIPSCs. In addition, the TRPV1 antagonist 5′-iodoresiniferatoxin (1 μM; 5′-iRFT; Tocris Bioscience) was dissolved in ethanol and diluted in ACSF (final concentration of ethanol <0.01% by volume).

DATA ANALYSIS

The recordings were analyzed with pClamp 10 software (Molecular Devices). Miniature IPSCs and EPSCs were analyzed offline using MiniAnalysis (Synaptosoft). The effects of temperature on mEPSCs and mIPSCs were analyzed within individual cells using the Kolmogorov-Smirnov test. The effects of temperature across neuron groups were analyzed using a paired two-tailed Student's t test. Values are expressed as means ± s.e.m.

RESULTS

TRPV1 POTENTIATES EXCITATORY NEUROTRANSMISSION TO DMV NEURONS IN TEMPERATURE-DEPENDENT MANNER

Patch-clamp recordings from NTS neurons demonstrated that increase of temperature potentiates excitatory neurotransmission in a TRPV1-dependent manner (Peters et al., 2010; Shoudai et al., 2010). To reveal the contribution of TRPV1 to temperature-dependent neurotransmission in the DMV, we used patch-clamp whole-cell recordings. The frequency and amplitude of mEPSCs were examined at −60 mV using Cs-gluconate solution in the recording pipettes to block K^+ currents (Bach and Smith, 2012). In control condition, the temperature of ACSF was maintained at 25°C. Then, the ACSF was heated up to 37°C within 5 min. A schematic illustration of the temperature protocol is depicted on **Figures 2B**, **4B.**

The increase of temperature from 25 to 37°C produced a significant increase in mEPSC frequency and amplitude in all recorded neurons (**Figure 1**). At 25°C, the average mEPSC frequency was 2.64 ± 0.1 events per second (range from 2.15 to 2.98 events per second; $n = 6$). Rapid increase of temperature to 37°C triggered a 351.7% increase of mEPSCs frequency to 12.02 ± 1.7 events per second (range from 4.34 to 17.95 events per second; $n = 6$; $P < 0.05$) (**Figure 1B**). The temperature-induced changes were rapid, reversible and did not diminish overtime in any of the recorded cells ($n = 6$) (**Figure 2B**).

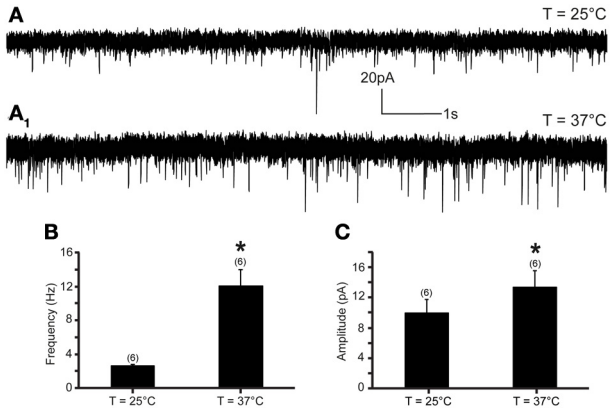

FIGURE 1 | Excitatory neurotransmission to DMV neurons is potentiated by TRPV1 at physiological temperatures. (A) Continuous recording of mEPSCs at 25°C **(A)** and after elevation of temperature from 25 to 37°C **(A_1)** in TTX (1 μM). **(B,C)**. Bar graph summarizing the effect of temperature on mEPSC frequency **(B)** and mEPSC amplitude **(C)**. *Significance ($p < 0.05$).

To test whether the temperature-dependent increase of mEPSC frequency was due to TRPV1 activation, 5′-iRFT, a selective TRPV1 antagonist was added to the ACSF for 30 min before recordings were performed. Application of 5′-iRFT (1 μM) prevented the increase of mEPSC frequency triggered by temperature elevation (**Figures 2A,B,D**). In the presence of 5′-iRFT the average mEPSC frequency was 1.24 ± 0.21 events per second (range from 0.96 to 1.88 events per second; $n = 6$) (**Figure 2D**, red trace). Rapid increase of temperature to 37°C in the presence of 5′-iRFT prevented the increase of mEPSC frequency. The average mEPSC frequency was 2.20 ± 0.26 events per second at 37°C (range from 1.51 to 2.96 events per second; $n = 6$; $P > 0.05$) (**Figure 2D**), which was not significantly different as compared to mEPSC frequency measured at 25°C. Our results suggest that the temperature-dependent potentiation of excitatory neurotransmission is driven by activation of TRPV1.

In addition, we assessed the effect of the rapid increase of temperature on mEPSC amplitude. We found that an increase of temperature from 25 to 37°C resulted in a significant increase of mEPSC amplitude (**Figures 1C**, **2C**). At 25°C the average mEPSC amplitude was 10.47 ± 1.6 pA (range from 7.25 to 14.97 pA; $n = 6$). Rapid increase of temperature to 37°C significantly increased the amplitude of mEPSCs in all recorded DMV neurons. The average mEPSC amplitude was 13.88 ± 1.8 pA (range from 8.73 to 19.09 pA; $n = 6$; $P < 0.05$) in ACSF at 37°C (**Figure 1C**). To determine if the temperature-dependent increase of amplitude is TRPV1 driven, amplitudes were compared in the presence and absence of 5-iRFT. Application of TRPV1 antagonist, 5′-iRFT, did not block the increase of mEPSC amplitude in response to temperature increase (**Figures 2C,E**, red trace). Failure to prevent the increase of mEPSC amplitude with a TRPV1 antagonist suggests that the effect occurs in a TRPV1-independent fashion.

In addition, increase of temperature to 37°C modulated mEPSC kinetics. Rise-time and decay time were both significantly reduced at 37°C (**Table 1**). The change in the mEPSC kinetics was not blocked by 5-iRFT application, suggesting that the effect also occurs in a TRPV1-independent fashion.

Temperature-induced currents were also investigated. Rapid increase of temperature produced a significant shift of the holding current. Rapid increase of temperature from 25 to 37°C shifted the holding current from -11.87 ± 1.9 pA (range −6.12 to −18.53) to -49.21 ± 6.7 pA (range −28.04 to −76.49; $n = 6$; $P < 0.05$) (**Figure 2F**). Application of 5′-iRFT did not block the inward shift in holding current (**Figure 2F**, red trace).

Our results suggest that rapid increase of temperature from 25 to 37°C had multiple effects, but potentiation of presynaptic release of excitatory neurotransmitters to DMV neurons is TRPV1-dependent.

TRPV1 POTENTIATES INHIBITORY NEUROTRANSMISSION TO DMV NEURONS IN A TEMPERATURE-DEPENDENT MANNER

The frequency and amplitude of mIPSCs were examined at 0 mV. Increase of temperature from 25 to 37°C produced a significant increase of mIPSC frequency and amplitude in all recorded neurons (**Figure 3**). At 25°C, the average mIPSC frequency was 1.10 ± 0.2 events per second (range from 0.27 to 1.93 events per second; $n = 7$). Rapid increase of temperature to 37°C triggered a 184.7% increase of mIPSC frequency to 2.93 ± 0.7 events per second (range from 0.63 to 6.11 events per second; $n = 7$; $P < 0.05$) (**Figure 3B**). The temperature-induced changes were rapid, reversible and did not diminish overtime ($n = 7$) (**Figure 4B**). To test whether the increase of mIPSC frequency was caused by TRPV1 activation, mIPSCs were recorded in the presence of 5′-iRFT, a TRPV1 antagonist. Application of 5′-iRFT (1 μM) prevented the increase of mIPSC frequency triggered by temperature elevation (**Figures 4A,B,D**). In the presence of 5′-iRFT, the mean mIPSC frequency was 0.86 ± 0.26 events per second (range from 0.20 to 1.77 events per second; $n = 6$). After rapid increase of temperature to 37°C in ACSF containing 5′-iRFT, we observed no significant changes in mIPSC frequency. The average mIPSC frequency was 0.72 ± 0.25 events per second (range from 0.35 to 1.89 events per second; $n = 6$; $P > 0.05$) (**Figure 4D**). Our results suggest that the temperature-dependent potentiation of inhibitory neurotransmission is driven by activation of TRPV1.

Next, we assessed the effect of temperature elevation on mIPSC amplitude. We found that rapid increase of temperature from 25 to 37°C significantly increased the amplitude of mIPSCs (**Figures 3C**, **4C**). At 25°C, the mean mIPSC amplitude was 29.18 ± 1.5 pA (range from 24.54 to 35.75 pA, $n = 7$). Rapid increase of temperature to 37°C significantly increased amplitude of mIPSCs in all recorded DMV neurons. The average amplitude was increased to 35.84 ± 3.6 pA (range from 24.46 to 50.11 pA; $n = 7$; $P < 0.05$) at 37°C (**Figure 3C**). Application of the TRPV1 antagonist, 5′-iRFT, did not block the increase of mIPSC amplitude in response to temperature increase (**Figures 4C,E**, red trace). Failure to block the increase of mIPSC amplitude with a TRPV1 antagonist suggests that the effect occurs in a TRPV1-independent fashion.

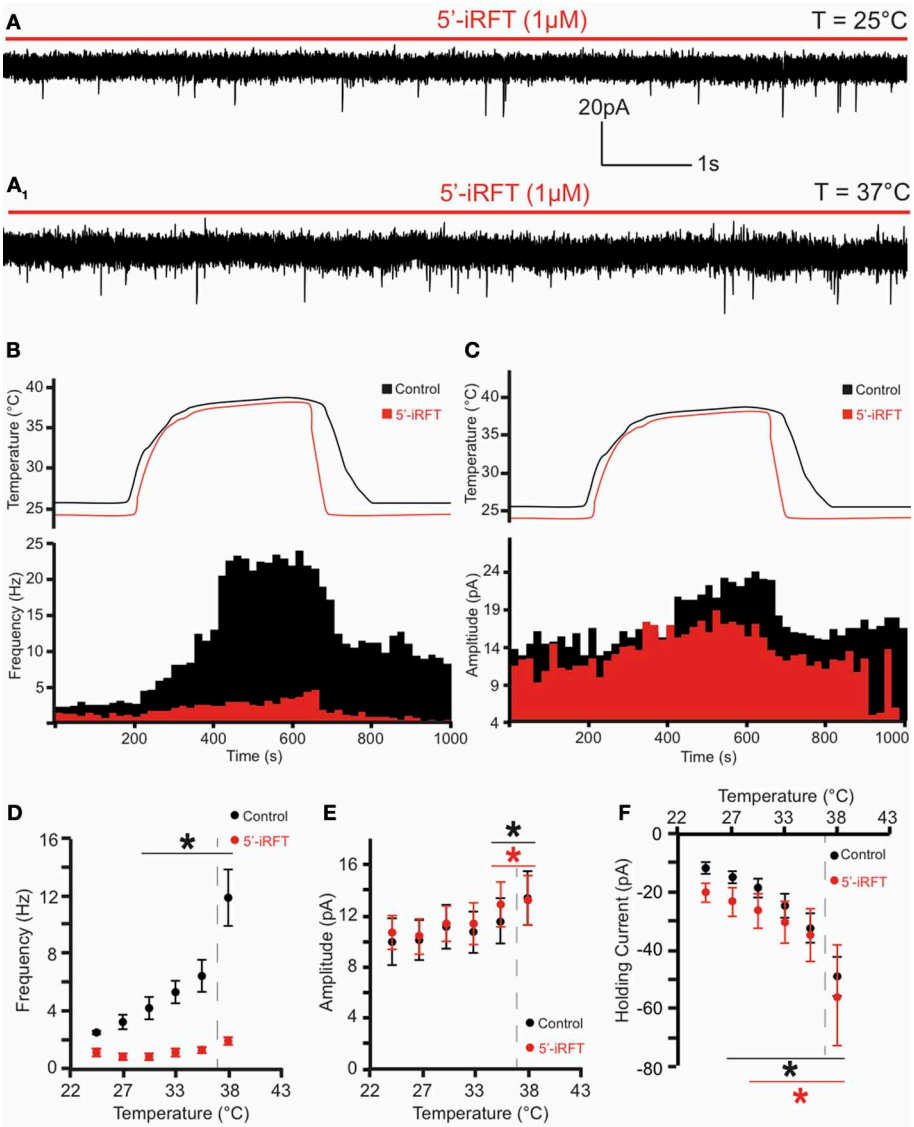

FIGURE 2 | TRPV1 antagonist prevents the potentiation of excitatory neurotransmission caused by TRPV1 activation to DMV neurons. (A) Continuous recording of mEPSCs in the presence of 5′-iRFT (1μM) and TTX (1μM) at 25°C **(A)** and after increase of temperature from 25°C to 37°C **(A_1)**. **(B,C)**. The effect of TRPV1 antagonist on the increase of mEPSC frequency **(B)** and amplitude **(C)**. **(D–F)**. Summary for temperature response on mEPSC frequency **(D)**, mEPSC amplitude **(E)**, and total inward current **(F)** ($n = 6$). Black traces indicate control conditions. Red traces indicate recordings conducted in the presence of 5′-iRFT, a TRPV1 antagonist. Dashed-line indicates physiological temperature. *Significance ($p < 0.05$).

In addition, increase of temperature to 37°C modulated mIPSC kinetics. Rise-time and decay time were both significantly reduced at 37°C (**Table 1**). The change in mIPSC kinetics was not blocked by 5-iRFT application, suggesting that the effect also occurs in a TRPV1-independent fashion.

Finally, temperature-induced currents were investigated. Rapid increase of temperature produced a significant shift of the holding current. Rapid increase of temperature from 25 to 37°C shifted the holding current from 49.32 ± 13.5 pA at 25°C to 202.3 ± 38.3 pA at 37°C ($n = 7$; $P < 0.05$) (**Figure 4F**). Application of 5′-iRFT did not block the outward shift in holding current (**Figure 4F**, red trace).

Our results suggest that rapid increase of temperature form 25 to 37°C potentiate presynaptic release of inhibitory neurotransmitters to DMV neurons in TRPV1-dependent manner.

DISCUSSION

The results of our study provide novel information about TRPV1-dependent regulation of excitatory and inhibitory neurotransmission in the DVC. Our data demonstrate that TRPV1 modulates synaptic transmission of DMV neurons in two different ways. First, at 37°C, mEPSC frequency is increased due to presynaptic activation of TRPV1. Second, mIPSC frequency is increased due to presynaptic activation

Table 1 | Rise time and decay time response to temperature changes in DMV neurons in control condition and in the presence of 5-iRFT.

		T = 25°C		T = 37°C	
	n Cells	**Mean**	**Range**	**Mean**	**Range**
mEPSCs					
Rise time (ms)	6	1.76 ± 0.4	1.07–2.73	1.07 ± 0.3*	0.56–2.30
Decay time (ms)	6	4.23 ± 1.0	1.98–8.89	2.54 ± 0.8*	1.14–6.71
in 5′-iRFT					
Rise time (ms)	6	1.02 ± 0.2	0.60–1.71	0.80 ± 0.2*	0.42–1.71
Decay time (ms)	6	1.85 ± 0.2	1.47–2.73	1.37 ± 0.1*	1.03–1.77
mIPSCs					
Rise time (ms)	7	1.83 ± 0.2	0.91–2.07	0.89 ± 0.1*	0.65–1.59
Decay time (ms)	7	6.82 ± 0.3	5.88–7.91	2.37 ± 0.3*	1.39–2.72
in 5′-iRFT					
Rise time (ms)	6	2.57 ± 0.3	1.09–4.30	1.80 ± 0.2*	0.88–2.58
Decay time (ms)	6	10.74 ± 0.5	8.20–12.37	5.49 ± 0.5*	3.55–7.87

Significance ($P < 0.05$)

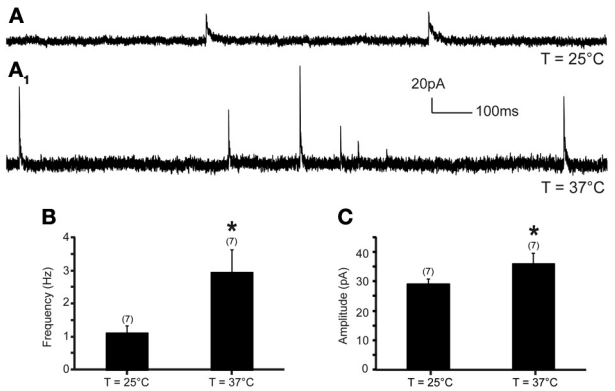

FIGURE 3 | Inhibitory neurotransmission to DMV neurons is potentiated by TRPV1 at physiological temperatures. (A). Continuous recording of mIPSCs at 25°C **(A)** and after increase of temperature from 25 to 37°C **(A_1)** in TTX (1 μM). **(B,C)**. Bar graph summarizing the effect of temperature on mIPSC frequency **(B)** and mIPSC amplitude **(C)**. *Significance ($p < 0.05$).

of TRPV1. Our results show that TRPV1 is involved in the regulation of both excitatory and inhibitory neurotransmission to DMV neurons. Physiological temperatures, in our case 37°C, activate presynaptic TRPV1, thus increasing excitatory and inhibitory neurotransmitters release to DMV neurons.

It has been shown previously that activation of TRPV1 by capsaicin resulted in increased mIPSC and mEPSC frequency in DMV neurons (Derbenev et al., 2006). TRPV1 is localized on both excitatory and inhibitory presynaptic terminals synapsing with DMV neurons and TRPV1 activation produces an increase of neurotransmitter release from these presynaptic terminals. Also, it has been shown that TRPV1 drives asynchronous synaptic activity to the NTS independently of afferent activity (Peters et al., 2010; Shoudai et al., 2010). Here we demonstrated that physiological range of temperature (37°C) alone drives frequency of mEPSCs and mIPSCs in TRPV1-dependent manner.

It has been reported that TRPV1 has a thermal threshold of 43°C *in vitro* (Caterina et al., 1997; Tominaga et al., 1998; Premkumar and Ahern, 2000; Gavva et al., 2007; Yao et al., 2010). The heat-induced activation of TRPV1 is caused by a negative shift of the voltage dependence of activation. At 0 mV and 25°C, the probability of opening is ∼0.10 while at 35°C, the probability of opening is ∼0.40. At −60 mV, probability of opening stays low, reaching ∼0.10 at 35°C (Voets et al., 2004). Protons and PKC sensitize TRPV1 to lower temperatures by increasing the negative shift of voltage dependence of activation (Premkumar et al., 2002; Voets et al., 2004). Seeing the robust activation of TRPV1 even at −60 mV, it is plausible that TRPV1 is potentiated in the DVC. Clearly, further studies are needed to elucidate the exact mechanisms of sensitization of TRPV1 in the DVC.

5′-iRFT application was used to block TRPV1 in some of our recordings. Previously, it has been shown that in control conditions, 5′-iRFT does not effect either excitatory or inhibitory inputs to DMV neurons at 1 μM concentration (Zsombok et al., 2011a). In contrast, our data show that 5′-iRFT significantly reduced mEPSC frequency: mESPC frequency was 2.64 ± 0.1 events per second in the control group (range from 2.15 to 2.98 events per second; $n = 6$) and 1.24 ± 0.21 events per second in the 5′-iRFT group (range from 0.96 to 1.88 events per second; $n = 6$; $P < 0.05$). Our differential findings could be explained by the fact that the 5′-iRFT effect was investigated across group and not across individual neurons: the difference of basal frequency between the control group and the 5′-iRFT group is likely due to variability between the neurons recorded in each group. Even though the basal mEPSC frequency is lower in the 5′-iRFT group, we would expect similar temperature-dependent increase of mEPSC frequency if 5′-iRFT were not present in the ACSF.

Our data also indicate that a rapid increase of temperature results in an increase of mPSC amplitude in a linear fashion, and 5′-iRFT failed to block this increase (**Figures 2E**, **4E**) suggesting that temperature-induced increase of mPSC amplitude is TRPV1 independent. Furthermore, mPSC kinetics were influenced by temperature in the same linear-fashion. Decay-time and rise-time were significantly reduced at 37°C compared to 25°C (**Table 1**). As the temperature increased, the 10–90% rise time and decay time constant of mIPSC and mEPSC decreased. This is consistent with previous studies demonstrating relationship between temperature and PSC kinetics (Taschenberger and Gersdorff von, 2000; Wall et al., 2002; Kushmerick et al., 2006; Postlethwaite et al., 2007). Temperature increase from 25 to 37°C accelerated mEPSC kinetics and increased mEPSC amplitude in the calyx of Held due to a temperature-dependent scaling of reaction rate constant of AMPA receptors. Specifically, the changes were caused by accelerated agonist binding, unbinding and kinetics of AMPA receptors (Postlethwaite et al., 2007). We can speculate that the same scaling of reactions rates might occur in the DMV due to increase of temperature.

It is well established that DMV neurons receive synaptic inputs from the NTS and provide tonic inputs to visceral organs

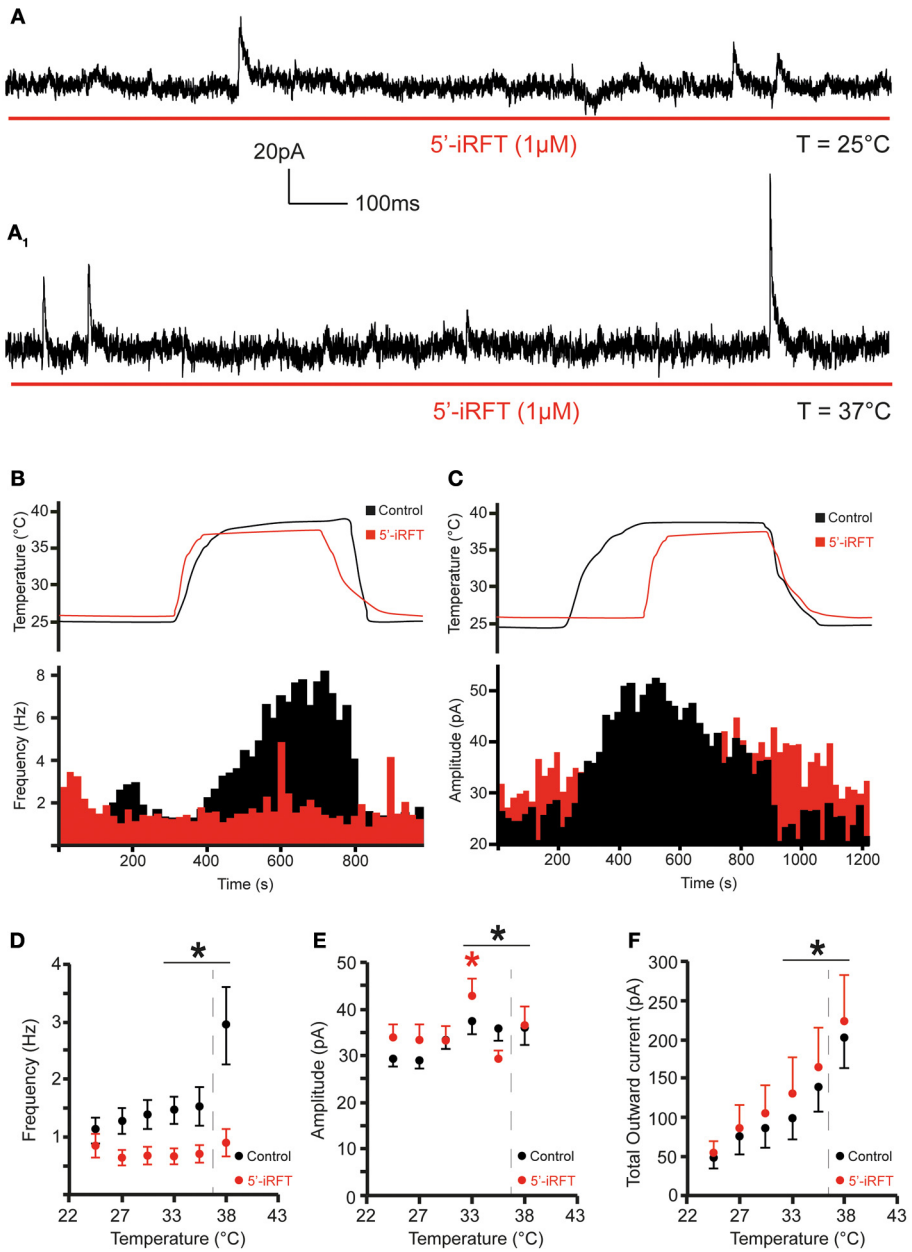

FIGURE 4 | TRPV1 antagonist prevents the increase of inhibitory neurotransmission to DMV neurons caused by TRPV1 activation. **(A)**. Continuous recording of mIPSCs in the presence of 5′-iRFT (1 μM) and TTX (1 μM) at 25°C **(A)** and after rise of temperature from 25 to 37°C **(A_1)**. **(B,C)**. The effect of TRPV1 antagonist on the increase of mIPSC frequency **(B)** and amplitude **(C)** (red traces are recordings with 5′-iRFT). **(D–F)**. Summary for temperature response on mIPSC frequency **(D)**, mIPSC amplitude **(E)**, and total outward current **(F)** ($n = 7$). Black traces indicate control conditions. Red traces indicate recordings conducted in the presence of 5′-iRFT, a TRPV1 antagonist. Dashed-line indicates physiological temperature. *Significance ($p < 0.05$).

(Travagli and Rogers, 2001). Also, DMV neurons exhibit slow, spontaneous, pacemaker-like activity by tonically firing action potentials (Barrett et al., 2006; Travagli et al., 2006; Browning and Travagli, 2011). Microinjections of glutamate or GABA receptor antagonists into the DVC confirmed that inhibitory inputs play a significant role in regulating the rate of the pacemaker-like activity of DMV neurons, while the excitatory inputs were not involved (Browning and Travagli, 2011). This suggests that the NTS provides tonic GABAergic inputs to the DMV to regulate its activity, while excitatory inputs to the DMV have little effect on the activity of the DMV. Our study suggests that both the excitatory and inhibitory inputs are tonically potentiated at physiological temperature due to the presence of presynaptic TRPV1. The presence of TRPV1 on GABAergic terminals could thus constitute an

additional regulatory mechanism of the vagal tone. Furthermore, tonic TRPV1 activation could reduce the pacemaker-like activity of DMV neurons and therefore reduce the motor vagal output.

Our study revealed that TRPV1 tonically drives excitatory and inhibitory inputs to the DMV at physiological temperatures. These findings provide new insights into TRPV1 function in the CNS and the autonomic nervous system. While TRPV1 serves primarily as a noxious stimuli integrator in the peripheral nervous system, our study suggests that TRPV1 exerts different functions in the CNS. At physiological temperatures, TRPV1 plays a novel role in the neurotransmission of the DMV, and therefore also contributes to the vagal motor output and the control of visceral organs.

AUTHOR CONTRIBUTIONS

Imran J. Anwar performed experiments; Imran J. Anwar analyzed data; Imran J. Anwar and Andrei V. Derbenev interpreted results of experiments; Imran J. Anwar prepared figures; Imran J. Anwar and Andrei V. Derbenev edited and revised manuscript; Imran J. Anwar and Andrei V. Derbenev approved final version of manuscript; Andrei V. Derbenev conception and design of research; Imran J. Anwar and Andrei V. Derbenev drafted manuscript.

ACKNOWLEDGMENTS

We thank Dr. Andrea Zsombok, Dr. Hong Gao, and Amanda Krantz for valuable comments on the manuscript.

REFERENCES

Bach, E. C., and Smith, B. N. (2012). Presynaptic NMDA receptor-mediated modulation of excitatory neurotransmission in the mouse dorsal motor nucleus of the vagus. *J. Neurophysiol.* 108, 1484–1491. doi: 10.1152/jn.01036.2011

Bailey, E. F. (2008). A tasty morsel: the role of the dorsal vagal complex in the regulation of food intake and swallowing. Focus on "BDNF/TrkB signaling interacts with GABAergic system to inhibit rhythmic swallowing in the rat," by Bariohay et al. *Am. J. Physiol. Regul. Integr. Comp. Physiol.* 295, R1048–1049. doi: 10.1152/ajpregu.90701.2008

Barrett, K. E., Ghishan, F. K., Merchant, J. L., Said, H. M., and Wood, J. D. (eds.). (2006). *Physiology of the Gastrointestinal Tract*, *4th Edn.* Vol. 1–2. Waltham: Academic Press.

Bauer, S., Hay, M., Amilhon, B., Jean, A., and Moyse, E. (2005). *In vivo* neurogenesis in the dorsal vagal complex of the adult rat brainstem. *Neuroscience* 130, 75–90. doi: 10.1016/j.neuroscience.2004.08.047

Bessac, B. F., and Jordt, S. E. (2008). Breathtaking TRP Channels: TRPA1 and TRPV1 in Airway Chemosensation and Reflex Control. *Physiology* 23, 360–370. doi: 10.1152/physiol.00026.2008

Bevan, S., and Yeats, J. (1991). Protons activate a cation conductance in a subpopulation of rat dorsal root ganglion neurones. *J. Physiol. (Lond.)* 433, 145–161.

Browning, K. N., and Travagli, R. A. (2011). Plasticity of vagal brainstem circuits in the control of gastrointestinal function. *Auto. Neurosci. Basic Clin.* 161, 6–13. doi: 10.1016/j.autneu.2010.11.001

Caterina, M. J., Schumacher, M. A., Tominaga, M., Rosen, T. A., Levine, J. D., and Julius, D. (1997). The capsaicin receptor: a heat-activated ion channel in the pain pathway. *Nature* 389, 816–824. doi: 10.1038/39807

Cavanaugh, D. J., Chesler, A. T., Jackson, A. C., Sigal, Y. M., Yamanaka, H., Grant, R., et al. (2011). Trpv1 Reporter mice reveal highly restricted brain distribution and functional expression in arteriolar smooth muscle cells. *J. Neurosci.* 31, 5067–5077. doi: 10.1523/JNEUROSCI.6451-10.2011

Cristino, L., de Petrocellis, L., Pryce, G., Baker, D., Guglielmotti, V., and Di Marzo, V. (2006). Immunohistochemical localization of cannabinoid type 1 and vanilloid transient receptor potential vanilloid type 1 receptors in the mouse brain. *Neuroscience* 139, 1405–1415. doi: 10.1016/j.neuroscience.2006.02.074

Davis, S. F., Derbenev, A. V., Williams, K. W., Glatzer, N. R., and Smith, B. N. (2004). Excitatory and inhibitory local circuit input to the rat dorsal motor nucleus of the vagus originating from the nucleus tractus solitarius. *Brain Res.* 1017, 208–217. doi: 10.1016/j.brainres.2004.05.049

Davis, S. F., Williams, K. W., Xu, W., Glatzer, N. R., and Smith, B. N. (2003). Selective enhancement of synaptic inhibition by hypocretin (orexin) in rat vagal motor neurons: implications for autonomic regulation. *J. Neurosci.* 23, 3844–3854.

Derbenev, A. V., Monroe, M. J., Glatzer, N. R., and Smith, B. N. (2006). Vanilloid-Mediated heterosynaptic facilitation of inhibitory synaptic input to neurons of the rat dorsal motor nucleus of the vagus. *J. Neurosci.* 26, 9666–9672. doi: 10.1523/JNEUROSCI.1591-06.2006

Fawley, J. A., Peters, J. H., and Andresen, M. C. (2011). GABAB-mediated inhibition of multiple modes of glutamate release in the nucleus of the solitary tract. *J. Neurophysiol.* 106, 1833–1840. doi: 10.1152/jn.00476.2011

Gao, H., Miyata, K., Bhaskaran, M. D., Derbenev, A. V., and Zsombok, A. (2012). Transient Receptor Potential Vanilloid Type 1-Dependent regulation of liver-related neurons in the paraventricular nucleus of the hypothalamus diminished in the Type 1 diabetic mouse. *Diabetes* 61, 1381–1390. doi: 10.2337/db11-0820

Gavva, N. R., Bannon, A. W., Surapaneni, S., Hovland, D. N., Lehto, S. G., Gore, A., et al. (2007). The Vanilloid Receptor TRPV1 Is tonically activated *in vivo* and involved in body temperature regulation. *J. Neurosci.* 27, 3366–3374. doi: 10.1523/JNEUROSCI.4833-06.2007

Gavva, N. R., Treanor, J. J. S., Garami, A., Fang, L., Surapaneni, S., Akrami, A., et al. (2008). Pharmacological blockade of the vanilloid receptor TRPV1 elicits marked hyperthermia in humans. *Pain* 136, 202–210. doi: 10.1016/j.pain.2008.01.024

Glatzer, N. R., and Smith, B. N. (2005). Modulation of synaptic transmission in the rat nucleus of the solitary tract by endomorphin-1. *J. Neurophysiol.* 93, 2530–2540. doi: 10.1152/jn.00429.2004

Grandl, J., Kim, S. E., Uzzell, V., Bursulaya, B., Petrus, M., Bandell, M., et al. (2010). Temperature-induced opening of TRPV1 ion channel is stabilized by the pore domain. *Nat. Neurosci.* 13, 708–714. doi: 10.1038/nn.2552

Jay, G. W. (2007). *Chronic Pain*. Boca Raton: Informa Healthcare.

Ji, R.-R., Samad, T. A., Jin, S.-X., Schmoll, R., and Woolf, C. J. (2002). p38 MAPK activation by NGF in primary sensory neurons after inflammation increases TRPV1 levels and maintains heat hyperalgesia. *Neuron* 36, 57–68. doi: 10.1016/S0896-6273(02)00908-X

Kushmerick, C., Renden, R., and Gersdorff von, H. (2006). Physiological temperatures reduce the rate of vesicle pool depletion and short-term depression via an acceleration of vesicle recruitment. *J. Neurosci.* 26, 1366–1377. doi: 10.1523/JNEUROSCI.3889-05.2006

Moriyama, T., Higashi, T., Togashi, K., Iida, T., Segi, E., Sugimoto, Y., et al. (2005). Sensitization of TRPV1 by EP1 and IP reveals peripheral nociceptive mechanism of prostaglandins. *Mol. Pain* 1, 3. doi: 10.1186/1744-8069-1-3

Patwardhan, A. M., Akopian, A. N., Ruparel, N. B., Diogenes, A., Weintraub, S. T., Uhlson, C., et al. (2010). Heat generates oxidized linoleic acid metabolites that activate TRPV1 and produce pain in rodents. *J. Clin. Invest.* 120, 1617–1626. doi: 10.1172/JCI41678

Peters, J. H., McDougall, S. J., Fawley, J. A., and Andresen, M. C. (2011). TRPV1 Marks synaptic segregation of multiple convergent afferents at the rat medial solitary tract nucleus. *PLoS ONE* 6:e25015. doi: 10.1371/journal.pone.0025015

Peters, J. H., McDougall, S. J., Fawley, J. A., Smith, S. M., and Andresen, M. C. (2010). Primary afferent activation of thermosensitive trpv1 triggers asynchronous glutamate release at central neurons. *Neuron* 65, 657–669. doi: 10.1016/j.neuron.2010.02.017

Pingle, S. C., Matta, J. A., and Ahern, G. P. (2007). Capsaicin receptor: TRPV1 a promiscuous TRP channel. *Handb. Exp. Pharmacol.* 155–171. doi: 10.1007/978-3-540-34891-7_9

Postlethwaite, M., Hennig, M. H., Steinert, J. R., Graham, B. P., and Forsythe, I. D. (2007). Acceleration of AMPA receptor kinetics underlies temperature-dependent changes in synaptic strength at the rat calyx of Held. *J. Physiol. (Lond.)* 579, 69–84. doi: 10.1113/jphysiol.2006.123612

Premkumar, L. S., Agarwal, S., and Steffen, D. (2002). Single-channel properties of native and cloned rat vanilloid receptors. *J. Physiol. (Lond.)* 545, 107–117. doi: 10.1113/jphysiol.2002.016352

Premkumar, L. S., and Ahern, G. P. (2000). Induction of vanilloid receptor channel activity by protein kinase C. *Nature* 408, 985–990. doi: 10.1038/35050121

Shoudai, K., Peters, J. H., McDougall, S. J., Fawley, J. A., and Andresen, M. C. (2010). Thermally active TRPV1 tonically drives central spontaneous glutamate release. *J. Neurosci.* 30, 14470–14475. doi: 10.1523/JNEUROSCI.2557-10.2010

Taschenberger, H., and Gersdorff von, H. (2000). Fine-tuning an auditory synapse for speed and fidelity: developmental changes in presynaptic waveform, EPSC kinetics, and synaptic plasticity. *J. Neurosci.* 20, 9162–9173.

Terenzi, R., Romano, E., Manetti, M., Peruzzi, F., Nacci, F., Matucci-Cerinic, M., et al. (2013). Neuropeptides activate TRPV1 in rheumatoid arthritis fibroblast-like synoviocytes and foster IL-6 and IL-8 production. *Ann. Rheum. Dis.* 72, 1107–1109. doi: 10.1136/annrheumdis-2012-202846

Tominaga, M., Caterina, M. J., Malmberg, A. B., Rosen, T. A., Gilbert, H., Skinner, K., et al. (1998). The cloned capsaicin receptor integrates multiple pain-producing stimuli. *Neuron* 21, 531–543. doi: 10.1016/S0896-6273(00)80564-4

Travagli, R. A., Gillis, R. A., Rossiter, C. D., and Vicini, S. (1991). Glutamate and GABA-mediated synaptic currents in neurons of the rat dorsal motor nucleus of the vagus. *Am. J. Physiol.* 260, G531–G536.

Travagli, R. A., Hermann, G. E., Browning, K. N., and Rogers, R. C. (2006). Brainstem circuits regulating gastric function. *Annu. Rev. Physiol.* 68, 279–305. doi: 10.1146/annurev.physiol.68.040504.094635

Travagli, R. A., and Rogers, R. C. (2001). V. Fast and slow extrinsic modulation of dorsal vagal complex circuits. *Am. J. Physiol. Gastrointest. Liver Physiol.* 281, G595–G601.

Venkatachalam, K., and Montell, C. (2007). TRP Channels. *Annu. Rev. Biochem.* 76, 387–417. doi: 10.1146/annurev.biochem.75.103004.142819

Voets, T., Droogmans, G., Wissenbach, U., Janssens, A., Flockerzi, V., and Nilius, B. (2004). The principle of temperature-dependent gating in cold- and heat-sensitive TRP channels. *Nature* 430, 748–754. doi: 10.1038/nature02732

Wall, M. J. M., Robert, A. A., Howe, J. R. J., and Usowicz, M. M. M. (2002). The speeding of EPSC kinetics during maturation of a central synapse. *Eur. J. Neurosci.* 15, 785–797. doi: 10.1046/j.1460-9568.2002.01910.x

Yao, J., Liu, B., and Qin, F. (2010). Kinetic and energetic analysis of thermally activated TRPV1 Channels. *Biophys. J.* 99, 1743–1753. doi: 10.1016/j.bpj.2010.07.022

Zsombok, A., Bhaskaran, M. D., Gao, H., Derbenev, A. V., and Smith, B. N. (2011a). Functional plasticity of central TRPV1 receptors in brainstem dorsal vagal complex circuits of streptozotocin-treated hyperglycemic mice. *J. Neurosci.* 31, 14024–14031. doi: 10.1523/JNEUROSCI.2081-11.2011

Zsombok, A., Gao, H., Miyata, K., Issa, A., and Derbenev, A. V. (2011b). Immunohistochemical localization of transient receptor potential vanilloid type 1 and insulin receptor substrate 2 and their co-localization with liver-related neurons in the hypothalamus and brainstem. *Brain Res.* 1398, 30–39. doi: 10.1016/j.brainres.2011.04.048

Zygmunt, P. M., Petersson, J., Andersson, D. A., Chuang, H., Sørgård, M., Di Marzo, V., et al. (1999). Vanilloid receptors on sensory nerves mediate the vasodilator action of anandamide. *Nature* 400, 452–457. doi: 10.1038/22761

Conflict of Interest Statement: The authors declare that the research was conducted in the absence of any commercial or financial relationships that could be construed as a potential conflict of interest.

Received: 30 September 2013; accepted: 26 November 2013; published online: 13 December 2013.

Citation: Anwar IJ and Derbenev AV (2013) TRPV1-dependent regulation of synaptic activity in the mouse dorsal motor nucleus of the vagus nerve. Front. Neurosci. 7:238. doi: 10.3389/fnins.2013.00238

This article was submitted to Autonomic Neuroscience, a section of the journal Frontiers in Neuroscience.

frontiers in
NEUROSCIENCE

ORIGINAL RESEARCH ARTICLE
published: 08 August 2014
doi: 10.3389/fnins.2014.00232

Leptin into the rostral ventral lateral medulla (RVLM) augments renal sympathetic nerve activity and blood pressure

Maria J. Barnes[1]* and David H. McDougal[2]

[1] *Nutrition and Neural Signaling Laboratory, Pennington Biomedical Research Center, Baton Rouge, LA, USA*
[2] *Neurobiology of Metabolic Dysfunction Laboratory, Pennington Biomedical Research Center, Baton Rouge, LA, USA*

Edited by:
Andrea Zsombok, Tulane University, USA

Reviewed by:
Kirsteen Browning, Penn State College of Medicine, USA
Alexandre A. Silva, University of Mississippi Medical Center, USA

****Correspondence:***
Maria J. Barnes, Nutrition and Neural Signaling Laboratory, Pennington Biomedical Research Center, 6400 Perkins Road, Baton Rouge, LA 70808, USA
e-mail: maria.barnes@pbrc.edu

Leptin is a hormone released from adipose tissue. While this hormone normally acts to reduce feeding behavior and increase energy expenditure, in obesity, resistance to these effects occurs even though the hormone is released in large amounts. Although leptin no longer works to suppress feeding in the obese, leptin retains its potent effects on other autonomic functions such as blood pressure regulation. Leptin has been associated with hypertension and increased sympathetic autonomic activity. Therefore, leptin is emerging as a major contributor to the hypertensive state observed in obesity. Sympathetic control of blood pressure is maintained principally by autonomic reflex control circuits in the caudal brainstem. The rostral ventral-lateral medulla (RVLM) is the primary regulator of the sympathetic nervous system, sending excitatory fibers to sympathetic preganglionic neurons to regulate sympathetic control over resistance vessels and blood pressure. Previous studies from our laboratory have shown that neurons in the ventral lateral medulla express leptin receptors (ObRb). Our present study using pseudo-rabies multi-synaptic retrograde tract tracing and immunohistochemical methods revealed that neurons within the RVLM that send sympathetic projections to the kidney express leptin receptors. Acute microinjection of leptin (1 and 3 μg; 40 nL) into the RVLM evoked a significant increase in Mean Arterial Pressure (MAP) and renal sympathetic nerve activity (RSNA). When the 3 μg dose of leptin was preceded with a leptin antagonist, (SLAN-4; 1 ng), it attenuated the cardiovascular response of leptin. Taken together, these data suggest that leptin's actions within the RVLM may influence blood pressure and renal sympathetic nerve activity.

Keywords: leptin, renal sympathetic nerve activity, blood pressure, rostral ventral lateral medulla, neurons

INTRODUCTION

Leptin is an adipocyte-derived hormone which signals the availability of peripheral energy stores. Circulating leptin levels act as a long term signal of the amount of fat stored in white adipose tissue, while short term fluctuations in leptin levels convey information regarding acute changes in caloric intake. This information is integrated centrally by the autonomic nervous system to regulate a variety of homeostatic functions, most notably food intake and energy expenditure (Morris and Rui, 2009; Myers et al., 2009; Galic et al., 2010; Kelesidis et al., 2010). One mechanism by which leptin affects energy expenditure is by increasing sympathetic tone (Eikelis et al., 2003; Morris and Rui, 2009; Myers et al., 2009).

This increase of sympathetic outflow can produce profound effects on various homeostatic functions including the modulation of cardiovascular dynamics such as arterial blood pressure (Friedman, 2002; Correia and Rahmouni, 2006). Leptin also regulates blood pressure via augmentation of renal sympathetic nerve activity (RSNA); events which are believed to play a significant role in the development of hypertension (Hall et al., 2010). This change in RSNA and blood pressure after leptin administration is absent in experimental animals that have defective leptin receptors (i.e., Zucker Rats and db/db mice), suggesting that these effects are leptin receptor mediated (Haynes et al., 1997; Rahmouni et al., 2003).

The majority of leptin signaling studies have been conducted in the hypothalamus, and acute administration of leptin into regions of the hypothalamus associated with control of cardiovascular functions has been shown to increase RSNA and blood pressure (Marsh et al., 2003; Shih et al., 2003; Rahmouni and Morgan, 2007). However, the long form of the leptin receptor (ObRb) is located throughout the central nervous system (Patterson et al., 2011), and there is growing evidence that extrahypothalamic leptin signaling plays a critical role in autonomic regulation (Myers et al., 2009). In fact, the caudal hindbrain, which contains several populations of preautonomic neurons, may be a critical site for mediating leptin's effect on sympathetic outflow (Grill and Kaplan, 2002; Grill, 2010). For example, acute injection of leptin into the nucleus of the solitary tract (NST), located in the dorsal hindbrain, has been shown to increase RSNA (Mark et al., 2009; Ciriello and Moreau, 2013).

The rostral ventral lateral medulla (RVLM), located within the hindbrain, contains neurons which play a key role in determining peripheral sympathetic vasomotor tone and blood pressure (Guyenet, 2006). The RVLM integrates multiple descending and cervical-thoracic (barosensor) inputs regulating sympathetic outflow. The RVLM is a "pre-sympathetic" structure in that it sends axons to the intermediolateral cell column; the source of sympathetic preganglionic neurons. Our laboratory reported that leptin receptors are expressed by adrenergic/noradrenergic C1/A1 cells located in the ventrolateral medulla (Barnes et al., 2010), which overlaps the RVLM. Therefore, the possibility exists that preautonomic blood pressure neurons in the RVLM may express leptin receptors and that leptin may regulate blood pressure and RSNA directly by increasing the activity of these neurons. The present study was conducted to determine if RVLM neurons projecting through multi-synaptic pathways to the kidney indeed express leptin receptors and whether acute administration of leptin into the RVLM influences RSNA as well as cardiovascular dynamics.

MATERIALS AND METHODS

ANIMALS

Male Long Evan rats (8–10 weeks old) obtained from Charles Rivers were used in these studies. All animals were maintained in a room with a 12:12 light-dark cycle with constant temperature and humidity, and given food and water *ad libitum*. All experimental protocols were performed according to the guidelines set forth by the National Institutes of Health and were approved by the Institutional Animal Care and Use Committees at the Pennington Biomedical Research Center.

PSEUDO RABIES VIRUS INJECTIONS

Co-localization of ObRb on RVLM neurons with projections to the kidney

Long Evans rats ($n = 5$) were anesthetized with a ketamine (90 mg/kg) and xylazine (9 mg/kg) cocktail. Using aseptic technique, a flank incision was made to expose the left kidney. Animals received two injections (2 μl each) of pseudo rabies virus 152 (PRV), green fluorescent trans-neuronal tracer virus, into the cortex of the kidney using a Hamilton syringe. The injection site was immediately sealed with liquid bandage (Thermo Fisher Scientific, Pittsburgh PA). The kidney was returned into its appropriate position; overlying skin was sutured with Vicryl and the animal was returned to its home cage for recovery. Four (4) days after the injection, animals were anesthetized with urethane (1 mg/kg) and transcardially perfused with 0.1 M Phosphate-Buffered Saline (PBS) followed by 4% paraformaldehyde. Brains were removed and processed for immunohistochemical demonstration of trans-neuronal tract-tracing and leptin receptor expression.

IMMUNOHISTOCHEMISTRY

The hindbrain was cut into 30 micron thick sections on a freezing microtome, washed three times with 0.1 M PBS, placed in a blocking solution of 10% goat serum (Jackson ImmunoResearch, West Grove PA) containing 0.3% Triton X-100 (Sigma Aldrich, Saint Louis, MO) for 60 min and incubated for 72 h at 4°C in the primary antibody, chicken anti-ObRb [(1:50) (Neuromics, Edina MN)]. Sections were then washed three times with 0.1 M PBS followed by 60 min incubation in Alexa 594 goat anti-chicken antibody [(1:100) (Invitrogen, Grand Island NY)] followed by three rinses with 0.1 M PBS prior to being mounted on slides with ProLong Gold anti-fade reagent (Invitrogen, Grand Island NY). No additional immunohistochemical processing was necessary to visualize the green fluorescent protein expression induced by our PRV injections. Note that heat-induced antigen retrieval method used in our previous studies of leptin receptor expression in the hindbrain (Barnes et al., 2010) led to quenching of the green fluorescent signal induced via our renal injections of PRV. Therefore, comparable ObRb staining was accomplished by both increasing the concentration of the primary antibody to 1:50 and increasing the incubation time from 12 to 72 h, as described above.

QUANTIFICATION OF IMMUNOHISTORY

Histological sections containing the majority of the anterior to posterior extent of the hindbrain [(9–14.5 mm post Bregma); (Paxinos and Watson, 2007)] were examined for evidence of PRV and ObRb positive cell bodies in the ventral half of the hindbrain. Sections were visualized with an Axioplan 2 upright microscope (Carl Zeiss Microscopy, Thornwood, NY) equipped with a Lambda LS 175W Xenon arc lamp. A FITC filter set (EX HQ487/25, EM GQ535/40, D Q505lp) was used to visualize the green PRV staining, while a CY3 filter set (EX HQ535/50, EM HQ610/75, D Q565lp) was used to visualize the ObRb staining. Images of positive staining were captured using a CoolSnap HQ CCD camera (Photometrics, Tucson, AZ). Slidebook Software (v2.0; Intelligent Imaging Innovations, Denver CO) was used to generate two dimensional montages of the entire ventral hindbrain of each section which demonstrated positive staining using a Plan Apochromat 20×/0.75 NA objective (Carl Zeiss Microscopy, Thornwood, NY). The numbers of PRV and ObRb positive cells within hindbrain nuclei, as well as the numbers of double labeled cells in each image were quantified.

PHYSIOLOGICAL EFFECTS OF LEPTIN INJECTION INTO RVLM

Measurement of renal sympathetic nerve activity and blood pressure

Male Long Evan rats ($n = 6$ per group) were anesthetized with long acting thiobutabarbital (inactin) [(150 mg/kg); (Sigma Aldrich, St. Louis, MO)] which has minimal interference with autonomic reflexes (Buelke-Sam et al., 1978). Using aseptic techniques, a trachea tube was inserted to allow the airway of the animal to remain patent. The left femoral artery was catheterized with PE 20 tubing attached to an AD Instrument transducer for measurement of blood pressure with a PowerLab data acquisition system (AD Instruments, Colorado Springs, CO). The animals were placed in a stereotaxic frame; the occipital plate was removed to expose the hindbrain. A flank incision was made to expose the right kidney and the renal nerve. The renal nerve was separated from the renal vein and renal artery, placed on bipolar platinum-iridium electrodes (A-M Systems, Carlsborg WA) and secured with kwik cast gel (World Precision Instruments, Sarasota, FL). Renal sympathetic nerve activity (RSNA) and mean arterial pressure (MAP) and heart rate (HR) were monitored continuously. Once preparatory surgery and instrumentation was completed,

animals were allowed to stabilize for 60 min. A triple barrel glass micropipette (total tip diameter was 150 micron) containing glutamate [(10 mM); (Sigma Aldrich, St. Louis, MO)], saline (0.9%), leptin [(0.3, 1, or 3 μg); (Peprotech, Rocky Hill, NJ)] or a superactive rat leptin antagonist [(1 ng); (SLAN-4); (Shpilman et al., 2011; Gertler and Elinav, 2014); (Protein Laboratories Rehovot)] was lowered into the RVLM at the following coordinates relative to the calamus scriptorius (2.9 mm rostral, 1.9 mm lateral, 2.7 mm ventral). Confirmation of pipette location was accomplished with nano-injections of glutamate (40 nL, 10 mM), as described by Goodchild et al. (1982), which elicited rapid increases in blood pressure. Similar techniques have been used in previous investigations of the RVLM in regulation of autonomic function (e.g., Adams et al., 2007). After confirmation of the injection site via glutamate, animals were allowed to recover for 30 min prior to the start of the experiment. Each animal served as its own control.

Triple barrel pipettes were filled and administered (40 nL) accordingly: glutamate (10 mM)—0.9% saline—leptin (0.3 μg); glutamate—saline—leptin (1 μg); glutamate—saline—leptin (3 μg); glutamate—saline—SLAN-4 (1 ng); glutamate—SLAN-4—leptin (3 μg); glutamate—saline—Chicago Blue.

STATISTICS

Physiological experiments

Each animal served as its own control. MAP and RSNA were monitored continuously throughout the experiment; measurement of these parameters was analyzed at 4 min intervals. Time course response of MAP is shown in **Figures 4A**, **5A** as a percent change from baseline. Statistical analysis of mean MAPs before and after the first CNS injection were not significantly different (data not shown); therefore, "baseline" mean MAP for each animal was defined as that value at time −15 min. Changes in MAP and RSNA occurring after the second CNS injection were statistically analyzed across all groups.

Raw RSNA was corrected by subtraction of background noise as determined at the termination of the experiment. These corrected values were used to determine the percent change of RSNA from baseline (i.e., mean corrected values obtained 15 min following the first injection). Analysis of the peak MAP responses and RSNA were made using One-Way ANOVA followed by Bonferroni *post-hoc* multiple comparison tests. Statistics were performed using GraphPad Prism Version 5.01 (LaJolla CA). All values are expressed as mean ± s.e.m. p-value < 0.05 was considered statistically significant.

RESULTS

HISTOLOGY

ObRb positive cells in the ventral medulla were found in the C1/A1 cell group and the ventromedial region

Cells in the ventral hindbrain that were positive for ObRb staining (i.e., expressed leptin receptors) were localized in one of four regions: the C1/A1 cell column, ventromedial medulla (VMM), caudal raphe, and A5 cell group. The ObRb staining in the C1/A1, caudal raphe, and A5 was quite distinct and easily assigned to these medullary nuclei based on Paxinos and Watson (2007) (**Figure 1**). In contrast, the staining in the VMM was diffuse and often overlapped adjacent nuclei such as the paragigantocellular nuclear subdivisions, the reticular nucleus subdivisions, and the inferior olive (**Figure 2A**). ObRb positive cells ($ObRb^+$) were defined as those cells which displayed extensive cytoplasmic ObRb staining (see insets of **Figures 1**, **2C**), as opposed to cells which merely displayed isolated ObRb punctate staining. An average of 420 ± 87 $ObRb^+$ cells were observed in C1/A1, 146 ± 32 $ObRb^+$ cells were observed in VMM, 107 ± 87 $ObRb^+$ cells were observed in A5, and 26 ± 14 $ObRb^+$ cells were observed in the caudal raphe (**Table 1**).

Pseudo rabies (PRV) positive neurons identified in the ventral hindbrain after injection in the cortex of the left kidney

Our PRV kidney injection paradigm labeled cells in C1/A1, VMM, caudal raphe and A5 (**Figure 2**). An average of 88 ± 30 PRV^+ cells were observed in C1/A1, 113 ± 81 PRV^+ cells were observed in VMM, 35 ± 21 PRV^+ cells were observed in A5, and 73 ± 42 PRV^+ cells were observed in the caudal raphe (**Table 1**). PRV^+ cells in C1/A1 were concentrated in the rostral portion of the cell column, consistent with specific labeling of RVLM neurons. There were no differences in the number of PRV^+ cell on the contralateral and ipsilateral hemispheres relative to the site of renal injection. These results confirm a number of previous studies which employed PRV injection into the renal cortex (Schramm et al., 1993; Huang and Weiss, 1999; Sly et al., 1999; Weiss et al., 2001), as well as studies employing PRV injected into organs which receive substantial sympathetic inputs (Strack et al., 1989a,b; Sved et al., 2001).

A subset of hindbrain neurons projecting through multi-synaptic pathways to the kidney expressed ObRb

A subset of PRV labeled neurons within the hindbrain were also leptin receptor expressing cells (**Figure 2**). An average of 59 ± 19 double labeled cells were observed in C1/A1, 50 ± 38 double labeled cells were observed in VMM, 30 ± 19 double labeled cells were observed in A5, and 16 ± 12 double labeled cells were observed in the caudal raphe. Thus, approximately 67% of C1/A1 cells that were PRV+ also expressed leptin receptors compared to 45% in VMM, 22% in caudel raphe and 85% of all PVR^+ cells in A5 (**Table 1**).

PHYSIOLOGY

RVLM identified by nano-injection of glutamate

RVLM neurons were identified by nano-injection of glutamate which elicited a minimum increase of 15 mmHg in blood pressure within 15 s (**Figure 3**) and an increase in RSNA which preceded the change in blood pressure (**Figures 3B,C**). The effect of glutamate on blood pressure and RSNA had a short duration; all parameters returned to baseline within 15 min. At the conclusion of the experiments, a subset of animals was injected with Chicago Blue to further verify the location of the injection site (**Figure 3A**).

Microinjection of leptin into the RVLM produced an increase in mean arterial pressure (MAP) and renal sympathetic nerve activity (RSNA)

Long Evan rats received one of three doses of leptin into the RVLM to observe the effect on MAP and RSNA (**Figure 4**). **Figure 4A** displays the percent change in MAP over time in

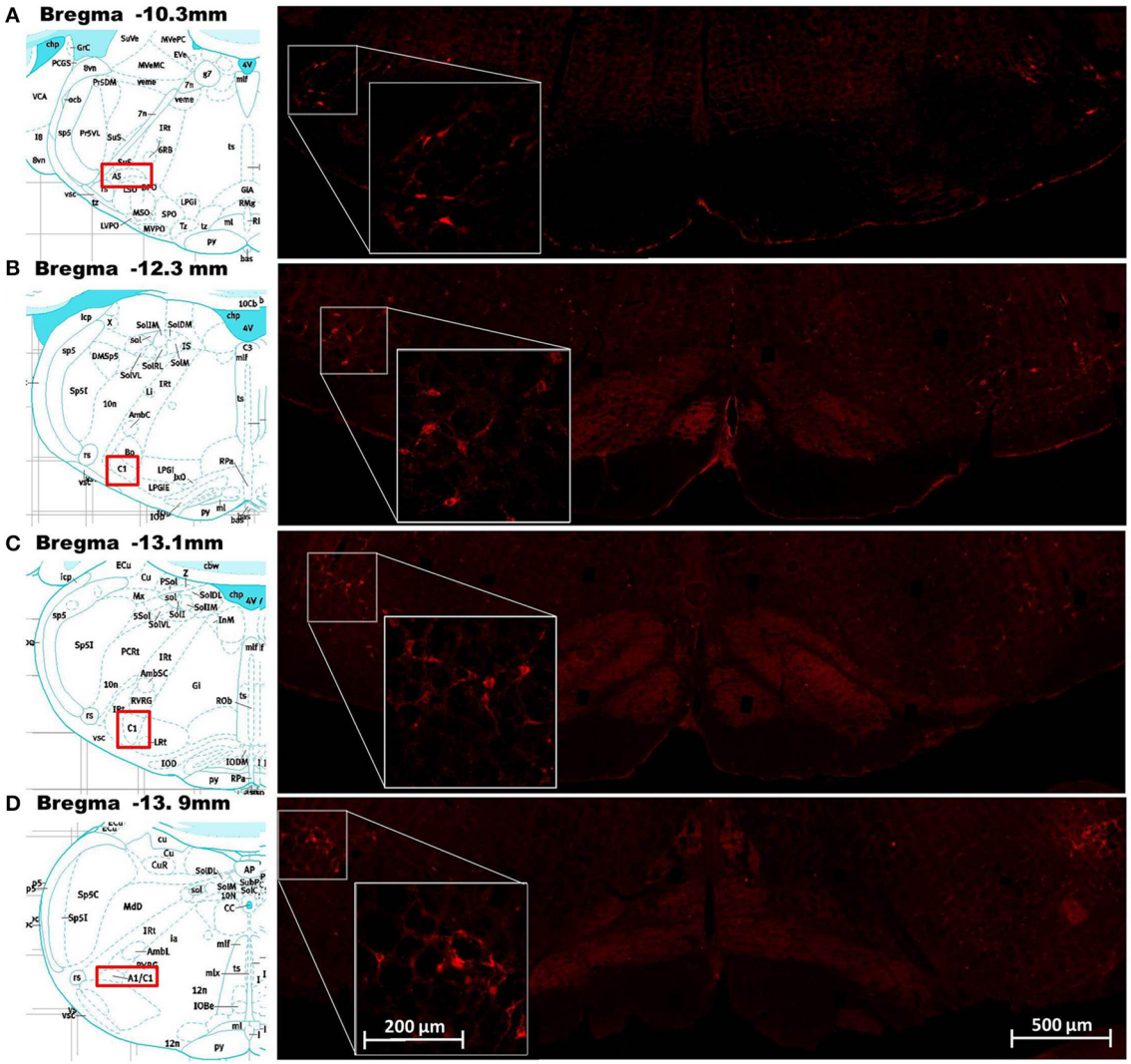

FIGURE 1 | Demonstration of leptin receptor (ObRb) positive cells at various points along the rostrocaudal axis of the ventral hindbrain. Images in the right column show corresponding histological staining for ObRb (red labeled cells) in the ventral hindbrain at the level of the A5 cell group **(A)**, RVLM **(B)**, C1 cell group **(C)**, and A1 cell group **(D)**. Insets on the right column show histological staining of ObRb at higher magnification in order to show cellular detail. The A5, RVLM, and C1/A1 cell groups described by Paxinos and Watson (2007) are represented in the pictographs, reprinted with permission, in the left column. Scale bars = 200 microns (insets) and 500 microns.

response to saline, 0.3, 1, or 3 µg of leptin injected into the RVLM. Analysis of percent change in MAP was conducted with one-way ANOVA which compared the MAP at 12 min following injection between each experimental condition (**Figure 4B**). In response to leptin (1 and 3 µg) MAP increased 8.3 ± 2.9% and 7.6 ± 2.1% respectively. The MAP response to these treatments was significantly different from saline (−1.7 ± 1.6%) and leptin (0.3 µg) (−2.4 ± 1.0%) [$F_{(3,\ 14)} = 8.019$; $p < 0.05$]. One-way analysis of MAP prior to and following the first injection (saline) was not statistically different (data not shown).

A One-Way ANOVA was also conducted to compare the effect of each treatment on the percent change of RSNA. There was a significant effect [$F_{(3,\ 24)} = 7.493$; $p < 0.05$] of leptin (1 and 3 µg) on the percent change of RSNA when compared to saline and leptin (0.3 µg). Leptin (1 and 3 µg) increased RSNA 49 and 34% respectively, whereas saline changed RSNA 1% and leptin (0.3 µg) caused a 12% increase.

Microinjection of rat superactive leptin antagonist (SLAN-4) eliminates leptin-induced increases in MAP and RSNA

The role of leptin receptors within the RVLM as it relates to cardiovascular parameters was assessed using the rat superactive leptin antagonist, SLAN-4. The time course response of MAP after administering leptin and SLAN-4 into the RVLM is presented in **Figure 5A**. A One-Way ANOVA of peak responses measured at 12 min following the second injection demonstrated a statistically significant effect of treatment [$F_{(3,\ 16)} = 16.64$; $p < 0.05$]. Leptin (3 µg) administration resulted in a 7.6 ± 2.1%

increase in MAP while SLAN-4 alone resulted in a 3.6 ± 0.8% decrease at the same time point. When SLAN-4 was administered into the RVLM prior to leptin (3 μg), leptin administration failed to produce an increase in MAP, and a decrease of 3.2 ± 0.6% was observed. 12 min following the second injection, the MAP responses to leptin (3 μg) alone was significantly different from the response to saline, SLAN-4, and SLAN-4 plus leptin (3 μg). The MAP response to SLAN-4 alone and SLAN-4 plus leptin (3 μg) were not significantly different from saline (Bonferroni *post-hoc t*-tests; $p < 0.05$) (**Figure 5B**). A One-Way ANOVA of percent change in RNSA across treatment was statistically significant [$F_{(3,\ 19)} = 8.288$; $p < 0.05$]. Following saline injection, leptin (3 μg) administration resulted in a 34% increase in RNSA while SLAN-4 resulted in a 20% decrease. When SLAN-4 was administered into the RVLM prior to leptin (3 μg), a 13% decrease in RNSA was observed. The change in RNSA in response to leptin (3 μg), SLAN-4, and SLAN-4 plus leptin (3 μg), were all significantly different from saline control injections (Bonferroni *post-hoc t*-tests; $p < 0.05$) (**Figure 5C**).

DISCUSSION

Our previous work demonstrated the presence of leptin receptor (ObRb) staining on tyrosine hydroxylase positive neurons in the medulla which make up the C1/A1 cell group (Barnes et al., 2010). The current report has built on this observation and further quantified the relative distribution of leptin receptor positive ($ObRb^+$) cells in various nuclei of the ventral medulla. We have demonstrated that the vast majority of $ObRb^+$ cells are present in C1/A1 cell column and this staining extends along the complete anterior to posterior extent of this cell group (**Figure 1**; **Table 1**). Several $ObRb^+$ cells were also observed in the caudal raphe, but the relative number of cells present was minor in comparison to C1/A1 cell group. Furthermore, through the use of PRV, a polysynaptic retrograde tracer, we demonstrated that a substantial subpopulation of neurons that express leptin receptors (ObRb) projects to the kidney. We determined that a large percentage of kidney projecting neurons in both the C1/A1 cell group and the A5 cell group express ObRb, approximately 67 and 85% respectively. We quantified additional neurons that had leptin receptors and projected to the kidney in the VMM and caudal raphe, approximately 45 and 22% respectively (**Table 1**).

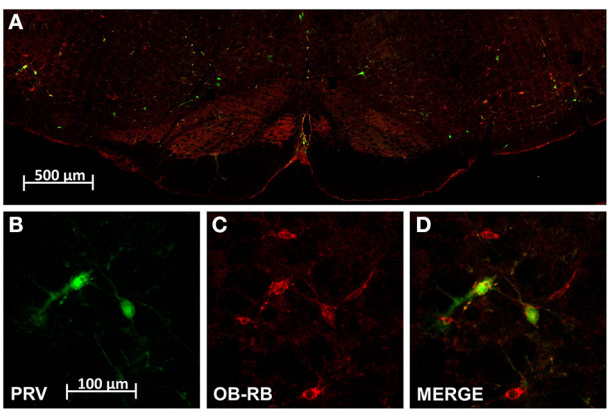

FIGURE 2 | Dual localization of leptin receptors (ObRb; red) and pseudo rabies virus infected cells (PRV; green) resulting from renal PRV injection. (A) Is a low power montage of the complete ventral half of the medulla at the level of the RVLM. **(B–D)** Are high magnification of cell cluster in left RVLM shown in **(A)** demonstrating PRV positive RVLM neurons **(B)**, ObRb expressing RVLM neurons **(C)**, and double labeled RVLM neurons **(D)**. Scale bar = 100 microns.

As stated previously, the labeling pattern resulting from our renal PRV injections is consistent with a number of previous studies utilizing the same or similar techniques (Strack et al., 1989a; Schramm et al., 1993; Huang and Weiss, 1999; Sly et al., 1999; Weiss et al., 2001). Injections of trans-neuronal tract tracing into the cortex of the kidney have been consistently shown to retrogradely label hindbrain neurons within the RVLM, VMM, A5 cell group, and the caudal raphe. However, our observation that significant subsets of these labeled neurons are $ObRb^+$ is completely novel. Previous studies investigating the phenotype of kidney projecting hindbrain neurons have reported that a subpopulation of these cells express tyrosine hydroxylase (TH), phenylethanolamine-N-methyltransferase (PNMT) and/or 5-hydroxytryptamine (5-HT), i.e., are catecholaminergic, noradrenergic, or serotonergic neurons (Huang and Weiss, 1999). Additionally, it has been shown that a small subset (<15%) of neurons in the ventral hindbrain that projects to the kidney express nitric oxide synthase (nNOS). Further studies will be needed to identify which of these neuronal subpopulations also express ObRb.

Microinjection of leptin into the RVLM, the rostral most subdivision of the C1/A1 which houses neurons associated with control of vasomotor tone and blood pressure (Pilowsky and Goodchild, 2002; Guyenet, 2006), caused an increase in both MAP, approximately 9 mmHg, and RSNA, approximately 50%. Furthermore, when microinjection of leptin (3 μg) was preceded by focal administration of the leptin antagonist, SLAN-4 (1 ng), this leptin mediated cardiovascular response was eliminated. In

Table 1 | Distribution of leptin receptor (ObRb) expressing and psuedorabies virus (PRV) infected cells in the ventral hindbrain (mean ± s.e.m., *n* = 5).

Hindbrain region	Number of ObRb positive cells	Number of PRV infected cells	Number of double labeled cells	% of PRV cells positive for ObRb
A5	107 ± 11	35 ± 21	30 ± 19	85 ± 4
C1/A1	420 ± 87	88 ± 30	59 ± 19	67 ± 2
VMM	146 ± 32	113 ± 81	50 ± 38	45 ± 7
Caudal raphe	26 ± 14	73 ± 42	16 ± 12	22 ± 13

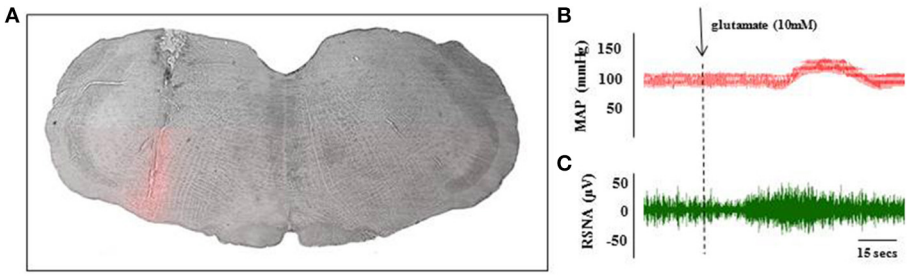

FIGURE 3 | Histological and physiological verification of RVLM injection site. A subset of animals received Chicago Blue injection at the end of the glutamate identification procedure to verify histological placement of pipette. Coronal sections through the hindbrain were used to identify the injection site at the level of the RVLM **(A)**. Scale bar = 500 microns. Microinjection of glutamate (10 mM; 40 nL) into the RVLM evoked transient increase in MAP **(B)** and renal sympathetic nerve activity **(C)** within 30 s of injection. These parameters returned to baseline levels within 15 min of the injection.

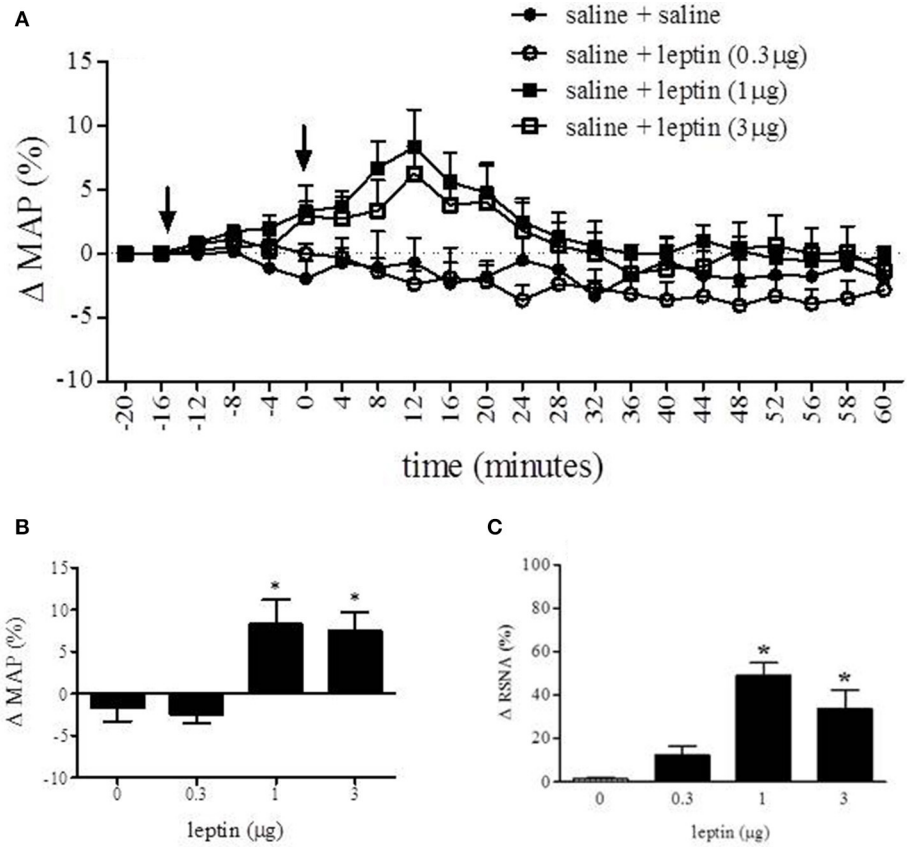

FIGURE 4 | Nano-injection of leptin into the RVLM increased MAP and RSNA. Nano-injection of leptin (1 and 3 μg; 40 nL) into the RVLM increased MAP **(A)**. Analysis of percent change in MAP was conducted with One-Way ANOVA which compared the MAP at 12 min following injection between each experimental condition **(B)**. Peak response of leptin (1 and 3 μg) was 8.9 ± 2.9% and 7.6 ± 2.1% respectively. The MAP response to these treatments was significantly different from saline (−1.6 ± 1.6%) and leptin (0.3 μg) (−2.4 ± 1.0%). Leptin (1 and 3 μg) increased RSNA **(C)** 49 and 34%, respectively. (Bonferroni *t*-tests; $*p < 0.05$); arrows indicate time of first (−15 min) and second (0 min) injection. Analysis of percent change following the first inject was not statistically different from values obtained prior to the first injection.

addition, microinjection of SLAN-4 into the RVLM, with or without leptin co-administration, caused a significant reduction in RSNA, approximately 13 and 20% respectively. The response produced by the highly specific leptin antagonist, SLAN-4, alone suggests that leptin receptor activation in the RVLM has an effect on tonic RSNA activity. These data are the first demonstration that neurons within the RVLM express functional leptin receptors and can respond to leptin by increasing RSNA and mean arterial blood pressure. Taken together, our results suggest that leptin may regulate renal sympathetic tone and ultimately

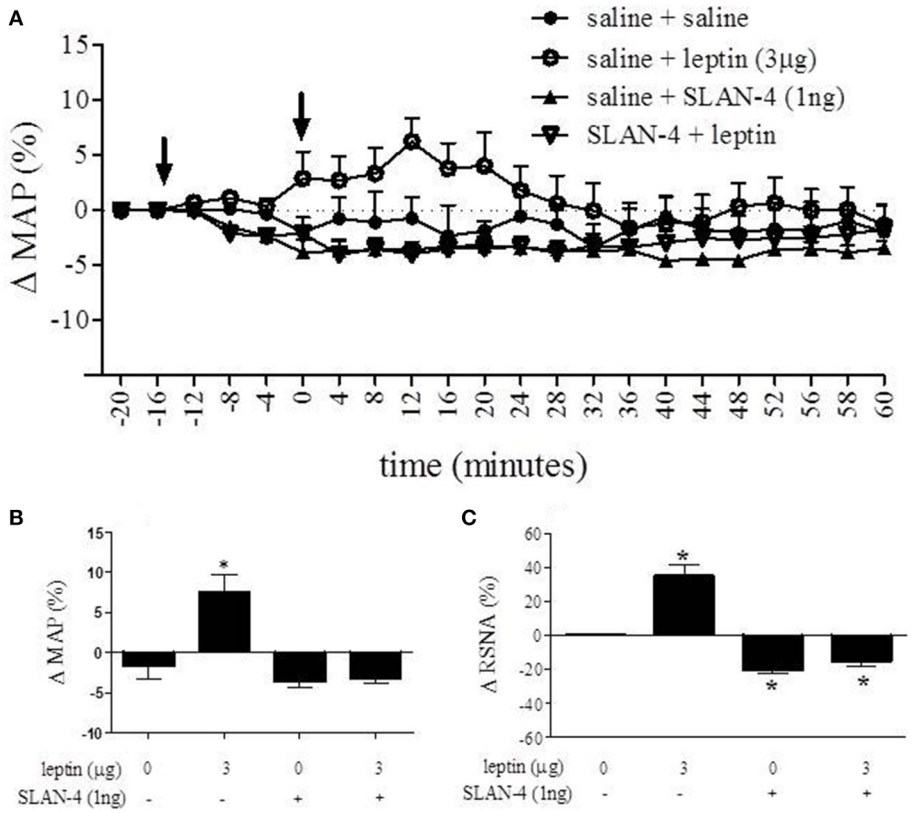

FIGURE 5 | Nano-injection of rat superactive leptin antagonist (SLAN-4) attenuated the leptin-induced increase in MAP and RSNA and decreased basal RSNA. Time course response of MAP after administering leptin and SLAN-4 into the RVLM is presented in **(A)**. 12 min following the second injection, MAP was increased following saline + leptin relative to saline + saline controls, while saline + SLAN-4 and SLAN-4 + leptin treatment did not significantly alter MAP relative to saline + saline treatment **(B)**. In contrast, saline + leptin treatment caused a significant increase in RNSA, while saline + SLAN-4 and SLAN-4 + leptin treatment caused a significant decrease in RNSA relative to saline + saline controls. **(C)** (Bonferroni *t*-tests; $^*p < 0.05$).

blood pressure by modulating the activity of neurons within the RVLM.

Leptin's influence on cardiovascular dynamics is well established. Intracerebroventricular (ICV) injection of leptin has been shown to increase RSNA and/or MAP in a variety of animal models (Dunbar et al., 1997; Casto et al., 1998; Matsumura et al., 2000; Rahmouni et al., 2003; Rahmouni and Morgan, 2007; Prior et al., 2010). Furthermore, direct microinjection of leptin into discrete hypothalamic nuclei (i.e., ventromedial, dorsomedial, arcuate, and paraventricular nuclei) and the nucleus of the solitary tract (NTS), leads to increases in MAP and RSNA (Marsh et al., 2003; Shih et al., 2003; Montanaro et al., 2005; Rahmouni and Morgan, 2007; Mark et al., 2009; Ciriello and Moreau, 2012). In the majority of these studies, changes in both MAP and RSNA were observed with peak changes observed at approximately 15–25 min post injection. These response dynamics were similar to those observed in the present study (see **Figures 4A**, **5A**). The magnitude of our observed leptin induced changes in MAP were also similar to the above microinjection studies which reported changes in MAP from approximately 8 (Marsh et al., 2003) to 17 mmHg (Shih et al., 2003; Rahmouni and Morgan, 2007), with the exception of Ciriello and Moreau (2012), which reported a maximum increase of approximately 32 mmHg following microinjection into the NTS. In contrast, our leptin mediated increases in RSNA were slightly less than that reported in other microinjection studies, which ranged from approximately 65% (Ciriello and Moreau, 2012) to 110% (Mark et al., 2009). Furthermore, the dose of leptin required for maximal response in both MAP and RSNA in the current study (1 μg) was similar to that reported by Mark et al. (2009) in the NTS, but greater than that required by Ciriello and Moreau (2012) in the NTS (0.1 μg) and other studies utilizing microinjection of leptin (0.02–0.5 μg) in hypothalamic nuclei (Marsh et al., 2003; Shih et al., 2003; Rahmouni and Morgan, 2007). These differences may be caused by the reduced density of ObRb receptors in the RVLM (see **Figure 1**) relative to NTS (e.g., Barnes et al., 2010) and the hypothalamus (e.g., Zhang et al., 2011).

One of the most intriguing finding in the present study is that pharmacological blockade of leptin receptor signaling in the RVLM via the newly developed leptin antagonist, SLAN-4, lead to decreased MAP and RSNA. SLAN-4 is a rat superactive leptin antagonist with similar properties to the recently developed mouse superactive leptin antagonist (Shpilman et al., 2011). These mutated leptin molecules have been shown to have potent effects on feeding and body weight *in vivo* (Elinav et al., 2009; Shpilman et al., 2011; Chapnik et al., 2013). These data provides

further support to the role of leptin in regulating cardiovascular parameters. Indeed, administering leptin results in a significant increase in blood pressure and renal sympathetic activity. Taken together, our findings suggest that endogenous leptin may act locally at the level of the RVLM to influence blood pressure in the normotensive state.

AUTHOR CONTRIBUTIONS

Maria J. Barnes and David H. McDougal were involved in the study concept and design, performing the experiments, acquisition, analysis and interpretation of data, and drafting of the manuscript.

GRANT SUPPORT

Research reported in this publication was supported by: The National Institute of Diabetes and Digestive and Kidney Diseases under Award Number K01DK078588, the National Institute of Neurological Disorders and Stroke under Award Number NS55866 and National Institute of General Medical Sciences under Award Number GM103528 of the National Institutes of Health. This work used the facilities of the Pennington Cell Biology and Bioimaging Core, which is supported in part by COBRE (NIH 8 P20 GM103528) and NORC (NIH 2P30DK072476) center grants from the National Institutes of Health.

ACKNOWLEDGMENTS

The authors would like to thank Dr. Christopher Morrison for graciously providing the 152 green fluorescent trans-neuronal tracer pseudo rabies virus.

REFERENCES

Adams, J. M., Madden, C. J., Sved, A. F., and Stocker, S. D. (2007). Increased dietary salt enhances sympathoexcitatory and sympathoinhibitory responses from the rostral ventrolateral medulla. *Hypertension* 50, 354–359. doi: 10.1161/HYPERTENSIONAHA.107.09184

Barnes, M. J., Rogers, R. C., Van Meter, M. J., and Hermann, G. E. (2010). Co-localization of TRHR1 and LepRb receptors on neurons in the hindbrain of the rat. *Brain Res.* 1355, 70–85. doi: 10.1016/j.brainres.2010.07.094

Buelke-Sam, J., Holson, J. F., Bazare, J. J., and Young, J. F. (1978). Comparative stability of physiological parameters during sustained anesthesia in rats. *Lab. Anim. Sci.* 28, 157–162.

Casto, R. M., Vanness, J. M., and Overton, J. M. (1998). Effects of central leptin administration on blood pressure in normotensive rats. *Neurosci. Lett.* 246, 29–32. doi: 10.1016/S0304-3940(98)00223-7

Chapnik, N., Solomon, G., Genzer, Y., Miskin, R., Gertler, A., and Froy, O. (2013). A superactive leptin antagonist alters metabolism and locomotion in high-leptin mice. *J. Endocrinol.* 217, 283–290. doi: 10.1530/JOE-13-0033

Ciriello, J., and Moreau, J. M. (2012). Leptin signaling in the nucleus of the solitary tract alters the cardiovascular responses to activation of the chemoreceptor reflex. *Am. J. Physiol. Regul. Integr. Comp. Physiol.* 303, R727–R736. doi: 10.1152/ajpregu.00068.2012

Ciriello, J., and Moreau, J. M. (2013). Systemic administration of leptin potentiates the response of neurons in the nucleus of the solitary tract to chemoreceptor activation in the rat. *Neuroscience* 229, 88–99. doi: 10.1016/j.neuroscience.2012.10.065

Correia, M. L. G., and Rahmouni, K. (2006). Role of leptin in the cardiovascular and endocrine complications of metabolic syndrome. *Diabetes Obes. Metab.* 8, 603–610. doi: 10.1111/j.1463-1326.2005.00562.x

Dunbar, J. C., Hu, Y. G., and Lu, H. Q. (1997). Intracerebroventricular leptin increases lumbar and renal sympathetic nerve activity and blood pressure in normal rats. *Diabetes* 46, 2040–2043. doi: 10.2337/diab.46.12.2040

Eikelis, N., Schlaich, M., Aggarwal, A., Kaye, D., and Esler, M. (2003). Interactions between leptin and the human sympathetic nervous system. *Hypertension* 41, 1072–1079. doi: 10.1161/01.HYP.0000066289.17754.49

Elinav, E., Niv-Spector, L., Katz, M., Price, T. O., Ali, M., Yacobovitz, M., et al. (2009). Pegylated leptin antagonist is a potent orexigenic agent: preparation and mechanism of activity. *Endocrinology* 150, 3083–3091. doi: 10.1210/en.2008-1706

Friedman, J. M. (2002). The function of leptin in nutrition; weight, and physiology. *Nutr. Rev.* 60, S1–S14. doi: 10.1301/002966402320634878

Galic, S., Oakhill, J. S., and Steinberg, G. R. (2010). Adipose tissue as an endocrine organ. *Mol. Cell. Endocrinol.* 316, 129–139. doi: 10.1016/j.mce.2009.08.018

Gertler, A., and Elinav, E. (2014). Novel superactive leptin antagonists and their potential therapeutic applications. *Curr. Pharm. Des.* 20, 659–665. doi: 10.2174/13816128113199990014

Goodchild, A. K., Dampney, R. A., and Bandler, R. (1982). A method for evoking physiological responses by stimulation of cell bodies, but not axons of passage, within localized regions of the central nervous system. *J. Neurosci. Methods* 6, 351–363. doi: 10.1016/0165-0270(82)90036-X

Grill, H. J. (2010). Leptin and the systems neuroscience of meal size control. *Front. Neuroendocrinol.* 31, 61–78. doi: 10.1016/j.yfrne.2009.10.005

Grill, H. J., and Kaplan, J. M. (2002). The neuroanatomical axis for control of energy balance. *Front. Neuroendocrinol.* 23, 2–40. doi: 10.1006/frne.2001.0224

Guyenet, P. G. (2006). The sympathetic control of blood pressure. *Nat. Rev. Neurosci.* 7, 335–346. doi: 10.1038/nrn1902

Hall, J. E., Da Silva, A. A., Do Carmo, J. M., Dubinion, J., Hamza, S., Munusamy, S., et al. (2010). Obesity-induced hypertension: role of sympathetic nervous system, leptin, and melanocortins. *J. Biol. Chem.* 285, 17271–17276. doi: 10.1074/jbc.R110.113175

Haynes, W. G., Morgan, D. A., Walsh, S. A., Mark, A. L., and Sivitz, W. I. (1997). Receptor-mediated regional sympathetic nerve activation by leptin. *J. Clin. Invest.* 100, 270–278. doi: 10.1172/JCI119532

Huang, J., and Weiss, M. L. (1999). Characterization of the central cell groups regulating the kidney in the rat. *Brain Res.* 845, 77–91. doi: 10.1016/S0006-8993(99)01937-X

Kelesidis, T., Kelesidis, I., Chou, S., and Mantzoros, C. S. (2010). Narrative review: the role of leptin in human physiology: emerging clinical applications. *Ann. Intern. Med.* 152, 93. doi: 10.7326/0003-4819-152-2-201001190-00008

Mark, A. L., Agassandian, K., Morgan, D. A., Liu, X., Cassell, M. D., and Rahmouni, K. (2009). Leptin signaling in the nucleus tractus solitarii increases sympathetic nerve activity to the kidney. *Hypertension* 53, 375–380. doi: 10.1161/HYPERTENSIONAHA.108.124255

Marsh, A. J., Fontes, M. A., Killinger, S., Pawlak, D. B., Polson, J. W., and Dampney, R. A. (2003). Cardiovascular responses evoked by leptin acting on neurons in the ventromedial and dorsomedial hypothalamus. *Hypertension* 42, 488–493. doi: 10.1161/01.HYP.0000090097.22678.0A

Matsumura, K., Abe, I., Tsuchihashi, T., and Fujishima, M. (2000). Central effects of leptin on cardiovascular and neurohormonal responses in conscious rabbits. *Am. J. Physiol.* 278, R1314–R1320.

Montanaro, M. S., Allen, A. M., and Oldfield, B. J. (2005). Structural and functional evidence supporting a role for leptin in central neural pathways influencing blood pressure in rats. *Exp. Physiol.* 90, 689–696. doi: 10.1113/expphysiol.2005.030775

Morris, D. L., and Rui, L. Y. (2009). Recent advances in understanding leptin signaling and leptin resistance. *Am. J. Physiol.* 297, E1247–E1259. doi: 10.1152/ajpendo.00274.2009

Myers, M. G., Munzberg, H., Leinninger, G. M., and Leshan, R. L. (2009). The geometry of leptin action in the brain: more complicated than a simple ARC. *Cell Metab.* 9, 117–123. doi: 10.1016/j.cmet.2008.12.001

Patterson, C. M., Leshan, R. L., Jones, J. C., and Myers, M. G. (2011). Molecular mapping of mouse brain regions innervated by leptin receptor-expressing cells. *Brain Res.* 1378, 18–28. doi: 10.1016/j.brainres.2011.01.010

Paxinos, G., and Watson, C. (2007). *The Rat Brain in Stereotaxic Coordinates*. Amsterdam; Boston: Academic Press/Elsevier.

Pilowsky, P. M., and Goodchild, A. K. (2002). Baroreceptor reflex pathways and neurotransmitters: 10 years on. *J. Hypertens.* 20, 1675–1688. doi: 10.1097/00004872-200209000-00002

Prior, L. J., Eikelis, N., Armitage, J. A., Davern, P. J., Burke, S. L., Montani, J. P., et al. (2010). Exposure to a high-fat diet alters leptin sensitivity and elevates renal sympathetic nerve activity and arterial pressure in

rabbits. *Hypertension* 55, 862–868. doi: 10.1161/HYPERTENSIONAHA.109.141119

Rahmouni, K., Haynes, W. G., Morgan, D. A., and Mark, A. L. (2003). Role of melanocortin-4 receptors in mediating renal sympathoactivation to leptin and insulin. *J. Neurosci.* 23, 5998–6004.

Rahmouni, K., and Morgan, D. A. (2007). Hypothalamic arcuate nucleus mediates the sympathetic and arterial pressure responses to leptin. *Hypertension* 49, 647–652. doi: 10.1161/01.HYP.0000254827.59792.b2

Schramm, L. P., Strack, A. M., Platt, K. B., and Loewy, A. D. (1993). Peripheral and central pathways regulating the kidney: a study using pseudorabies virus. *Brain Res.* 616, 251–262. doi: 10.1016/0006-8993(93)90216-A

Shih, C. D., Au, L. C., and Chan, J. Y. H. (2003). Differential role of leptin receptors at the hypothalamic paraventricular nucleus in tonic regulation of food intake and cardiovascular functions. *J. Biomed. Sci.* 10, 367–378. doi: 10.1007/BF02256428

Shpilman, M., Niv-Spector, L., Katz, M., Varol, C., Solomon, G., Ayalon-Soffer, M., et al. (2011). Development and characterization of high affinity leptins and leptin antagonists. *J. Biol. Chem.* 286, 4429–4442. doi: 10.1074/jbc.M110.196402

Sly, D. J., Colvill, L., Mckinley, M. J., and Oldfield, B. J. (1999). Identification of neural projections from the forebrain to the kidney, using the virus pseudorabies. *J. Auton. Nerv. Syst.* 77, 73–82. doi: 10.1016/S0165-1838(99)00031-4

Strack, A. M., Sawyer, W. B., Hughes, J. H., Platt, K. B., and Loewy, A. D. (1989a). A general pattern of CNS innervation of the sympathetic outflow demonstrated by transneuronal pseudorabies viral infections. *Brain Res.* 491, 156–162.

Strack, A. M., Sawyer, W. B., Platt, K. B., and Loewy, A. D. (1989b). CNS cell groups regulating the sympathetic outflow to adrenal gland as revealed by transneuronal cell body labeling with pseudorabies virus. *Brain Res.* 491, 274–296.

Sved, A. F., Cano, G., and Card, J. P. (2001). Neuroanatomical specificity of the circuits controlling sympathetic outflow to different targets. *Clin. Exp. Pharmacol. Physiol.* 28, 115–119. doi: 10.1046/j.1440-1681.2001.03403.x

Weiss, M. L., Chowdhury, S. I., Patel, K. P., Kenney, M. J., and Huang, J. (2001). Neural circuitry of the kidney: NO-containing neurons. *Brain Res.* 919, 269–282. doi: 10.1016/S0006-8993(01)03030-X

Zhang, Y., Kerman, I. A., Laque, A., Nguyen, P., Faouzi, M., Louis, G. W., et al. (2011). Leptin-receptor-expressing neurons in the dorsomedial hypothalamus and median preoptic area regulate sympathetic brown adipose tissue circuits. *J. Neurosci.* 31, 1873–1884. doi: 10.1523/JNEUROSCI.3223-10.2011

Conflict of Interest Statement: The authors declare that the research was conducted in the absence of any commercial or financial relationships that could be construed as a potential conflict of interest.

Received: 07 October 2013; accepted: 14 July 2014; published online: 08 August 2014.
Citation: Barnes MJ and McDougal DH (2014) Leptin into the rostral ventral lateral medulla (RVLM) augments renal sympathetic nerve activity and blood pressure. Front. Neurosci. ***8****:232. doi: 10.3389/fnins.2014.00232*
This article was submitted to Autonomic Neuroscience, a section of the journal Frontiers in Neuroscience.